Trabajo Fin de Grado
Ingeniería de la Energía

Current Sensing in LV Distribution Panels through the use of Magnetic Field Sensors

Medida de Corrientes en Cuadros de Distribución BT mediante el uso de Sensores de Campo Magnético

Autor: Enrico Leorato
Tutores: Prof. Juan Carlos del Pino López
Prof. Pedro Luis Cruz Romero

Dep. de Ingeniería Eléctrica
Escuela Técnica Superior de Ingeniería
Universidad de Sevilla

Sevilla, 2016

Trabajo Fin de Grado
Ingeniería de la Energía

Current Sensing in LV Distribution Panels through the use of Magnetic Field Sensors

Medida de Corrientes en Cuadros de Distribución BT mediante el uso de Sensores de Campo Magnético

Autor:
Enrico Leorato

Tutores:
Prof. Juan Carlos del Pino López
Prof. Pedro Luis Cruz Romero

Dep. de Ingeniería Eléctrica
Escuela Técnica Superior de Ingeniería
Universidad de Sevilla

Sevilla, 2016

Trabajo Fin de Grado: Current Sensing in LV Distribution Panels through the use of Magnetic Field Sensors

Autor: Enrico Leorato

Tutores: Prof. Juan Carlos del Pino López
Prof. Pedro Luis Cruz Romero

El tribunal nombrado para juzgar el Proyecto arriba indicado, compuesto por los siguientes miembros:

Presidente:

Vocales:

Secretario:

Acuerdan otorgarle la calificación de:

Sevilla, 2016

El Secretario del Tribunal

A mi familia

A mi novia

A mis maestros

ACKNOWLEDGEMENTS

Por primero querría agradecer mis tutores, en particular el profesor Pino López que me ha permitido emprender esto proyecto, ayudándome con el uso de los softwares y siendo siempre presente y disponible por cada uno de los infinitos problemas que hemos tenido que afrontar durante el desarrollo del proyecto.

Me complace particularmente el hecho que con el uso de Comsol empecé desde un nivel igual a cero, hasta llegar en estos meses a un buen nivel de conocimiento del programa, aunque si no ha sido fácil y he pasado muchas noches donde me hubiera gustado quemar el ordenador.

Por el soporte moral tengo que agradecer mi novia que siempre ha sido presente y me ha consulado cuando nada funcionaba o tenía problemas.

Un agradecimiento especial también a Sevilla que tiene un color y un calor especial. Para mí será siempre la ciudad más hermosa del mundo y la experiencia Erasmus que he emprendido aquí cambiará para siempre mi idea del mundo, de las otras culturas y de todo lo que está afuera de la nuestra "confort zone". Sin hablar, además, de la satisfacción personal que se tiene cuando se habla otro idioma.

Gracias, al final, a mi templanza, que me permitió de estudiar y trabajar por más de 5 años sin tener que pedir nada a mi familia, que la quiero mucho.

ABSTRACT

In power systems currents that usually flow through flat copper or aluminium conductors called bus bars. Therefore, there is a practical demand for bus bars to be employed in current measurement applications.

The present investigation, taking into account this practical demand, has as its objective the development of a cheap and automatic current monitoring system applicable to electrical bus bars.

The requirement to develop a low cost system is the first step in order to obtain a possible future industrial production of this system and it affected the choice of the hardware tools used in this project.

The bus bars taken into consideration in this project are employed in an electrical LV distribution panel intended for use in the industrial sector.

The panel is employed for the supply of four different 3-phase circuits that provide energy to distinct groups of electrical loads.

This automatic system of monitoring has the purpose of measuring the current flowing through every bar with the future goal to check, at any time, electrical information of the electrical system, such as the load curve that denotes every circuit.

The application developed in this investigation assumes that the magnetic field around a bus bar, at a certain distance, is proportional to the applied current at all times. Thus, it is possible to find out the electrical information of a bus bar by measuring and analysing the emanated magnetic field.

In order to analyse the Magnetic field, it has been taken into consideration, principally for the cost-effectiveness, the implementation of a number of Magnetoresistive sensors installed into the panel and supported by an Arduino® board, specially programmed for the case in study.

The main develop of the project was realized using a 3D model of the distribution panel, designed with the support of the Solidworks® software and subsequently implemented in the COMSOL Multiphysics® simulation software for FEM analysis.

The use of the FEM simulation software has been fundamental in order to find out the correct position and configuration of the sensors. The main goal obtained with the FEM simulations it was the elimination of the influence of stray MFs in the sensors measures through the setting of an anti-differential configuration of the sensors.

At the end of the work it has been reached an advanced level of the project, with the correct functioning of the simulating measurement system and the implementation of an Arduino® algorithm to control the board supported the sensors.

The correct functioning of the simulating system was figure out with a graphical study of the measured currents trends, developed in a Matlab® environment.

TABLE OF CONTENTS

LIST OF TABLES

LIST OF FIGURES

LIST OF SYMBOLS AND ABBREVIATIONS

AMR	Anisotropic Magnetoresistance	
MF	Magnetic Field	
I	current	A
ω	Angular frequency	rad/s
J	Current density (volume)	A/m^2
D	Electric displacement	C/m^2
E	Electric field	V/m
σ	Electrical conductivity	S/m
j, i	Imaginary unit	-
H	Magnetic field	A/m
B	Magnetic flux density	T
A	Magnetic potential (vector)	Wb/m
$\vec{B}_x$	Magnetic flux density, vector component x	T
$\vec{B}_y$	Magnetic flux density, vector component y	T
$\vec{B}_z$	Magnetic flux density, vector component z	T
$\left[\vec{B}\right]$	Magnetic flux density matrix	µT
$\left[\vec{I}\right]$	Matrix of currents	A
$\left[\vec{B}(t)\right]$	Time dependent magnetic flux density matrix	µT
$\left[\vec{I}(t)\right]$	Time dependent matrix of currents	A
$[K]$	Matrix of constant elements	
$[K]_{corr}$	Matrix of corrective coefficients	
MCU	Microcontroller unit	
ADC	Analog-to-Digital converter	

1 INTRODUCTION

"Measurement is the first step that leads to control and eventually to improvement.
If you can't measure something, you can't understand it.
If you can't understand it, you can't control it.
If you can't control it, you can't improve it."

-H. James Harrington-

The application developed in this investigation assumes that the magnetic field around a bus bar, at a certain distance, it's proportional to the applied current at all times. Thus, it's possible to find out the electrical information of a bus bar by measuring and analysing the emanated magnetic field.

This type of application of current measurement it was implemented, in this study, in order to develop an automatic system for the monitoring of the currents that flow through a group of bus bars.

This automatic system of measurement it's destined for a L.V. electric panel employed in the industrial sector. The panel is operated for the supply of four different circuits that provide energy to distinct groups of electrical loads. The circuits in consideration are 3-phase circuits, thus every circuit it's composed by three different bus bars referred to the phases R, S, T.

The purpose of the study it's to monitor the current of every bar in order to know, at any time, the load curve that denotes every circuit.

This technology, in order to be practical and applicable in this and other electric panels, must require that the monitoring device should be compact, easy for installation, and make no contact with the bars. With these features, the technology can monitor the load curve for every circuit in every moment without having to apply a direct and manual measure of the parameters.

The main difficulty encountered, in the development of the project, was the implementation of a system able to achieve the immunity from stray magnetic fields, which can significantly disturb the measurement accuracy.

To fulfil this objective there have been implemented, for every bus bar, two Magnetoresistive sensors in the anti-differential configuration, as explained in the next paragraph. These sensors belong to the category of Hall effect sensors, also known as open-loop current sensors [*1, 2*], better described in the paragraph [..].

Considering the difficulty to develop the present investigation with practical methods it was used a theoretical approach based on a modelling of the problem with a Finite Element Method (FEM).

The modelling with a FEM permit to make various studies of the problem and it permit to simulate the behaviour of various electric parameters depending to the settings. In this particular case, the big advantages in the use of a FEM have been principally the possibility to set infinite value for the input current (useful for the implementation of the various tests) and the possibility to feed, or not, every singular bar of every circuit.

The FEM software used in this investigation is COMSOL Multiphysics® used with the support of Solidworks® for the geometrical part and the support of Matlab® for the graphical results part.

Regarding the practice development of the study, namely the real monitoring of the current in the panel, it was used a control system composed by the Magnetoresistive sensors supported by an Arduino® board programmed with an appropriate software.

1.1 Magnetoresistive sensors

Magnetoresistance (MR) is defined as the property of a material to change the value of its electrical resistance when an external magnetic field is applied to it.

The first Magnetoresistive effect was discovered by William Thomson (better known as Lord Kelvin) in 1851.

Whit his experiments discovered that in a piece of iron the resistance increases when the current is in the same direction as the magnetic force and decreases when the current is at 90° to the magnetic force. Making, subsequently, the same experiment with nickel he founds that the piece of iron was affected in the same way but the magnitude of the effect was greater. This effect is referred to as anisotropic magnetoresistance (AMR).

On a theoretical level, depending on the magnetic field conditions, the material has a minimum and maximum resistance, Rmin and Rmax respectively, where Rmin is taken as the reference resistance value and its variation can be expessed by the ratio:

$$MR = \frac{(R_{max} - R_{min})}{R_{min}} \times 100\%$$

being MR the percentage of the magnetoresistive effect in the material or device. [*3,4*]

The mains different magnetoresistive mechanisms are: anisotropic magnetoresistance (AMR), giant magnetoresistance (GMR) and tunnel magnetoresistance (TMR).

1.1.1 AMR effect

Thomson's experiments are an example of AMR, property of a material in which a dependence of electrical resistance on the angle between the direction of electric current and direction of magnetization is observed.

The maximum resistance is obtained when the magnetic field direction is parallel to the current flow, while the minimum value occurs when the magnetic field and the electric current have perpendicular directions. This effect is a characteristic of ferromagnetic alloys, such as Fe and Ni compounds, and arises from spin orbit interactions among the 3d shells electrons. It is related with the scattering of the conduction electrons in d orbitals (spin-orbit coupling), being the scattering probability higher when these orbitals are parallel to the current direction, resulting in different scattering cross sections for perpendicular and parallel configurations.

The orientation of d orbitals is set by the magnetic field orientation. The largest AMR effect at room temperature was observed for Ni1-xCox presenting a value of 6%.

AMR of new materials is being investigated and magnitudes up to 50% have been observed in some ferromagnetic uranium compounds.

Actually the AMR effect is used in a wide array of sensors for measurement of Earth's magnetic field (electronic compass), for electric current measuring (by measuring the magnetic field created around the conductor), for traffic detection and for linear position and angle sensing. The biggest AMR sensor manufacturers are Honeywell, NXP Semiconductors, and Sensitec GmbH. [*5*]

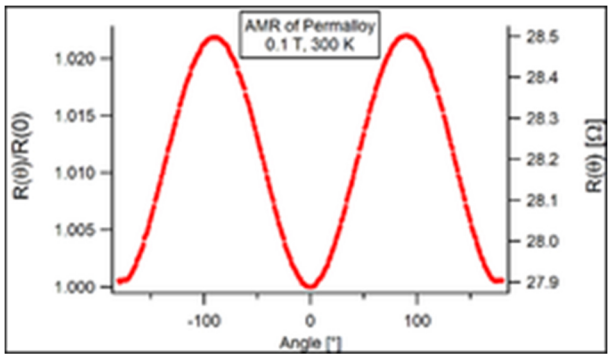

Fig. 1.1 Resistance of a thin Permalloy film as a function of the angle of an applied external field.

1.1.2 The 3-axis Magnetoresistive sensors: HMC5883L

The MR sensors used in this project are three-axis sensors named HMC5883L and produced by the Honeywell company (USA).

The Honeywell HMC5883L is a surface-mount, multi-chip module designed for low-field magnetic sensing with a digital interface for applications such as low-cost compassing and magnetometry.

The device utilizes Anisotropic Magnetoresistive technology (AMR), mentioned in the previous paragraph, and includes high-resolution HMC118X series magneto-resistive sensors plus an ASIC (Application Specific Integrated Circuit) containing amplification and a 12-bit ADC with high accuracy.

The HMC5883L is a 3.0x3.0x0.9mm surface mount 16-pin and for its size it finds also diverse applications in Mobile Phones, Netbooks, Consumer Electronics, Auto Navigation Systems, and Personal Navigation Devices.

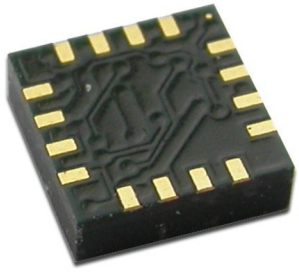

Fig. 1.2 Honeywell HMC5883L Magnetoresistive sensor

The main characteristics and strong points of the sensor are:

- Small size, that permit a highly integration in the electric panel;
- Low cost and good cost-effectiveness;
- Low-Cost functionality test after assembly in production;
- Low voltage operations (2.16 to 3.6V) and low power consumption (100 μA), also compatible with batteries;
- High resolution;
- High speed: 160 Hz maximum output rate;
- Operating temperature range: -30 ÷ 85 °C.

Where the main important characteristics that lead to choose this sensor for the implementation in the present project are: the low coast advantage, the small size and the big operating temperature range that allows to bear the heat produced by the bars.

1.2 Theoretical considerations for the MF measure

Focusing to the goal of the work, the target is to measure the MF generate by an electric bar of the electric panel trying to not measure the stray MFs producing by the other bars.

To simplify the problem, it is possible to considerate an electric conductive wire, like a cable, in which flows an electric current. As a consequence of this current flow, a magnetic field will arise and surround the electric wire forming concentric circles around the wire, like in the following image.

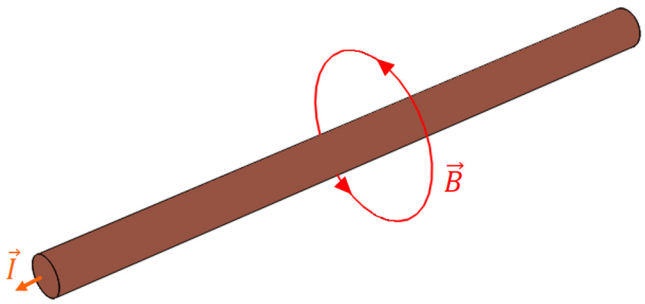

Fig. 1.3 Distribution of MF around an electric wire

Now if is taken into consideration that the MF surrounds the cable in the form of circular lines, it's intuitive to think that for the purpose of measure the value of MF it could be sufficient measure the primary magnetic field in a point into the space close to the cable.

This it can be true if the magnetic field produced by the current it's not influenced by other stray MFs produced, for example, from other active conductors or electrical devices present near the cable.

On the other side, if it's taken into consideration the presence of another powered electric wire close to the main, it's necessary to considerate that there will be some components of MF generated by the second wire that may have influence in the measure of the main MF produced by the first wire.

A solution to this problem can be found with a more practical approach, using an electronic stratagem. This consist on a simultaneous use of two Magnetoresistive sensors instead of one with the accuracy of positioning these sensors in order to measure the same magnitude of MF.

The idea is to eliminate the effects produced by the other powered bars with the implementation of two Hall effect sensors in anti-differential configuration, in order to cancel the common mode magnetic fields while the output signal is doubled.

For doing this we have to install one MF sensor on one side of the conductive wire and configure it to monitor a first directional magnetic field induced by the current. Then is necessary to install a second MF sensor positioned in the other side of the conductor, substantially opposite to the first sensor, and configure it to monitor a second directional MF. That MF is substantially opposite in direction to the first directional magnetic field, like is represent in the image below.

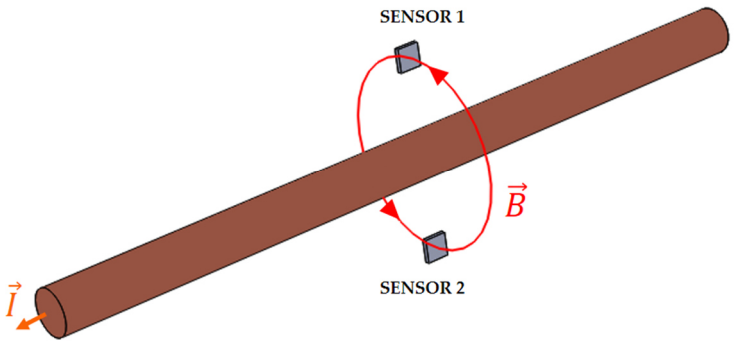

Fig. 1.4 Disposition of sensors for an electric wire

Referring to the image, if we consider the vertical plane cutting the sensors and the line of MF in a perpendicular way, it's possible to note that the lines of MF can be incoming or outgoing to the considerate plane.

Then, for the fact that the sensors have an anti-differential configuration, one of them will measure the value of a component of MF but with negative sign, getting two value with the same sign.

Consequently, the result sum of the two values will be the double of the real MF value in this moment (neglecting the probable measure errors and the uniformities of the MF distribution in the space).

On the other hand, it's take now in consideration the case of two powered electric wire, positioned at a respective distance much bigger than the distance between the two sensors. In this case the line of MF, produced by the current flowing in the second wire, will be both incoming in the plane in consideration i.e. incoming in the sensor surface, as can be seen in the next image.

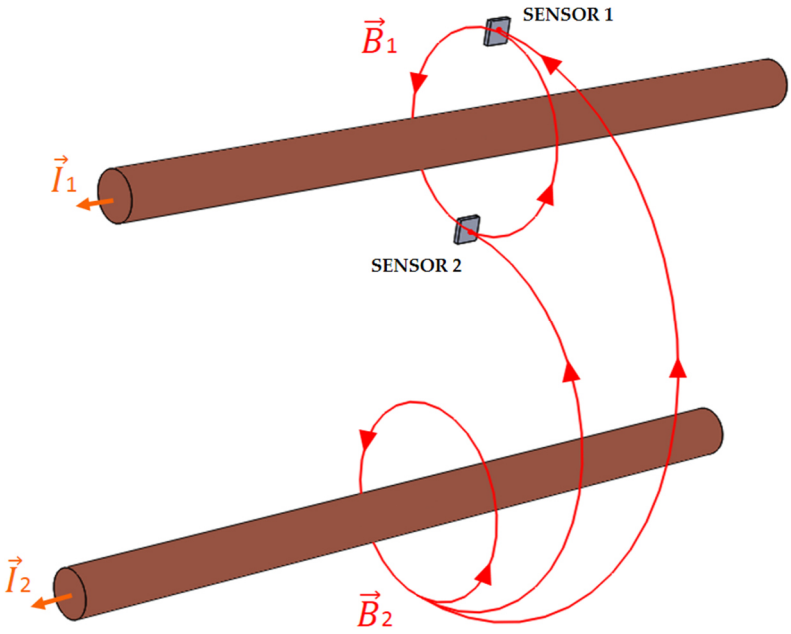

Fig. 1.5 Detection of MF by the sensors. Case with two electric wires

Going now to sum the two component measured by the sensors the obtained result will be, thanks to the anti-differential configuration, the difference of the two measures instead the sum obtaining the almost total elimination of the contribute of stray field in the measure.

To doing this there is a processing component supporting the sensors, it's configured to receive feedback from the first and the second magneto-resistive sensor and generate an anti-differential output from the feedback.

Is important to note that the anti-differential configuration works perfectly with homogenous stray fields. Therefore, considering the fact that the magnetic field gradient decreases with the distance, if the surrounding nonhomogeneous stray fields are away from the transducer they can be considered as homogeneous.

In reality, when multiple alimented conductors are arranged in parallel, the magnetic field gradient decreases with the distance. This means that the cancelation of the effects caused by surrounding conductors it will be better if they will be at greater distance.

All these considerations are obviously applicable to the electric bars in study in this project, creating an automatic system for the monitoring of the MF and consequently for the monitoring of the electric current flowing in the bars.

The next image represent the idea just explained referring it to the case with the bus bars presented in the electric panel.

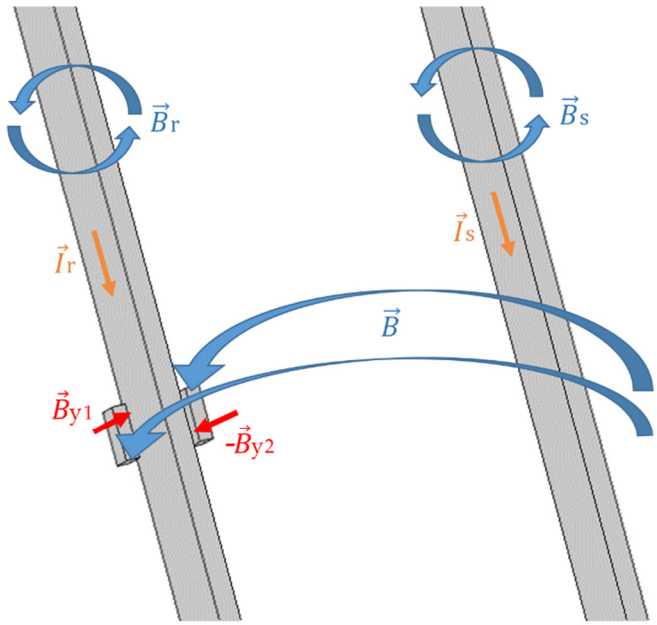

Fig. 1.6 Detection of MF by the sensors. Case with two bus bars.

In the image are represented with the vectors $\vec{B}_{y1}$ and $-\vec{B}_{y2}$ the settings adopted in order to use the sensors in anti-configuration mode. As explained before, the two sensors measure a component of the MF (in this case the vector component y) but setting these measure with a different sign it brings to eliminate the part of measure influenced by the stray magnetic fields.

The final result will be a double measure of the magnetic field produced by the interest bar, with also an another adds term (error) that consider the fact that the sensors are closed but they aren't in the same point.

Indeed, considering that the distance from every bar is in the order of some cm and the distance between two sensors will be in the orders of 1.5 cm is normal to think that the sensors will detect a value of MF a little bit different, especially for the MF contribution by the nearest bars.

1.2.1 FEM approach to simulate a Magnetoresistive sensor

After the firsts tests to ascertain the proper functioning of the model it was possible to elaborate the firsts simulations in order to point out the veracity of the theoretical hypothesis explained in the previous paragraph.

To obtain this it was necessary, first of all, simulate the presence of these sensors in the FEM model, i.e. simulate a point of measure in the considerate space around the bars. Secondly it was necessary to determine a good site for the installation of the sensors remembering the real geometry of the electric panel.

To model the sensors in Comsol has been used a tool in the post processing section named ‘’Domain Point Probe’’ that allows to evaluate the value of MF in a fixed point in the space and also to evaluate the three mains vector components of the MF: $\vec{B}_x$, $\vec{B}_y$ and $\vec{B}_z$.

This last feature was useful to model the panel because also the halls sensors are able to measure the electric field along a specific direction.

2 THEORETICAL FRAMEWORK

2.1 Ampere Law

In classical electromagnetism, Ampère's circuital law, discovered by André-Marie Ampère in 1823, relates the integrated magnetic field around a closed loop to the electric current passing through the loop and therefore relates magnetic fields to electric currents that produce them.

In its original form, Ampère's circuital law relates a magnetic field to its electric current source. The law can be written in two forms described below, the "integral form" and the "differential form". [6]

2.1.1 Integral form

In SI units, the "integral form" of the original Ampère's circuital law is a line integral of the magnetic field around some closed curve C (arbitrary but must be closed). The curve C in turn bounds both a surface S which the electric current passes through (again arbitrary but not closed—since no three-dimensional volume is enclosed by S), and encloses the current.

The mathematical statement of the law is a relation between the total amount of magnetic field around some path (line integral) due to the current which passes through that enclosed path (surface integral). It can be written in a number of forms. [7]

In terms of total current, which includes both free and bound current, the line integral of the magnetic B-field (in tesla, T) around closed curve C is proportional to the total current I_{enc} passing through a surface S (enclosed by C):

(1.1) $$\oint_C B \cdot dl = \mu_0 \iint_S J \cdot dS = \mu_0 I_{enc}$$

where J is the total current density (in ampere per square metre, Am^{-2}).

Alternatively, in terms of free current, the line integral of the magnetic H-field (in ampere per metre, Am^{-1}) around closed curve *C* equals the free current $I_{f,\,enc}$ through a surface *S*:

(1.2) $$\oint_C H \cdot dl = \iint_S J_f \cdot dS = I_{f,enc}$$

where J_f is the free current density only.

The B and H fields are related by the constitutive equation:

(1.3) $$B = \mu_0 \cdot H$$

where μ_0 is the magnetic constant.

2.1.2 Differential form

By the Stokes' theorem, this equation can also be written in a "differential form". Again, this equation only applies in the case where the electric field is constant in time, meaning the currents are steady (time-independent, else the magnetic field would change with time); see below for the more general form.

In SI units, the equation states for total current:

(1.4) $$\nabla \times B = \mu_0 J$$

and for free current

(1.5) $$\nabla \times H = J$$

where ∇× is the curl operator.

2.2 Principal laws used for the computation

In order to calculate the magnetic field generating by the currents and its distribution the simulation software will use these laws of electromagnetism:

- Ampere Law:

$$\nabla \times H = J \qquad (1.6)$$

- Gauss law for magnetism:

$$B = \nabla \times A \qquad (1.7)$$

- Definition of magnetic field:

$$E = -j\omega A \qquad (1.8)$$

3 ELECTRIC PANEL PRESENTATION

3.1 Electrical panel features

The electrical panel in consideration is a panel for the distribution of LV implemented in a MV/LV substation and employed principally in the industrial sector.

The electric panel is principally composed by:

- External aluminium structure;
- Electric bus bars made of aluminium;
- Plastic parts for support the bus bars and for the protection against direct contact with live parts;
- 12 fuses

Electrical features:

- In = 400 A
- Vn = 400 V

The dimensions of the structure are presented in the next paragraph.

Fig. 3.1 Photo of the electric distribution panel

3.2 Development of the geometry in Solidworks®

In order to realize the geometry of the model it was used the CAD software Solidworks® in which is possible to draw the geometry in 3D.
In the next image are represented the final model drawn in the CAD software and subsequently imported in the Comsol software for the analysis.
In the figure 3.2 is shown the original model and in the figure 3.6 is shown the same model but with a prolongation of the final part of the bars with the length of 120 cm. This because the external domain it will be much bigger of the panel size and for this it will necessary to prolong the bars, in order to connect them to the external domain and close the paths for the currents. On the other hand, otherwise, there would be a not real distribution of the MFs caused by the small size of the domain.

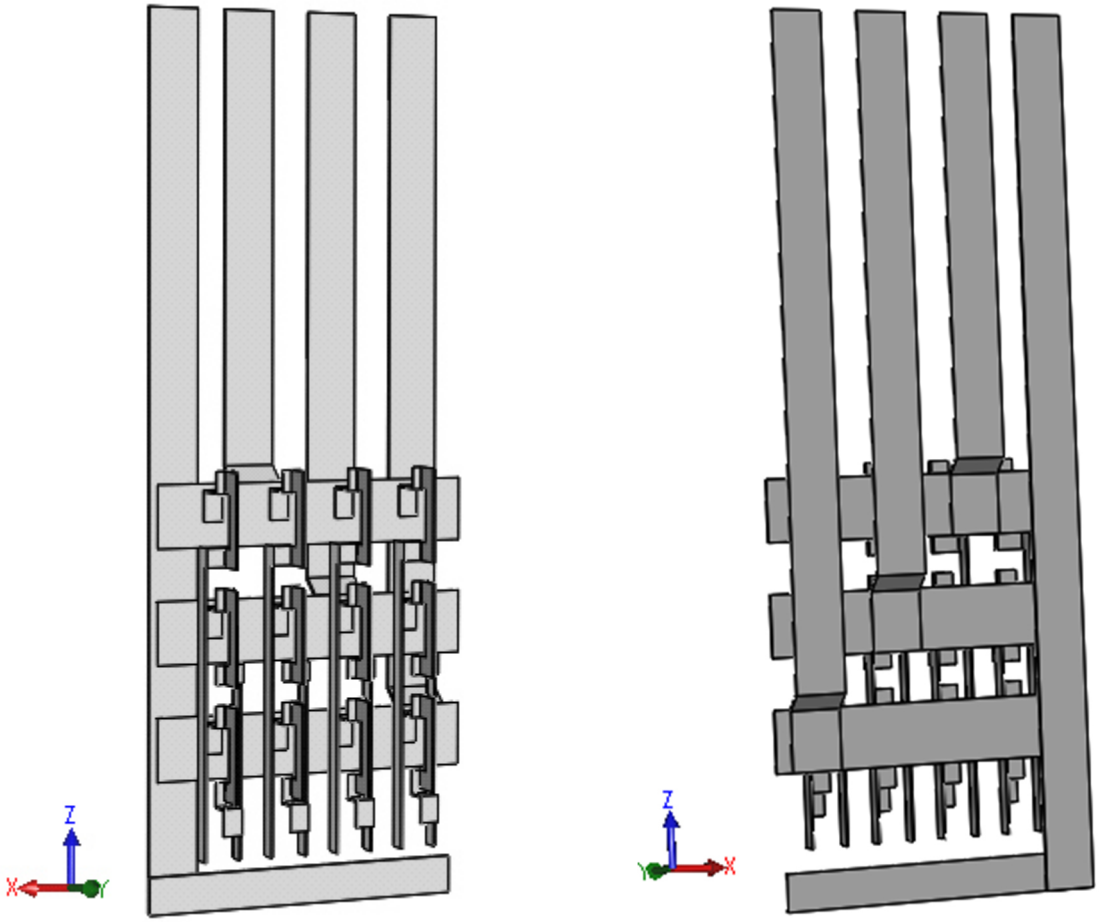

Fig. 3.2 3D CAD model of the electric panel

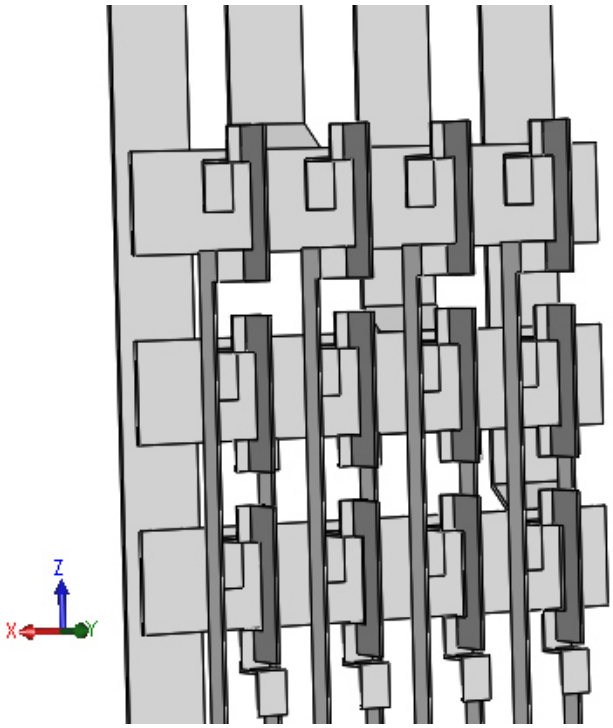

Fig. 3.3 3D CAD model of the electric panel

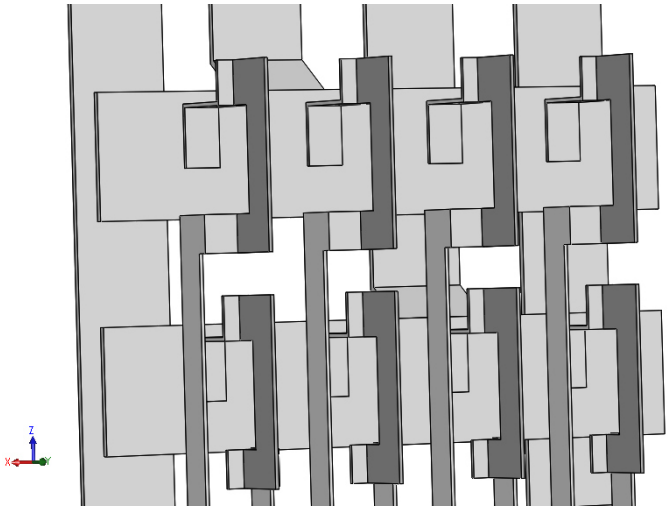

Fig. 3.4 3D CAD model of the electric panel

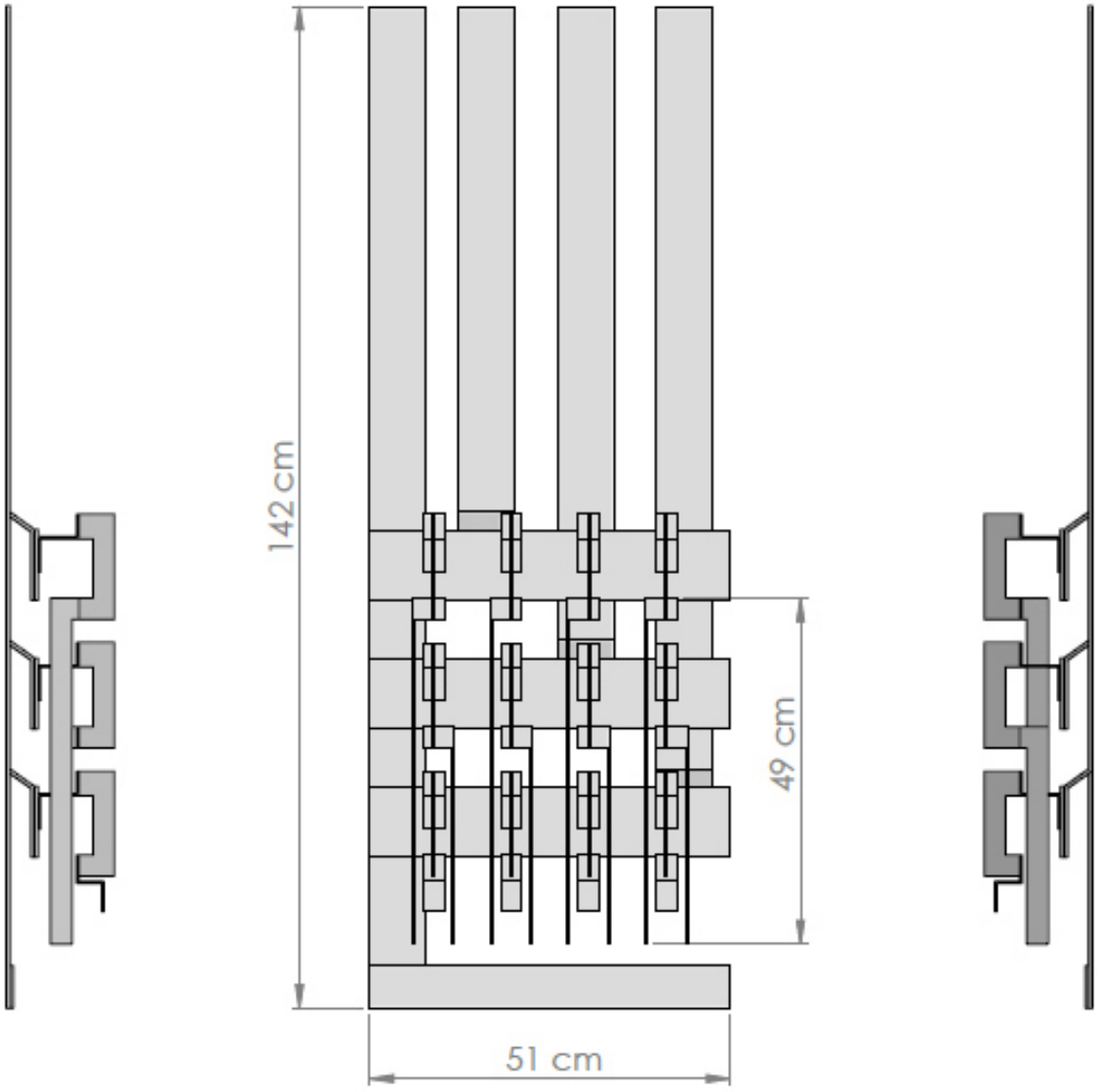

Fig. 3.5 Axonometric drawing of the original model

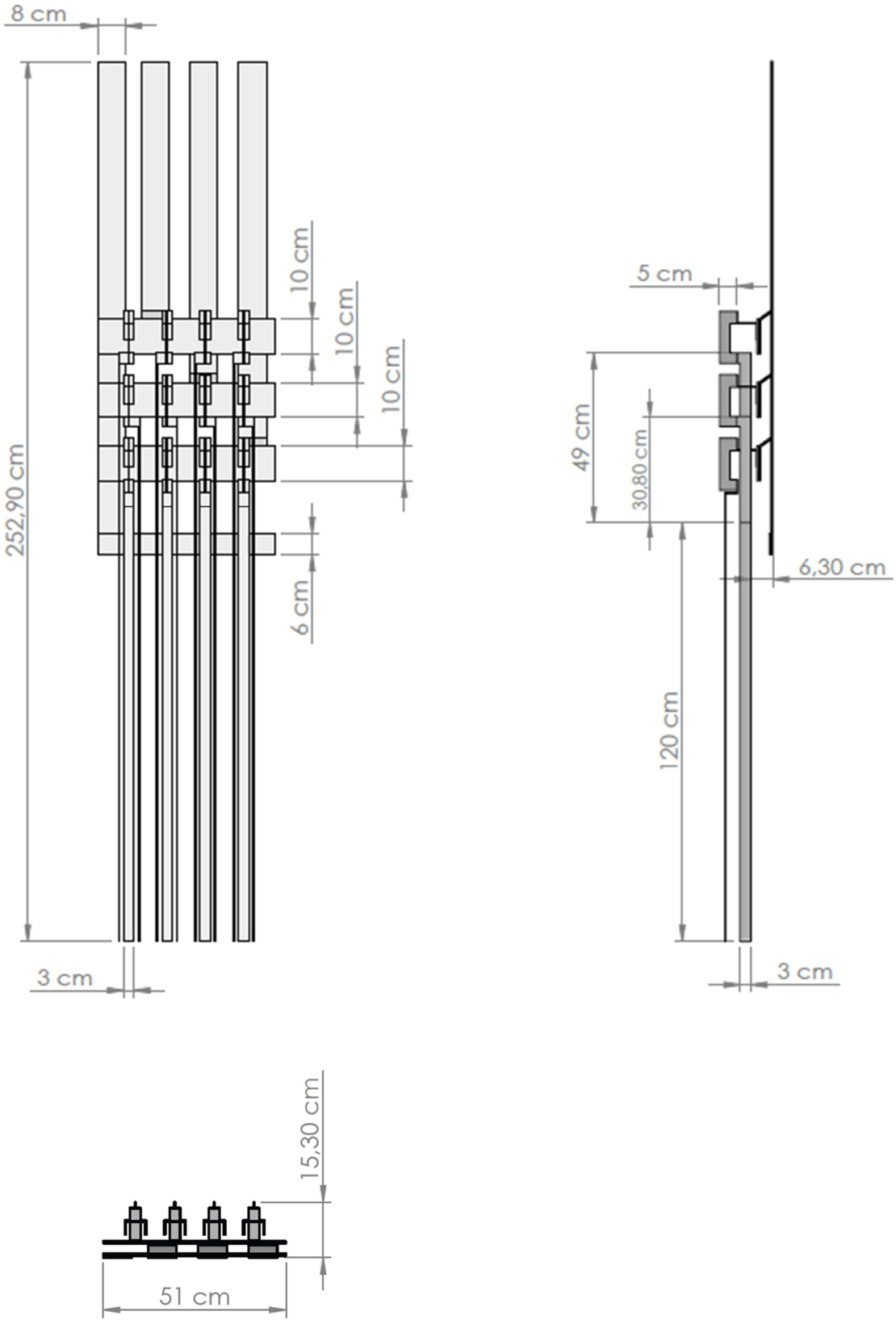

Fig. 3.6 Axonometric drawing of the model with prolonged bars

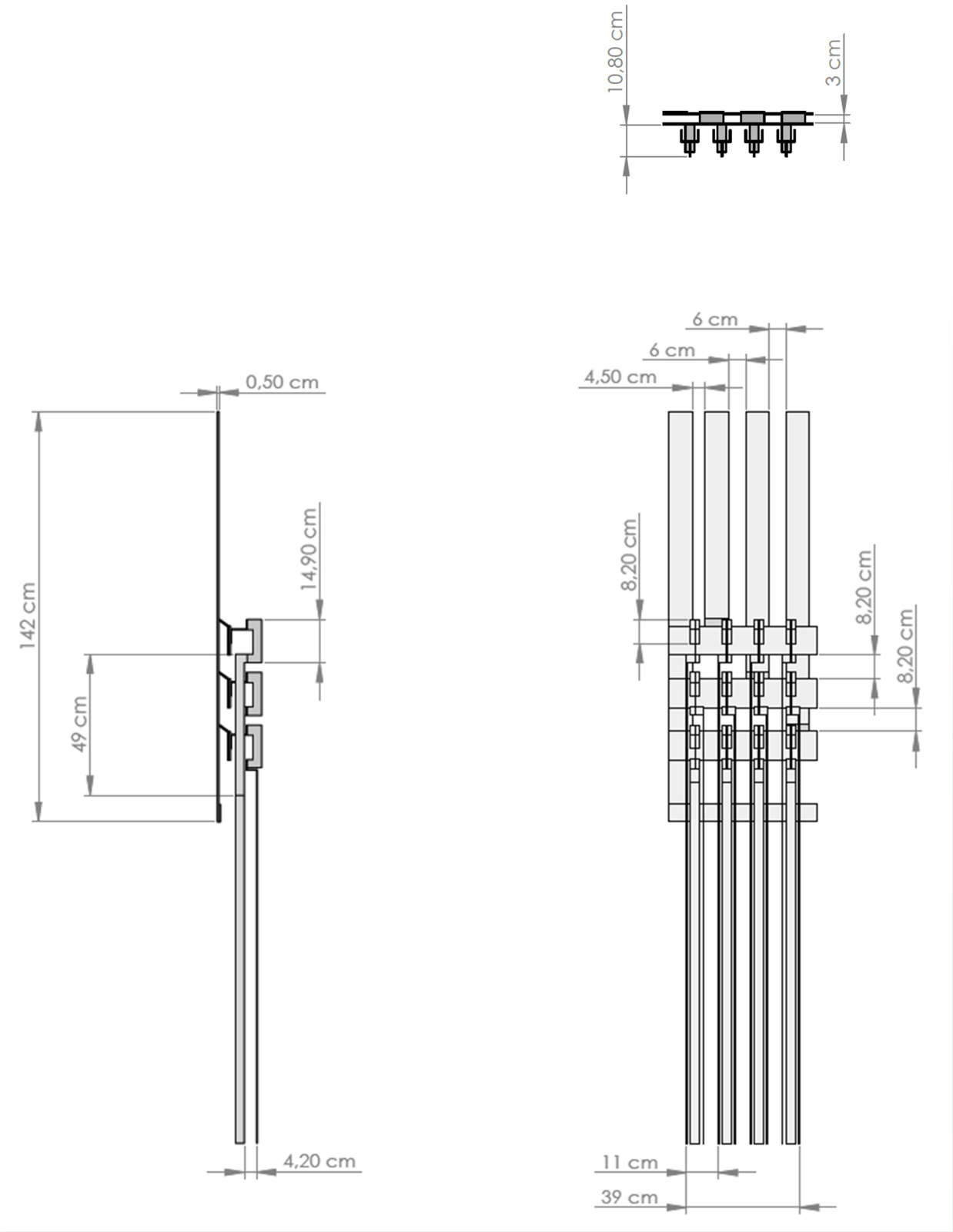

Fig. 3.7 Axonometric drawing of the model with prolonged bars

3.3 Geometry implementation in Comsol Multiphysics®

For the implementation of the geometry in Comsol it was used the tool that permits to import Solidworks projects in the Comsol GUI ensuring that all the measures were read correctly from the software and all the parts were considered as solid parts.

At this point there were inserted other two blocks positioned around the panel designed, in order to form the external domain and consequently the way to return for the currents, as it will be explained in the chapter [5].

The two blocks represented in the figures *3.8, 3.9* are characterized by the following measures:

	Width [cm]	*Depth [cm]*	*Height [cm]*
Block 1	*70*	*30*	*252.7*
Block 2	*300*	*200*	*252.7*

Tab. 3.1 Size of domain blocks

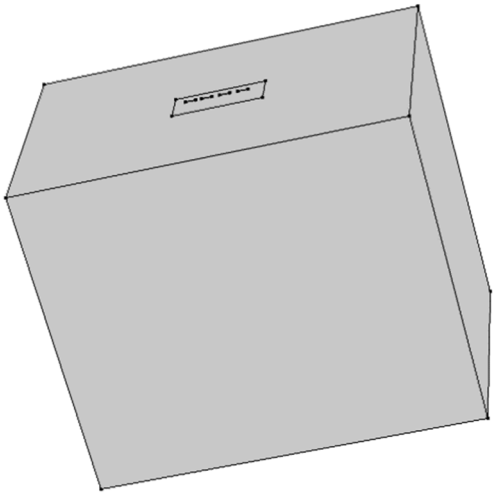

Fig. 3.8 Block 2

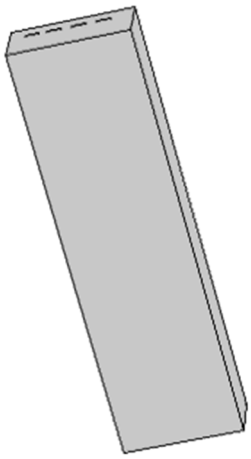

Fig. 3.9 Block 1

4 MATERIAL

There are a lot of consideration to do regarding the materials with which is made the subject of study because all the results are dependent on the electrical materials properties.

In this particular case the electrical panel is made principally of these materials:

- Aluminium, with which are made the bus bars and the external carcase;
- Plastic, with which are made a lot of parts acting as support for some components of the panel and significantly to protect the user against unintentional direct contacts with live parts;
- Copper, for the support where will be insert the fuses;
- Steel, of the nuts and bolts used to fix the various parts of the panel.

Most of these materials will be not taken into consideration in the modelled study of the electric panel, as it's explained in the next paragraph.

4.1 Materials hypothesis for the Comsol Multiphysics® simulation.

As introduced before, not all the parts that composed the panel have been taken into account in the construction of the Comsol model, this because not all the parts are interested in the flow of current neither are particularly influent in the expansion of the magnetic field in the air.

Furthermore, as seen before, it would not be possible to make a drawing with all the single parts really present in the panel and substantially in the Comsol model there have been represented the aluminium bars and the fuse support, that are the parts of interest, omitting the others parts.

Moreover, we have to consider the geometric simplification of the fuse support that implies the omitting of the copper parts and the consideration of a single piece of aluminium.

The result of all these considerations bring to consider in the simulation software all the solid parts (bus bars) made of aluminium and all the others parts, surrounding the actives parts, to be made of air.

After these considerations is possible to set, in the Comsol GUI, the respective material to every part of the model through the appropriate tool.

In the subsequent developments of the project will be taken into consideration these two different material approaches:

- Consider the bus bars made of aluminium, like in the reality case, in order to study the model including the effects of the mutual inductance;
- Consider the bus bars made of air, in order to study the model neglecting the mutual inductance effects between the bars.

These approach will be better taken up in the chapter [10].

In the next tables are represented the characteristics of the materials used for the simulations:

	Value	Unit
Relative permeability	1	-
Relative permittivity	1	-
Electrical conductivity	10	[S/m]

Tab. 4.1 Characteristics of air

	Value	Unit
Relative permeability	1	-
Relative permittivity	1	-
Electrical conductivity	3.77E+07	[S/m]

Tab. 4.2 Characteristics of aluminium

As it can be seen, for the air it was used an Electric conductivity of 10 [S/m] so as to speed up the simulations. This change it will be not influent in the calculation of the results.

5 SETTING OF THE PHYSIC OF THE STUDY

A fundamental part of the study of a model in Comsol is the setting of the physic i.e. the setting of the type of study we need to take into consideration.

In the particular model take into account in this project the type of study chosen it's a Magnetic field study. This type of study allows to set a current or a potential difference to the element of interest with the purpose of calculate the respective Magnetic field produced, its distribution in the space and also it enable to see the distribution of the current density in the object.

Another fundamental part is the selection of a domain of study. About this it has been taken into consideration principally the time domain. This for the fact that the current that flows through the panel bars is an alternating current depending on time, the frequency took into consideration is the industrial frequency of 50 Hz.

In addition to the domain of time it was used a steady-state analysis of the same in order to find out some constant value that will be explained in next paragraphs.

5.1 Setting of a current

For the setting of the currents it has been used an easy and practice way that consist in considerate the subject of the study like a coil in which it's possible to set a close path for the current.

In order to do this, in the software there are nodes named "Coil" that are used to simplify the setup of magnetostatic and low-frequency electromagnetic models.

In many such applications, the magnetic field is generated by electric currents flowing in conductive materials (for example, cables, wires, coils, or solenoids) and the coil features can be used to easily model these structures and to translate lumped quantities (currents and voltages) into distributed quantities (current densities and electric fields).

There are two types of coil features, the Single-Turn Coil and the Multi-Turn Coil which differ by the physical system represented.

The Multi-Turn Coil feature implements a homogenized model of a coil consisting of numerous tightly-wound conducting wires, separated by an electrical insulator.

On the other hand, the Single-Turn Coil feature models a single, solid region of a conducting material (for example, metal) in which the current flows and this is the case that most befits to our study.

After the choice of the Singe-Turn Coil tool and after the selection of the parts that represent the aluminium bars it's necessary to set the current that will flows through the circuit and consequently generates the magnetic field.

All the coil features can be excited either with current and voltage excitation and the supplied value or expression is translated to a current density or electric field applied to the domain in consideration.

The excitation is applied by means of specialized subnodes:

- Boundary Feed subnode, in which is possible to set the input current in the interest boundary, thus creating a way in for the current in the turn coil;

- Ground subnode, that enforces the coil potential to be zero on the selected boundaries.

The lumped voltage and current of the coil correspond respectively to the integral of the electric field along the coil length and to the integral of the current density on a cross section. [*8*]

With these settings we created a path for the current that actually is not a close path, for doing a close path we have to introduce an important topic for the FEM simulations: the study of the Boundary Conditions.

5.1.1 Boundary conditions

As a consequence of the computed current flow, a magnetic field arises and surrounds the wire. This is a vector field, having both a magnitude and direction, and can be computed from Ampère's law. We are interested in learning how to model this magnetic field and how it interacts with other objects.

A reasonable computational model of an electric wire, fed by a current, might look like the image below.

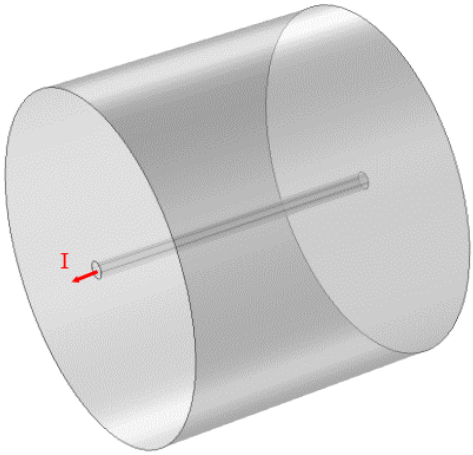

Fig. 5.1 Model of an electric wire with FEM

First, we can see that there is a cylinder around the wire, this represents the air domain. This is the computational domain within which we are solving for the magnetic field and this is a finite-sized domain, yet the magnetic field will actually extend infinitely far away from the wire.

The field intensity will drop off with the inverse of distance to a straight wire, so the field magnitude will be quite small far away from the wire. Although it will never be precisely zero, we can reasonably truncate our modeling domain to a finite-sized space for not require a big computational effort to solve.

By choosing a finite modeling region around the wire, we are assuming that we are only interested in the fields in this region and this choice of finite-sized region introduces an assumption at the boundaries. Indeed, we need to consider some boundary conditions along the boundaries of the cylinder or whatever surrounding domain shape we choose, the mains boundary conditions available in Comsol are the Magnetic Insulation and the Perfect Magnetic Conductor conditions.

The Magnetic Insulation condition can be physically interpreted as a boundary to a domain that has infinite electrical conductivity. That is, the Magnetic Insulation condition implies that our wire is enclosed within a sphere of very high conductivity. Currents can flow and be induced on a magnetic insulation boundary. Mathematically speaking, the magnetic insulation fixes the field variable that is being solved for to be zero at the boundary; it is a homogeneous Dirichlet boundary condition.

On the other hand, the Perfect Magnetic Conductor boundary condition can be thought of as the opposite boundary condition. Mathematically, it enforces the homogeneous Neumann condition, meaning the derivative of the solution field in the direction normal to the boundary is zero. No current can flow, nor be induced on, a perfect magnetic conductor boundary. [*9,10*]

Since our wire extends to the boundaries of the modelling domain, concerning in what was explained in the previous paragraph, we need to provide a current return path via the Magnetic Insulation boundary condition to allows the current to flow through this domain.

The Magnetic Insulation boundary condition represents a mirror symmetry plane for the magnetic field, in fact the magnetic field will be exactly mirrored as you cross the plane. This boundary condition also means that the magnetic field is zero in the normal direction to the boundary. That is, the magnetic field must be

tangential to this boundary. As a consequence, this boundary condition has the physical interpretation of a boundary through which current can only flow in the normal direction.

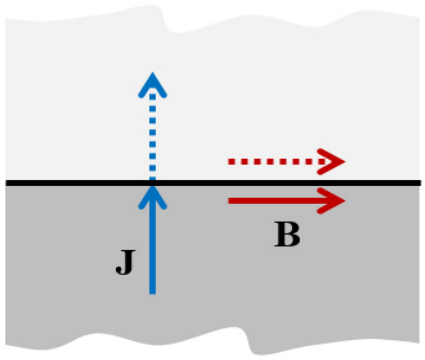

Fig. 5.2 Magnetic insulation boundary condition

5.2 Modelling of a basic electrical conductor in Comsol Multiphysics

As we have just seen, one of the most basic points in modelling an electric wire is the concept of a closed current path.

In the case of study Whenever we are modelling an electrical conductor, or any magnetic field excited by a current flow, we must have a closed path of current and our models must satisfy this condition to be valid.

If we would try to impose a current flowing through an open circuit conductor, that would be equivalent to implying that the current (electrons) instantaneously moves from one end of the open circuit to the other, and this would violate Maxwell's equations.

Moving on our particular case, we have a current that flows through the bars and, as a consequence of the computed current flow, a magnetic field arises and surrounds the bars.

Taking into account a single bus bar, it has been imposed a grounded boundary condition at one of the sides, meaning an imposition of an electric potential of zero. Subsequently it has been imposed a higher electric potential on the other side. At this point, however, it's necessary to set a path for the current in order to obtain a close circuit for its return.

This problem can be solved considering some boundary conditions along the boundaries of the blocks represented the external domain, discussed in the previously paragraph. Therefore, in order to set a close path for the current it was necessary to insert around the model a block representing the external domain and set for it an appropriate boundary condition.

In this project it has been considered a boundary condition that represents a perfect electrical conductor for the return of current, namely a Magnetic Insulation boundary condition.

For the physical interpretation of this, it can be assumed that the conductor sits inside of a cylindrical metal container. As a consequence of the boundary condition, the current, which is flowing along the wire from one side to the other, it will flow back along the surface of the modelled domain as shown in the image below.

In this way it was possible to apply an electric current to the bars and obtain a perfect simulation of its flow in the conductive material.

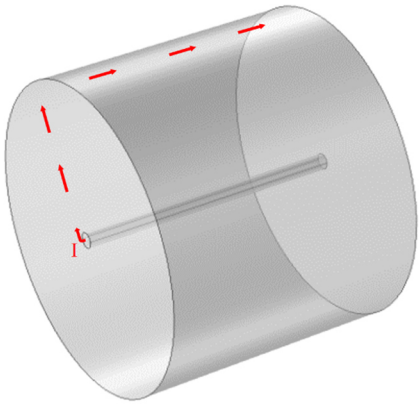

Fig. 5.3 Model of a conductor. Return of current through the external domain.

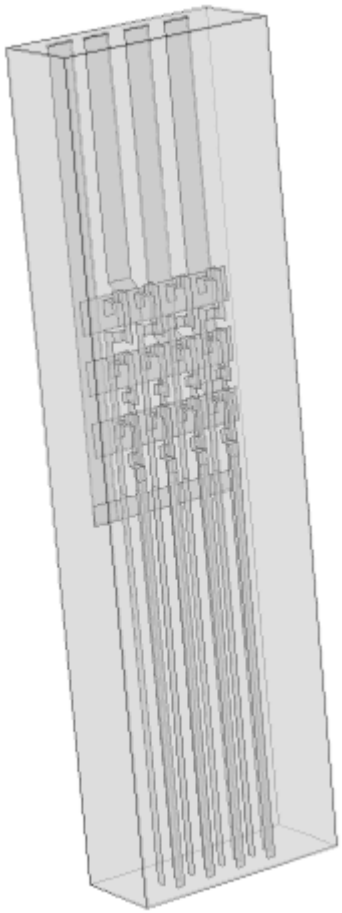

Fig. 5.4 Model of the electric panel with the respective domain

6 MESH IMPLEMENTATION

The finite element method approximates the solution within each element, using some elementary shape function that can be constant, linear, or of higher order.

Substantially the finite element mesh serves two purposes, for first subdivides the CAD geometry being modelled into smaller pieces, or elements, over which it is possible to write a set of equations describing the solution to the governing equation. Then the mesh is also used to represent the solution field to the physics being solved.

Exists four different 3D element types that are tets, bricks, prisms, and pyramids:

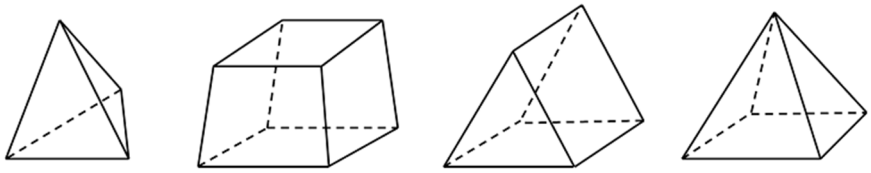

Fig. 6.1 3D elements types

These four elements can be used, in various combinations, to mesh any 3D model (for 2D models, there are available triangular and quadrilateral elements).

Tetrahedral elements are the default element type for most physics within Comsol Multiphysics and any 3D volume, regardless of shape or topology, can be meshed with tets. They are also the only kind of elements that can be used with adaptive mesh refinement.

The other three element types (bricks, prisms, and pyramids) should be used only when it is motivated to do so. It is first worth noting that these elements will not always be able to mesh a particular geometry. [11]

For these considerations in our model of study has been chosen a tetrahedral mesh approach for the mesh construction, considering also that is possible in this way to custom the proprieties of the mesh.

In the next figures are shown the graphical representation of the mesh for every part of the model. Are considered three different sizes of mesh, as it can be seen in the tables. For the external domains (block 1 and block 2) have been chosen types of mesh with larger size elements in order to reduce the computing time.

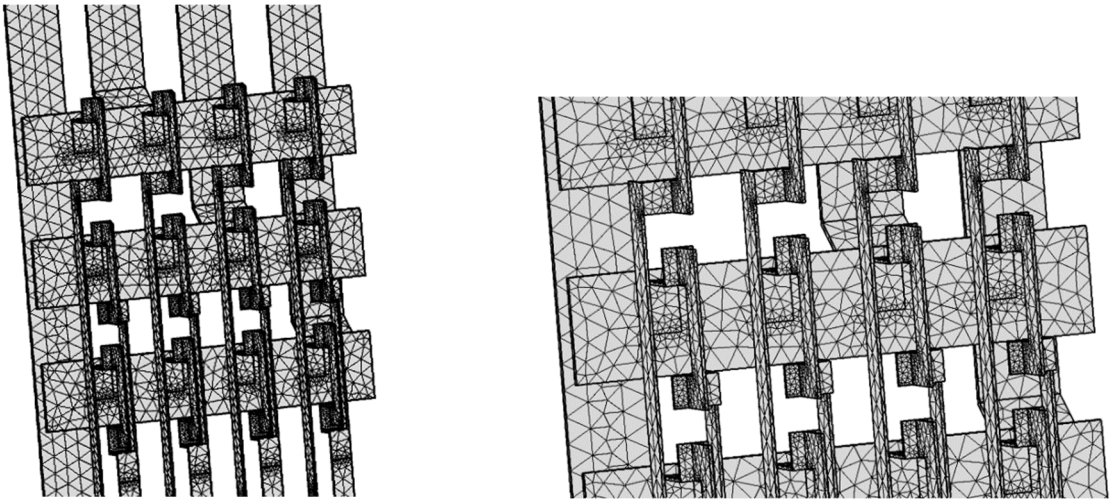

Fig. 6.2 Tetrahedral mesh n° 1

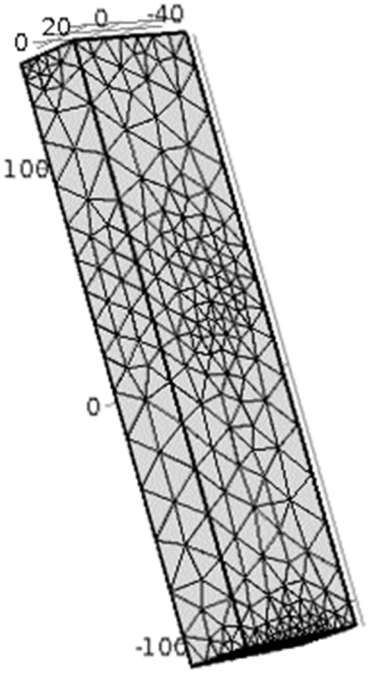

Fig. 6.3 Tetrahedral mesh n°2

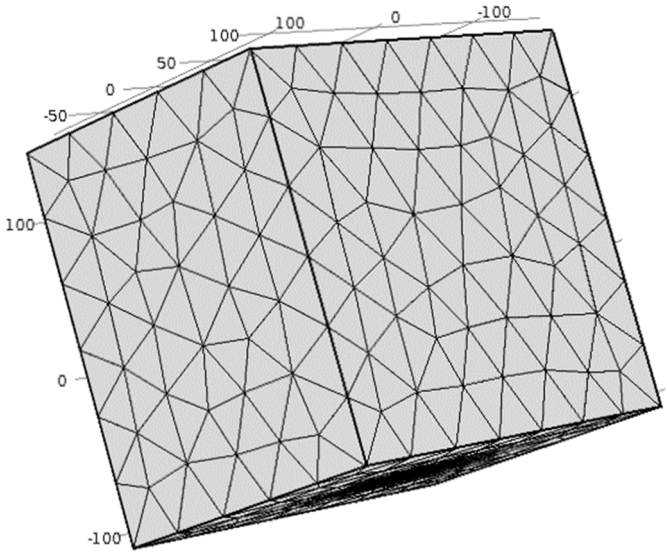

Fig. 6.4 Tetrahedral mesh n°3

6.1 Mesh characteristics

Tab. 6.1 Tetrahedral mesh n°1

	Value
Maximum element size [cm]	*25.3*
Minimum element size [cm]	*2.3*
Minimum element growth rate	*1.5*
Curvature factor	*0.6*
Resolution of narrow regions	*0.5*

Tab. 6.2 Tetrahedral mesh n°2

	Value
Maximum element size [cm]	*25.3*
Minimum element size [cm]	*2.5*
Minimum element growth rate	*1.5*
Curvature factor	*0.6*
Resolution of narrow regions	*0.5*

Tab. 6.3 Tetrahedral mesh n°3

	Value
Maximum element size [cm]	*45*
Minimum element size [cm]	*8.4*
Minimum element growth rate	*1.6*
Curvature factor	*0.7*
Resolution of narrow regions	*0.4*

7 FIRST APPROACH OF STUDY: CONSIDERATION OF A 2D CUT-PLANE

In this section there will be described the main reasons that brought into consideration the possibility to start the simulations with the FEM software in a 2D representation instead of a 3D representation.

This it's possible considering a plane obtained "cutting" the 3-dimensional model in a given plane of interest.

This cutting plane will form an area in which it will be possible to find a location for the sensors, namely, in the simulating case, a good location for the measure points created with the appropriate Comsol tool.

Obviously every test in 2D will be followed by a 3D test considering the same points of measure, including so also the effects of the MF caused by the bars not considerate in the 2D model.

The main criteria that led to the use of a 2D approach were:

- reduction of the geometric complexity;
- reduction of the physic complexities due to the setting of the currents and their repartition in all the circuits;
- focalization in a more reduced area;
- reduction of the heavy computation in order to reduce the computation time.

The last point in particular has a great influence in the present case because change the model slightly means re-solving the model study and for computation-heavy models (like the 3D model in subject) this it can lead to have a big time-consuming process.

7.1 The choose of the cut-planes for the 2D study

One of the most difficult point in the development of the FEM model it was to choose an opportune 2D cut plane for the simulation of the sensors measurement.

The main difficulties founded there were caused by the geometry complexity of the electric panel in the real physic case. This because, as it can be seen in the photos, there are a lot of plastic parts that don't allow to install a sensor wherever we want. Moreover, there are other parts in which it's not convenient the installation of a sensor because of the high concentration of different magnetic fields that could be influence the measures.

For these reasons it was essential to considerate in every case both the simplified model and the real electric panel, in order to assure the connection between the theoretical simulation and the real physic realization.

The two planes selected for the study are the follows:

- A plane x-y obtained slicing the model at the height of z = 35.25 cm;
- A plane x-z obtained slicing the model at the height of y = 11.4 cm;
- A plane x-z obtained slicing the model at the height of y= 6.9 cm;

In this way it was divided the study of the model into the two following possible dispositions of sensors:

- First possible disposition of sensors, composed by the first two cut-planes (z = 35.25 cm and y =11.4 cm);
- Second possible disposition of sensors, composed by the thirth cut-plane (y=6.9 cm).

In the first disposition were considered two different planes for the fact that in the first cut plane there are present the electrics bars referred to the phases R and S but there are not present the T-phase bars.

Therefore, the first option contains two different planes of disposition for the sensors: the first cut-plane for the sensors used for the bars referred to the phases R-S and the second cut-planes for the sensors used in the T-phase bars.

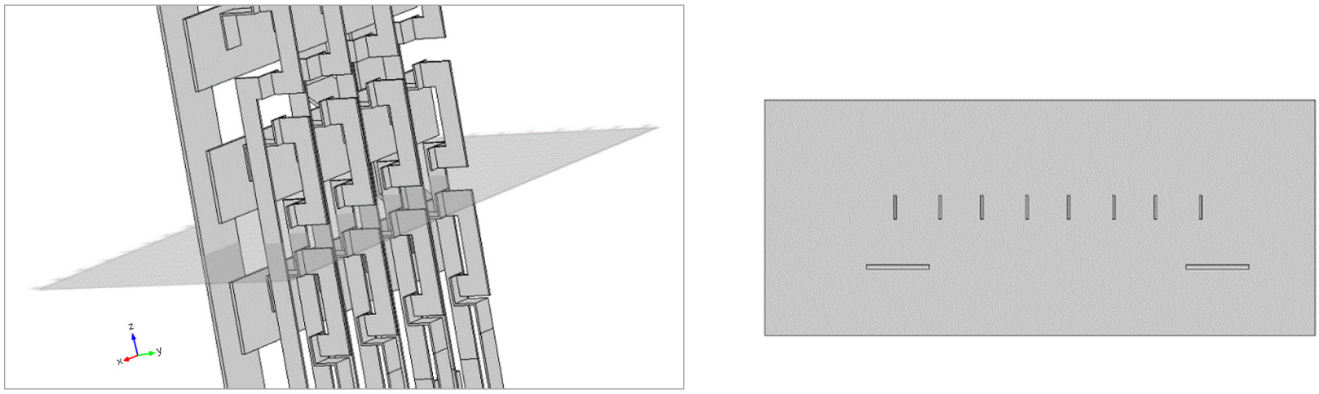

Fig. 7.1 Cut-plane for the R-S bars sensors of the first disposition, 3D and 2D views

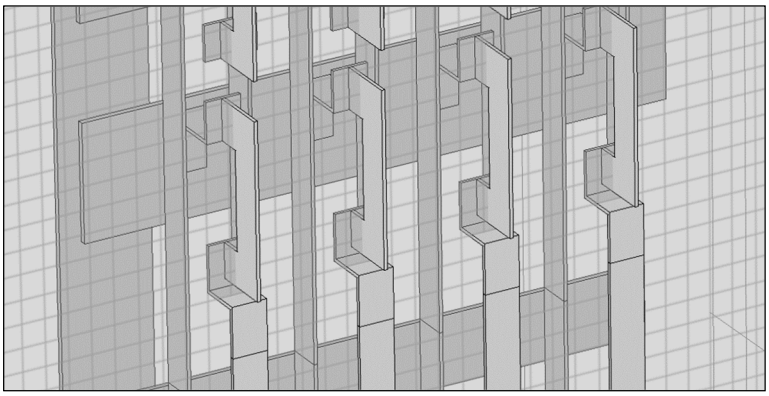

Fig. 7.2 Cut-plane for the T-bars sensors of the first disposition, 3D view

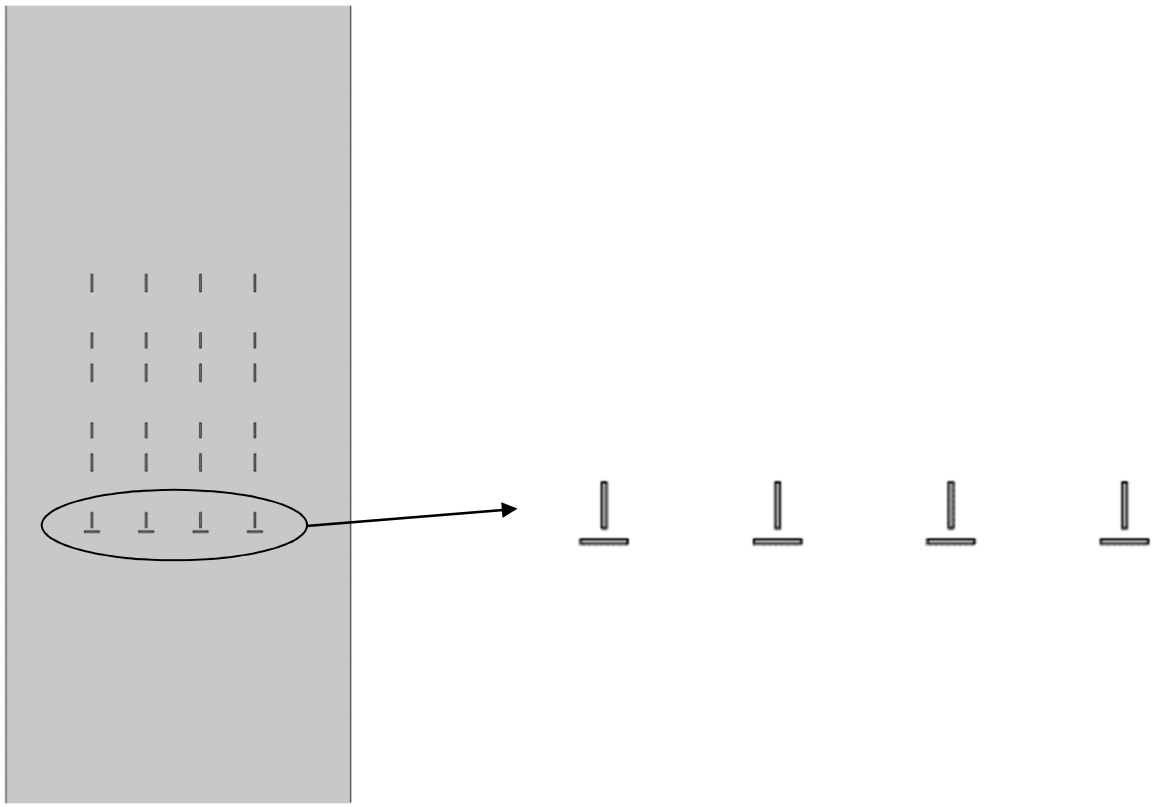

Fig. 7.3 Cut-plane for the T-bars sensors of the first disposition, 3D view.

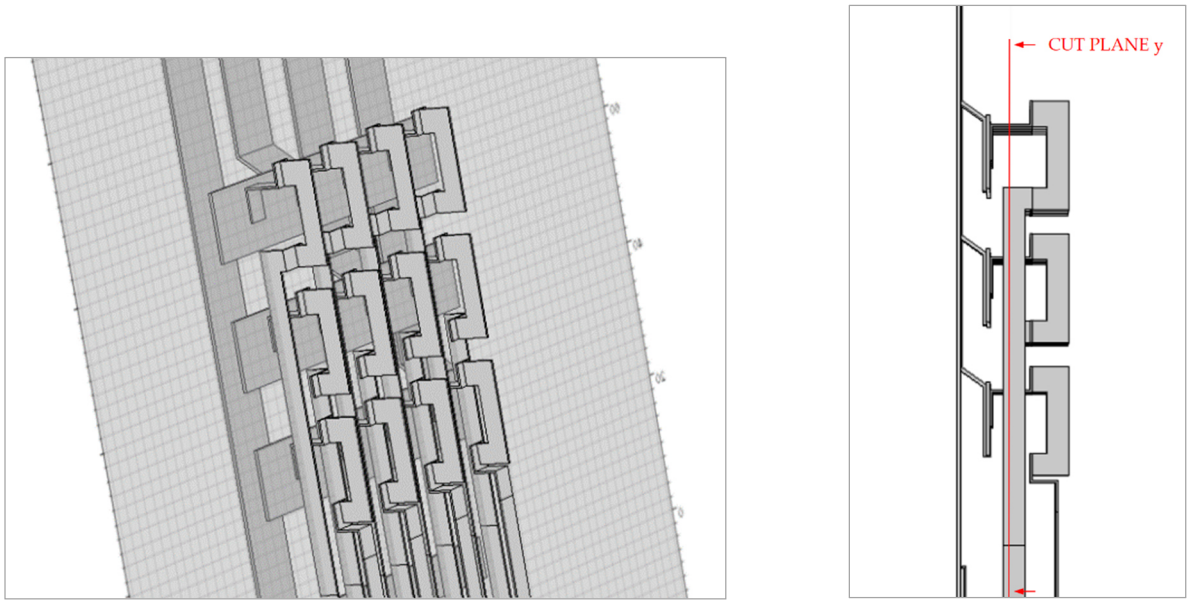

Fig. 7.4 Cut-plane for the second disposition, 3D view

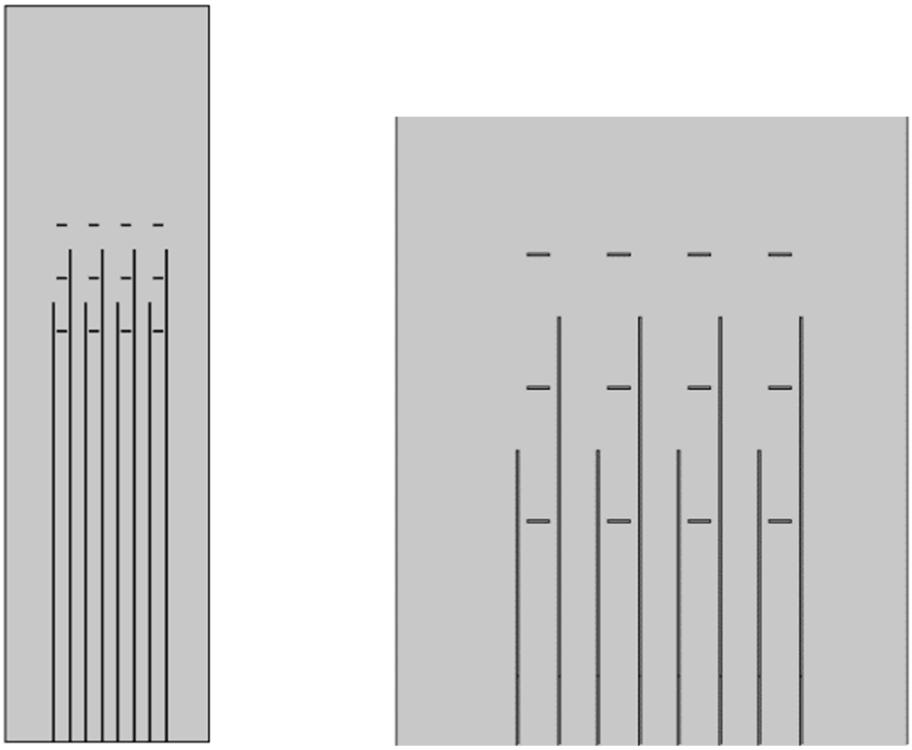

Fig. 7.5 Cut-plane for the second disposition, 2D view

8 POSITIONING OF THE MEASURE POINTS IN THE SIMULATING SOFTWARE

The presence of the sensors, as explained before, was simulated in the simulation model with the use of a virtual tool that allows to measure the MF and its vector components in a given point.

The main steps for the implementation of the measuring points in the 2D cut-plane there have been:

- Consider the position in which it's possible to insert the sensor in the real electric panel, trying to follow a certain physic symmetry;
- Find the site with the lesser distance between the sensors;
- Find out the vector component of the MF more adapt for the measure of the MF in the point taken into consideration in the previous step;
- Make a brief study about the distribution of the MF around the electric bars. This in order to find out the site near the bar that present the higher magnitude of the MF for the vector component taken into consideration;

To explain the principal decisions adopted it is better to divide the problem into the two different cut planes taken into account.

8.1 First possible disposition of measure sensors

The first alternative of sensors disposition, as seen before, is divided into two different cut-planes, one is the cut plane at the height of z=35.25 cm from the point zero and the other one is a cut plane at the high of y= 11.4 cm.

For the first cut-plane it has been chosen to insert all the sensors respecting to a horizontal line with a view to simplify the future installation making it more easy and fast.

For the second cut-plane it was adopted the same criteria of the reference line. For the position site there weren't a lot of alternatives because of the small length of the T bars. Because of this, it was thought to the eventual possibility to cut a small part of plastic for the insertion of one of the two sensors for every circuit.

8.1.1 Disposition of the R-S sensors in the z cut-plane

In the following image are indicated with the black points the points of measure set out in the Comsol Multiphysic simulation, these points represent the positions chosen for the sensors in this plane.

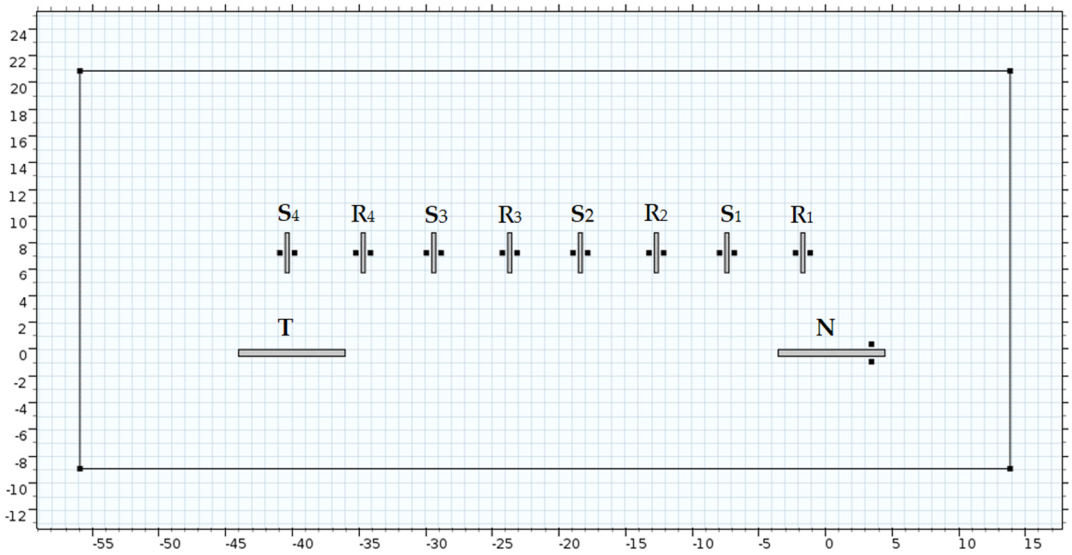

Fig. 8.1 Points of measure in the 2D cut-plane

For the positioning of the points in this plane have been chosen the right and left side of the bars, because in this way it is possible to minimize the distance between the sensors. For the same reason it was chosen to dispose other two points in the upper and lower part of the neutral bar.

After that it was necessary to discover the component of the MF that gave the higher level of MF, this in order not to fall in the future risk to have such a low value of MF to induce in making error caused by the sensibility of the sensors.

For pointed out this it was necessary make some measure in a couple of point near the bars confronting the components $\vec{B}_x$ and $\vec{B}_y$ and picking out the vector component with the higher value.

In the next table are listed some measures made in different points close to the bars and it's possible to observe that for the points 1 and 2 it's preferable to set the Comsol tool for measure the component $\vec{B}_y$ of the field and, on the other hand, for the points 4 and 5 closed to the neutral bar, it's better to make a measure of the $\vec{B}_x$ component of the MF.

Point	$\vec{B}_x$ [μT]	$\vec{B}_y$ [μT]
1	*-24,696*	*248,43*
2	*25,066*	*254,83*
3	*20,87*	*210,01*
4	*-114,81*	*23,361*
5	*-93,254*	*15,795*

Tab. 8.1 Values of different vector components of MF for different points

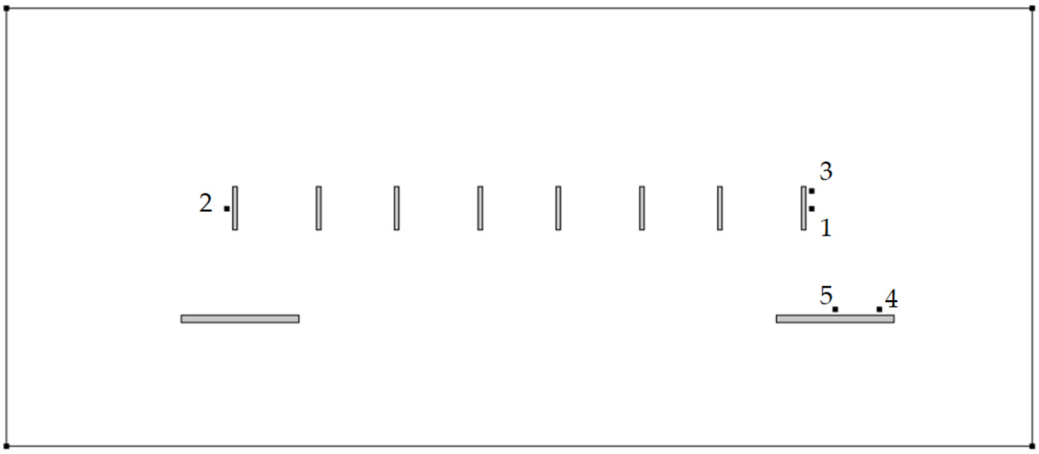

Fig. 8.2 Points of measure referred to the table 8.1

Regarding to the points 3 and 5 they represent other probes made in order to establish the best measuring position around the bars. In fact, with the point 3 have been evaluated the changes in magnitude of the MF respect to the point 1, one more time in the interest to find the higher value of MF and equally for the points 5 and 4.

From the table above it is possible to note that it is preferable to set the measure tools in the points 1 and 4 because of the higher component of the field.

Other important considerations to do are about the choice of the distance of installation between the detectors and the bars. To figure out the best distance it was considered that the sensors can't be installed too close to the bars, because of the heat released by the bars during the normal operation. It was established for this reason a minimum distance of 0,4 cm between all the sensors installed in this project and the bars.

About a possible increase of the distance from 0,4 cm to higher distance first of all is important to note that an increase of the distance between a sensor and a bar means an increase of the distance between the two sensors. This it can cause a following increase of measure errors because are compromised the initial hypothesis for the elimination of the external magnetic field.

Another concept to take in mind is that moving with the sensor away to the bars implies a decrease of the magnitude of MF monitored by the detectors. To avoid this, there have been made some tests in order to figure out the best configuration of installation.

One of the tests was made with the bar of the phase R1 shows in the next image. In this case were considered the points 1 and 2 situated at a distance of 0,4 cm from the bar and the point 3 and 4 at a distance of 1 cm.

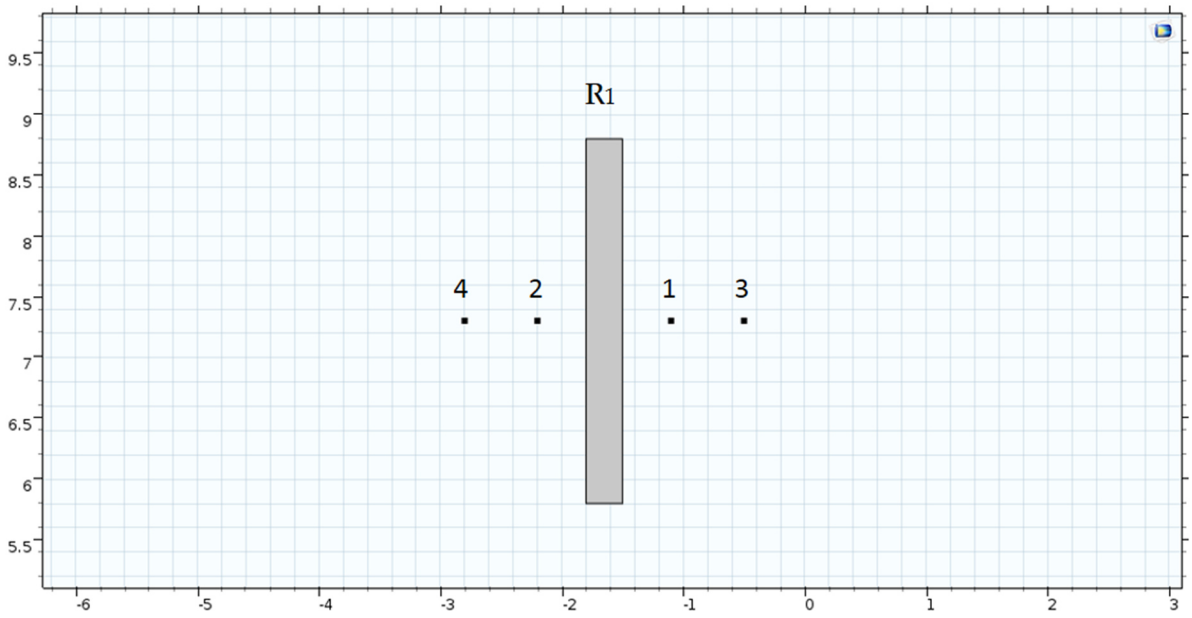

Fig. 8.3 Points of measure referred to the table 8.2

As can be seen in the next table, for the point 1 and 2, more close to the bar, it can be detected a higher magnitude of MF and so these points are preferable in order to reduce the possible errors.

Point	$\vec{B}_y$ [μT]
1	*166.93*
2	*157.09*
3	*127.25*
4	*117.58*

Tab. 8.2 Values of $\vec{B}_y$ referred to the points in the fig. 8.3

In the next figures are illustrated some graphical solution, obtained with the simulation in the Comsol model, that confirms the reasons of the choices just explained.

The simulations have been computed feeding the bars with an input current of 10[A].

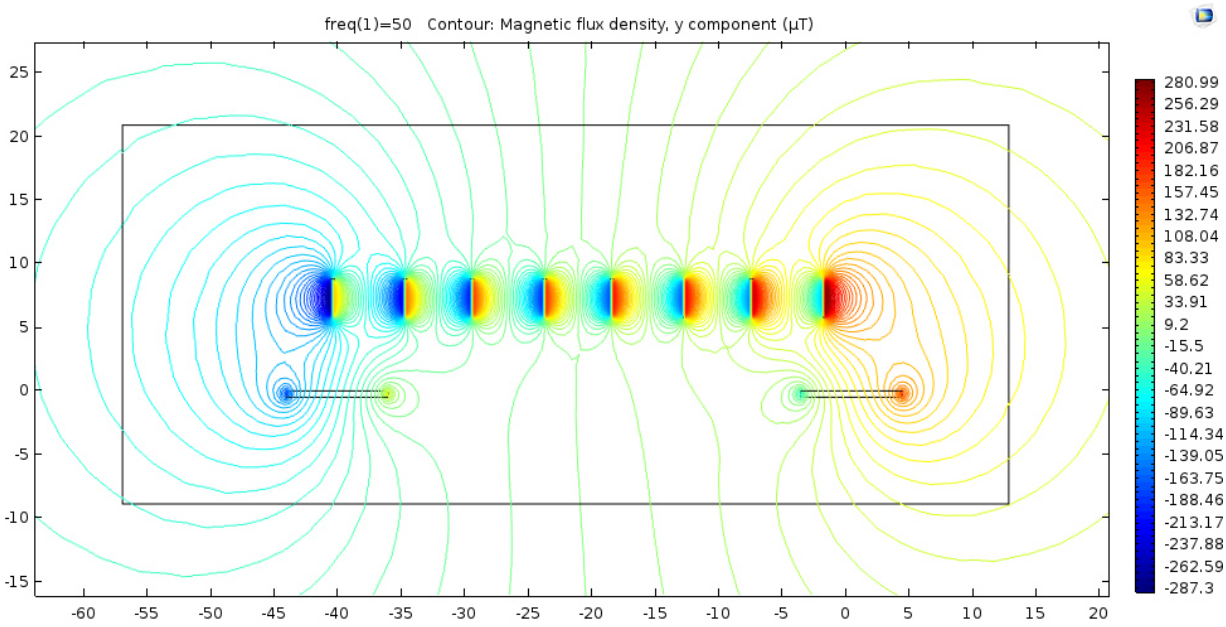

Fig. 8.4 Magnetic flux density considering only the y component of the MF, input current: 10 A.

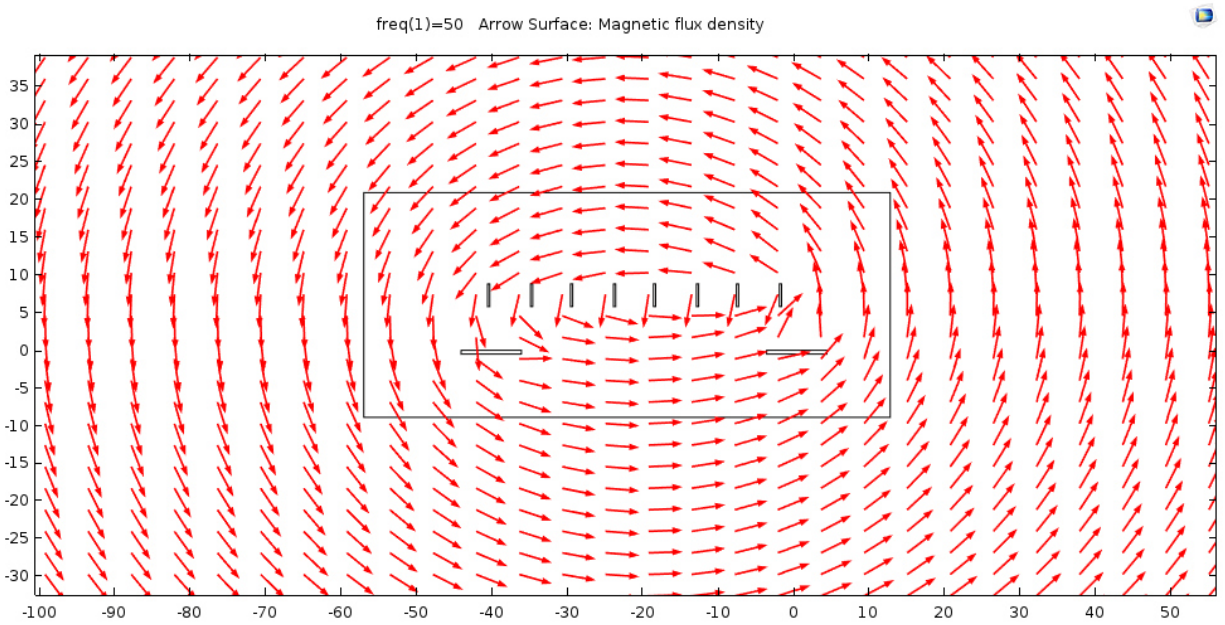

Fig. 8.5 Magnetic flux density considering only the y component of the MF, input current: 10 A.

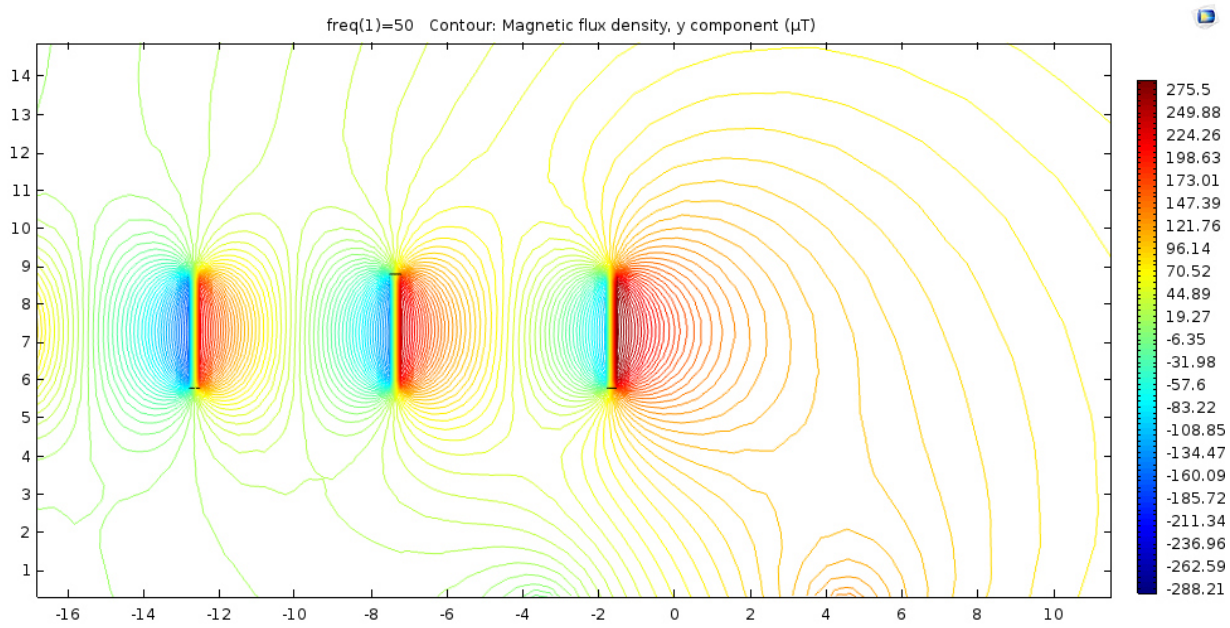

Fig. 8.6 Magnetic flux density of the phases R1, S1, R2 considering only the y component of the MF, input current: 10 A.

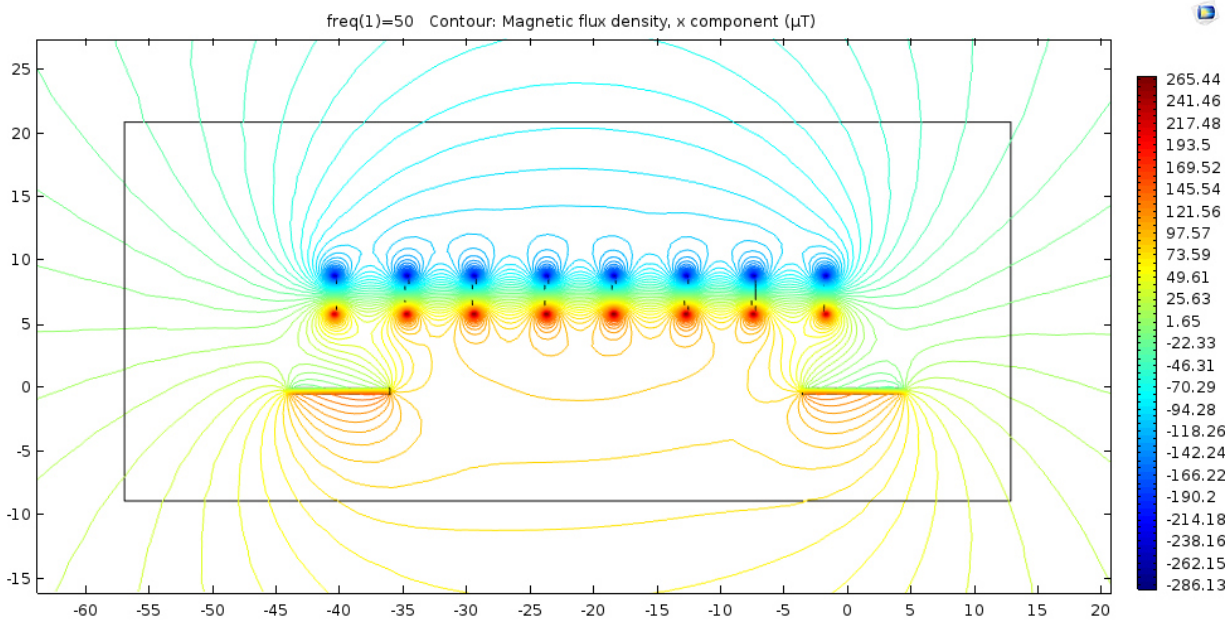

Fig. 8.7 Magnetic flux density considering only the x component of the MF, input current: 10 A.

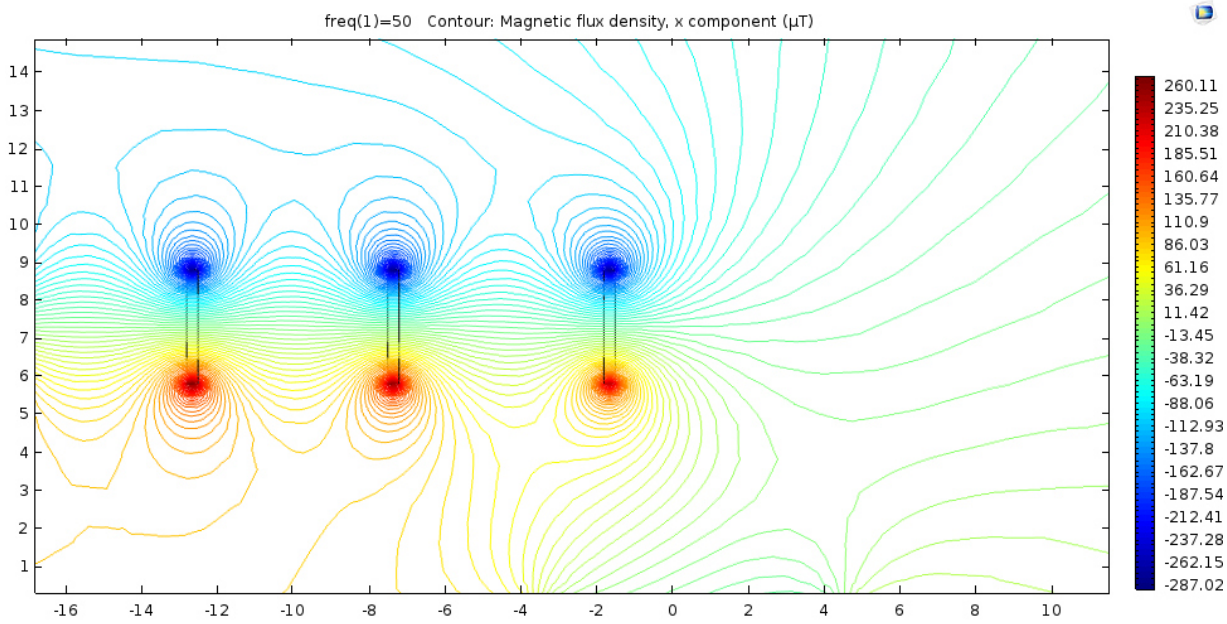

Fig. 8.8 Magnetic flux density of the phases R1, S1, R2 considering only the x component of the MF, input current: 10 A.

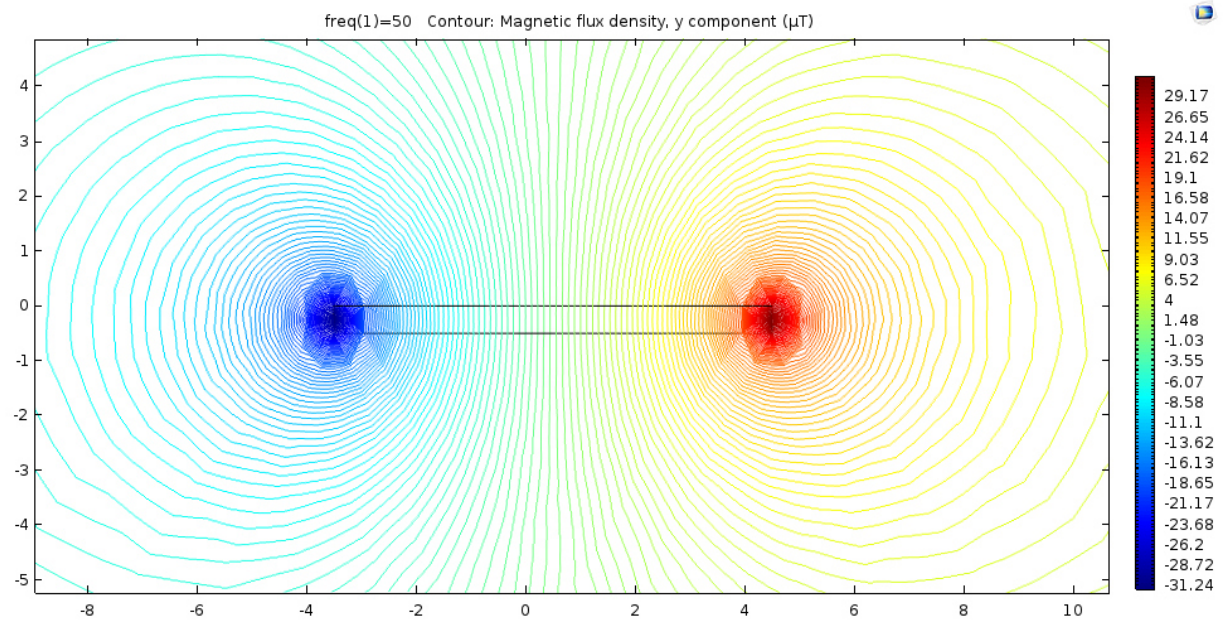

Fig. 8.9 Magnetic flux density of the neutral bar considering only the y component of the MF, input current: 10 A.

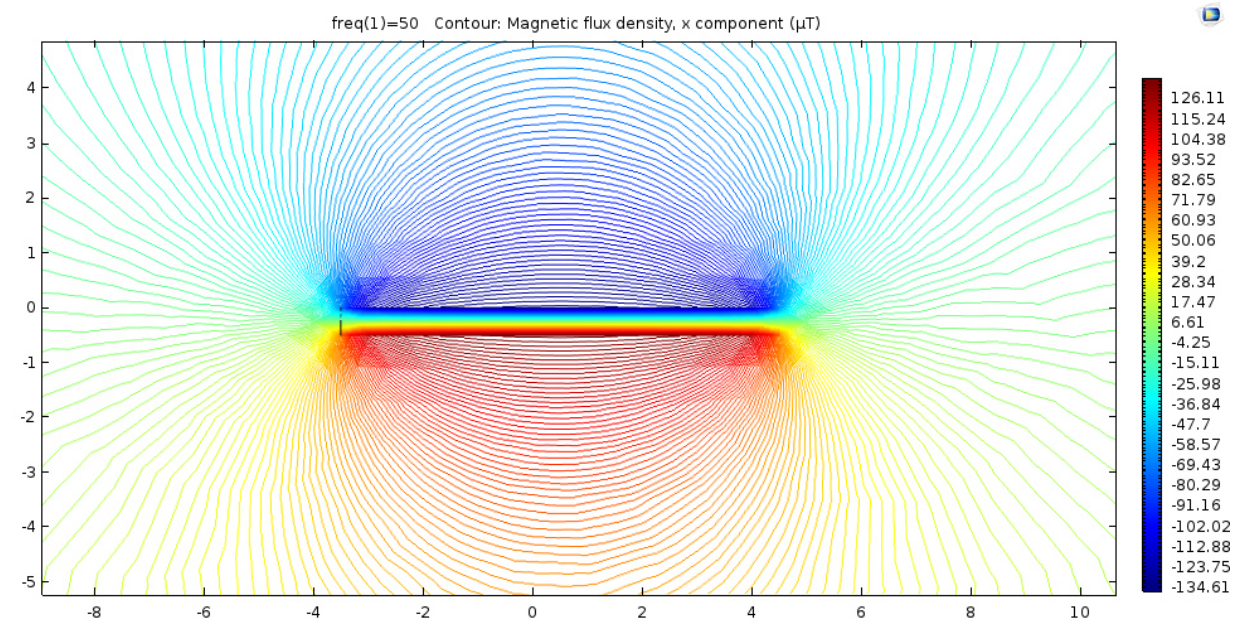

Fig. 8.10 Magnetic flux density of the neutral bar considering only the y component of the MF, input current: 10 A.

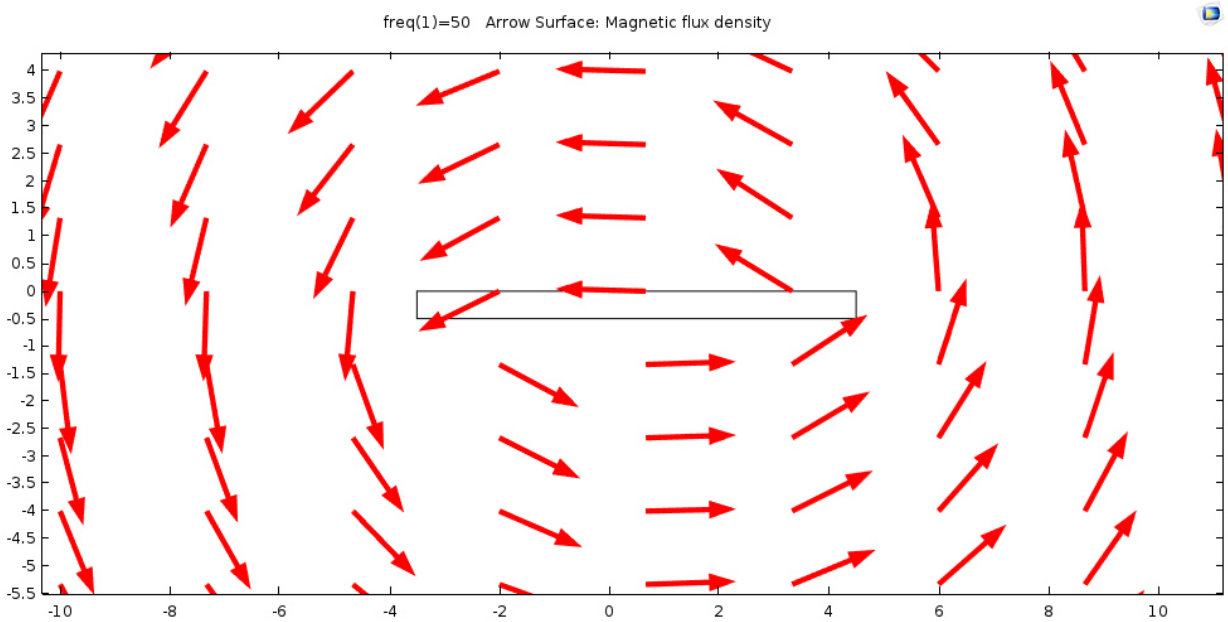

Fig. 8.11 Direction of the Magnetic flux density of the neutral bar considering the x and y component of the MF, input current: 10 A

8.1.2 Disposition of the T sensors in the y cut-plane

For the disposition of the sensors T have been done the same steps of the previous case, in order to reach a good level of measure for the points in consideration.

In this case the distribution of the sensors in the cut-plane is the following:

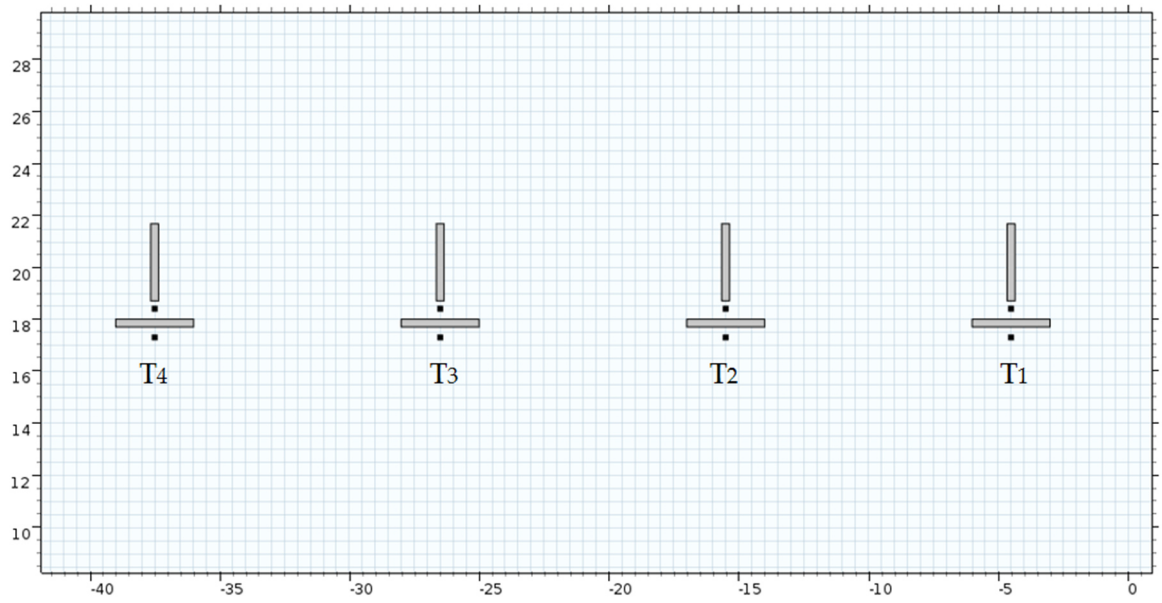

Fig. 8.12 Points of measure in the 2D cut-plane

Considering that a sensor has a size around to 1.5×1.5 [cm] and the electric bars have a width of 3 cm there was not a lot of space to change the position of the sensors.

For this reason, it was preferred to facilitate the installation inserting the sensors in the middle of the bars, taking advantage to the fact that there wasn't a big difference between the measures taken in the central position and in the lateral position.

The next step, as in the previous cut-plane, it was find out the best vector component of MF to use for the MF monitoring.

In order to do this there were considered the points selected in the next image for the bars T1 and T2 and were compared the results for the components $\vec{B}_x$ and $\vec{B}_y$ shown in the table [1].

The final choice was to consider the *x* vector component for the measures, this because this component had the higher magnitude of MF.

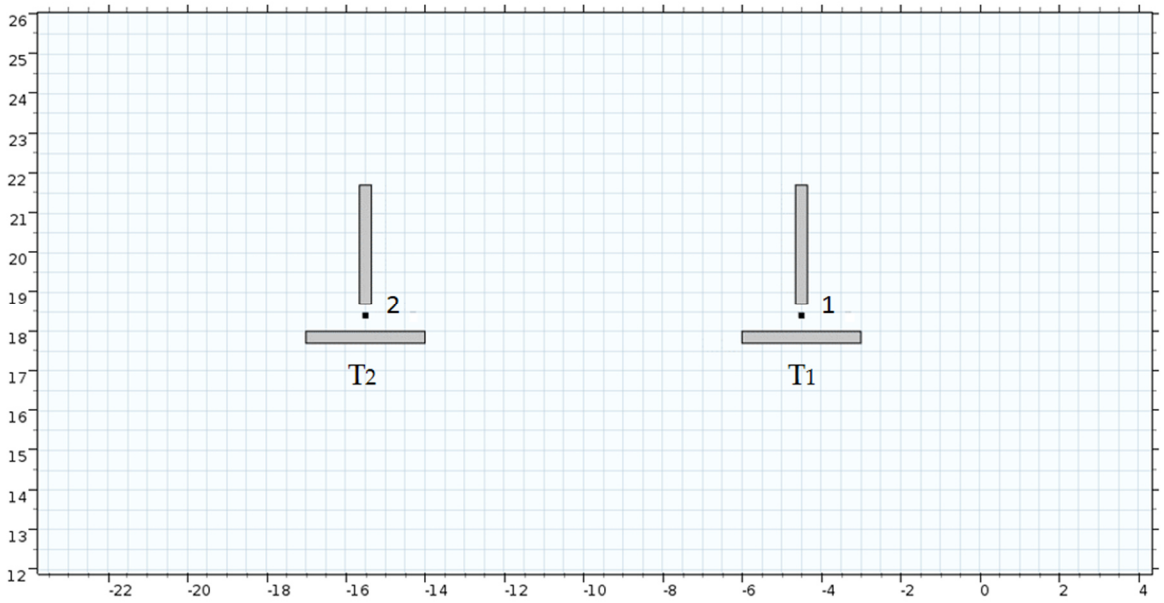

Fig. 8.13 Points of measure referred to the table 8.2

Point	$\vec{B}x$ [μT]	$\vec{B}y$ [μT]
1	*-296.57*	*19.769*
2	*-293.06*	*6.7005*

Tab. 8.3 Values of $\vec{B}_y$ referred to the points in the fig. 8.13

In the next figures are illustrated some graphical solutions, obtained with the simulations in the Comsol model, that confirms the reasons just explained.

The simulations have been computed feeding the bars with an input current of 10[A].

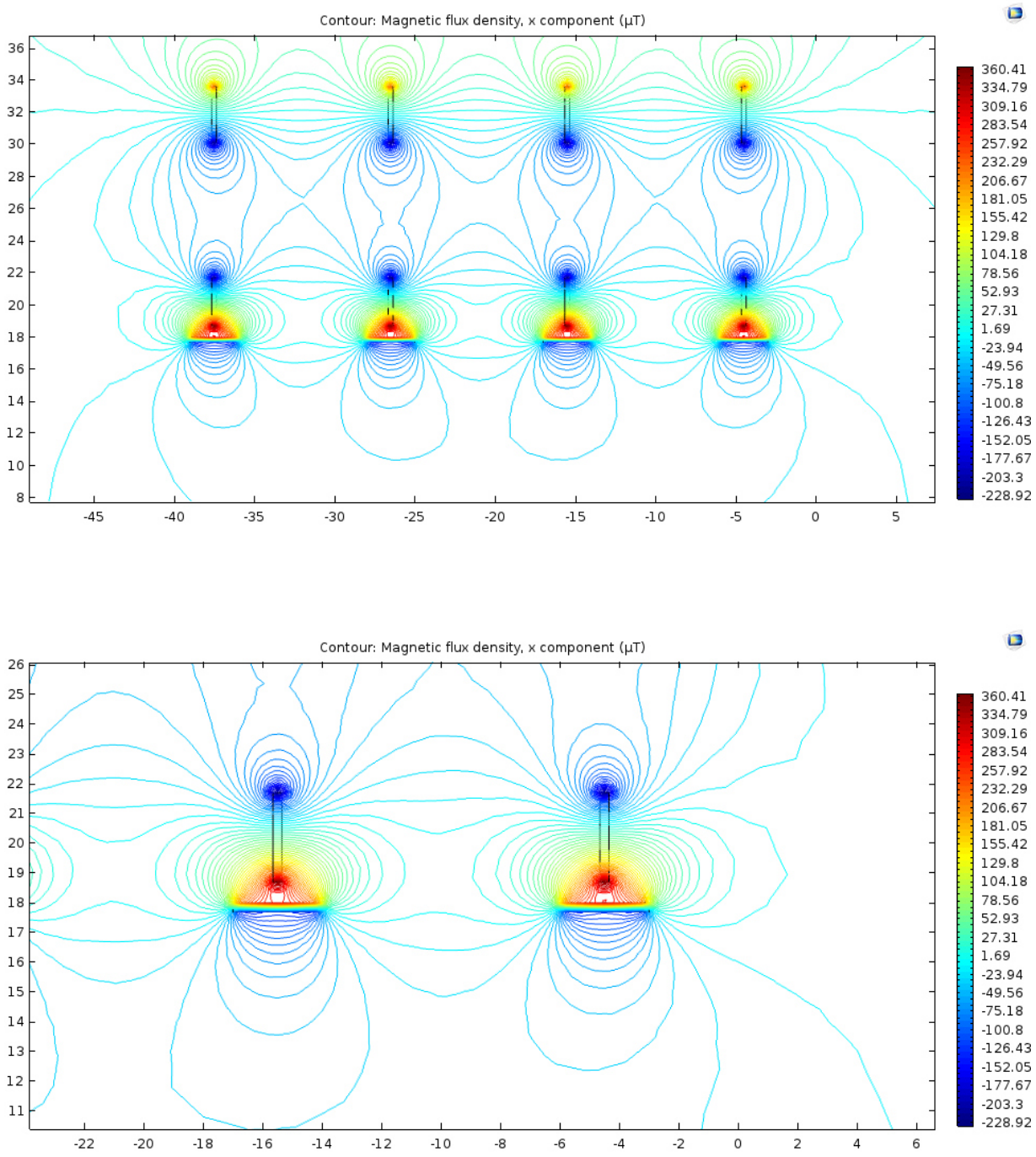

Fig. 8.14 Magnetic flux density of the phases T considering only the x component of the MF, input current: 10 A.

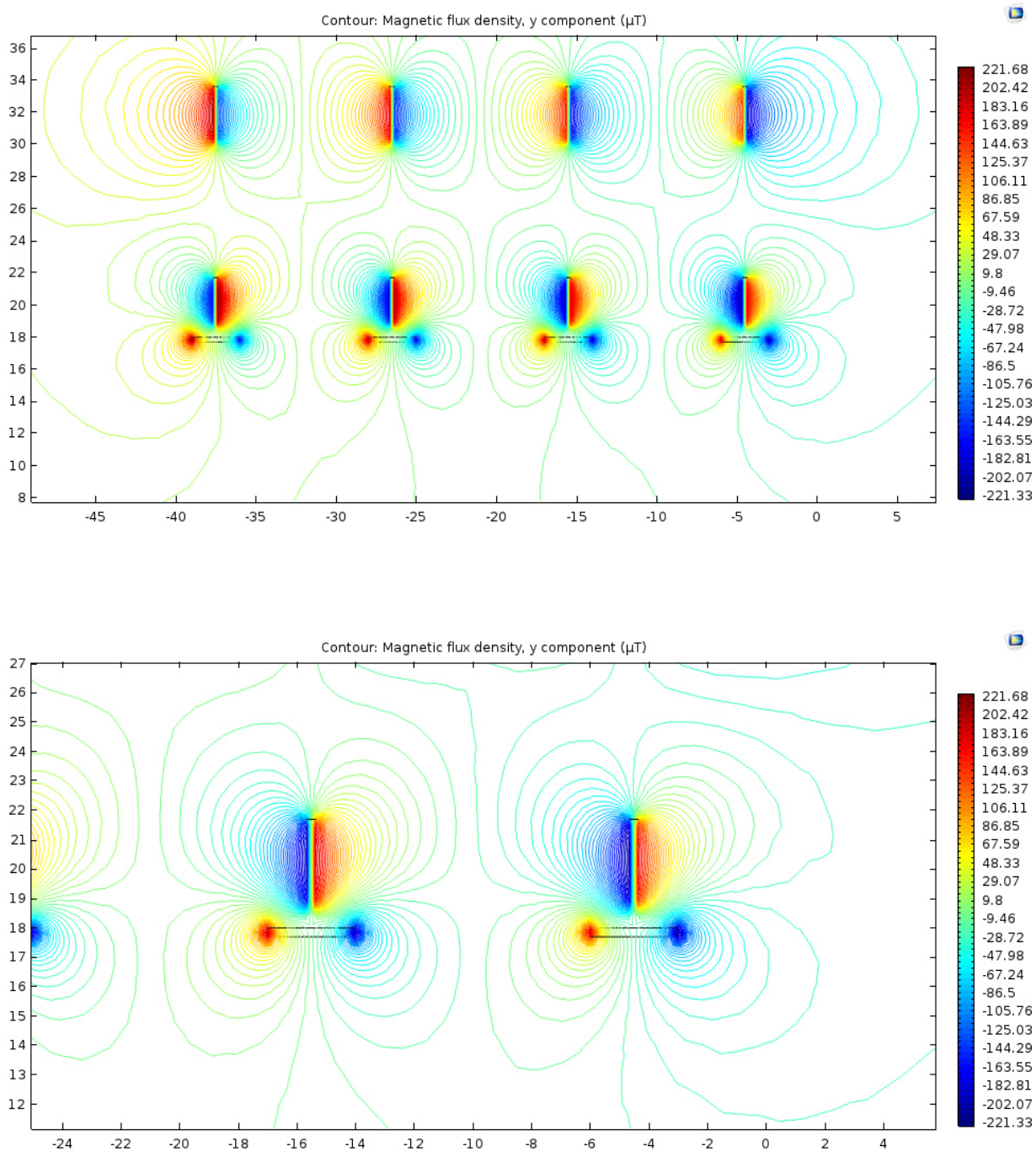

Fig. 8.15 Magnetic flux density of the phases T considering only the y component of the MF, input current: 10 A.

8.1.3 Final position of the sensors in the 3D model

- **Cut plane z**

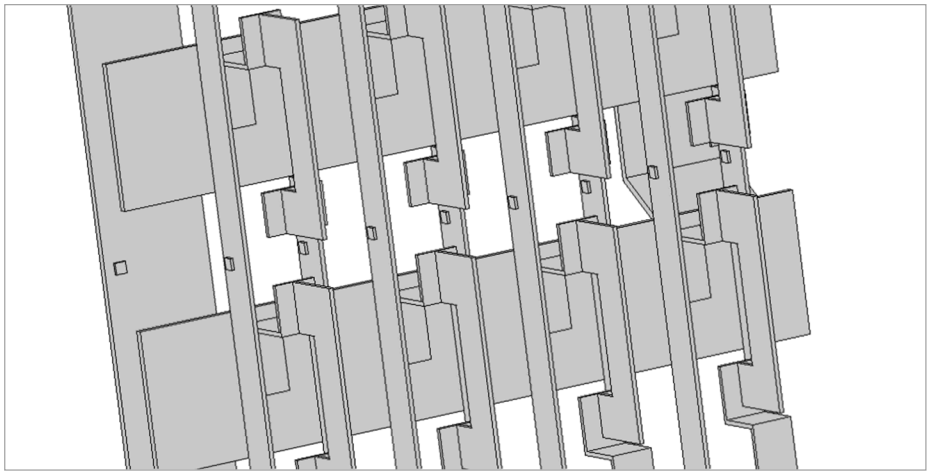

Fig. 8.16 Position of the sensor for the cut-plane z

Fig. 8.17 Position of the sensor for the cut-plane z

Fig. 8.18 Settings of the sensors adopted in order to delete the stray MFs contribution

- **Cut-plane y**

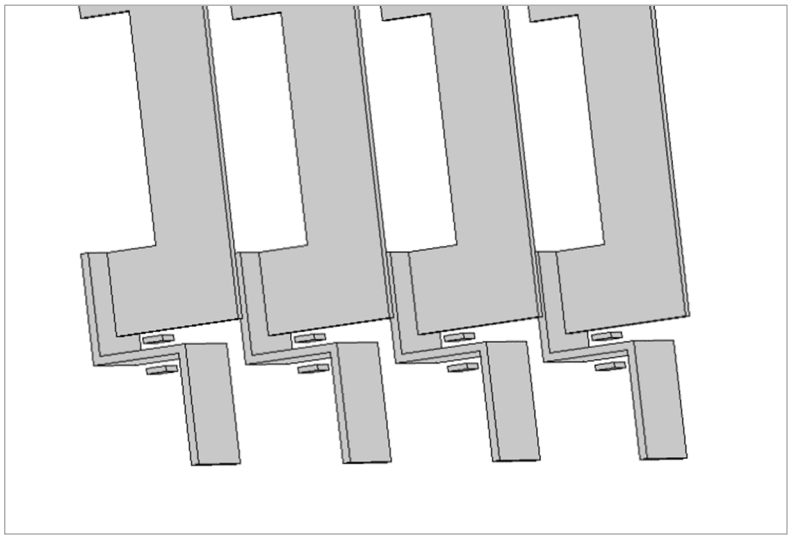

Fig. 8.19 Position of the sensor for the cut-plane y

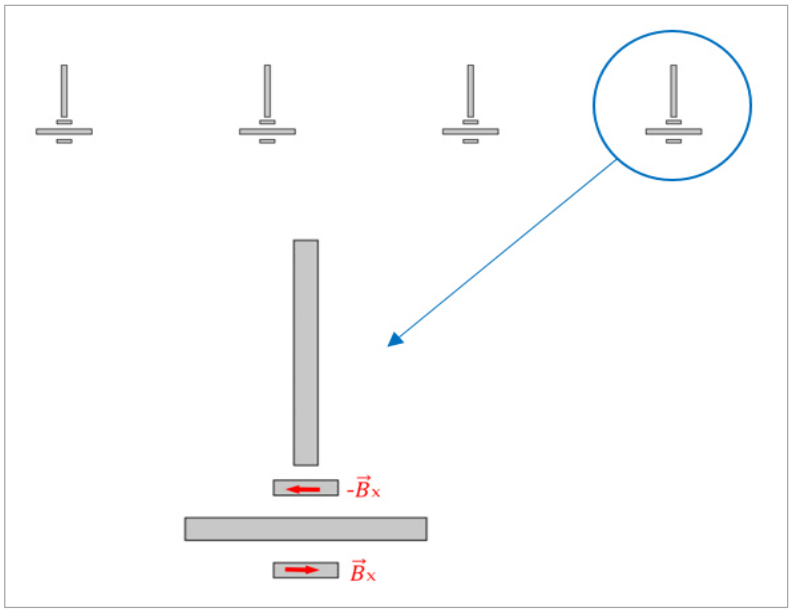

Fig. 8.20 Settings of the sensors adopted in order to delete the stray MFs contribution

8.2 Second possible disposition of measure sensors

The cut plane adopted for the second disposition of sensors is obtained cutting the 3D model with a plane parallel to the y-axis, at the height of y=6,9 cm. This cut-plane permits to considerate all the phases of all the circuit in a single plane and so presents the advantages to simplify and focus the 2D study in a single simulation.

In the same way of the first cut-plane it has been chosen to insert all the sensors respecting to a horizontal line in order to simplify the future installation. This despite to the fact that it will be necessary make certain changes to the electric panel cutting some plastic parts for the installation of one of the two sensor for every bar.

In the following image there are indicated the points of measure set out in the Comsol Multiphysic simulation, these points represent the positions of the sensors chosen for this plane.

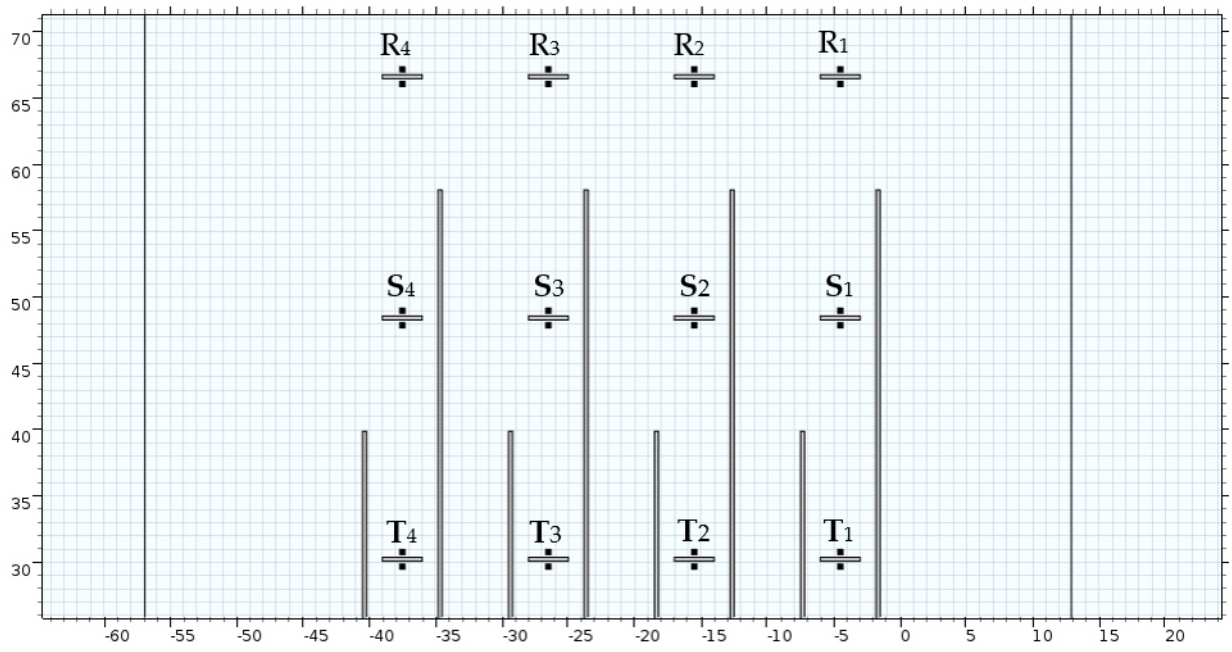

Fig. 8.21 Points of measure in the 2D cut-plane

For the setting of the sensor there have been taken the same steps done in the previous cases, in order to reach a good level of measure for the points in consideration.

As explained in the previous paragraph, considering that a sensor has a size around to 1.5×1.5 [cm] and the electric bars have a width of 3 cm there was not a lot of space to change the position of the sensors.

For this reason, it was preferred to facilitate the installation inserting the sensors in the middle of the bars, taking advantage to the fact that there wasn't a big difference between the measures taken in the central position and in the lateral position.

The next step, as in the previous cut-plane, it was find out the best vector component of MF to use for the MF monitoring.

In order to do this there were considered the points selected in the next image for the bars R2, S2, T2 and were compared the results for the components $\vec{B}_x$ and $\vec{B}_y$ shown in the table [1].

The final choice was to consider the *x* vector component of MF for the measures, this because this component had the higher magnitude of MF.

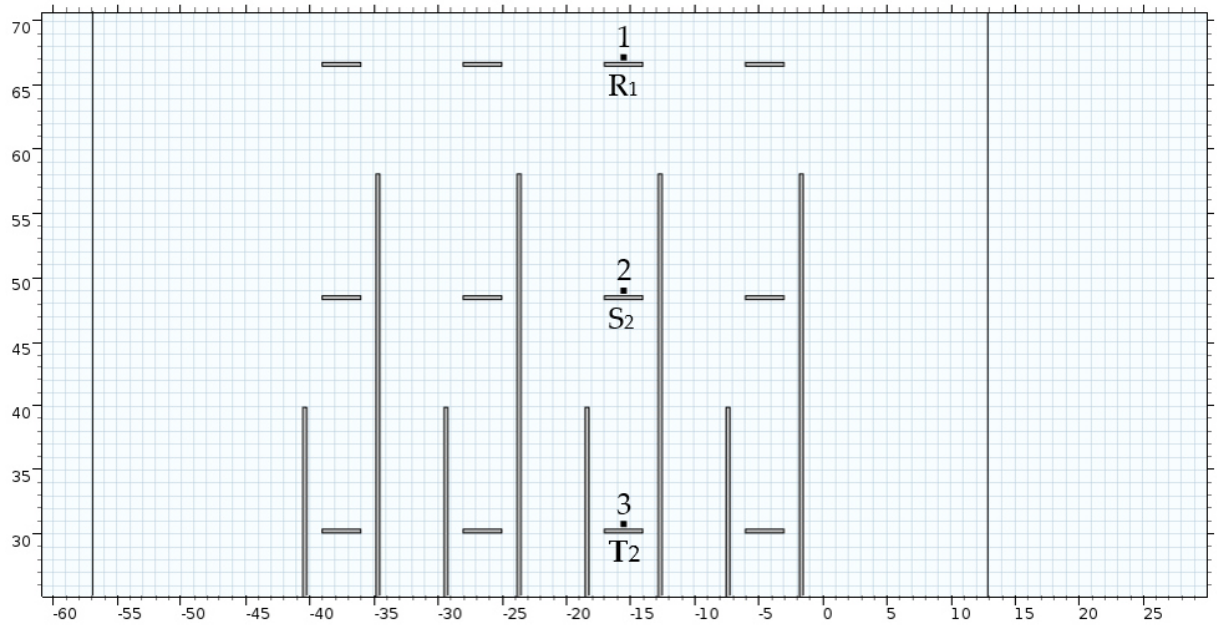

Fig. 8.22 Points of measure referred to the table 8.2

Point	$\vec{B}$x [μT]	$\vec{B}$y [μT]
1	*-221.11*	*16.345*
2	*-168.72*	*19.587*
3	*-117.08*	*16.863*

Tab. 8.4 Values of $\vec{B}_y$ referred to the points in the fig. 8.3

In the next figures are illustrated some graphical solutions, obtained with the simulations in the Comsol model, that confirms the reasons just explained.

An important consideration to consider is that the vertical bars presented in the images, that are the bars R-S presented in the model and cut by the cut-plane, have not been considered in the measures. This because the respective MF produced by that bars don't influence the vector component *x* of the MF.

For this reason, they have been considerate made of air and so not considerate as active in the model simulation

The simulations have been computed feeding the bars with an input current of 10[A].

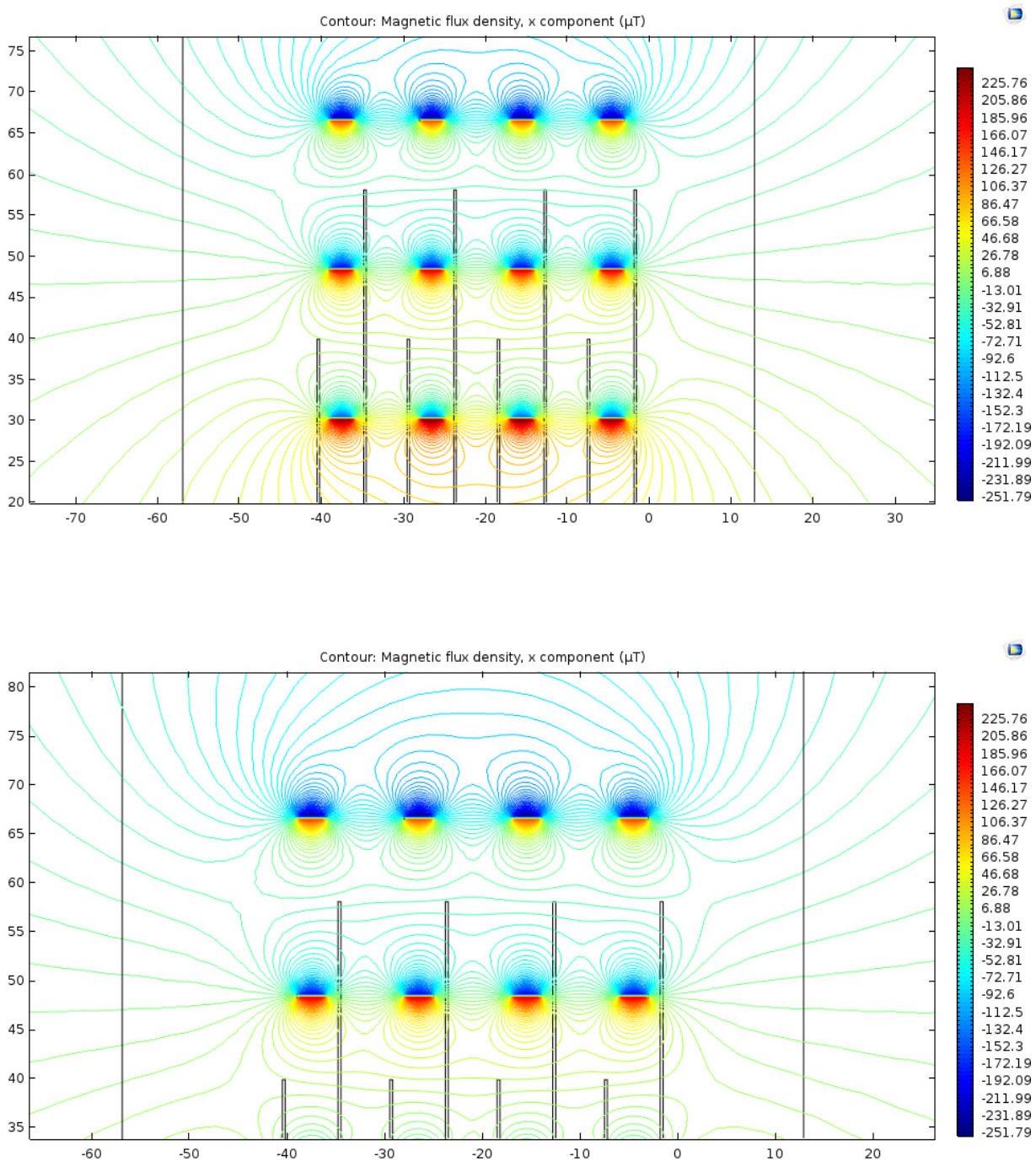

Fig. 8.23 Magnetic flux density considering only the x component of the MF, input current: 10 A.

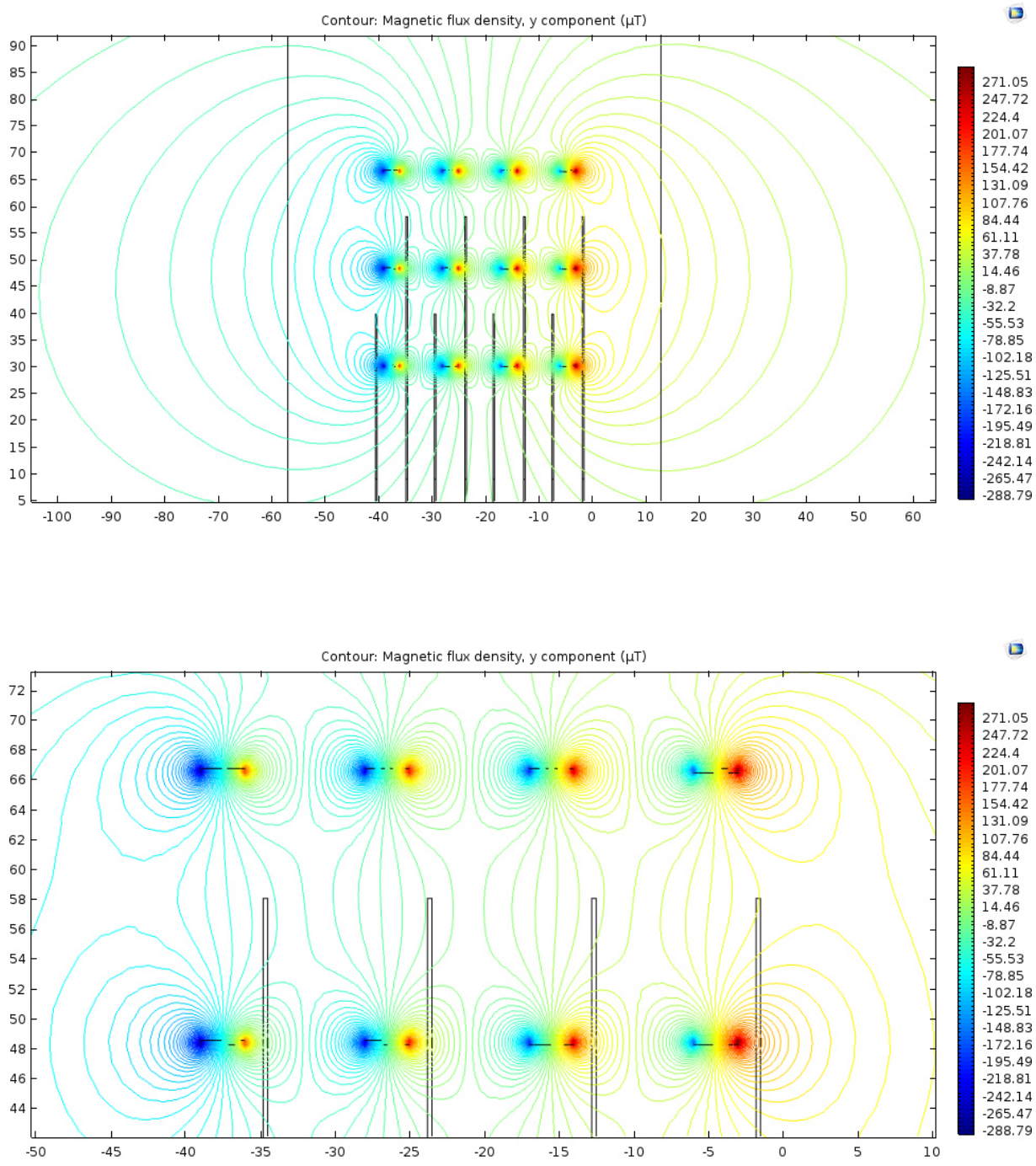

Fig. 8.24 Magnetic flux density considering only the y component of the MF, input current: 10 A.

8.3 Final position of the sensors in the 3D model

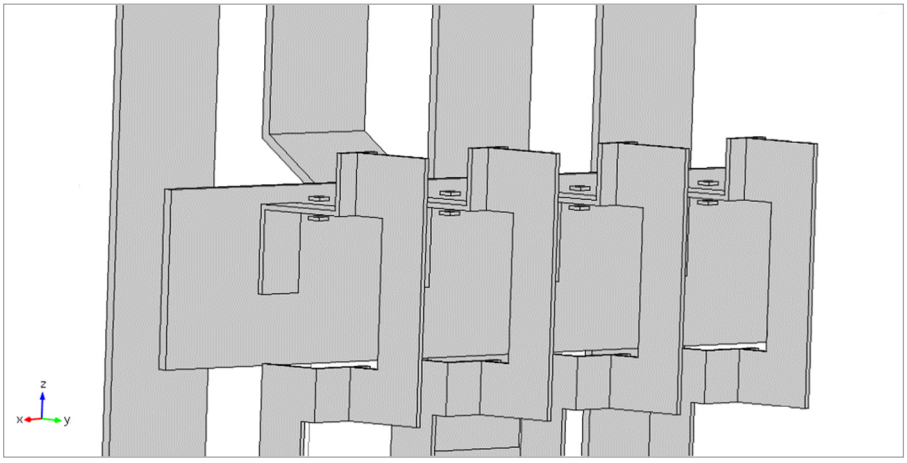

Fig. 8.25 Position of the sensor installed for the phase R

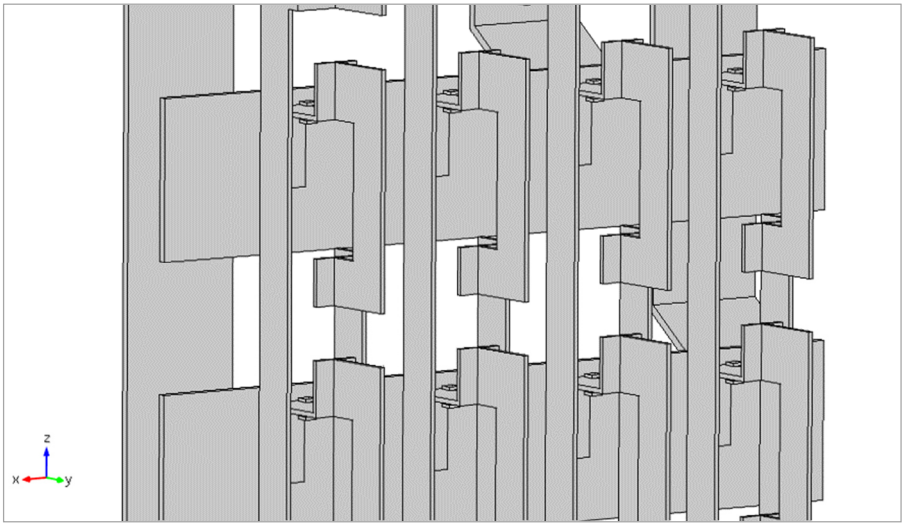

Fig. 8.26 Position of the sensor installed for the phases R and S

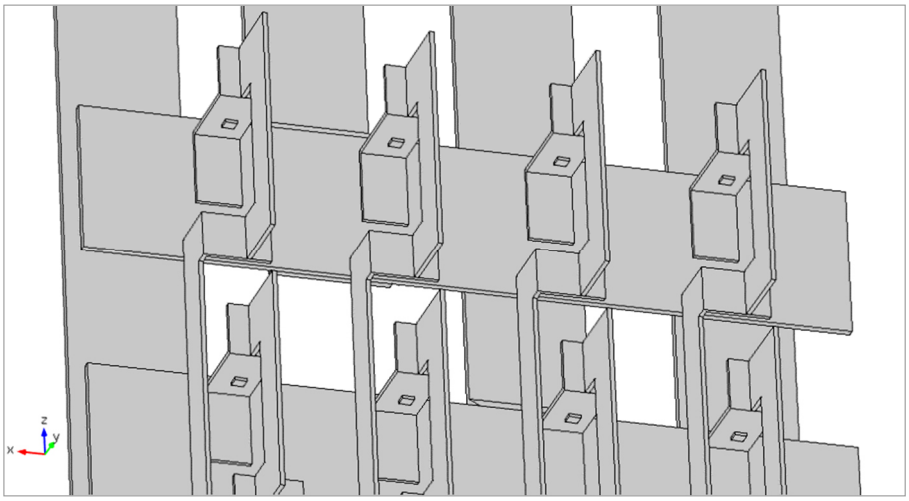

Fig. 8.27 Position of the sensor installed for the phases R and S

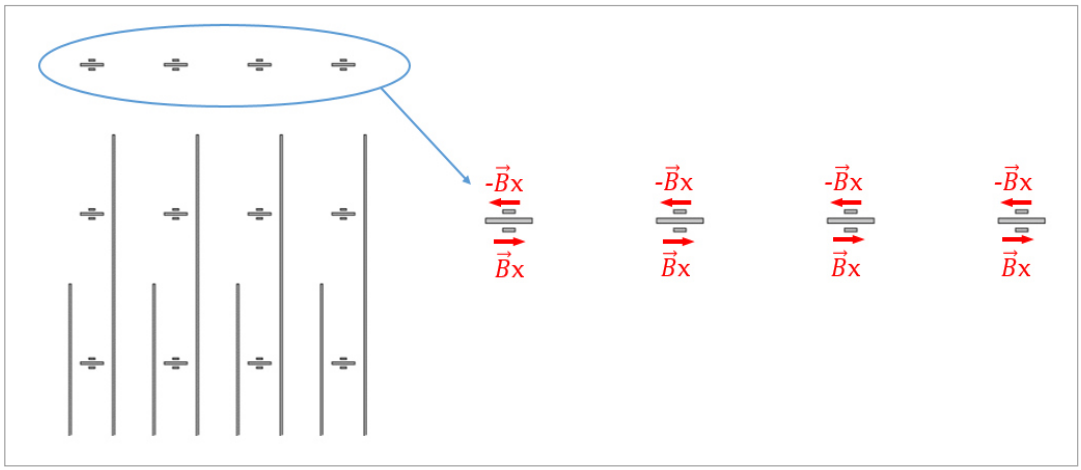

Fig. 8.28 Settings of the sensors adopted in order to delete the stray MFs contribution

9 DERIVATION OF THE VALUE OF CURRENT

In this section of the document are explained the principle steps and ideas that lead to obtain a functional automatization for the indirect monitoring of current, in every temporal instant, through the use of the MF sensors installed in the electric panel.

For first, it's important to think that the sensors in question will have to work in the temporal domain, because the electric panel will be subject to an alternative current with a frequency of 50 Hz.

For this reason, it is now important to leave the stationary domain, used for the previously probes, and move to the temporal domain in order to analyse the trend of MF measured in a temporal period. This measure will allow to know, consequently, the trend of the current flowing in every circuit that it's the purpose of the project.

Stepping back to the simulating model in Comsol it is important to remember the development of the MF in the space it's produced by the flow of a current and that current was set like an input, in order to obtain an estimation of the MF.

On the other point of view, it's important to note that in the really working of the systems that is being created is necessary to do almost the opposite, i.e. measure a Magnetic field in order to obtain the value of electric current flowing in every circuit.

At this point it is possible to realize that there is a connection between the measured MF and the input current. Once this relationship has been found, it's easy to recalculate the input current, having only the MF values and the relationship found.

9.1 Implementation of the matrix $[K]$

To find the relationship between the MF and the input current it was necessary to make a study in the steady-state of the temporal domain. This, in order to find a coefficient that could represents the relationship between the two know terms, ensuring also that this relation could be valid and constant in the temporal domain.

Writing the searched relationship in physics terms we will have this equation expressed as a function of time:

(1.9) $$\vec{B}(t) = k \cdot \vec{I}(t)$$

where K is the constant that represent the relationship between the MF measured $\vec{B}(t)$ and the input current in the domain of time $\vec{I}(t)$.

First of all, to simplify the problem, it has been tried to find this constant in the stationary domain by imposing the time equal to zero and obtaining:

(1.10) $$\vec{B}(t) = k \cdot \vec{I}(t) \qquad t = 0$$

$$\vec{B}(0) = k \cdot \vec{I}(0)$$

(1.11) $$\vec{B} = k \cdot \vec{I}$$

Now the only thing to do it's to find the value of *k* taking in consideration that $\vec{B}$ and $\vec{I}$ are known terms and also assure that the value of *k* remains valid and constant for different input currents.

Once obtained the constant *k* it is possible to use this constant in the cases in which $\vec{B}$ is a known term and $\vec{I}$ is unknown.

With the purpose of find the constant *k*, in the Comsol model has been imposed an input current for every bar of 1[A]. Subsequently it was used a sort of superposition principle in which it was considerate the effect caused by the supply of every bar in the measures of the sensors.

To apply the superposition principle there have been fed the bars one by one and it has been considered, for a determined bar, the sum of the measures taken with its two sensors. This in order to figure out the value of MF measured by a determinate couple of sensors installed in a bar, for every single bar fed.

In the end, every single value measured represents the constant term that we are looking for.

Considering the fact that we need to monitor the current that flows through every bar of every circuit it's convenient to group every result in a matrix, to simplify the management of the results.

This matrix will be named $[K]$ and will be formed by a number of single elements *k*, every row of the matrix it's referred to the sensors considered for the measure and every column is referred to the active bar fed. Therefore, every element *k* will be defined according to the sensor and the powered phase taken into consideration.

A generic representation of the matrix $[K]$ can be represented in the next page:

(1.12)

$$\left[\vec{B}\right] = \left[K\right] \cdot \left[\vec{I}\right]$$

$$\begin{bmatrix} B_{R1} \\ B_{S1} \\ B_{T1} \\ B_{R2} \\ B_{S2} \\ B_{T2} \\ B_{R3} \\ B_{S3} \\ B_{T3} \\ B_{R4} \\ B_{S4} \\ B_{T4} \end{bmatrix} = \begin{bmatrix} K_{R1R1} & K_{R1S1} & K_{R1T1} & K_{R1R2} & K_{R1S2} & K_{R1T2} & K_{R1R3} & K_{R1S3} & K_{R1T3} & K_{R1R4} & K_{R1S4} & K_{R1T4} \\ K_{S1R1} & K_{S1S1} & K_{S1T1} & K_{S1R2} & K_{S1S2} & K_{S1T2} & K_{S1R3} & K_{S1S3} & K_{S1T3} & K_{S1R4} & K_{S1S4} & K_{S1T4} \\ K_{T1R1} & K_{T1S1} & K_{T1T1} & K_{T1R2} & K_{T1S2} & K_{T1T2} & K_{T1R3} & K_{T1S3} & K_{T1T3} & K_{T1R4} & K_{T1S4} & K_{T1T4} \\ K_{R2R1} & K_{R2S1} & K_{R2T1} & K_{R2R2} & K_{R2S2} & K_{R2T2} & K_{R2R3} & K_{R2S3} & K_{R2T3} & K_{R2R4} & K_{R2S4} & K_{R2T4} \\ K_{S2R1} & K_{S2S1} & K_{S2T1} & K_{S2R2} & K_{S2S2} & K_{S2T2} & K_{S2R3} & K_{S2S3} & K_{S2T3} & K_{S2R4} & K_{S2S4} & K_{S2T4} \\ K_{T2R1} & K_{T2S1} & K_{T2T1} & K_{T2R2} & K_{T2S2} & K_{T2T2} & K_{T2R3} & K_{T2S3} & K_{T2T3} & K_{T2R4} & K_{T2S4} & K_{T2T4} \\ K_{R3R1} & K_{R3S1} & K_{R3T1} & K_{R3R2} & K_{R3S2} & K_{R3T2} & K_{R3R3} & K_{R3S3} & K_{R3T3} & K_{R3R4} & K_{R3S4} & K_{R3T4} \\ K_{S3R1} & K_{S3S1} & K_{S3T1} & K_{S3R2} & K_{S3S2} & K_{S3T2} & K_{S3R3} & K_{S3S3} & K_{S3T3} & K_{S3R4} & K_{S3S4} & K_{S3T4} \\ K_{T3R1} & K_{T3S1} & K_{T3T1} & K_{T3R2} & K_{T3S2} & K_{T3T2} & K_{T3R3} & K_{T3S3} & K_{T3T3} & K_{T3R4} & K_{T3S4} & K_{T3T4} \\ K_{R4R1} & K_{R4S1} & K_{R4T1} & K_{R4R2} & K_{R4S2} & K_{R4T2} & K_{R4R3} & K_{R4S3} & K_{R4T3} & K_{R4R4} & K_{R4S4} & K_{R4T4} \\ K_{S4R1} & K_{S4S1} & K_{S4T1} & K_{S4R2} & K_{S4S2} & K_{S4T2} & K_{S4R3} & K_{S4S3} & K_{S4T3} & K_{S4R4} & K_{S4S4} & K_{S4T4} \\ K_{T4R1} & K_{T4S1} & K_{T4T1} & K_{T4R2} & K_{T4S2} & K_{T4T2} & K_{T4R3} & K_{T4S3} & K_{T4T3} & K_{T4R4} & K_{T4S4} & K_{T4T4} \end{bmatrix} \begin{bmatrix} I_{R1} \\ I_{S1} \\ I_{T1} \\ I_{R2} \\ I_{S2} \\ I_{T2} \\ I_{R3} \\ I_{S3} \\ I_{T3} \\ I_{R4} \\ I_{S4} \\ I_{T4} \end{bmatrix}$$

Where the first array contains the values of MF measured by the sensors installed in the bars from R_1 to T_4 when all the bars of the circuits are powered with a current of 1[A] and the last array represents all the input currents of the bars.

For the arrays $\left[\vec{B}\right]$ and $\left[\vec{I}\right]$ the first subscript denotes the phase of the bar taken into account and the second denotes the circuit considered (e.g. for B_{R1}, R denote the bar corresponding to the phase R and 1 denotes the first circuit).

For the matrix $\left[K\right]$ is the same and also the first couple of subscripts denotes the sensor that make the measure and the second couple denotes the active phase considered.

9.2 How to figure out the value of current

Once obtained the matrix $[K]$ is possible to figure out the value of current that flows into the bars, considered as an unknown term, using the values of $\vec{B}$ when all, or a part of the circuits, are fed. Then it's possible to reach the goal to measure the currents using only the value of $\vec{B}$ measured by the sensor.
To do this, it is necessary to elaborate the following equation in the time domain:

(1.13) $$\left[\vec{B}(t)\right] = \left[K\right] \cdot \left[\vec{I}(t)\right]$$

in order to obtain:

(1.14) $$\left[\vec{I}(t)\right] = \left[K\right]^{-1} \cdot \left[\vec{B}(t)\right]$$

Where all the terms, excepted for the elements *k*, are time-dependents and represented by a sine wave function. In particular:

- $\left[\vec{I}(t)\right]$ is the array of currents composed by all the sinusoidal currents, with their proper electric displacement of 120 °, that flow through the electric bars in a determinate instant of time;
- $\left[\vec{B}(t)\right]$ is the array of values of MF find out with the Comsol model simulation in the points selected for the sensor installation, in a determinate instant of time.

The values of time taken into consideration are the values from t=0 [s] to t=0,02 [s] with intervals of 0,01 [s], namely:

$$t = (0;\ 0.001;\ 0.002 \ldots 0.019;\ 0.02)$$

9.2.1 Implementation with Matlab®

In order to verify the proper functioning of the system there have been made some scripts using the Matlab software with the purpose of evaluate the matrix $\left[\vec{I}(t)\right]$ and also to evaluate the possible error between the values of current found out with this method and the values of input current set in the Comsol model.

The script reported in the *Appendix A.1* is an example of Matlab algorithm used for test if the matrix $[K]$ derived with the Comsol model is correct.

In specific terms, the program, given $\left[\vec{B}\right]$ and $[K]$, tries to figure out if the relative $\left[\vec{I}\right]$ calculated with this method is equal to the original array of input current of the Comsol model.

The array of currents derived with this script will be equal to the input current array only if the matrix $[K]$ considered is correct. In the case taken into account the result has to be an array where all the currents have a value of 1[A] if the input currents were set to 1[A], or for example 50 [A] if the input currents were set to 50[A].

Another example of script used in this project is the algorithm present in the *Appendix A.2*.

This script yields the array of currents with the insertion, in the appropriate program lines, of the array $\left[\vec{B}(t)\right]$ and the matrix $[K]$ and makes a comparison between the original inputs currents and the currents find out with the matrix method, in order to discover the possible differences.

In the script is possible to individuate a matrix named B. This matrix is composed by the elements represented the measures of MF, made by the measure points, in the different instants of time considerate in the previous paragraph.

More specifically, every element of the matrix depends on:

- The sensor that make this measure (9 sensors in this case);
- The instant time considered (21 instants in this case);

building so a 21× 9 dimensions matrix.

It's important to underline that this is only an example of script and that the matrix $\left[\vec{B}(t)\right]$ can change according to the number of bars taken into consideration, as it will be possible to see in the next paragraphs.

Another element to note in the Matlab script it's the division of the solutions into two cases:

- A first case (called *Exact calculation*) in which it's calculated the array of current $\left[\vec{I}(t)\right]$ (called *Im* in the script) with the equation:

(1.15) $$\left[\vec{I}(t)\right]_{exact} = \left[K\right]^{-1} \cdot \left[\vec{B}(t)\right]$$

- A second case (called *Approximate calculation*) in which it's calculated the same array but with the equation:

(1.16) $$\left[\vec{I}(t)\right]_{approx.} = \frac{\left[\vec{B}(t)\right]}{\left[K\right]}$$

Furthermore, with the same algorithm is possible to calculate the error between the initial input current and the current calculated with the use of the matrix.

To do this there were implemented the following equations:

- For the error between the real input current and the current calculate with the *Exact calculation*:

(1.17) $$e_{exact} = \left[\vec{I}(t)\right]_{exact} - \left[\vec{I}(t)\right]_{input}$$

- For the error between the real input current and the current calculate with the *Approximate calculation*:

(1.18) $$e_{approx.} = \left[\vec{I}(t)\right]_{approx.} - \left[\vec{I}(t)\right]_{input}$$

After the computation of these parameters all the results will graph in order to show the correct trend of the current wave form and the errors.

10 STUDY OF THE ERROR - 2D CASE

In this section it will be shown the procedure to obtain the correct measure of current focusing in every particular cut-plane considerate, for first in the 2D-model and then in the respective 3D-model.

In every case it will be shown the respective K matrix utilized and the solutions in graphic form.

It's important to anticipate that for the probes there were considered these two different cases:

- A study of the model neglecting the phenomenon of the mutual inductance which may be incurred between the bars;
- A study considering the phenomenon of mutual inductance.

Indeed, for the fact that the bars are made of conductive material (aluminium), it would be interesting to study the effects caused by this phenomenon in the current distribution of the bars and so in the measuring system.

To simulate these two type of study it has been necessary to consider the same Comsol model in two differents configuration: for the first study (mutual inductance neglected) it have been taken into consideration all the bars and circuits made by air instead of aluminium, for the second it was considered the normal configuration with aluminium.

10.1 First disposition of measure sensors

10.1.1 K matrix

In this paragraph there are presented the matrices $[K]$ used for the calculation of the measured current. All the values of the matrix elements are in $[\mu T]$.

1. Case neglecting the mutual inductance effect

$K =$

SENSOR \ ACTIVE PHASE	R1	S1	R2	S2	R3	S3	R4	S4	T	N
R1	32.448	-0.63872	-0.17978	-0.079189	-0.046106	-0.029409	-0.020951	-0.015426	-0.014192	0.26106
S1	-0.63766	32.441	-0.73116	-0.17971	-0.083036	-0.0461	-0.03025	-0.020949	-0.018561	0.016993
R2	-0.17971	-0.73139	32.447	-0.63771	-0.17963	-0.07915	-0.04609	-0.029401	-0.024522	-0.045264
S2	-0.079154	-0.17966	-0.63783	32.444	-0.73108	-0.17969	-0.083028	-0.046095	-0.03387	-0.039465
R3	-0.046097	-0.083032	-0.17971	-0.7313	32.453	-0.63794	-0.17966	-0.079151	-0.044139	-0.02936
S3	-0.0294	-0.046089	-0.079147	-0.17961	-0.63741	32.43	-0.73094	-0.17969	-0.033091	-0.021429
R4	-0.020949	-0.030252	-0.046103	-0.083045	-0.17975	-0.73166	32.46	-0.63797	0.11414	-0.016435
S4	-0.015421	-0.020943	-0.029397	-0.04608	-0.079129	-0.17957	-0.63729	32.446	0.29887	-0.012736
T	0.014605	0.018754	0.02434	0.033251	0.045202	0.058239	0.026484	-0.3162	12.451	0.014702
N	-0.10356	0.054683	0.0536	0.039178	0.028929	0.02147	0.016761	0.013215	0.014712	12.451

This matrix, as explained before, was calculated based on the imposition of a current of 1[A] in every bar of every circuit one at a time, the results was obtained with a steady-state study of the model.

To obtain this matrix there have been considerate the electric bars present in the cut-plane z: R-bars, S-bars, neutral-bar and also the bar T because it may influence the measures of all the sensors in the plane and so it has

to take into consideration.

There were taken into account also two sensors near the bar T, that will not be installed in the electric panel. These sensors have been necessary in this case to complete the matrix, because, considering only the effects of the bar T on the others sensors and not the effects of the others bars on the sensors of the bar T it means have a different number of row and column in the matrix. a column of the matrix. This translates into have a non-square matrix and so a non-invertible matrix.

A think to notice it's that the highest values of MF are present in the diagonal of the matrix, this because in the diagonal there are considerate all the measures made by the sensors installed in proximity of the fed bars. These values also represent the true MFs that we have to measure.

This can suggest that the theoretical considerations made about the 2-sensors method could be true; this because all the others elements of the matrix have a very low value and so will affect the measures with a very low contribute.

2. Case considering the mutual inductance effect

$K =$

SENSOR \ ACTIVE PHASE	R1	S1	R2	S2	R3	S3	R4	S4	T	N
R1	32.448	-0.63872	-0.17978	-0.079189	-0.046106	-0.029409	-0.020951	-0.015426	-0.014192	0.26106
S1	-0.63766	32.441	-0.73116	-0.17971	-0.083036	-0.0461	-0.03025	-0.020949	-0.018561	0.016993
R2	-0.17971	-0.73139	32.447	-0.63771	-0.17963	-0.07915	-0.04609	-0.029401	-0.024522	-0.045264
S2	-0.079154	-0.17966	-0.63783	32.444	-0.73108	-0.17969	-0.083028	-0.046095	-0.03387	-0.039465
R3	-0.046097	-0.083032	-0.17971	-0.7313	32.453	-0.63794	-0.17966	-0.079151	-0.044139	-0.02936
S3	-0.0294	-0.046089	-0.079147	-0.17961	-0.63741	32.43	-0.73094	-0.17969	-0.033091	-0.021429
R4	-0.020949	-0.030252	-0.046103	-0.083045	-0.17975	-0.73166	32.46	-0.63797	0.11414	-0.016435
S4	-0.015421	-0.020943	-0.029397	-0.04608	-0.079129	-0.17957	-0.63729	32.446	0.29887	-0.012736
T	0.014605	0.018754	0.02434	0.033251	0.045202	0.058239	0.026484	-0.3162	12.451	0.014702
N	-0.10356	0.054683	0.0536	0.039178	0.028929	0.02147	0.016761	0.013215	0.014712	12.451

As can be seen, the matrix K in this case it's exactly the same as the previous one, even taking into account the mutual inductance effects.

This can be explained with the fact that we are studying the system in a stationary domain condition and the input currents are constant currents. Because of this, as it can be demonstrated in the next equations, the derivative of current respect to the time will be zero and there will not the formation of an electromotive force on the others bars.

(1.19) $$\varepsilon = -M\frac{di}{dt} \qquad with \qquad \frac{di}{dt} = 0$$

$$\rightarrow \varepsilon = 0$$

10.1.2 Matrix $\left[\vec{B}(t)\right]$

To monitor the correct functioning of the measure system it have been done some tests with different input currents. This in order to discover the development of the error between the indirect measurement of current and the real current flowing through the panel bars.

For every single case taken into consideration it will be represented the respective matrix $\left[\vec{B}(t)\right]$ used for the computation.

The following matrices $\left[\vec{B}(t)\right]$ are derived with the input currents set in this way:

$$\begin{aligned}
&\vec{I}_{R1} = I_1 \sin(2\pi\, 50\, t) \\
&\vec{I}_{R2} = I_2 \sin(2\pi\, 50\, t) \\
&\vec{I}_{R3} = I_3 \sin(2\pi\, 50\, t) \\
&\vec{I}_{R4} = I_4 \sin(2\pi\, 50\, t) \\
&\vec{I}_{S1} = I_1 \sin(2\pi\, 50\, t + 2\pi/3) \\
&\vec{I}_{S2} = I_2 \sin(2\pi\, 50\, t + 2\pi/3) \\
&\vec{I}_{S3} = I_3 \sin(2\pi\, 50\, t + 2\pi/3) \\
&\vec{I}_{S4} = I_4 \sin(2\pi\, 50\, t + 2\pi/3) \\
&\vec{I}_{T} = 4\ I_1 \sin(2\pi\, 50\, t + 4\pi/3)
\end{aligned} \qquad I_1 = I_2 = I_3 = I_4 = 1,\ 50,\ 100\ [A]$$

Where I_1, I_2, I_3, I_4 are the peak value of the alternative currents considered, the electrical system considered it's symmetric and balanced.

It's important to note that for the phase T the input current set was 4 time the current set for the other bars. This because the bar T in this case it's not a bar of an electric circuit but it's the principle phase-T bar in which flows a current that will split into the four circuits.

Below there are showed the resulting matrices according to their respective input currents; all the values are in [μT].

1. Case neglecting the mutual inductance effect

$|B(t)|_{1[A]} =$

Time [s]	R1	S1	R2	S2	R3	S3	R4	S4	T
0	-0.60782	27.792	-1.269	27.693	-1.238	27.797	-1.4402	27.139	-42.924
0.001	9.4855	21.152	9.0041	21.09	9.0488	21.106	8.5039	20.125	-48.843
0.002	18.639	12.309	18.307	12.276	18.371	12.306	17.84	11.464	-49.572
0.003	25.985	2.2465	25.836	2.2462	25.913	2.2868	25.447	1.667	-45.454
0.004	30.791	-8.0427	30.839	-8.0106	30.921	-7.9631	30.567	-8.3001	-36.88
0.005	32.58	-17.54	32.82	-17.479	32.9	-17.429	32.692	-17.45	-24.699
0.006	31.189	-25.323	31.598	-25.238	31.668	-25.191	31.626	-24.895	-10.112
0.007	26.709	-30.608	27.246	-30.508	27.298	-30.468	27.427	-29.883	5.4944
0.008	19.624	-32.89	20.237	-32.786	20.267	-32.757	20.553	-31.941	20.536
0.009	10.61	-31.936	11.239	-31.837	11.243	-31.822	11.659	-30.855	33.554
0.01	0.57718	-27.885	1.1605	-27.8	1.1392	-27.801	1.6442	-26.777	43.301
0.011	-9.4808	-21.155	-8.9992	-21.094	-9.0439	-21.11	-8.499	-20.128	48.841
0.012	-18.644	-12.273	-18.313	-12.24	-18.377	-12.27	-17.846	-11.429	49.522
0.013	-26.004	-2.174	-25.856	-2.174	-25.933	-2.2146	-25.469	-1.5971	45.37
0.014	-30.786	8.0436	-30.834	8.0115	-30.916	7.964	-30.562	8.3008	36.871
0.015	-32.577	17.529	-32.817	17.468	-32.896	17.418	-32.688	17.44	24.71
0.016	-31.175	25.304	-31.584	25.219	-31.653	25.172	-31.611	24.876	10.12
0.017	-26.715	30.609	-27.253	30.509	-27.305	30.469	-27.434	29.884	-5.485
0.018	-19.645	32.91	-20.259	32.805	-20.289	32.776	-20.575	31.96	-20.532
0.019	-10.647	31.989	-11.277	31.889	-11.281	31.874	-11.697	30.906	-33.578
0.02	-0.62133	27.963	-1.2061	27.878	-1.1849	27.879	-1.6906	26.853	-43.354

$|B(t)|_{50[A]} =$

Time [s]	R1	S1	R2	S2	R3	S3	R4	S4	T
0	-30.391	1389.6	-63.448	1384.6	-61.901	1389.8	-72.01	1357	-2146.2
0.001	474.29	1057.6	450.21	1054.5	452.45	1055.3	425.2	1006.2	-2442.1
0.002	931.95	615.44	915.37	613.81	918.55	615.3	892	573.2	-2478.6
0.003	1299.2	112.39	1291.7	112.37	1295.6	114.4	1272.3	83.408	-2272.7
0.004	1539.5	-402.09	1541.9	-400.49	1546	-398.11	1528.3	-414.96	-1844
0.005	1629.1	-877.01	1641.1	-873.95	1645	-871.46	1634.7	-872.52	-1235
0.006	1558.9	-1265.8	1579.4	-1261.6	1582.8	-1259.2	1580.7	-1244.4	-505.24
0.007	1336.2	-1530.9	1363.1	-1525.9	1365.7	-1523.9	1372.1	-1494.7	274.24
0.008	982.8	-1646.3	1013.5	-1641.1	1015	-1639.6	1029.3	-1598.8	1027
0.009	532.61	-1600	564.12	-1595	564.34	-1594.3	585.16	-1545.9	1679.4
0.01	29.717	-1396.2	58.92	-1392	57.859	-1392	83.129	-1340.8	2166.8
0.011	-474.92	-1056.9	-450.86	-1053.8	-453.1	-1054.6	-425.86	-1005.5	2442
0.012	-932.69	-614.96	-916.11	-613.33	-919.3	-614.82	-892.74	-572.73	2479
0.013	-1299.7	-110.47	-1292.3	-110.47	-1296.1	-112.5	-1272.8	-81.564	2270.4
0.014	-1539.3	403.64	-1541.8	402.03	-1545.9	399.65	-1528.2	416.44	1841.3
0.015	-1628	876.75	-1640	873.68	-1643.9	871.2	-1633.6	872.25	1233.7
0.016	-1557.4	1265.2	-1577.8	1260.9	-1581.3	1258.6	-1579.2	1243.8	503.85
0.017	-1334.4	1530.3	-1361.3	1525.3	-1363.9	1523.3	-1370.4	1494	-276.09
0.018	-982.96	1645.4	-1013.6	1640.2	-1015.1	1638.7	-1029.4	1597.9	-1025.3
0.019	-533.28	1598.3	-564.74	1593.4	-564.97	1592.6	-585.75	1544.3	-1675.6
0.02	-29.471	1396.2	-58.675	1392	-57.613	1392	-82.887	1340.8	-2167.2

$|B(t)|_{100[A]} =$

Time [s]	R1	S1	R2	S2	R3	S3	R4	S4	T
0	-60.782	2779.2	-126.9	2769.3	-123.8	2779.7	-144.02	2713.9	-4292.4
0.001	948.16	2113.9	900.04	2107.7	904.51	2109.3	850.05	2011.2	-4881.5
0.002	1863.8	1231.1	1830.6	1227.8	1837	1230.8	1783.8	1146.6	-4957.2
0.003	2597.7	225.94	2582.8	225.91	2590.4	229.97	2543.9	167.95	-4546.1
0.004	3079.9	-804.98	3084.7	-801.77	3092.9	-797.02	3057.5	-830.71	-3688.2
0.005	3258.3	-1754.2	3282.3	-1748.1	3290.3	-1743.1	3269.5	-1745.2	-2470.1
0.006	3117.6	-2531.6	3158.5	-2523.1	3165.4	-2518.4	3161.2	-2488.8	-1010.1
0.007	2671.7	-3061	2725.5	-3051	2730.7	-3047.1	2743.5	-2988.5	548.4
0.008	1965.3	-3292.3	2026.7	-3281.9	2029.7	-3279	2058.4	-3197.3	2054.1
0.009	1065.7	-3200.5	1128.7	-3190.5	1129.1	-3189.1	1170.8	-3092.2	3358.8
0.01	61.465	-2795.2	119.92	-2786.7	117.8	-2786.8	168.36	-2684.3	4334.8
0.011	-948.72	-2116.3	-900.55	-2110.1	-905.02	-2111.7	-850.51	-2013.6	4886.3
0.012	-1866	-1230.2	-1832.8	-1226.9	-1839.2	-1229.9	-1786.1	-1145.7	4959.5
0.013	-2600	-223.08	-2585.1	-223.06	-2592.7	-227.12	-2546.2	-165.16	4545.2
0.014	-3079.5	804.67	-3084.3	801.45	-3092.5	796.7	-3057.1	830.4	3688
0.015	-3257	1753	-3281	1746.8	-3289	1741.9	-3268.2	1744	2470
0.016	-3116.7	2530.4	-3157.6	2522	-3164.5	2517.3	-3160.3	2487.6	1010.6
0.017	-2671.5	3060.5	-2725.3	3050.5	-2730.4	3046.6	-2743.3	2988.1	-547.92
0.018	-1964.2	3290.3	-2025.5	3279.9	-2028.5	3277	-2057.1	3195.4	-2052.8
0.019	-1064.9	3198.3	-1127.9	3188.3	-1128.3	3186.9	-1169.9	3090.1	-3356.5
0.02	-61.111	2793.9	-119.54	2785.4	-117.42	2785.5	-167.96	2683	-4333.2

1. CASE CONSIDERING THE MUTUAL INDUCTANCE EFFECT

$|B(t)|_{1[A]} =$

Time [s]	R1	S1	R2	S2	R3	S3	R4	S4	T
0	-0.94151	19.699	-1.8639	19.568	-1.8395	19.598	-2.579	18.303	-41.631
0.001	8.7127	21.372	8.4175	21.355	8.456	21.352	7.8569	20.418	-50.742
0.002	17.964	12.798	17.834	12.808	17.89	12.824	17.334	12.028	-49.74
0.003	25.459	2.8306	25.498	2.8657	25.567	2.8975	25.1	2.3156	-44.67
0.004	30.462	-7.4153	30.665	-7.3578	30.74	-7.3141	30.405	-7.621	-35.646
0.005	32.488	-16.936	32.834	-16.862	32.907	-16.81	32.738	-16.81	-23.317
0.006	31.329	-24.798	31.783	-24.714	31.848	-24.66	31.859	-24.352	-8.7766
0.007	27.096	-30.217	27.611	-30.132	27.662	-30.081	27.853	-29.495	6.607
0.008	20.227	-32.691	20.752	-32.614	20.784	-32.57	21.136	-31.764	21.336
0.009	11.391	-31.991	11.871	-31.929	11.881	-31.897	12.359	-30.949	33.983
0.01	1.4268	-28.136	1.8161	-28.096	1.8021	-28.079	2.3603	-27.082	43.282
0.011	-8.6819	-21.525	-8.4234	-21.51	-8.4592	-21.51	-7.8761	-20.562	48.349
0.012	-17.939	-12.801	-17.837	-12.814	-17.891	-12.83	-17.34	-12.022	48.68
0.013	-25.437	-2.8306	-25.504	-2.8694	-25.571	-2.9004	-25.105	-2.3128	44.265
0.014	-30.438	7.4154	-30.667	7.354	-30.74	7.3114	-30.406	7.6213	35.5
0.015	-32.452	16.931	-32.823	16.853	-32.895	16.803	-32.725	16.805	23.272
0.016	-31.298	24.79	-31.774	24.702	-31.838	24.65	-31.849	24.343	8.7668
0.017	-27.085	30.225	-27.621	30.136	-27.671	30.087	-27.861	29.502	-6.6066
0.018	-20.218	32.701	-20.762	32.62	-20.792	32.578	-21.144	31.772	-21.336
0.019	-11.36	31.954	-11.86	31.889	-11.868	31.858	-12.347	30.91	-33.972
0.02	-1.4041	28.118	-1.8116	28.074	-1.7966	28.059	-2.3548	27.061	-43.315

$|B(t)|_{50[A]} =$

Time [s]	R1	S1	R2	S2	R3	S3	R4	S4	T
0	-47.075	984.94	-93.196	978.41	-91.973	979.89	-128.95	915.15	-2081.6
0.001	435.62	1068.7	420.86	1067.8	422.78	1067.7	392.84	1021	-2537.2
0.002	898.2	639.9	891.68	640.37	894.47	641.18	866.69	601.38	-2487.2
0.003	1273	141.54	1274.9	143.3	1278.4	144.88	1255	115.79	-2233.6
0.004	1523.2	-370.78	1533.3	-367.91	1537.1	-365.72	1520.3	-381.06	-1782.4
0.005	1624.4	-846.85	1641.7	-843.13	1645.4	-840.57	1636.9	-840.57	-1166.2
0.006	1566.1	-1239.6	1588.8	-1235.4	1592.1	-1232.8	1592.7	-1217.4	-438.72
0.007	1354.9	-1511	1380.7	-1506.8	1383.2	-1504.2	1392.8	-1474.9	330.37
0.008	1011.6	-1634.9	1037.8	-1631	1039.4	-1628.8	1057	-1588.5	1066.9
0.009	568.83	-1597.9	592.94	-1594.8	593.4	-1593.2	617.36	-1545.8	1699
0.01	70.962	-1406.1	90.488	-1404.1	89.786	-1403.3	117.71	-1353.4	2165.5
0.011	-434.22	-1075.7	-421.25	-1075	-423.04	-1075	-393.86	-1027.5	2418.8
0.012	-897.09	-640.15	-891.98	-640.77	-894.68	-641.58	-867.13	-601.2	2435.2
0.013	-1271.8	-141.54	-1275.1	-143.47	-1278.5	-145.02	-1255.2	-115.65	2213.3
0.014	-1522.1	370.81	-1533.5	367.75	-1537.2	365.62	-1520.5	381.11	1775.4
0.015	-1621.7	846.15	-1640.2	842.24	-1643.8	839.74	-1635.3	839.82	1163.2
0.016	-1565.5	1239.9	-1589.3	1235.5	-1592.5	1232.9	-1593	1217.5	438.58
0.017	-1354.3	1511.3	-1381.1	1506.9	-1383.6	1504.4	-1393.1	1475.2	-330.39
0.018	-1011.2	1635.5	-1038.4	1631.5	-1039.9	1629.4	-1057.5	1589.1	-1066.9
0.019	-568.57	1598.9	-593.54	1595.7	-593.95	1594.1	-617.86	1546.7	-1699
0.02	-70.335	1406.2	-90.649	1404.1	-89.905	1403.3	-117.8	1353.4	-2164.7

$|B(t)|_{100[A]} =$

Time [s]	R1	S1	R2	S2	R3	S3	R4	S4	T
0	-94.151	1969.9	-186.39	1956.8	-183.95	1959.8	-257.9	1830.3	-4163.1
0.001	871.24	2137.9	841.75	2136.3	845.6	2136	785.74	2042.7	-5075
0.002	1796.4	1279.8	1783.4	1280.8	1789	1282.4	1733.4	1202.8	-4974.2
0.003	2545.9	283.06	2549.8	286.57	2556.7	289.74	2510	231.56	-4467.2
0.004	3045.9	-741.46	3066.2	-735.71	3073.7	-731.33	3040.2	-762.02	-3564.3
0.005	3249	-1693.7	3283.6	-1686.3	3290.9	-1681.1	3274	-1681.1	-2331.9
0.006	3134.3	-2480.9	3179.7	-2472.5	3186.3	-2467.1	3187.4	-2436.3	-878.23
0.007	2709.9	-3022	2761.4	-3013.5	2766.5	-3008.4	2785.6	-2949.8	660.77
0.008	2022.6	-3268.8	2075.1	-3261.1	2078.2	-3256.8	2113.5	-3176.1	2133.3
0.009	1136.9	-3193.1	1185.1	-3186.9	1186	-3183.8	1233.9	-3088.9	3394.9
0.01	141.69	-2810.9	180.81	-2806.8	179.41	-2805.1	235.34	-2705.3	4332.2
0.011	-868.04	-2150.1	-842.05	-2148.6	-845.63	-2148.6	-787.24	-2053.7	4837.8
0.012	-1794.1	-1280.2	-1783.9	-1281.4	-1789.3	-1283.1	-1734.2	-1202.3	4871.6
0.013	-2543.8	-283.09	-2550.4	-286.95	-2557.1	-290.05	-2510.5	-231.3	4427.4
0.014	-3044.1	741.61	-3066.9	735.48	-3074.3	731.21	-3040.9	762.2	3550.8
0.015	-3242.9	1692	-3279.8	1684.2	-3287	1679.2	-3270	1679.3	2326.1
0.016	-3125	2475.2	-3172.5	2466.4	-3178.9	2461.2	-3180	2430.6	875.89
0.017	-2707.7	3021.6	-2761.2	3012.8	-2766.2	3007.8	-2785.2	2949.3	-660.38
0.018	-2020.6	3268.2	-2074.9	3260.1	-2078	3255.9	-2113.1	3175.4	-2132.6
0.019	-1136.6	3196.7	-1186.6	3190.1	-1187.4	3187.1	-1235.3	3092.2	-3398.7
0.02	-140.25	2810.4	-181.03	2806	-179.54	2804.5	-235.42	2704.7	-4332.2

10.1.3 Graphic results

In this section there are gathered all the graphical solutions that will permit to observe the influence of the error in the sensors measures.

The graphs were obtained with Matlab scripts similar to the script reported in the *Appendix A.2* but adapted to every single case.

For every image will be graph, for every powered bar, the trends of currents and errors with respect to time.

For the trends of currents there have been considered the exact and approximate cases explained before (Exact and Approximate measure) and also the real input current that flows through the bars in the simulated model (Real current).

The difference between the Real current trend and the trends of the other measures generates the graph that represents the Error with respect to time.

With the name ‘’Phase XY’’ it means that it’s taken into consideration the trend of current that flows into the bar connected to the X-phase of the panel in the circuit Y.

For example, ‘’Phase R1’’ it means that the graph is referred to the trend of current that flows in the bar connected ù

to the R-phase of the panel in the circuit 1.

The graph referred to the bar T present in the 2D cut-plane it was created only for completeness because is not foreseen the installation of magnetoresistive sensors for that bar.

For the firsts groups of graphs, it will be take into consideration a balanced electrical system and in the *section* [*1.18*] it will be considered a case of unbalanced electrical system.

1. Case neglecting the mutual inductance effect

- **PEAK VALUE = 1[A]**

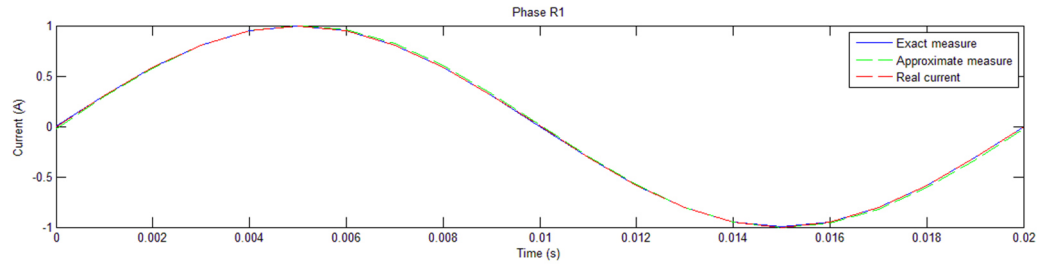

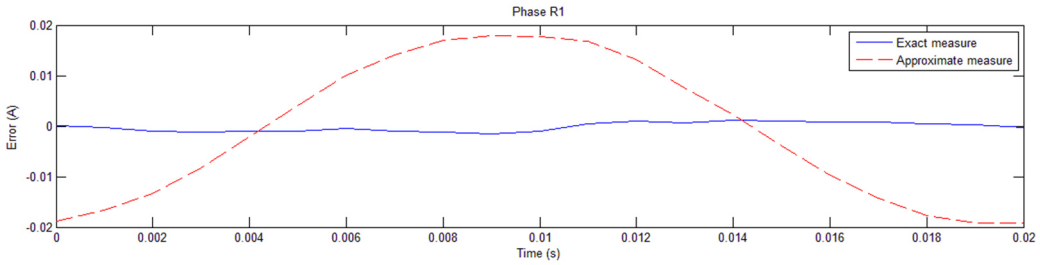

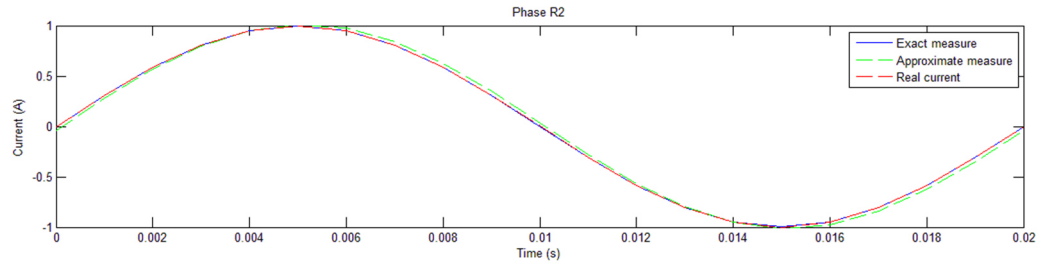

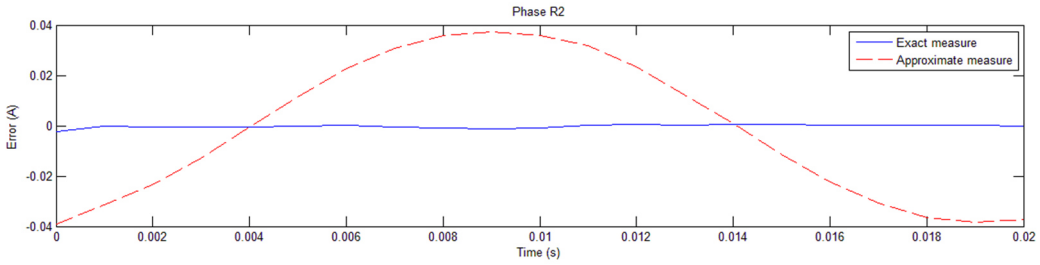

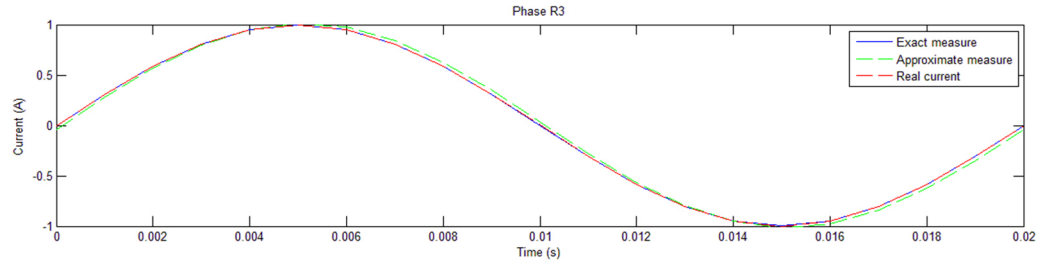
Phase R3
Exact measure
Approximate measure
Real current
Current (A)
Time (s)

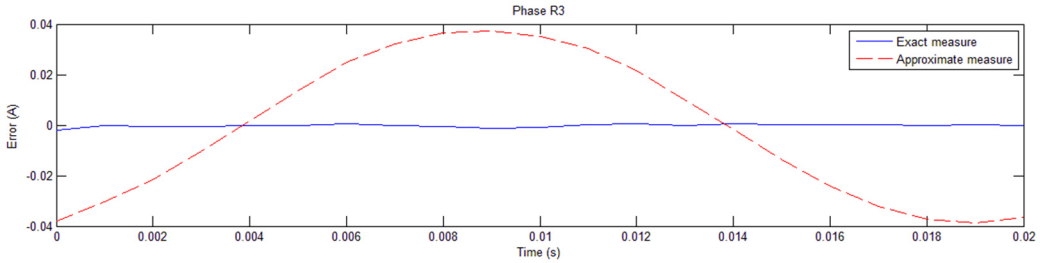
Phase R3
Exact measure
Approximate measure
Error (A)
Time (s)

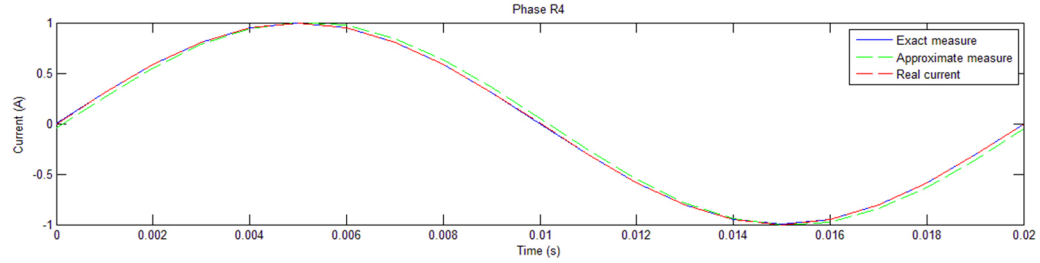
Phase R4
Exact measure
Approximate measure
Real current
Current (A)
Time (s)

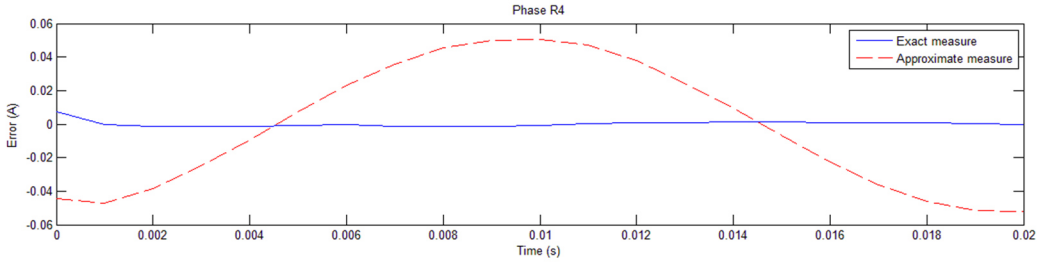
Phase R4
Exact measure
Approximate measure
Error (A)
Time (s)

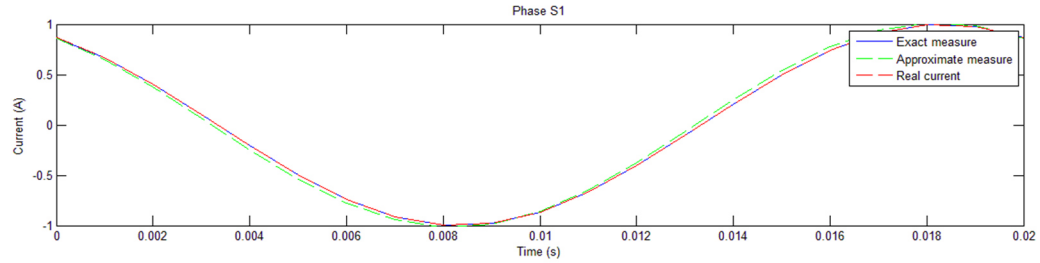
Phase S1
Exact measure
Approximate measure
Real current
Current (A)
Time (s)

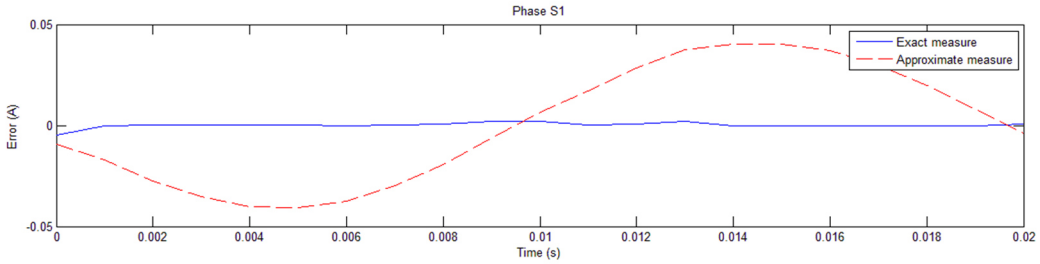
Phase S1
Exact measure
Approximate measure
Error (A)
Time (s)

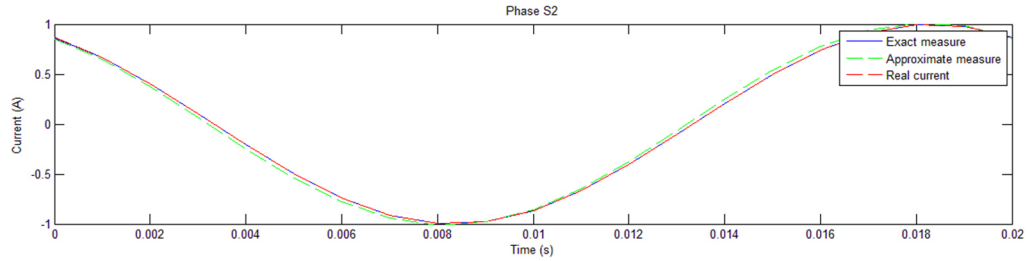
Phase S2
Exact measure
Approximate measure
Real current
Current (A)
Time (s)

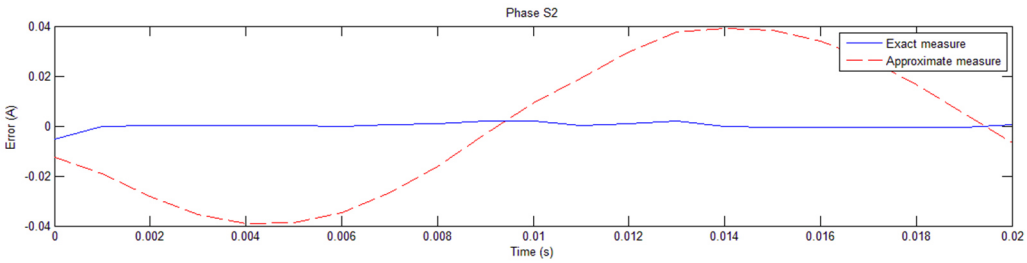
Phase S2
Exact measure
Approximate measure
Error (A)
Time (s)

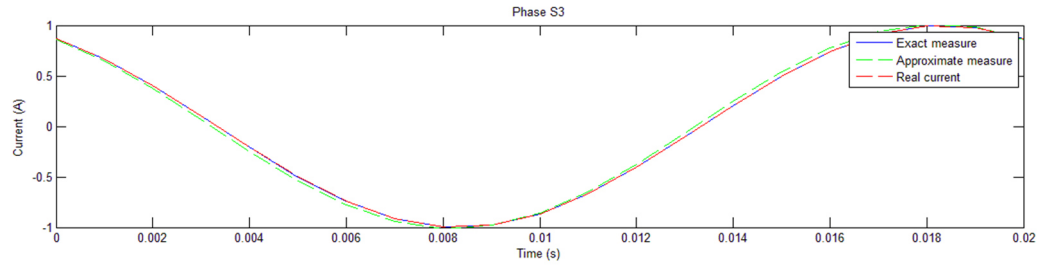
Phase S3
Exact measure
Approximate measure
Real current
Current (A)
Time (s)

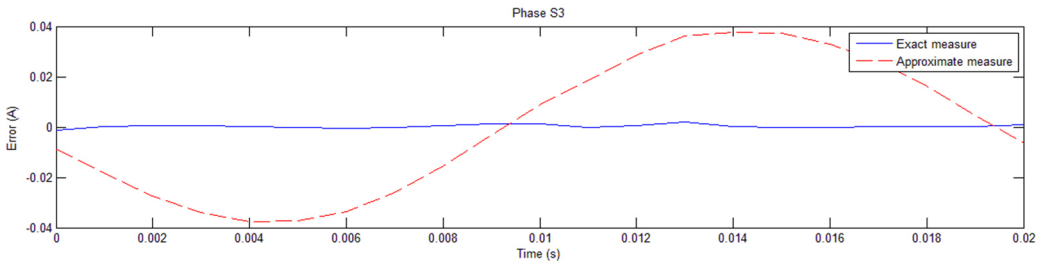
Phase S3
Exact measure
Approximate measure
Error (A)
Time (s)

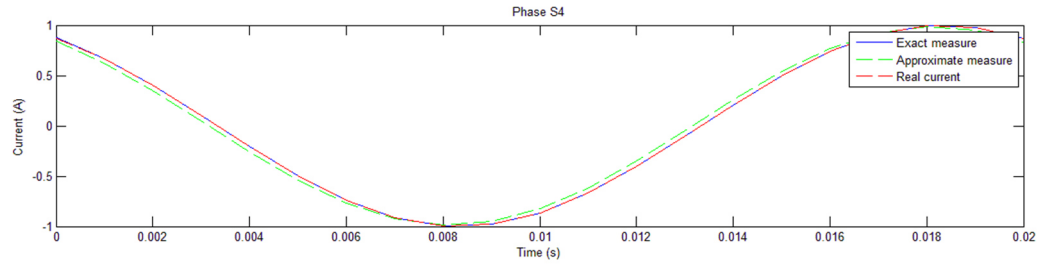
Phase S4
Exact measure
Approximate measure
Real current
Current (A)
Time (s)

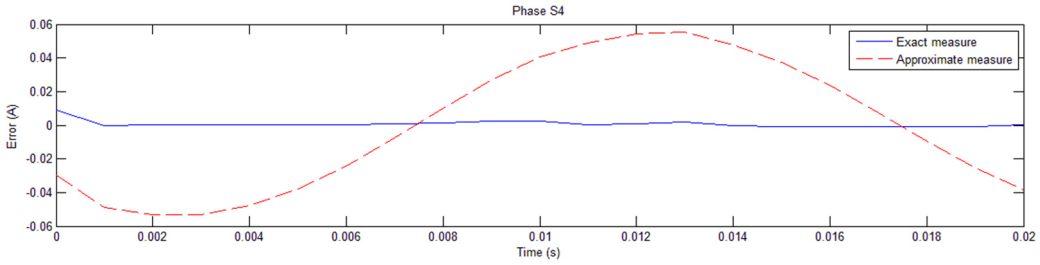
Phase S4
Exact measure
Approximate measure
Error (A)
Time (s)

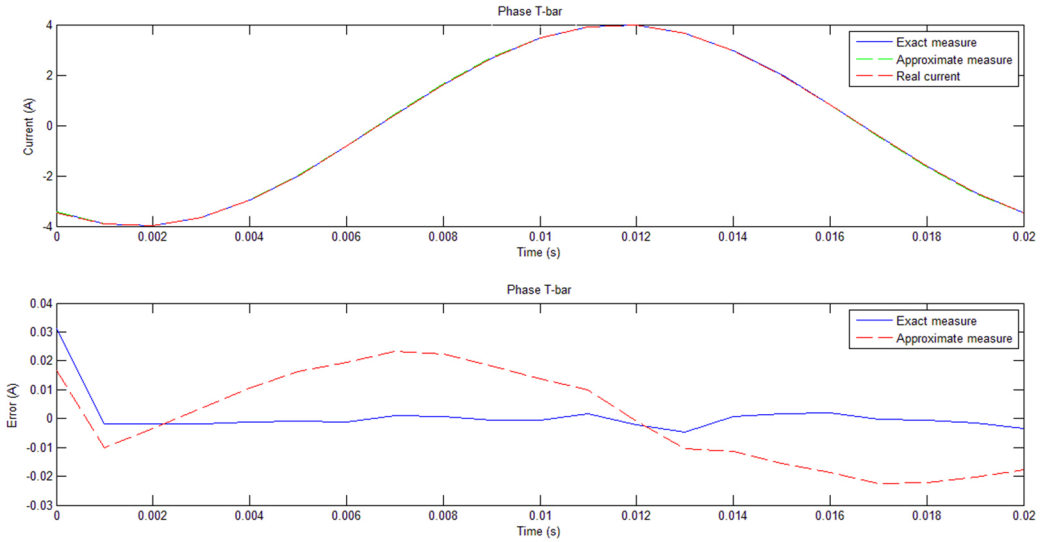

Considerations:

As it can be seen in the graphs, if it's taken into consideration the exact measure curve, it's evident that the error it's next to zero for every bar. This means that neglecting the effects of the mutual inductance the measurement system designed works perfectly.

It's possible to figure out the correct functioning of the measurement system also with the graphs displayed the current trend, in which it can be note the overlap of the real current curve with the measured current curve.

- **PEAK VALUE = 50[A]**

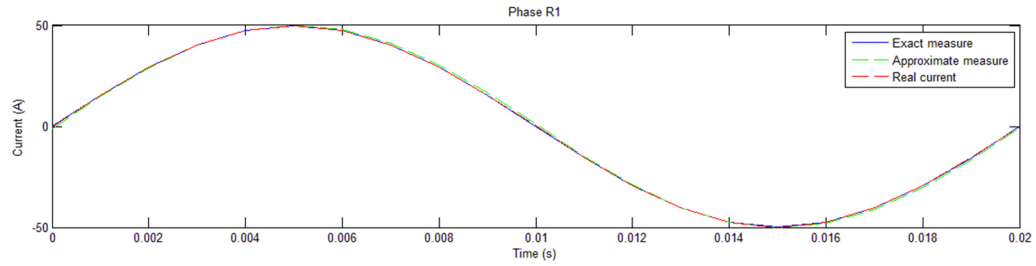

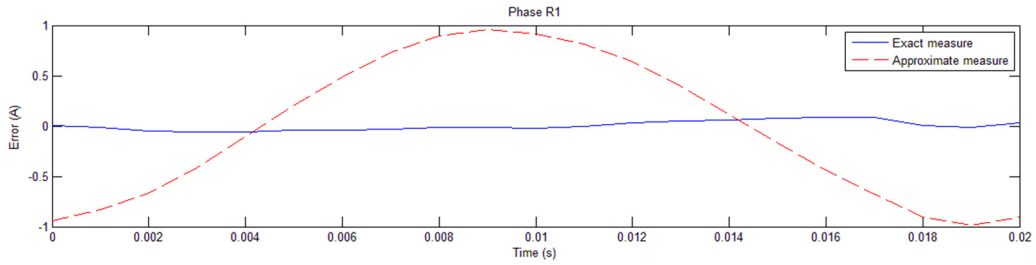

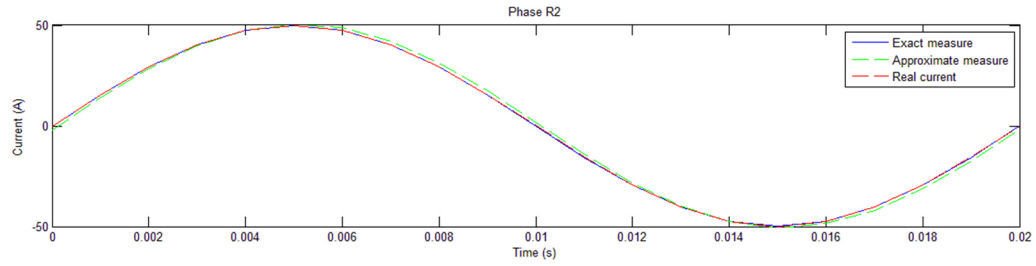

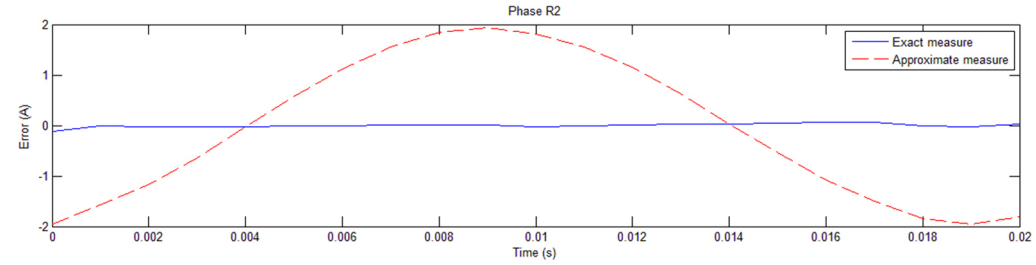

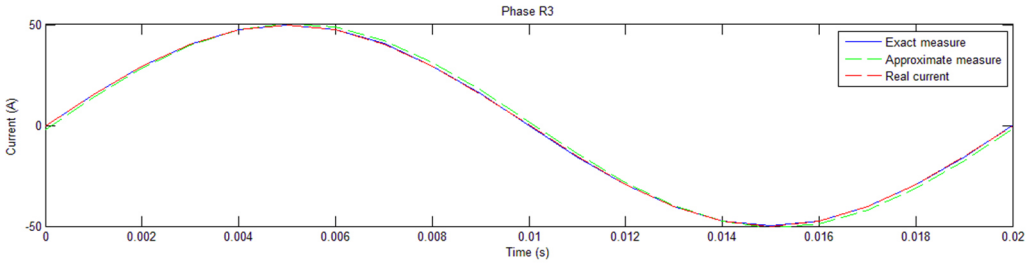
Phase R3
Exact measure
Approximate measure
Real current
Current (A)
Time (s)

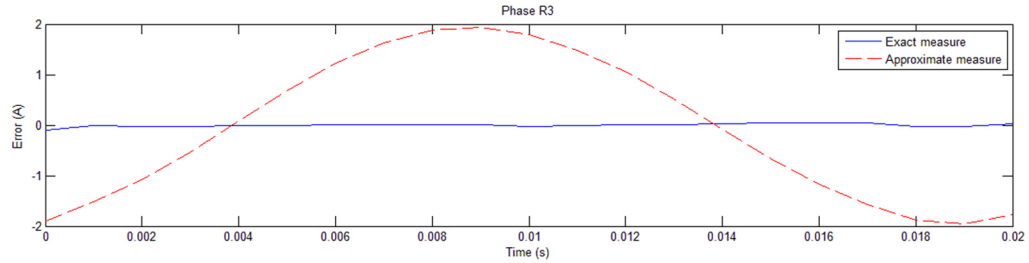
Phase R3
Exact measure
Approximate measure
Error (A)
Time (s)

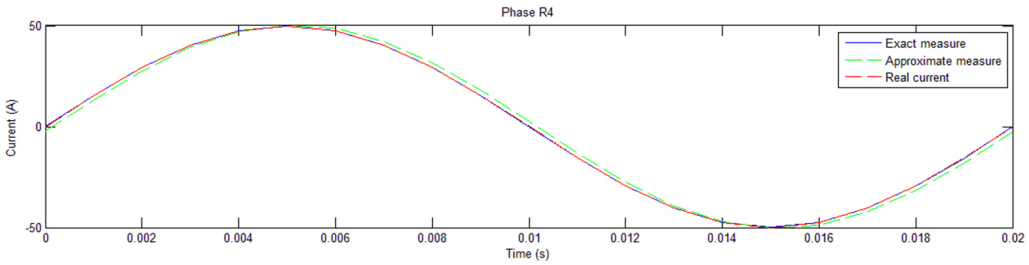
Phase R4
Exact measure
Approximate measure
Real current
Current (A)
Time (s)

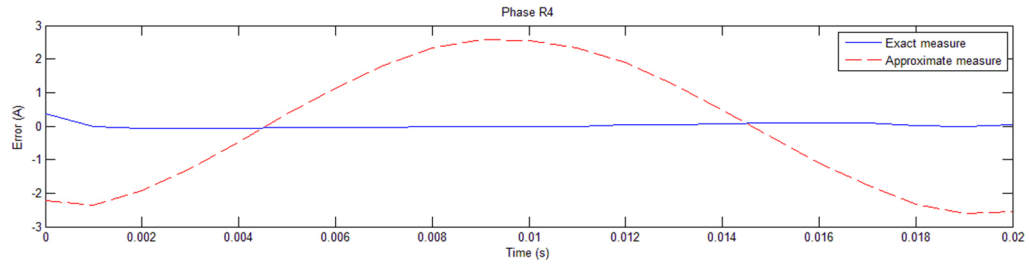
Phase R4
Exact measure
Approximate measure
Error (A)
Time (s)

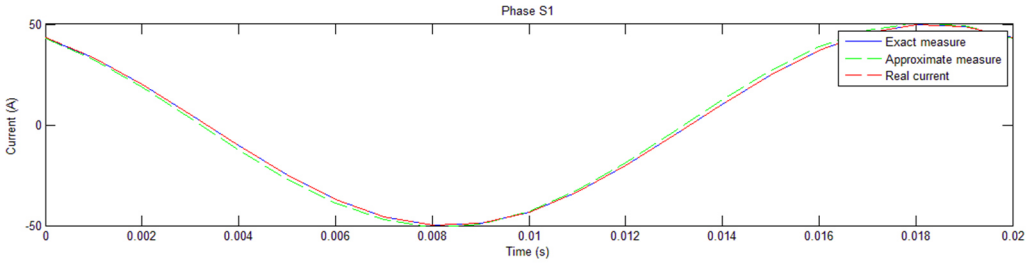
Phase S1
Exact measure
Approximate measure
Real current
Current (A)
Time (s)

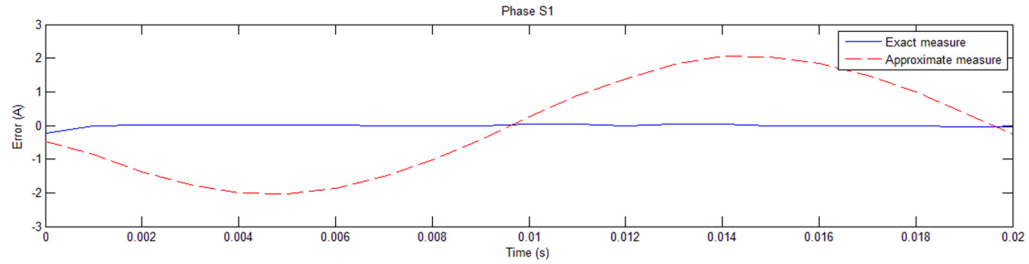
Phase S1
Exact measure
Approximate measure
Error (A)
Time (s)

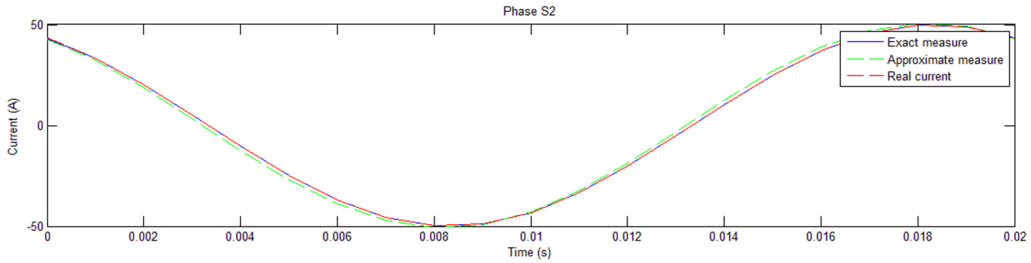
Phase S2
Exact measure
Approximate measure
Real current
Current (A)
Time (s)

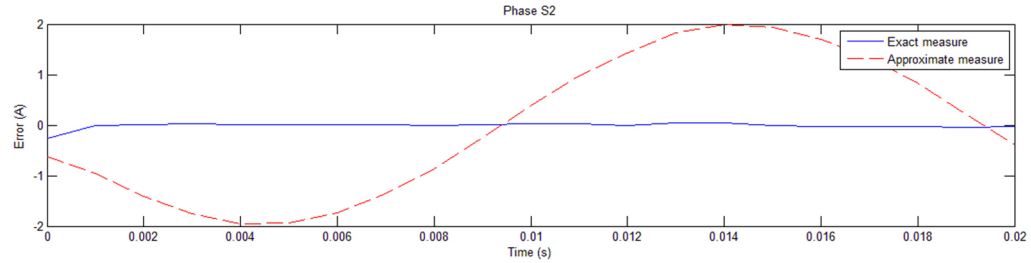
Phase S2
Exact measure
Approximate measure
Error (A)
Time (s)

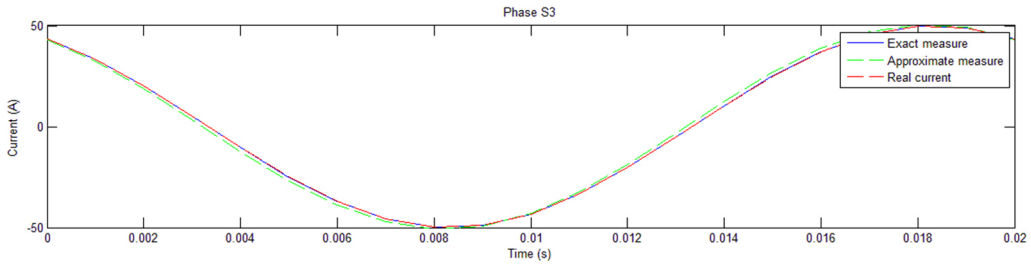
Phase S3
Exact measure
Approximate measure
Real current
Current (A)
Time (s)

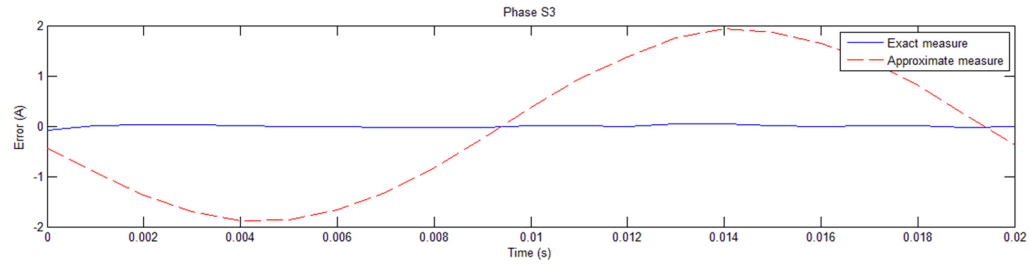
Phase S3
Exact measure
Approximate measure
Error (A)
Time (s)

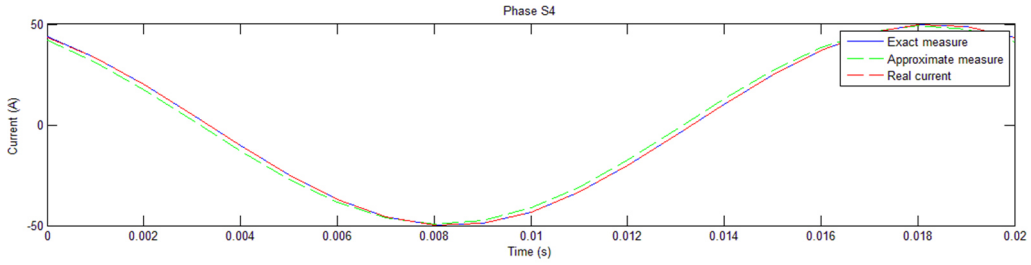
Phase S4
Exact measure
Approximate measure
Real current
Current (A)
Time (s)

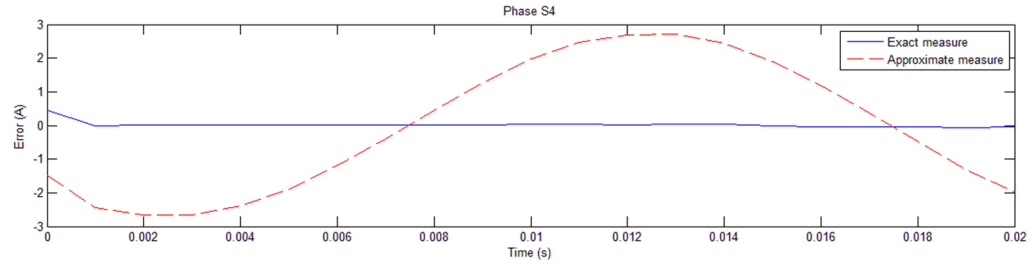
Phase S4
Exact measure
Approximate measure
Error (A)
Time (s)

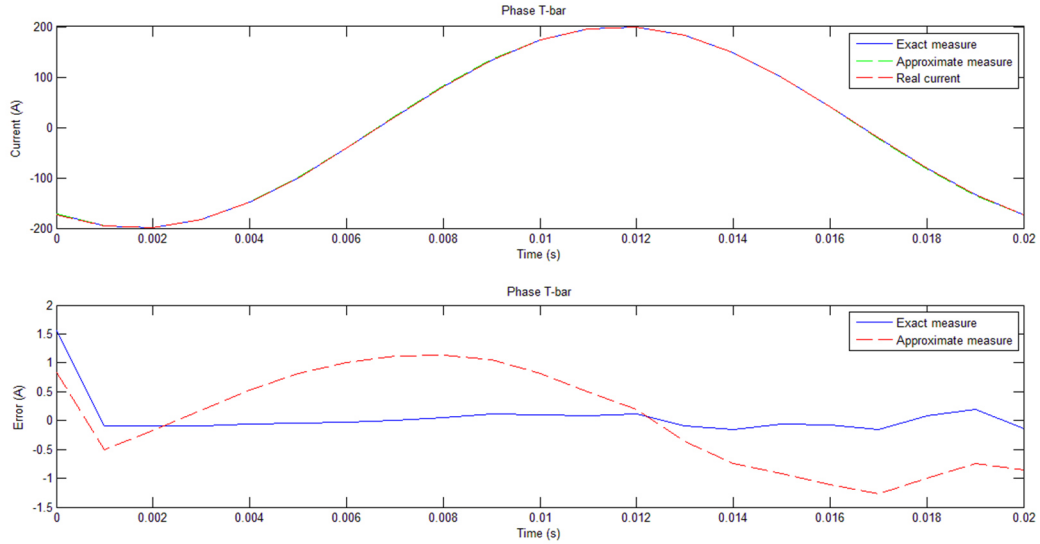

➢ **PEAK VALUE = 100 [A]**

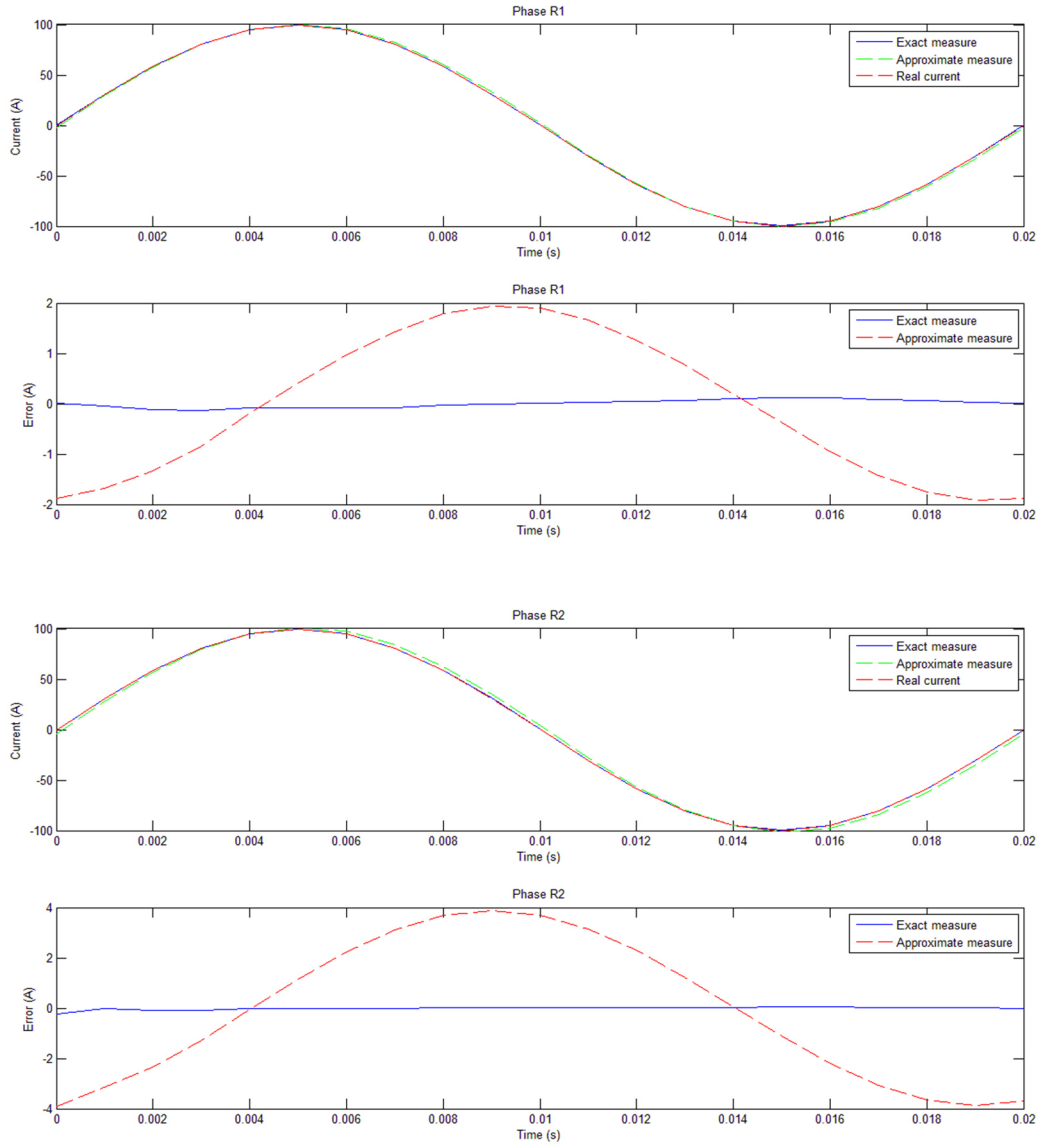

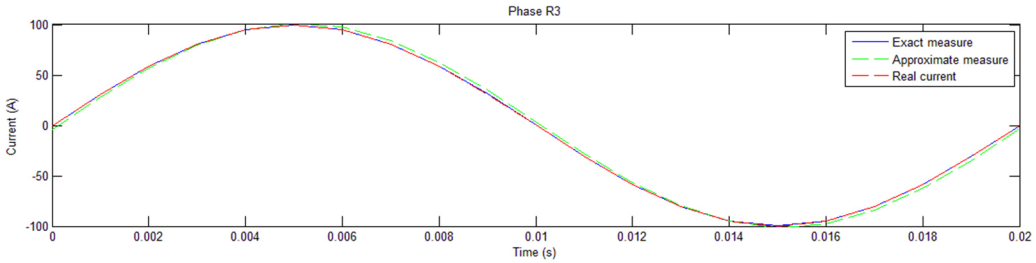
Phase R3
Exact measure
Approximate measure
Real current
Current (A)
Time (s)

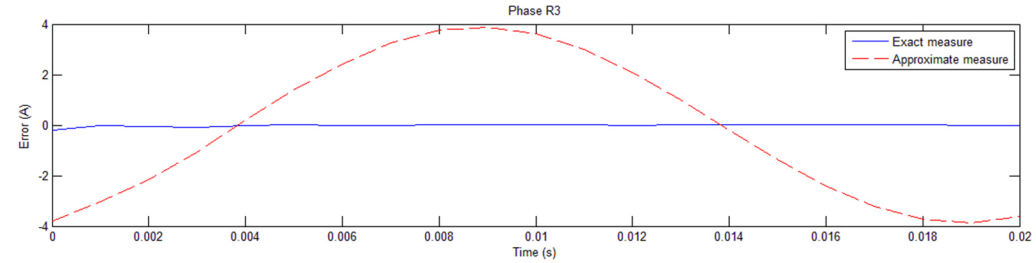
Phase R3
Exact measure
Approximate measure
Error (A)
Time (s)

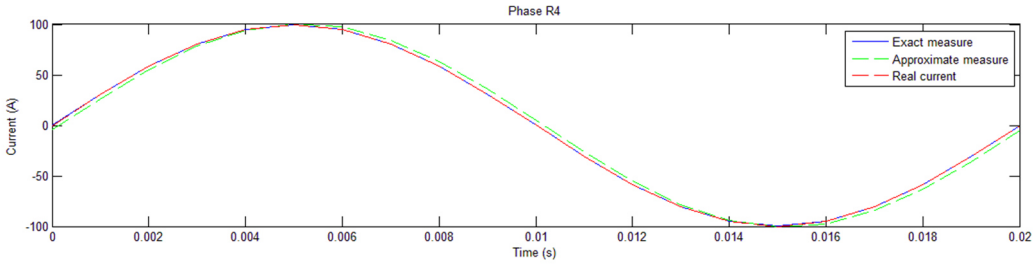
Phase R4
Exact measure
Approximate measure
Real current
Current (A)
Time (s)

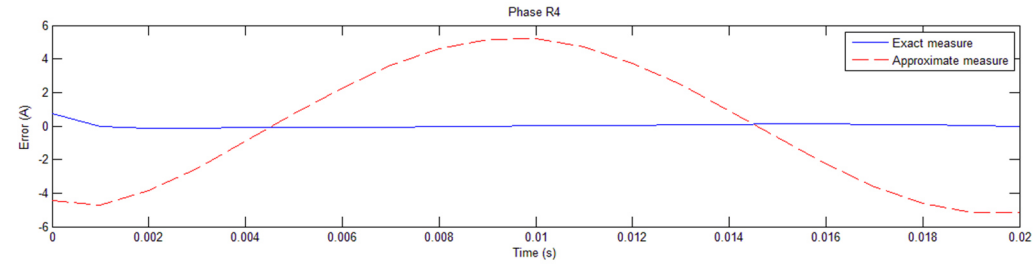
Phase R4
Exact measure
Approximate measure
Error (A)
Time (s)

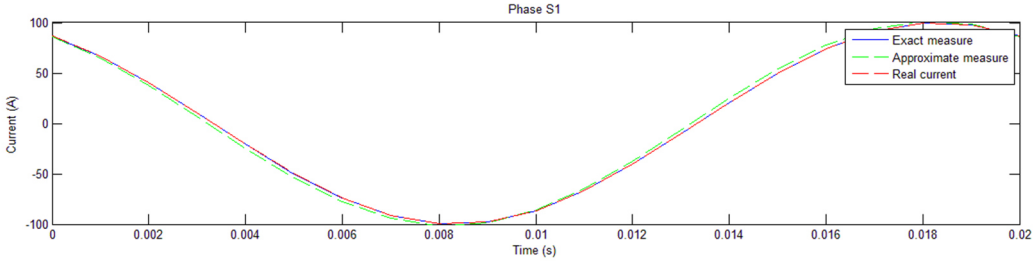
Phase S1
Exact measure
Approximate measure
Real current
Current (A)
Time (s)

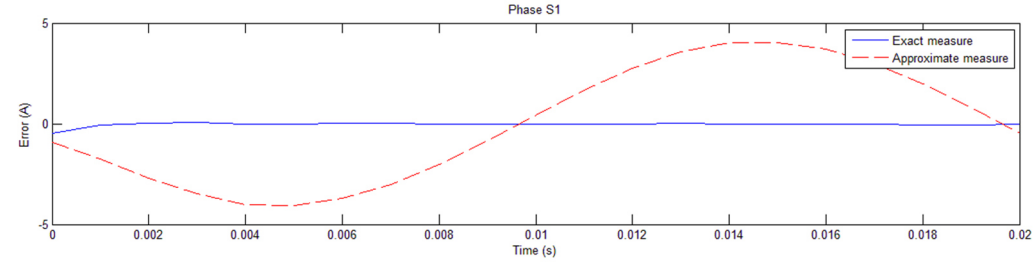
Phase S1
Exact measure
Approximate measure
Error (A)
Time (s)

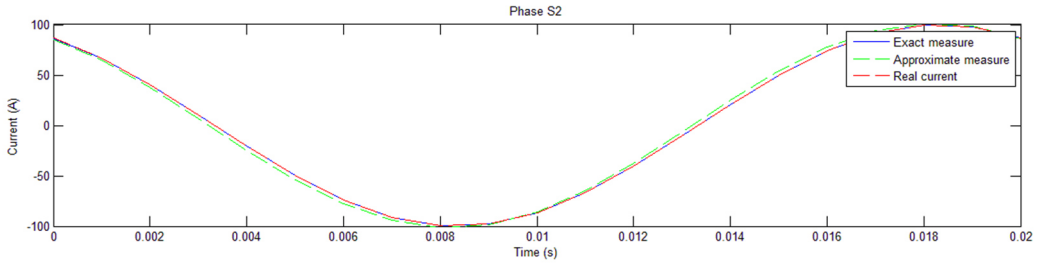
Phase S2
Exact measure
Approximate measure
Real current
Current (A)
Time (s)

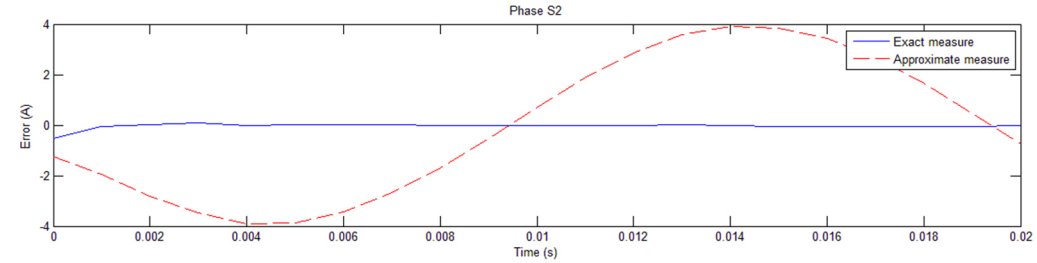
Phase S2
Exact measure
Approximate measure
Error (A)
Time (s)

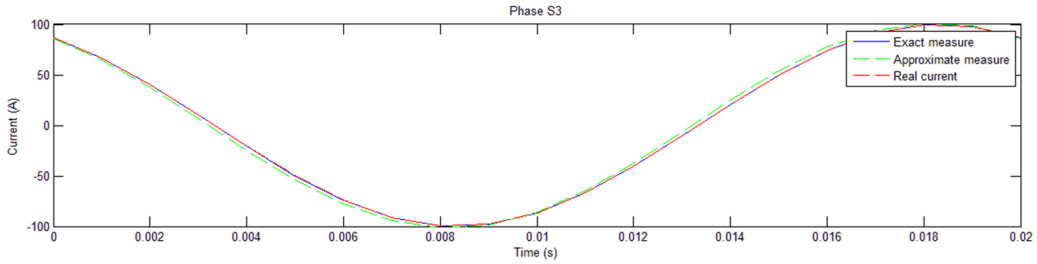
Phase S3
Exact measure
Approximate measure
Real current
Current (A)
Time (s)

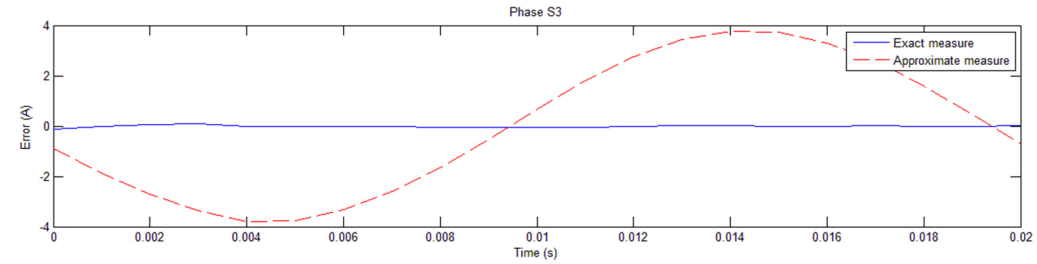
Phase S3
Exact measure
Approximate measure
Error (A)
Time (s)

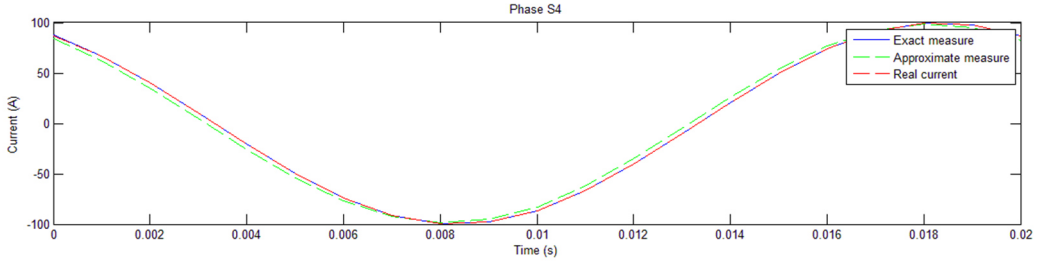
Phase S4
Exact measure
Approximate measure
Real current
Current (A)
Time (s)

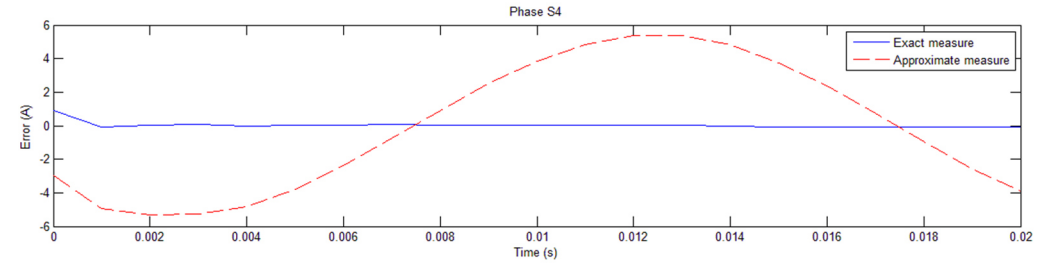
Phase S4
Exact measure
Approximate measure
Error (A)
Time (s)

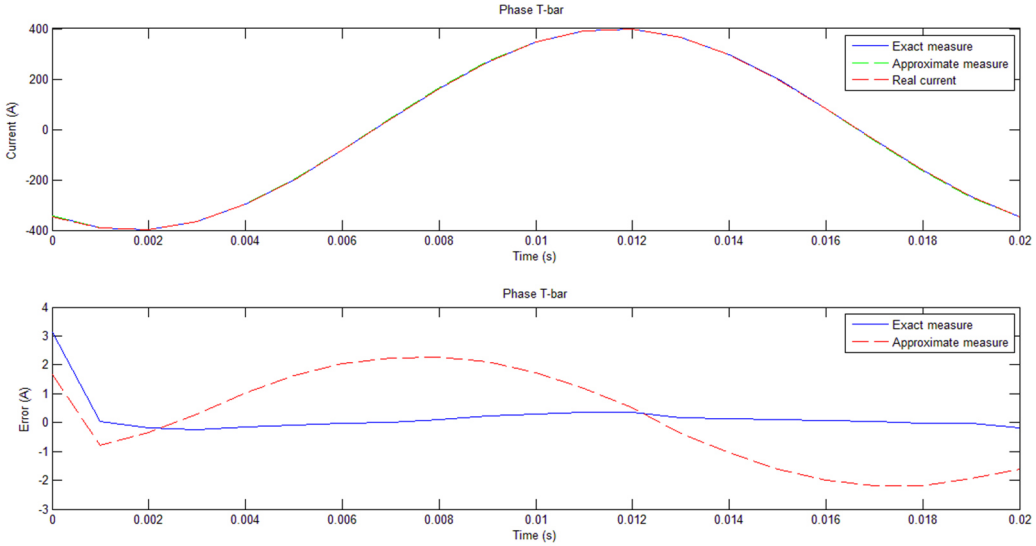

Considerations:

As can be seen by comparing the graphs obtained with the different currents, the relative error it's always next to zero and its report with the input current it's constant for every peak current considered.

2. Case considering the mutual inductance effect

- **PEAK VALUE = 1 [A]**

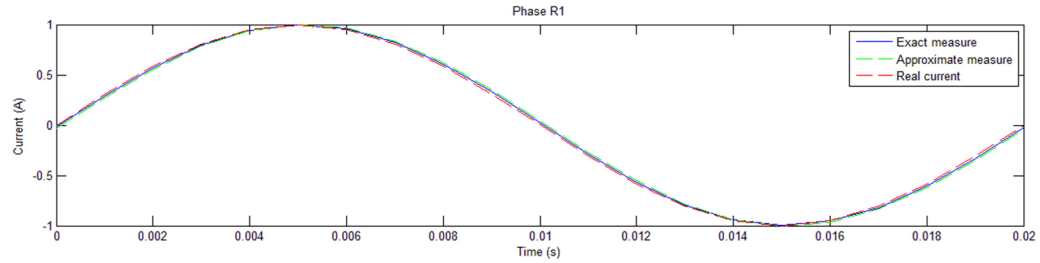

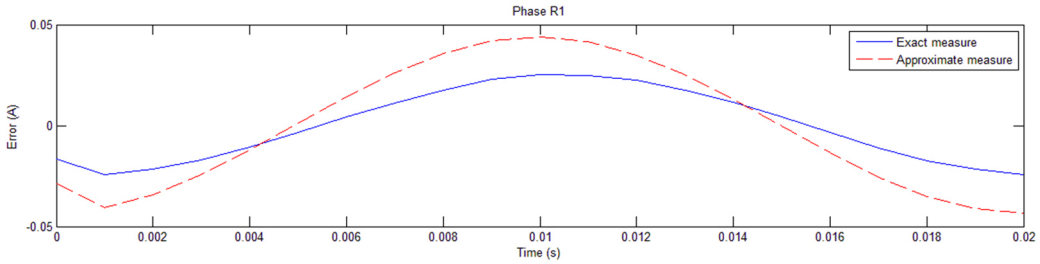

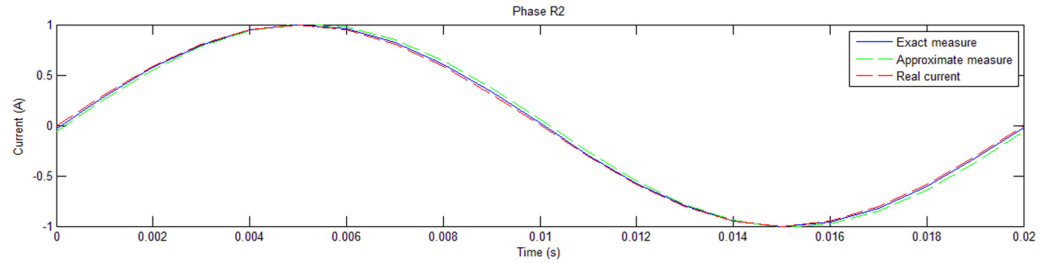

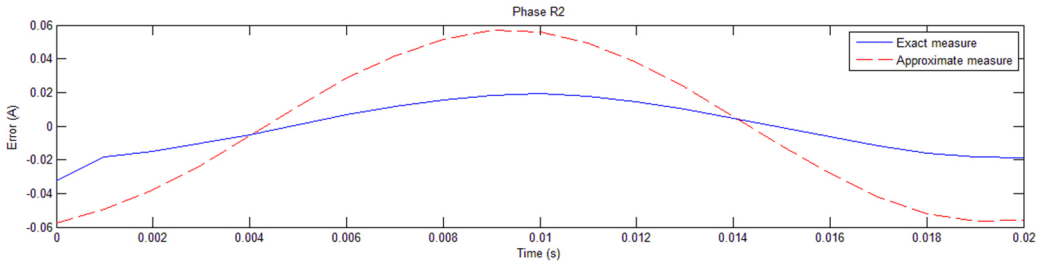

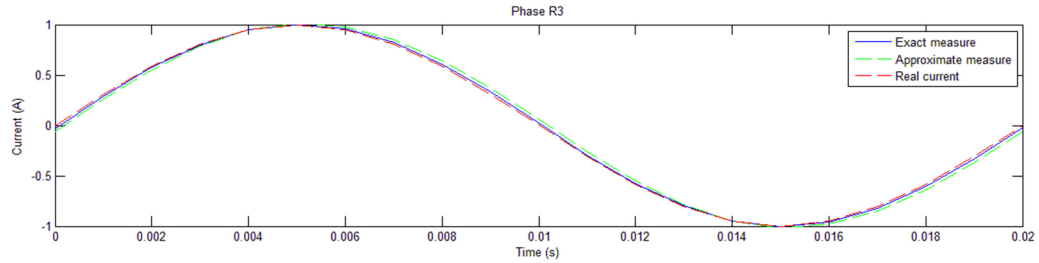
Phase R3
Exact measure
Approximate measure
Real current
Current (A)
Time (s)

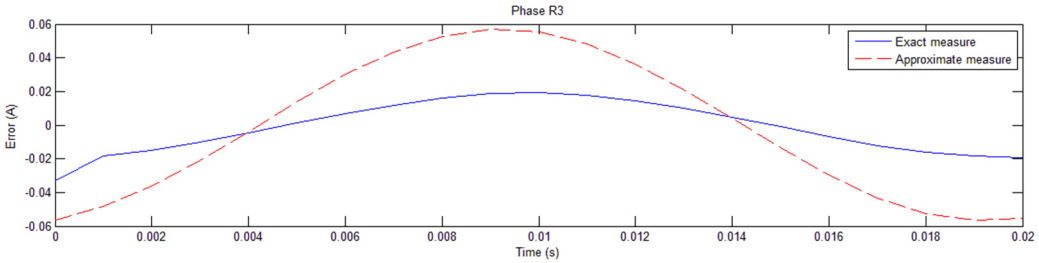
Phase R3
Exact measure
Approximate measure
Error (A)
Time (s)

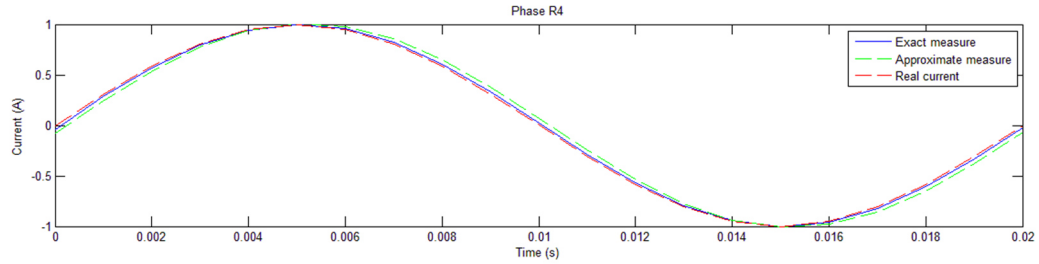
Phase R4
Exact measure
Approximate measure
Real current
Current (A)
Time (s)

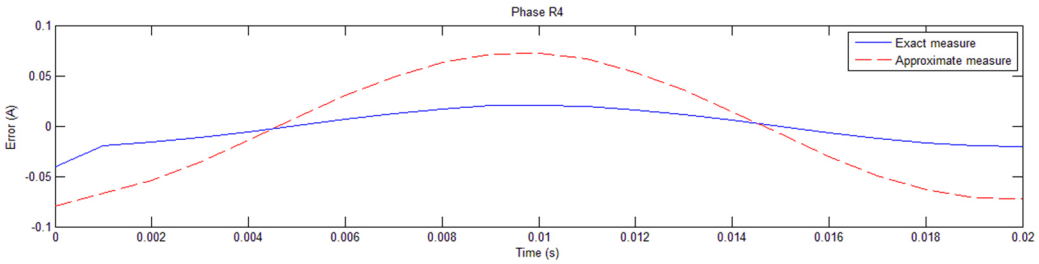
Phase R4
Exact measure
Approximate measure
Error (A)
Time (s)

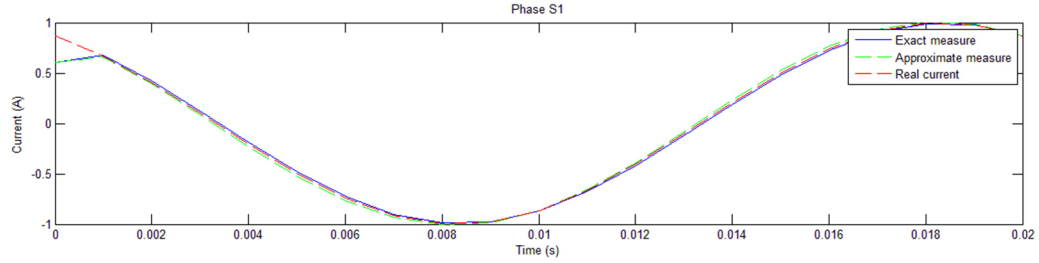
Phase S1
Exact measure
Approximate measure
Real current
Current (A)
Time (s)

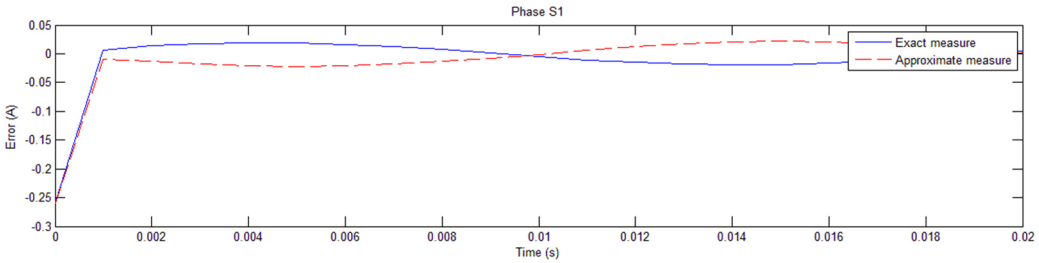
Phase S1
Exact measure
Approximate measure
Error (A)
Time (s)

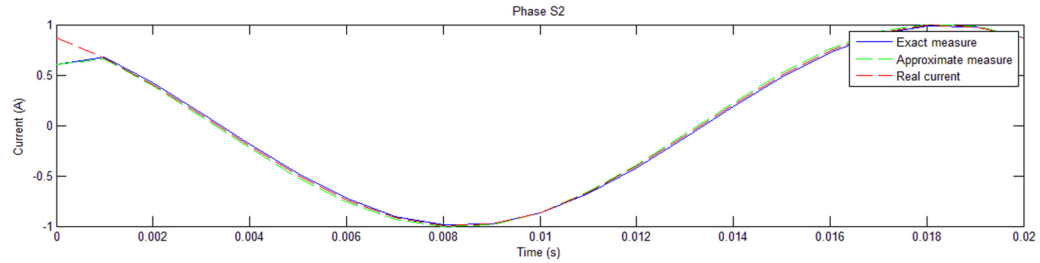
Phase S2
Exact measure
Approximate measure
Real current
Current (A)
Time (s)

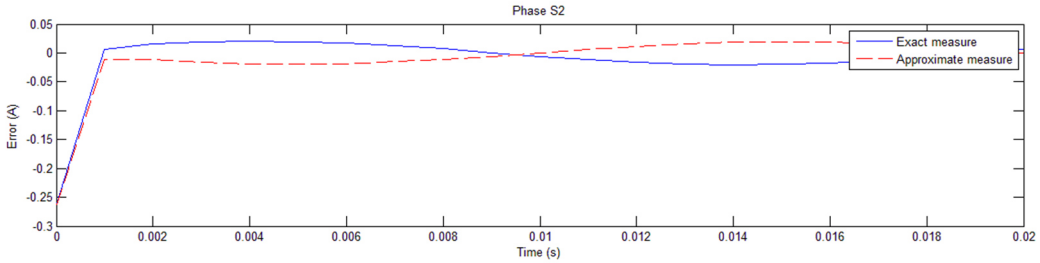
Phase S2
Exact measure
Approximate measure
Error (A)
Time (s)

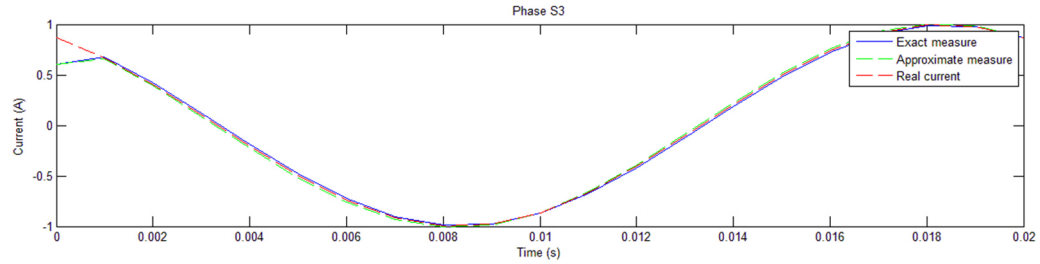
Phase S3
Exact measure
Approximate measure
Real current
Current (A)
Time (s)

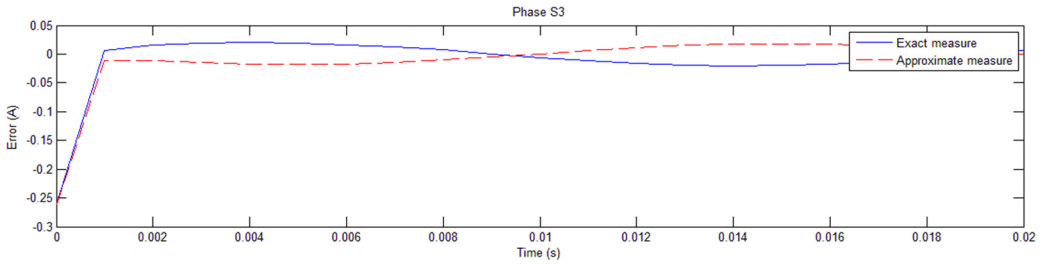
Phase S3
Exact measure
Approximate measure
Error (A)
Time (s)

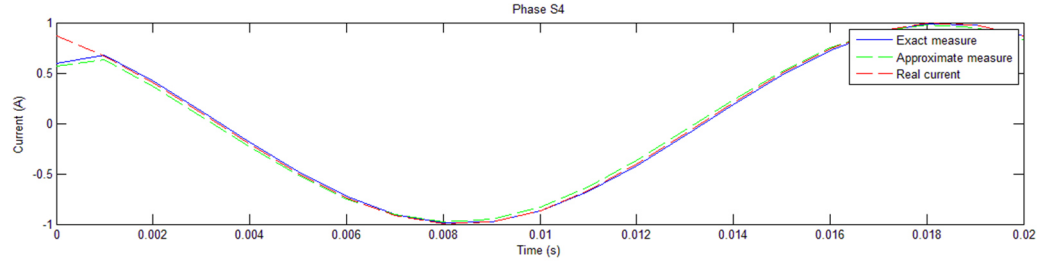
Phase S4
Exact measure
Approximate measure
Real current
Current (A)
Time (s)

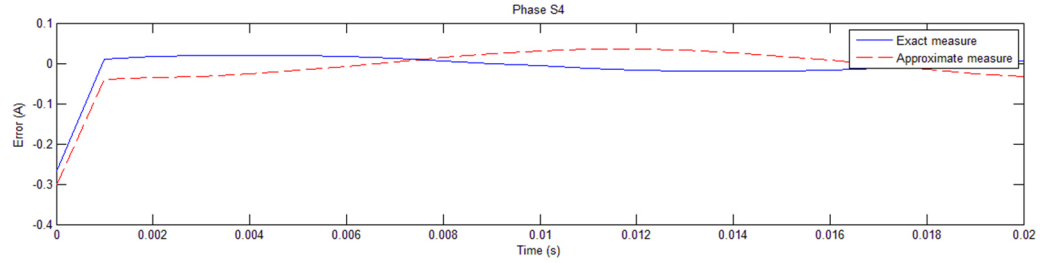
Phase S4
Exact measure
Approximate measure
Error (A)
Time (s)

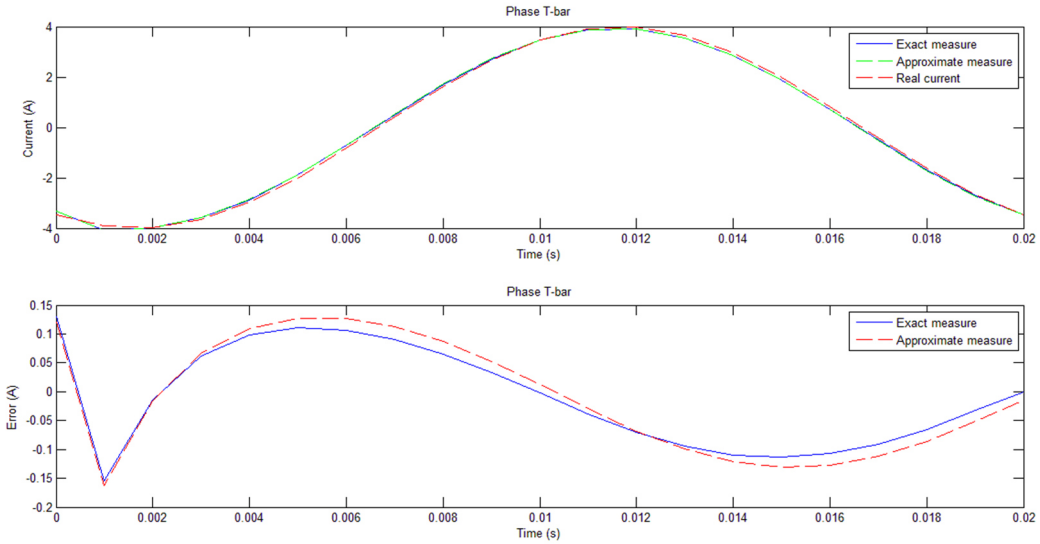

Considerations:

In this case it's considered the mutual inductance effect that influence the amount of current flowing through the bars and the effect of this phenomenon it's visible in the errors trends because they are a little bit different to the previous case.

In fact, it's important to remember that the results depend to the matrix K that it has been calculated in a steady-state domain in which are not considered the effects of the mutual inductance, as explained in the paragraph [..]. This cause that in the matrix K there are not considered the effects of the mutual inductance, as opposed to the matrix $\left[\vec{B}(t)\right]$ in which the components were computed in the time domain and so considering the mutual inductance effects.

The highest error caused by this fact it can be individuate in the phase S_4 in the instant time t= 0 [s] and it has an absolute value of: $e_{ass} = 0.2675.$

Considering that this value of absolute error is referred to a value of current of I = 0.866 [A] the respective relative error will be:

$$e_{rel} = \frac{0.2675}{0.866} = 30.889\%$$

As it will be seen in the next paragraphs it will be possible to eliminate this error with a corrective coefficient applicable only if the error will be proportional to every input current.

➢ **PEAK VALUE = 50 [A]**

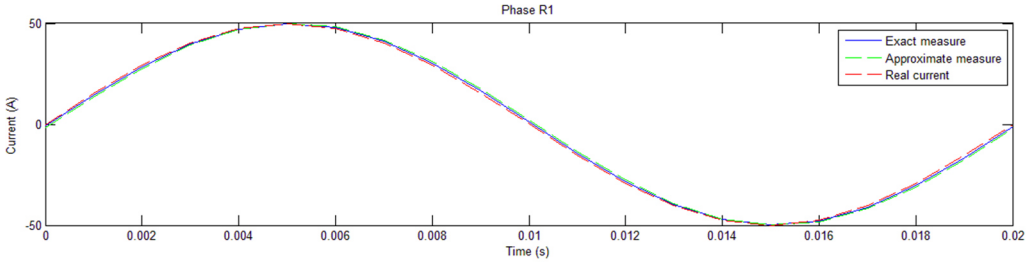

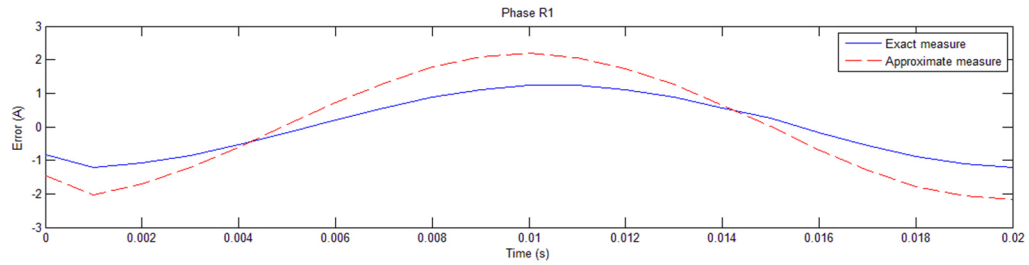

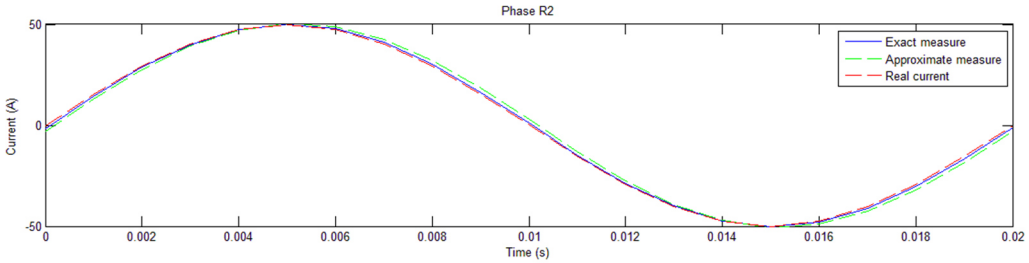

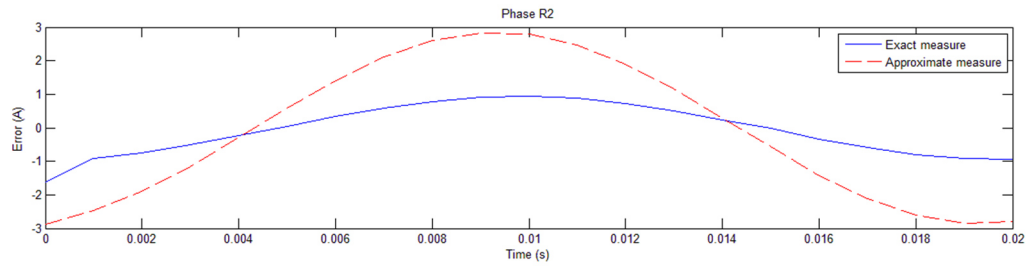

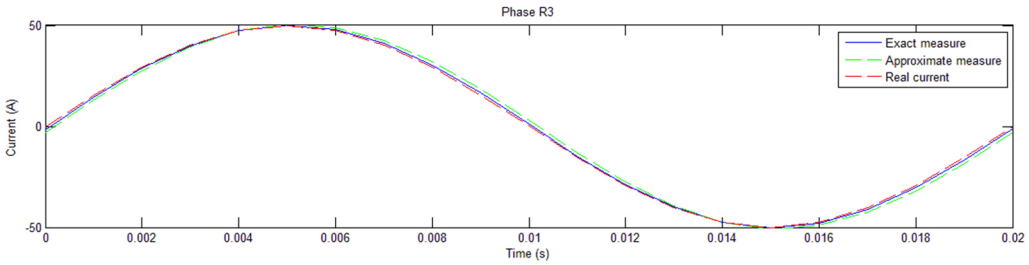

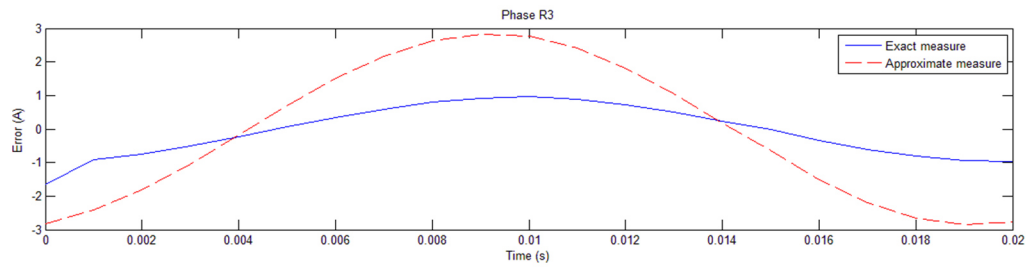

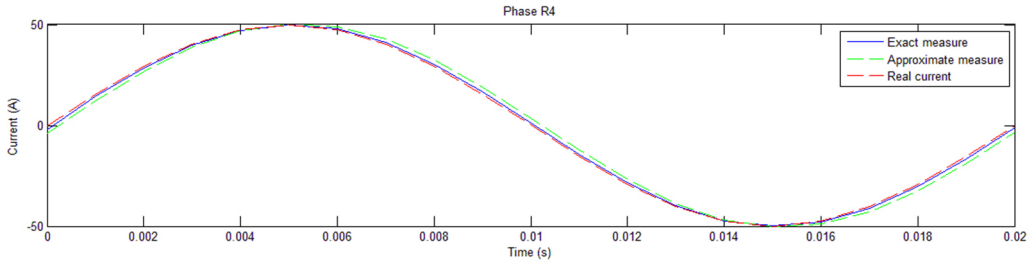
Phase R4
Exact measure
Approximate measure
Real current
Current (A)
Time (s)

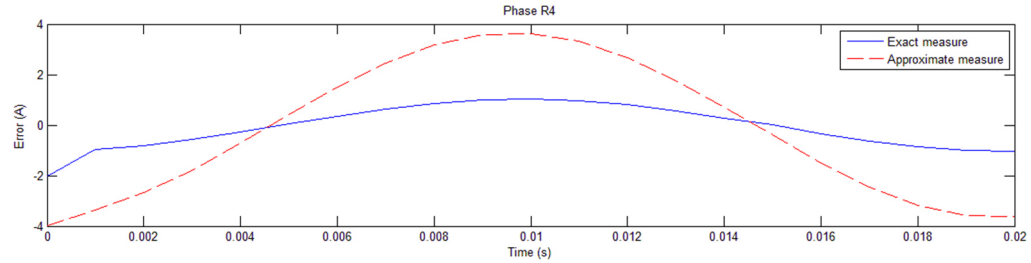
Phase R4
Exact measure
Approximate measure
Error (A)
Time (s)

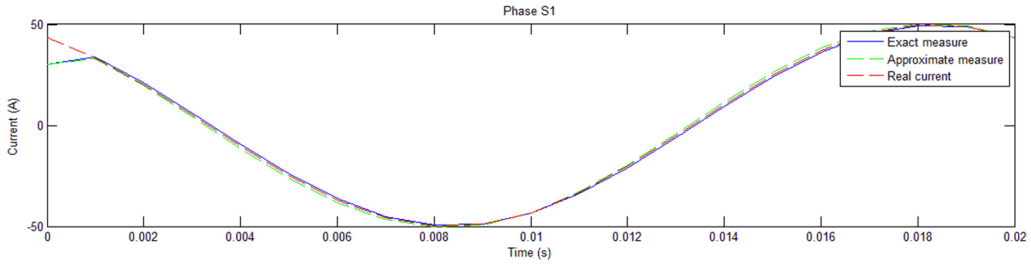
Phase S1
Exact measure
Approximate measure
Real current
Current (A)
Time (s)

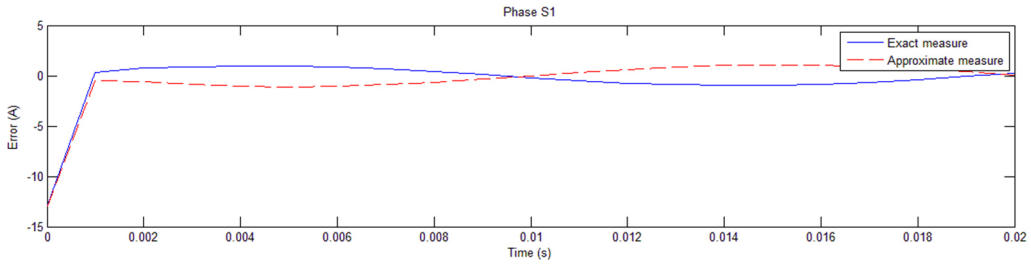
Phase S1
Exact measure
Approximate measure
Error (A)
Time (s)

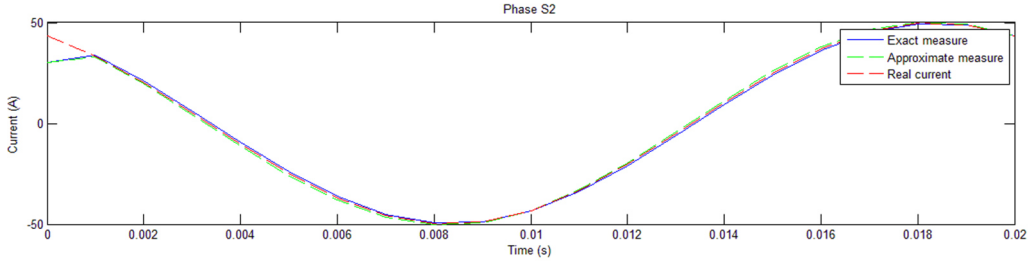
Phase S2
Exact measure
Approximate measure
Real current
Current (A)
Time (s)

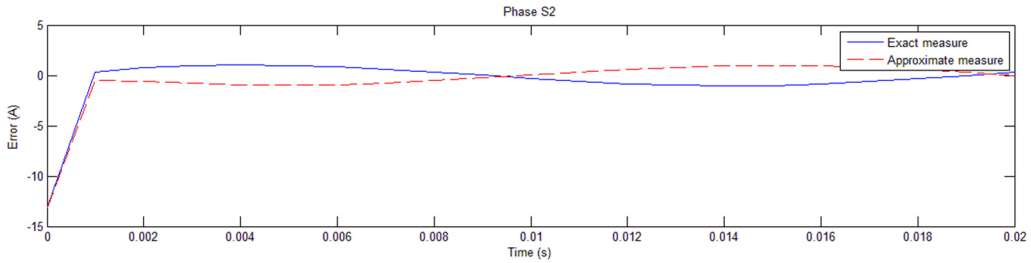
Phase S2
Exact measure
Approximate measure
Error (A)
Time (s)

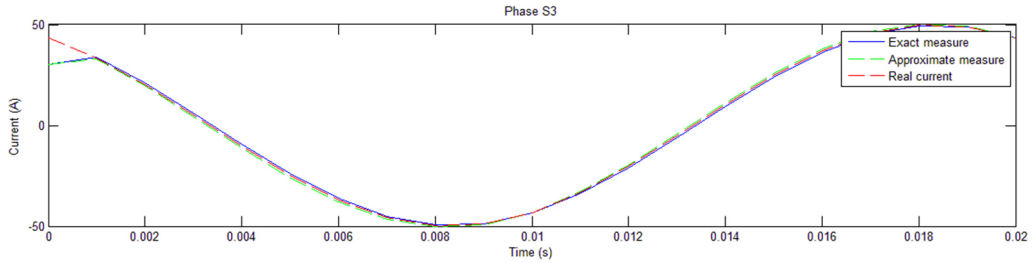
Phase S3
Current (A)
Time (s)
Exact measure
Approximate measure
Real current

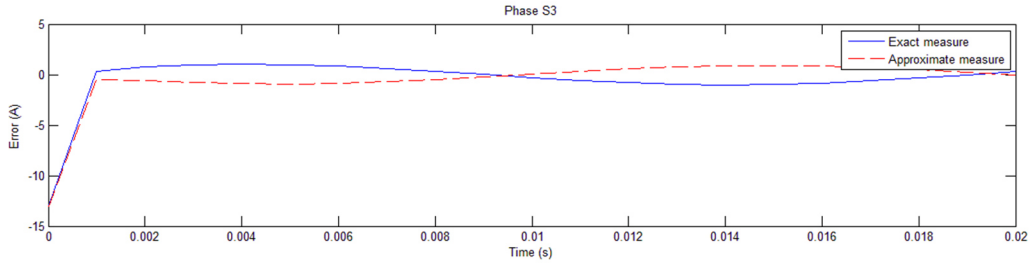
Phase S3
Error (A)
Time (s)
Exact measure
Approximate measure

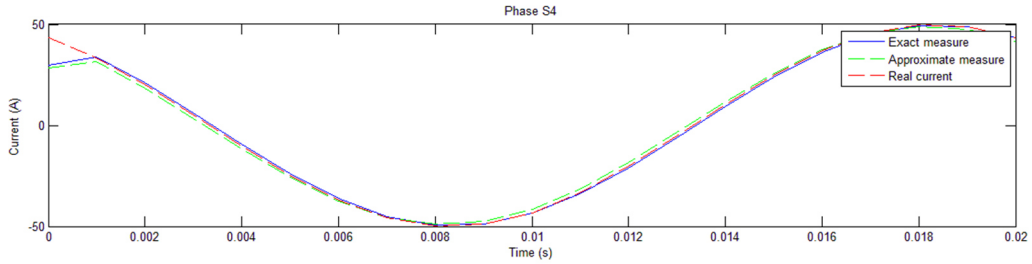
Phase S4
Current (A)
Time (s)
Exact measure
Approximate measure
Real current

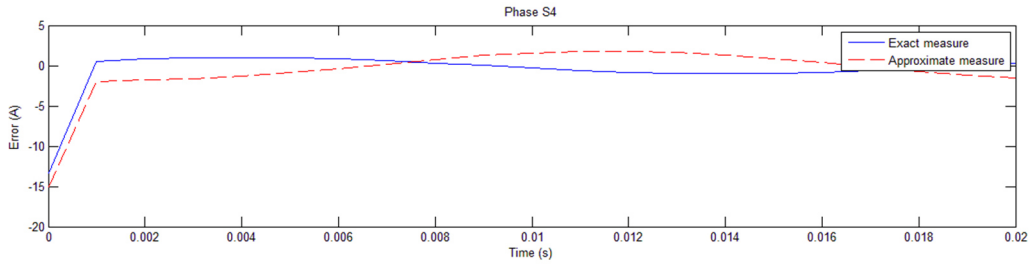
Phase S4
Error (A)
Time (s)
Exact measure
Approximate measure

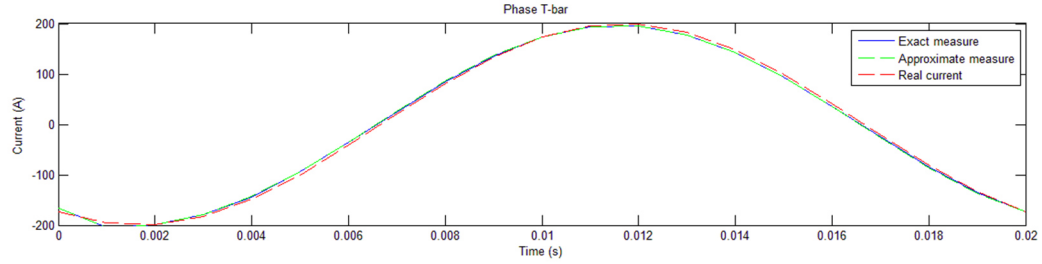
Phase T-bar
Current (A)
Time (s)
Exact measure
Approximate measure
Real current

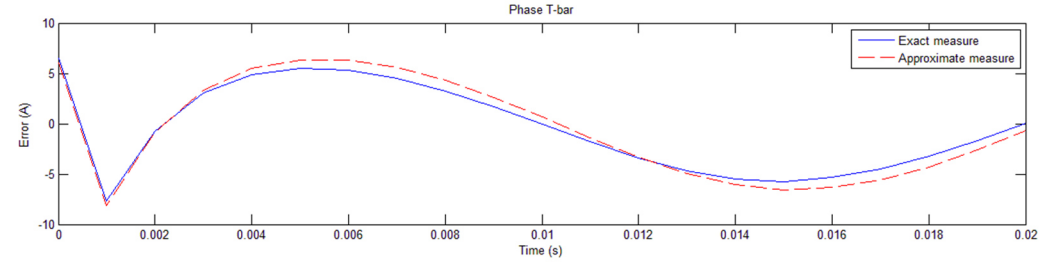
Phase T-bar
Error (A)
Time (s)
Exact measure
Approximate measure

- **PEAK VALUE = 100 [A]**

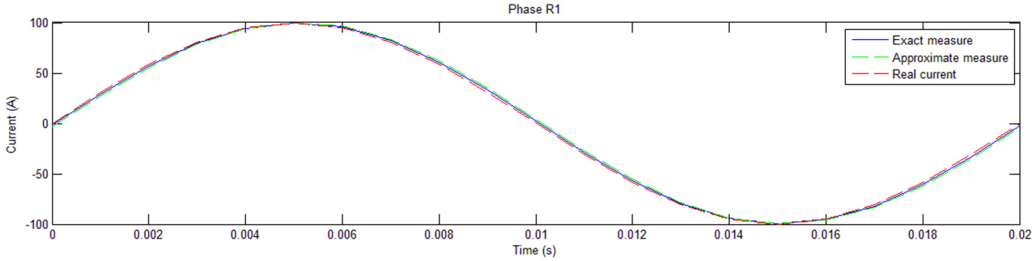

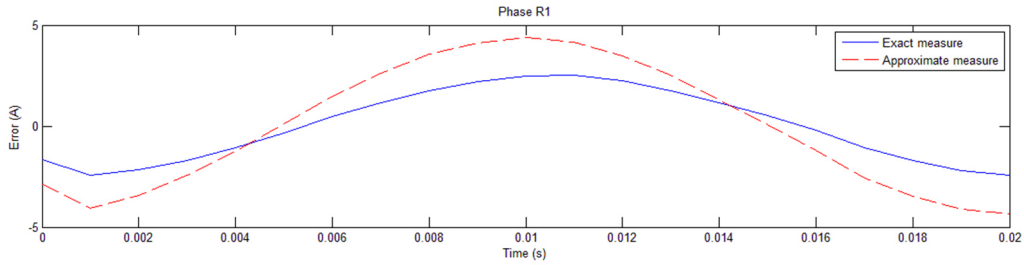

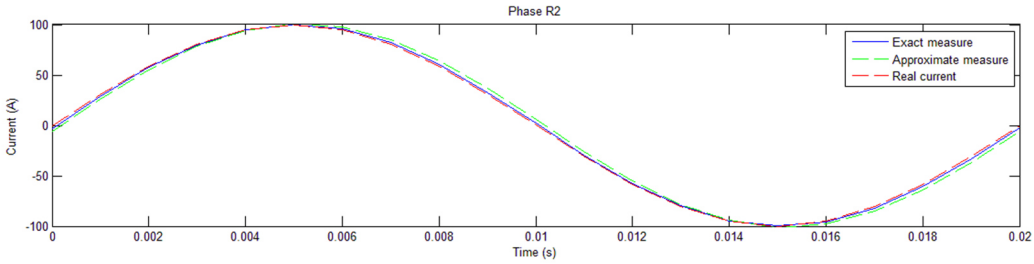

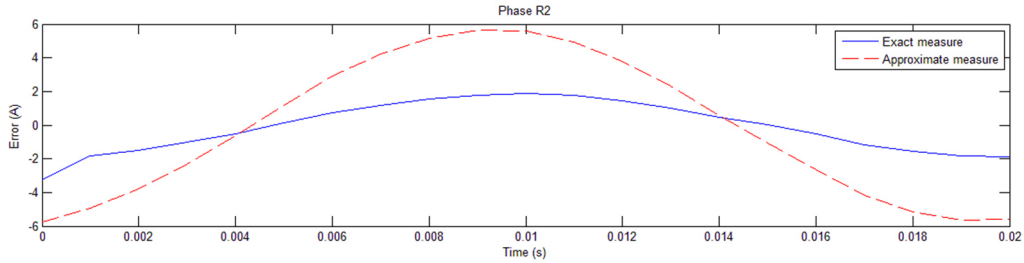

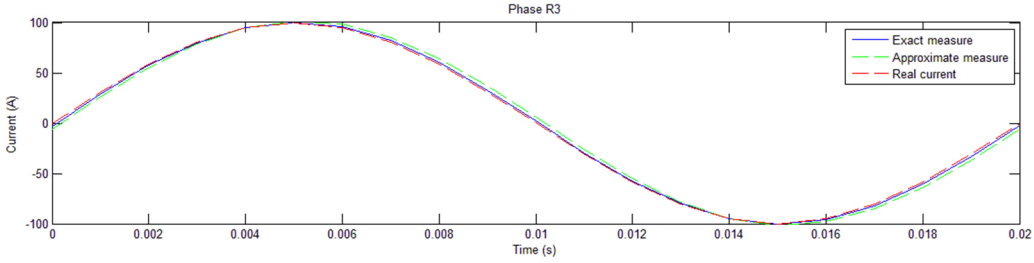

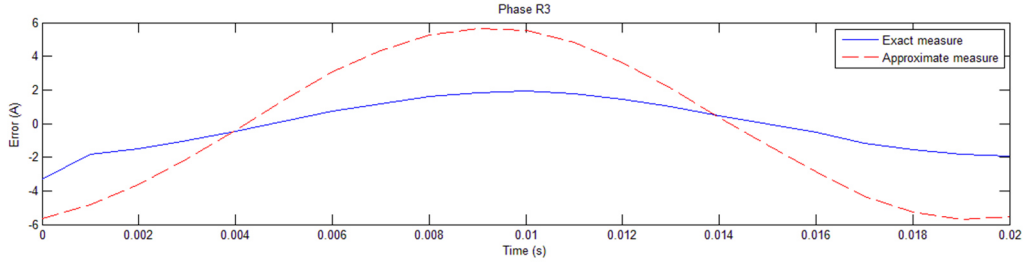

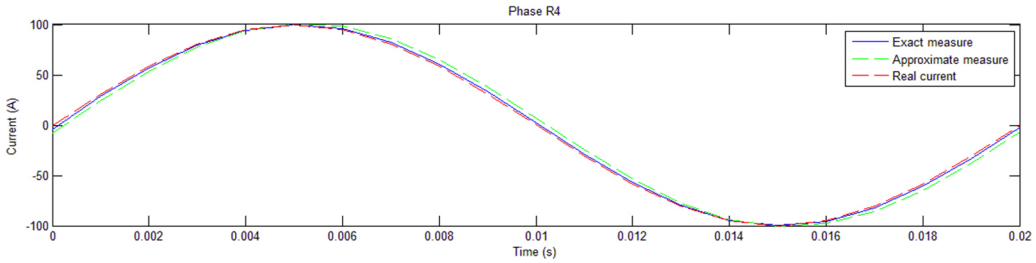
Phase R4
Exact measure
Approximate measure
Real current
Current (A)
Time (s)

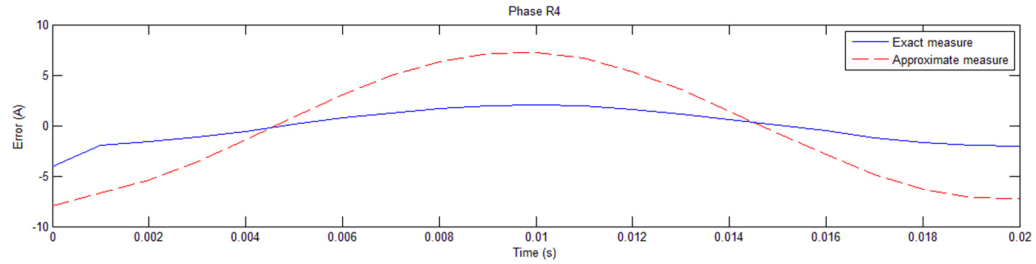
Phase R4
Exact measure
Approximate measure
Error (A)
Time (s)

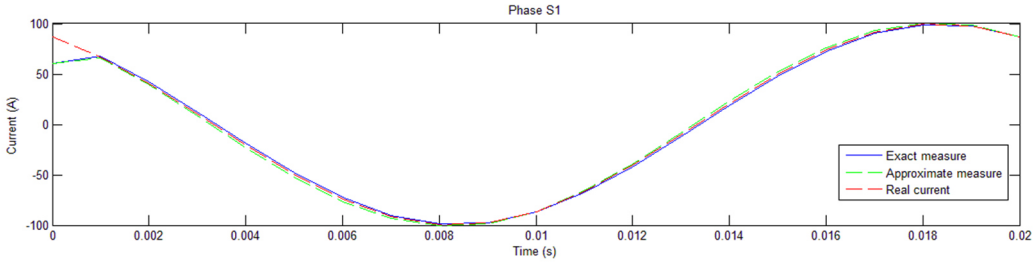
Phase S1
Exact measure
Approximate measure
Real current
Current (A)
Time (s)

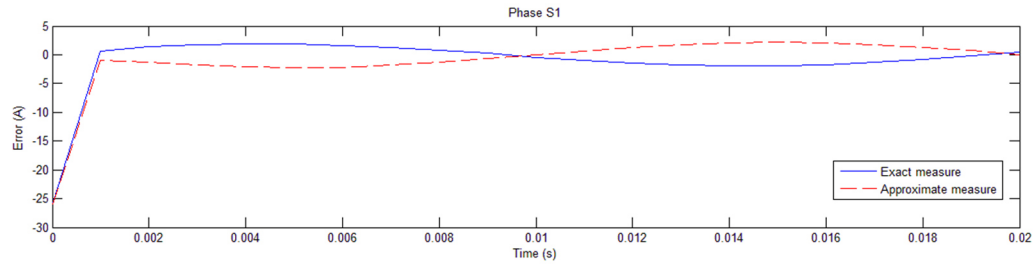
Phase S1
Exact measure
Approximate measure
Error (A)
Time (s)

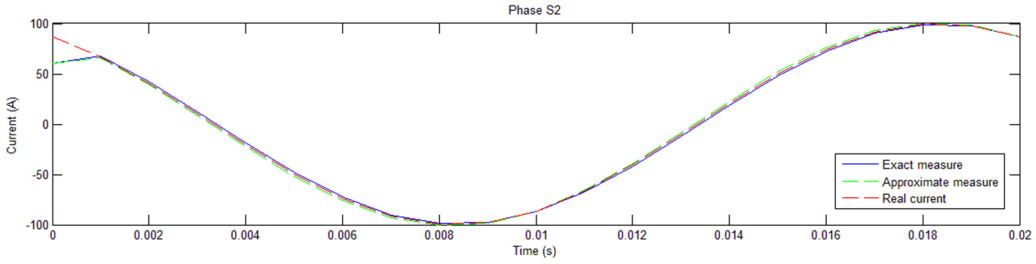
Phase S2
Exact measure
Approximate measure
Real current
Current (A)
Time (s)

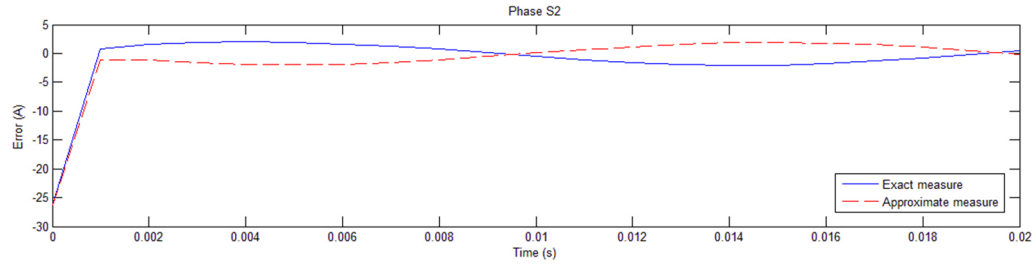
Phase S2
Exact measure
Approximate measure
Error (A)
Time (s)

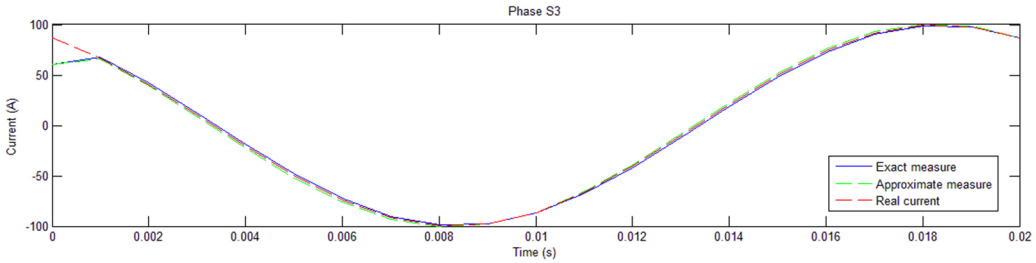
Phase S3
Current (A)
Time (s)
Exact measure
Approximate measure
Real current

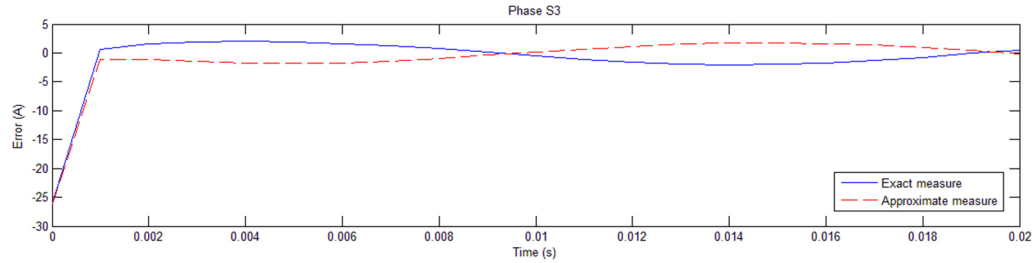
Phase S3
Error (A)
Time (s)
Exact measure
Approximate measure

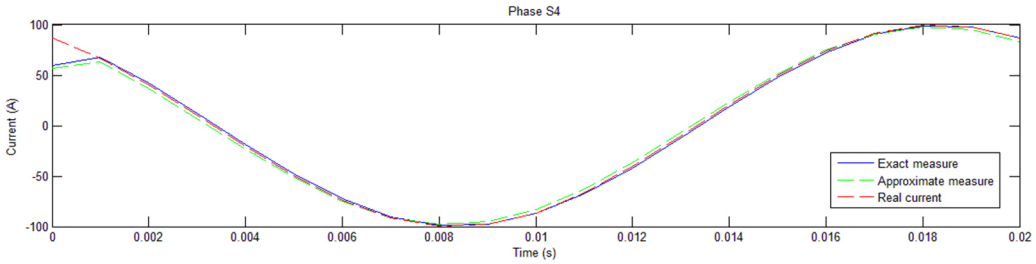
Phase S4
Current (A)
Time (s)
Exact measure
Approximate measure
Real current

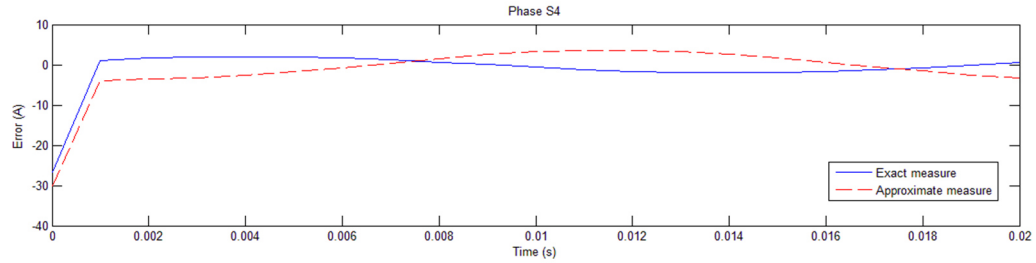
Phase S4
Error (A)
Time (s)
Exact measure
Approximate measure

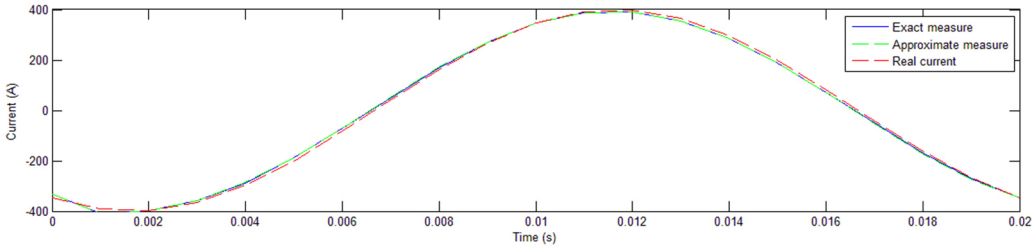
Current (A)
Time (s)
Exact measure
Approximate measure
Real current

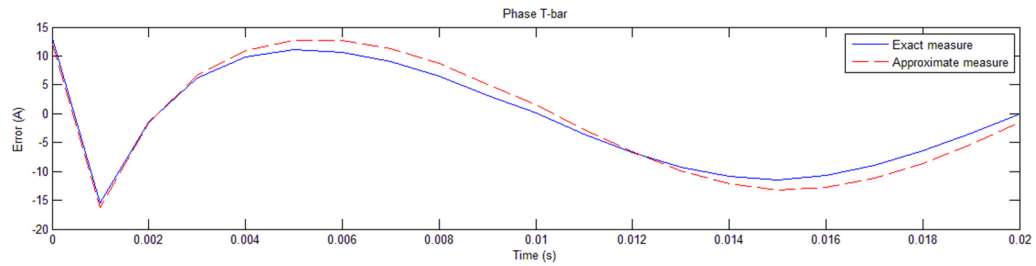
Phase T-bar
Error (A)
Time (s)
Exact measure
Approximate measure

Considerations:

As can be seen in the charts the development of the error in the time it's the same for the three different peak components used for the input current. This points to the fact that it may be possible to introduce an external factor in the equations in order to correct the errors in the current measure.

In the next paragraph it's explained how to derivate this external corrective coefficient and how it can correct the eventually measure errors.

10.2 Corrective coefficient for the measured current

The corrective coefficients in consideration will be grouped in a matrix that it's simply derived from the following equations:

(1.20) $$\left[K\right]_{corr} = \frac{\left[\vec{I}(t)\right]_{measured}}{\left[\vec{I}(t)\right]_{real}}$$

where:

$\left[K\right]_{corr}$ = matrix of the corrective coefficients;

$\left[\vec{I}(t)\right]_{measured}$ = matrix of the measured current;

$\left[\vec{I}(t)\right]_{real}$ = matrix of real currents flowing through the bars in the base case in which the sinusoidal currents are set with a peak value of 1A.

Then the implementation in the computing system will be done through the following expression:

(1.21) $$\left[\vec{I}(t)\right]_{correct} = \frac{\left[\vec{I}(t)\right]_{measured}}{\left[K\right]_{corr}}$$

Where $\left[\vec{I}(t)\right]_{correct}$ is the matrix of the currents measured corrected with the corrective coefficients matrix.

This will be true for every current and it will be implementable in the system only if every element of the matrix $\left[K\right]_{corr}$ it remains constant with the variation of the input current, initially set with a peak value of 1A to derive the matrix.

An example of corrective coefficients matrix for the case just studied it's represented in the next page.

$$|K|_{corr} = \begin{vmatrix}
inf & 0.7029 & inf & 0.6994 & inf & 0.7007 & inf & 0.6911 & 0.9623 \\
0.9217 & 1.0084 & 0.9408 & 1.0104 & 0.9402 & 1.0101 & 0.9368 & 1.0143 & 1.0394 \\
0.9632 & 1.0362 & 0.9748 & 1.0397 & 0.9747 & 1.0393 & 0.9727 & 1.0427 & 1.0037 \\
0.979 & 1.1719 & 0.9872 & 1.1843 & 0.9873 & 1.1822 & 0.9859 & 1.1874 & 0.9832 \\
0.9887 & 0.9068 & 0.9948 & 0.9018 & 0.995 & 0.903 & 0.9941 & 0.9026 & 0.967 \\
0.9967 & 0.9623 & 1.0011 & 0.9609 & 1.0012 & 0.9614 & 1.0009 & 0.9617 & 0.9448 \\
1.0046 & 0.9778 & 1.0072 & 0.9774 & 1.0074 & 0.9777 & 1.0074 & 0.9781 & 0.8723 \\
1.014 & 0.9857 & 1.0143 & 0.986 & 1.0146 & 0.9862 & 1.0153 & 0.9866 & 1.216 \\
1.0301 & 0.9921 & 1.0267 & 0.9928 & 1.0271 & 0.9929 & 1.0287 & 0.9933 & 1.0399 \\
1.0736 & 0.9988 & 1.0598 & 0.9999 & 1.0606 & 0.9999 & 1.0647 & 1.0004 & 1.0126 \\
inf & 0.7029 & inf & 0.6994 & inf & 0.7007 & inf & 0.6911 & 0.9623 \\
0.9193 & 1.0157 & 0.9425 & 1.018 & 0.9422 & 1.0178 & 0.9371 & 1.0183 & 0.9902 \\
0.9619 & 1.0366 & 0.9751 & 1.0404 & 0.975 & 1.0399 & 0.9725 & 1.0403 & 0.9823 \\
0.9781 & 1.172 & 0.9875 & 1.1857 & 0.9875 & 1.1834 & 0.986 & 1.1837 & 0.9743 \\
0.9879 & 0.9069 & 0.9949 & 0.9012 & 0.995 & 0.9025 & 0.9941 & 0.9031 & 0.963 \\
0.9956 & 0.962 & 1.0008 & 0.9604 & 1.0009 & 0.961 & 1.0004 & 0.9615 & 0.943 \\
1.0036 & 0.9775 & 1.0069 & 0.977 & 1.007 & 0.9773 & 1.0071 & 0.9778 & 0.8713 \\
1.0136 & 0.986 & 1.0147 & 0.9861 & 1.0149 & 0.9864 & 1.0156 & 0.9868 & 1.2159 \\
1.0297 & 0.9924 & 1.0272 & 0.9929 & 1.0275 & 0.9931 & 1.0291 & 0.9936 & 1.0399 \\
1.0706 & 0.9976 & 1.0589 & 0.9986 & 1.0595 & 0.9987 & 1.0637 & 0.9992 & 1.0123 \\
inf & 0.7029 & inf & 0.6994 & inf & 0.7007 & inf & 0.6911 & 0.9623
\end{vmatrix}$$

10.2.1 Test of the invariance of the matrix

An important test to do before to implement, in the measuring system, the corrective coefficient it's to assure that the relative error be constant for every current that can interest the bars.

To do this test it has been preferred to follow a simpler approach calculating the difference between two corrective coefficients matrices obtained with different input currents. An example of the various tests done is represented in the next matrix, in which it was calculated the difference between the corrective coefficient matrix computed with an input current of 50A and the matrix with an input current of 1A:

$$|K_{corr}|_{50A} - |K_{corr}|_{1A} = \begin{vmatrix}
0.0000 & 0.0000 & 0.0000 & 0.0000 & 0.0000 & 0.0000 & 0.0000 & 0.0000 & 0.0000 \\
0.0001 & 0.0001 & 0.0001 & 0.0001 & 0.0000 & 0.0001 & 0.0000 & 0.0001 & 0.0000 \\
0.0000 & 0.0000 & 0.0000 & 0.0000 & 0.0000 & 0.0001 & 0.0000 & 0.0000 & 0.0001 \\
0.0000 & 0.0001 & 0.0000 & 0.0001 & 0.0000 & 0.0000 & 0.0000 & 0.0000 & 0.0000 \\
0.0001 & 0.0001 & 0.0001 & 0.0001 & 0.0000 & 0.0000 & 0.0000 & 0.0000 & 0.0000 \\
0.0000 & 0.0000 & 0.0000 & 0.0001 & 0.0001 & 0.0001 & 0.0000 & 0.0001 & 0.0003 \\
0.0003 & 0.0003 & 0.0003 & 0.0002 & 0.0002 & 0.0001 & 0.0001 & 0.0001 & 0.0002 \\
0.0001 & 0.0001 & 0.0001 & 0.0001 & 0.0000 & 0.0001 & 0.0001 & 0.0001 & 0.0001 \\
0.0003 & 0.0002 & 0.0001 & 0.0001 & 0.0002 & 0.0001 & 0.0002 & 0.0002 & 0.0001 \\
0.0014 & 0.0010 & 0.0010 & 0.0010 & 0.0012 & 0.0010 & 0.0010 & 0.0010 & 0.0001 \\
0.0000 & 0.0000 & 0.0000 & 0.0000 & 0.0000 & 0.0000 & 0.0000 & 0.0000 & 0.0000 \\
0.0002 & 0.0005 & 0.0001 & 0.0005 & 0.0001 & 0.0005 & 0.0001 & 0.0005 & 0.0006 \\
0.0002 & 0.0001 & 0.0001 & 0.0001 & 0.0001 & 0.0002 & 0.0001 & 0.0002 & 0.0005 \\
0.0000 & 0.0000 & 0.0001 & 0.0000 & 0.0000 & 0.0000 & 0.0001 & 0.0001 & 0.0000 \\
0.0002 & 0.0001 & 0.0001 & 0.0001 & 0.0001 & 0.0002 & 0.0001 & 0.0001 & 0.0002 \\
0.0005 & 0.0004 & 0.0006 & 0.0004 & 0.0006 & 0.0005 & 0.0005 & 0.0005 & 0.0004 \\
0.0004 & 0.0003 & 0.0003 & 0.0003 & 0.0004 & 0.0004 & 0.0004 & 0.0003 & 0.0005 \\
0.0000 & 0.0000 & 0.0000 & 0.0001 & 0.0000 & 0.0000 & 0.0000 & 0.0001 & 0.0003 \\
0.0003 & 0.0003 & 0.0003 & 0.0003 & 0.0003 & 0.0003 & 0.0003 & 0.0003 & 0.0001 \\
0.0011 & 0.0008 & 0.0010 & 0.0008 & 0.0010 & 0.0007 & 0.0009 & 0.0007 & 0.0002 \\
0.0000 & 0.0000 & 0.0000 & 0.0000 & 0.0000 & 0.0000 & 0.0000 & 0.0000 & 0.0000
\end{vmatrix}$$

As can be seen, the difference between the two matrices obtained with different currents is next to zero and thus it means that the various corrective coefficients remain constants for different input currents. Consequently, also the relative error will be constant, as it can be understood in the previous graphs.

10.2.2 Results with the corrective coefficient

The following graphs considerate the trends of currents and errors with the implementation of the corrective coefficients as explained before.

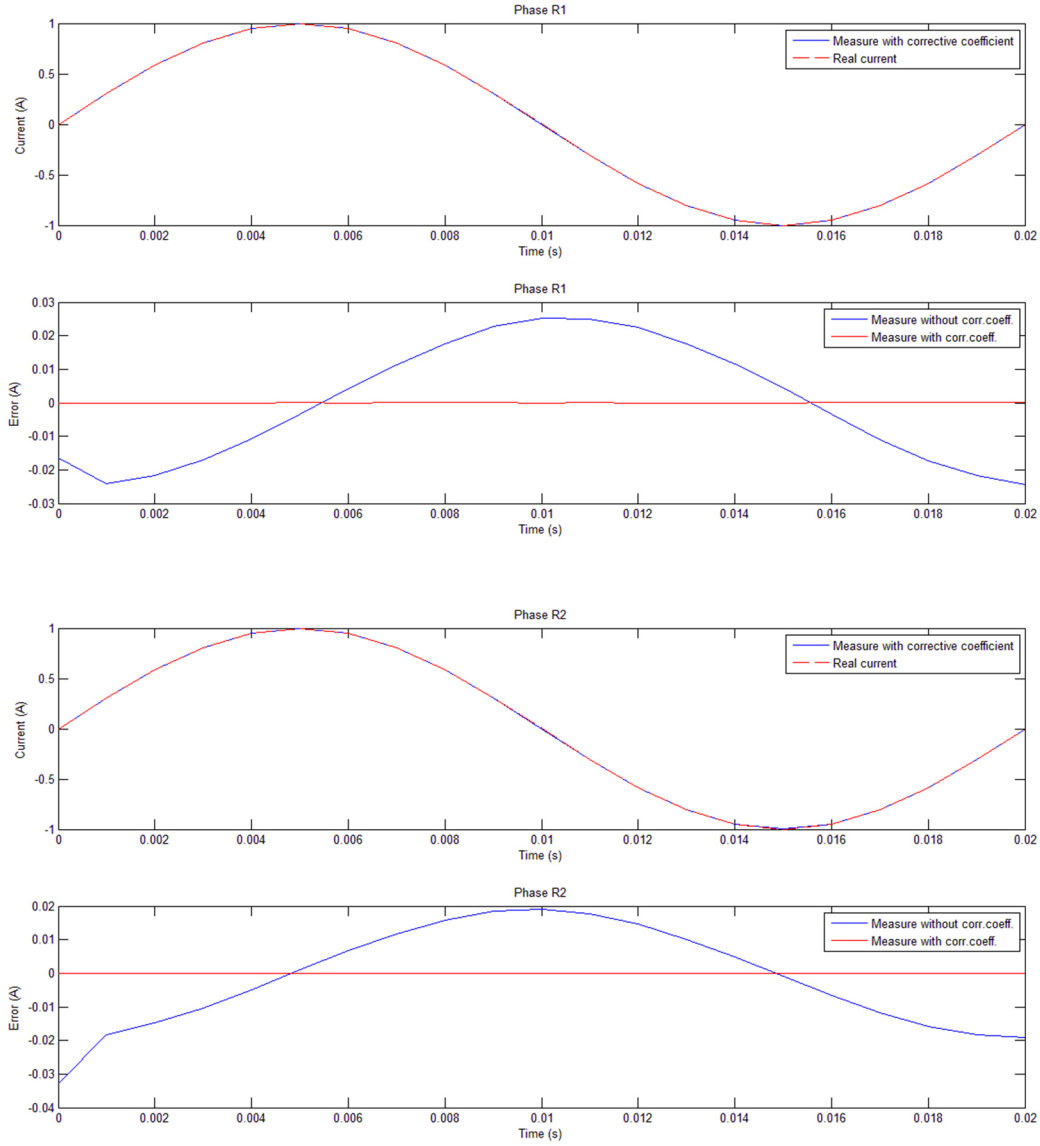

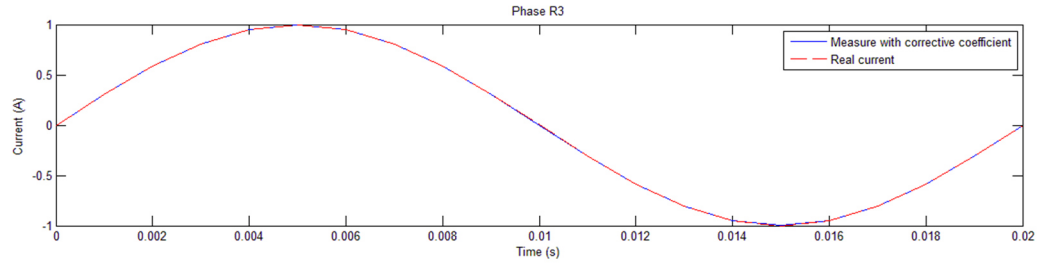
Phase R3
Measure with corrective coefficient
Real current
Current (A)
Time (s)

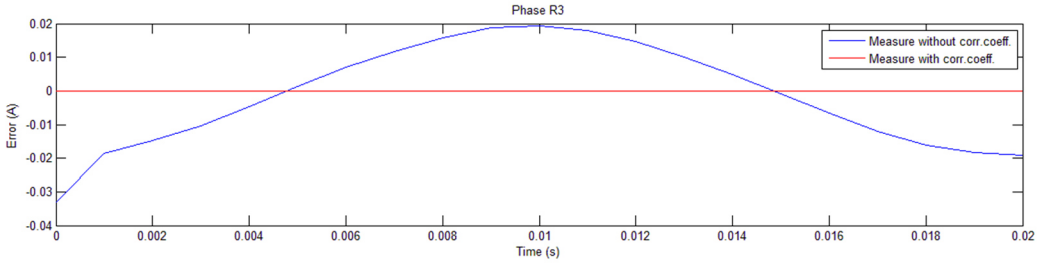
Phase R3
Measure without corr.coeff.
Measure with corr.coeff.
Error (A)
Time (s)

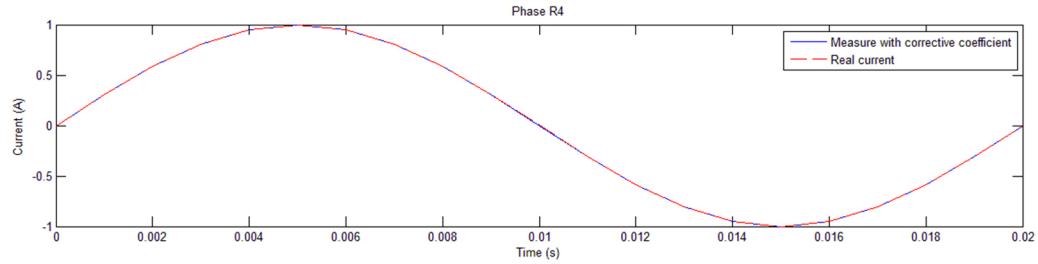
Phase R4
Measure with corrective coefficient
Real current
Current (A)
Time (s)

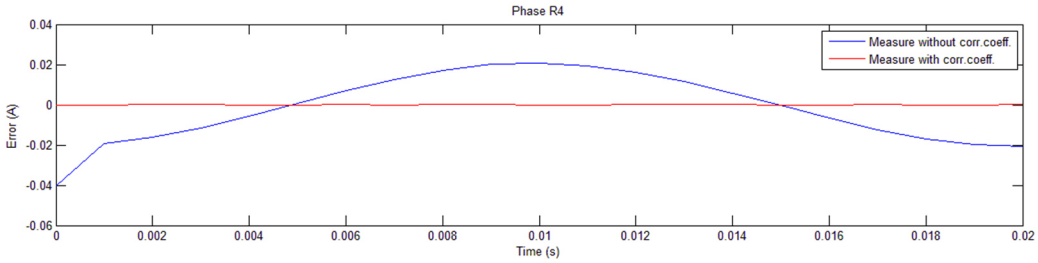
Phase R4
Measure without corr.coeff.
Measure with corr.coeff.
Error (A)
Time (s)

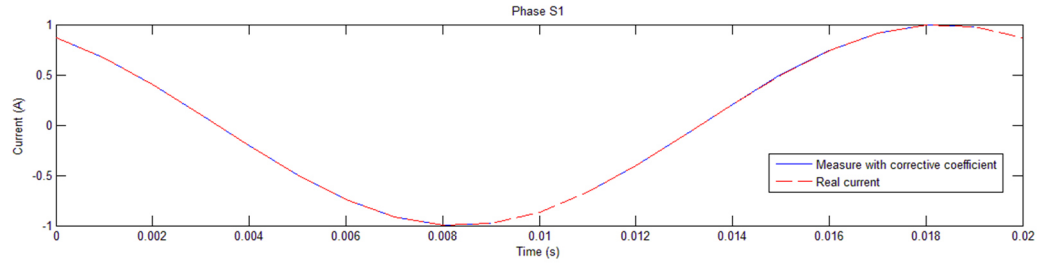
Phase S1
Measure with corrective coefficient
Real current
Current (A)
Time (s)

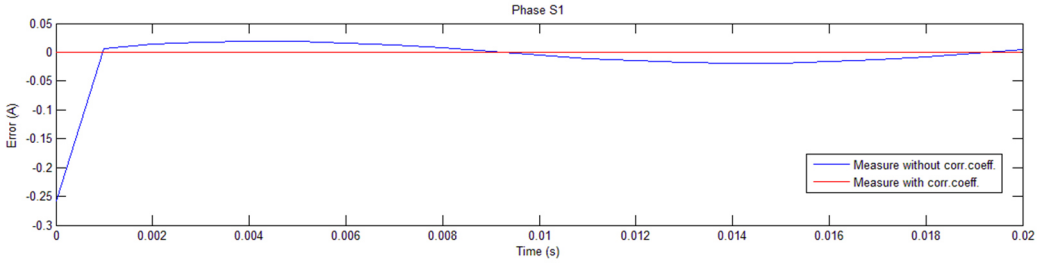
Phase S1
Measure without corr.coeff.
Measure with corr.coeff.
Error (A)
Time (s)

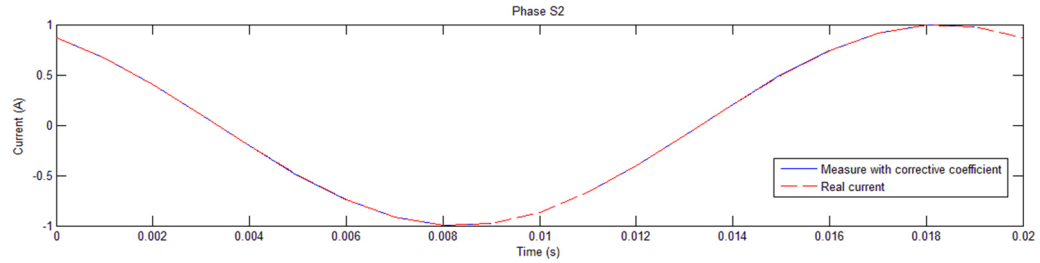
Phase S2
Current (A)
Time (s)
Measure with corrective coefficient
Real current

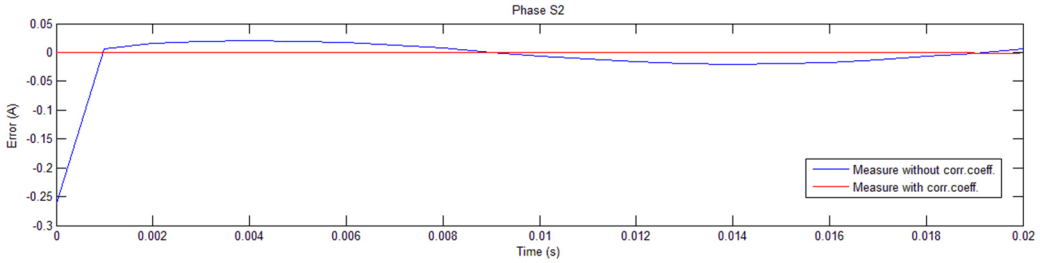
Phase S2
Error (A)
Time (s)
Measure without corr.coeff.
Measure with corr.coeff.

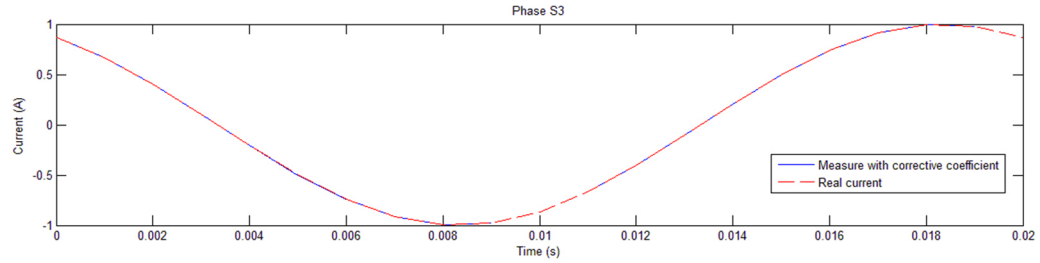
Phase S3
Current (A)
Time (s)
Measure with corrective coefficient
Real current

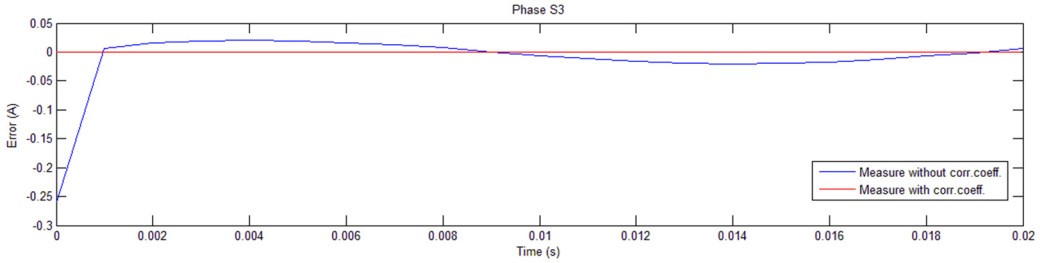
Phase S3
Error (A)
Time (s)
Measure without corr.coeff.
Measure with corr.coeff.

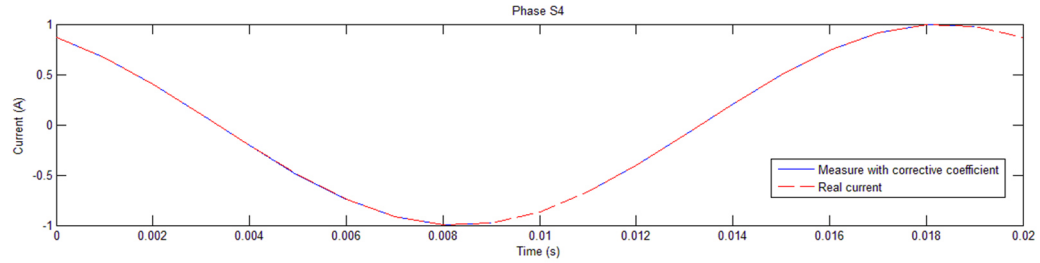
Phase S4
Current (A)
Time (s)
Measure with corrective coefficient
Real current

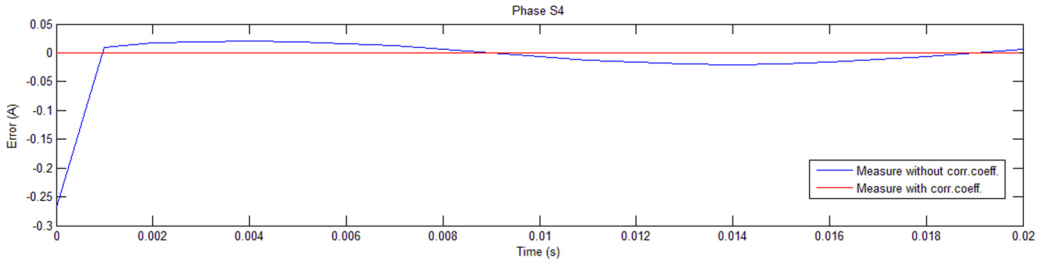
Phase S4
Error (A)
Time (s)
Measure without corr.coeff.
Measure with corr.coeff.

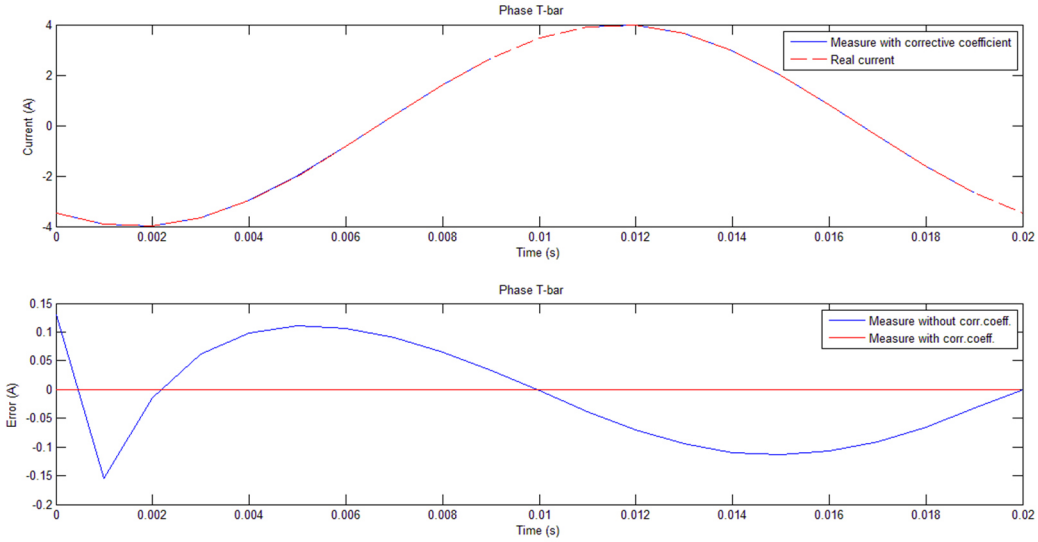

Considerations:

In the preceding graphs is possible to note that with the implementation of the correctives coefficients matrix the error in the measure it will be zero for every phase-bar considerate.

This consideration it's valid also for other input currents as can be seen in the following graphic example, so in this way it has been obtain a perfect virtual measure system for the monitoring of the currents flowing through the bars.

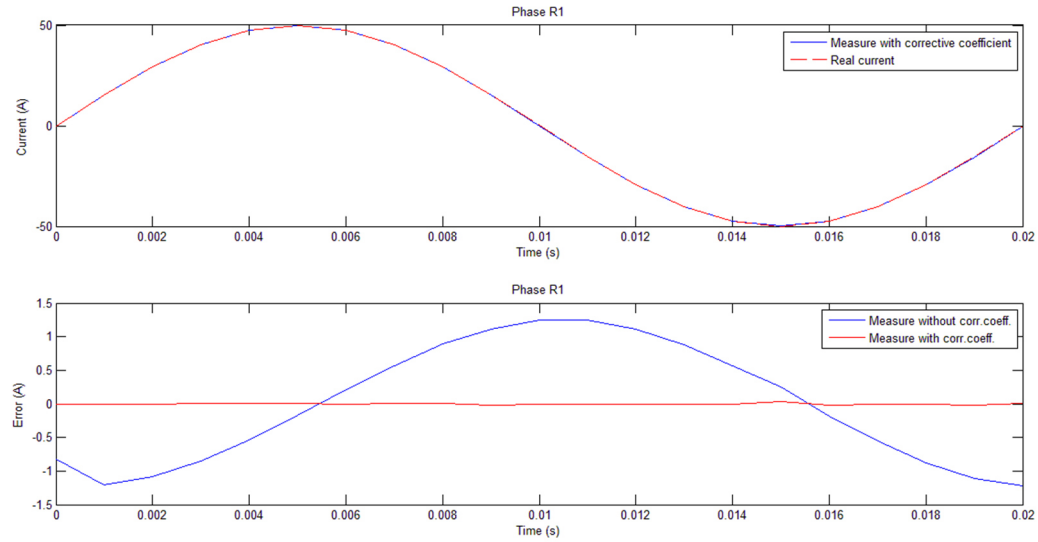

Fig. 10.1 Trends of currents and errors, case with corrective coefficient. Phase R_1, $I_{peak,input}$ = 50 A

10.3 A particular case: unbalanced electrical system

In this paragraph it will be taken into consideration the same system of the previous paragraphs but subject to unbalanced input currents for the phases R, S, T of every circuit.

This implies that there will be to considerate also a current that it flows in the neutral bar that will be the vector sum of all the currents flowing in all the circuits.

For this case, characterized by an unbalanced system, there will be completely described only the results for the cases that considered the mutual inductance effects.

The respected value of input currents set for the different circuits are:

$\vec{I}_{R1} = I_{r1} \sin(2\pi\ 50\ t)$	$I_{r1} = 10\ [A]$
$\vec{I}_{R2} = I_{r2} \sin(2\pi\ 50\ t)$	$I_{r2} = 30\ [A]$
$\vec{I}_{R3} = I_{r3} \sin(2\pi\ 50\ t)$	$I_{r3} = 40\ [A]$
$\vec{I}_{R4} = I_{r4} \sin(2\pi\ 50\ t)$	$I_{r4} = 50\ [A]$
$\vec{I}_{S1} = I_{s1} \sin(2\pi\ 50\ t + 2\pi / 3)$	$I_{s1} = 12\ [A]$
$\vec{I}_{S2} = I_{s2} \sin(2\pi\ 50\ t + 2\pi / 3)$	$I_{s2} = 32\ [A]$
$\vec{I}_{S3} = I_{s3} \sin(2\pi\ 50\ t + 2\pi / 3)$	$I_{s3} = 42\ [A]$
$\vec{I}_{S4} = I_{s4} \sin(2\pi\ 50\ t + 2\pi / 3)$	$I_{s4} = 51\ [A]$

Where $I_{r1} \ldots I_{s4}$ are the peak values of the alternative currents considered.

To impose the current that flows into the neutral bar it was used the expression:

$$\vec{I}_N = - \left(\sum_{n=1}^{4} \vec{I}_{Rn} + \sum_{n=1}^{4} \vec{I}_{Sn} \right)$$

Also for this case will be study the following two cases:

1. Case neglecting the mutual inductance effect

For this particular case there will not be included the graphs regarding the case neglecting the mutual inductance effect because it will not have a practical interest. Anyway, summarizing the results, it has been noted inspecting the graphs that, like in the balanced system, the error is very next to zero for every sensor considerate.

A graphical example of this case it can be the following:

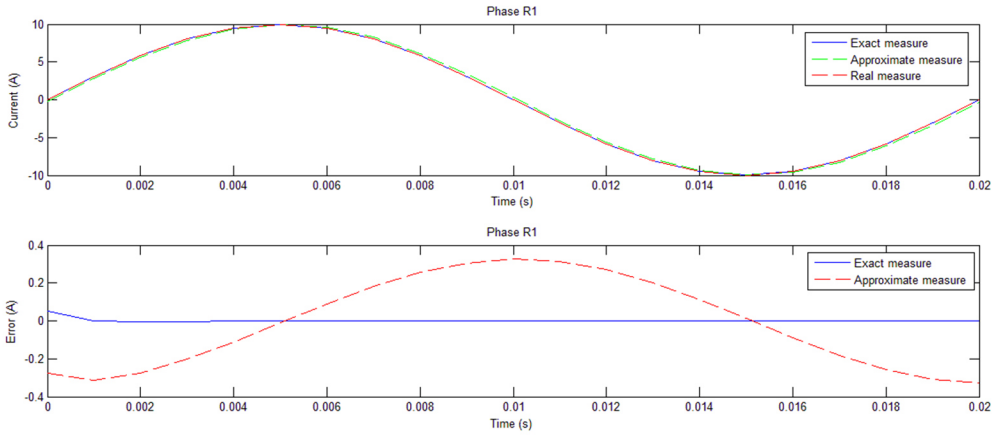

2. Case considering the mutual inductance effect

The matrix $\left[\vec{B}(t)\right]$ used for the computing of the results was:

$|B(t)|=$

Time [s]	R1	S1	R2	S2	R3	S3	R4	S4	N
0	-14.029	232.22	-40.35	627.38	-67.211	822.61	-109.33	960.28	-59.984
0.001	83.413	248.42	259.18	681.4	340.61	894.21	407.01	1064.6	-15.872
0.002	176.19	143.16	538.68	406.68	716.19	535.28	879.35	637.27	-1.4902
0.003	251.8	22.117	765.78	87.581	1022	117.89	1265.6	140.18	13.38
0.004	302.91	-101.24	918.36	-240.5	1228.3	-311.59	1528.6	-371.2	27.037
0.005	324.16	-214.76	980.44	-545.18	1313.6	-710.76	1641	-846.43	38.41
0.006	313.69	-307.24	946.59	-796.46	1270.4	-1040.3	1592.7	-1238.7	46.382
0.007	272.54	-369.66	820.16	-969.79	1102.9	-1268.1	1388.7	-1509.8	50.133
0.008	204.65	-395.81	613.29	-1048	827.26	-1371.4	1048.5	-1632.7	49.252
0.009	116.67	-382.9	346.21	-1022.7	470.4	-1339.4	605.42	-1594.4	43.765
0.01	17.502	-332.56	45.927	-897.49	68.4	-1176.4	104.16	-1400.3	33.893
0.011	-83.489	-250.56	-259.19	-686.82	-340.74	-901.46	-407.82	-1072.9	20.751
0.012	-176.28	-143.35	-538.82	-407.07	-716.38	-535.85	-879.76	-637.62	5.5844
0.013	-251.91	-22.161	-766.01	-87.631	-1022.3	-117.98	-1266	-140.13	-10.139
0.014	-302.94	101.22	-918.39	240.49	-1228.4	311.56	-1528.7	371.25	-24.491
0.015	-323.99	214.65	-979.88	544.91	-1312.9	710.4	-1640	846.02	-36.633
0.016	-313.71	307.25	-946.63	796.48	-1270.4	1040.3	-1592.8	1238.8	-45.191
0.017	-272.57	369.69	-820.25	969.89	-1103	1268.2	-1388.9	1509.9	-49.329
0.018	-204.67	395.83	-613.34	1048	-827.31	1371.5	-1048.6	1632.8	-48.689
0.019	-116.72	383.06	-346.36	1023.1	-470.6	1339.9	-605.68	1595	-43.388
0.02	-17.5	333.15	-45.907	899.09	-68.379	1178.5	-104.15	1402.8	-33.706

10.3.1 Graphical results

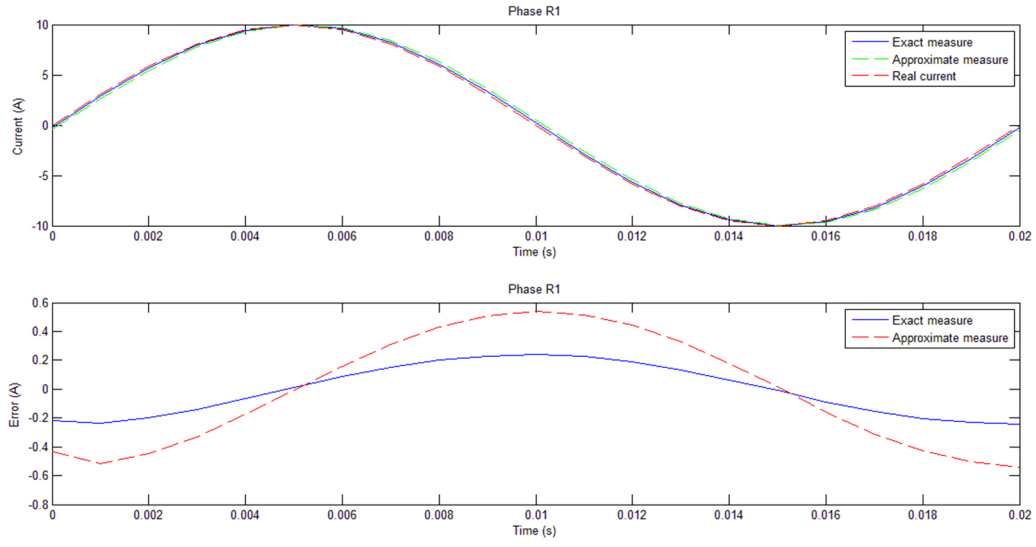

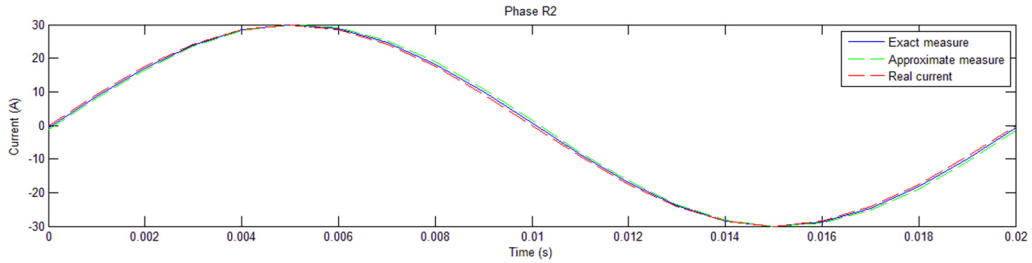
Phase R2
Exact measure
Approximate measure
Real current
Current (A)
Time (s)

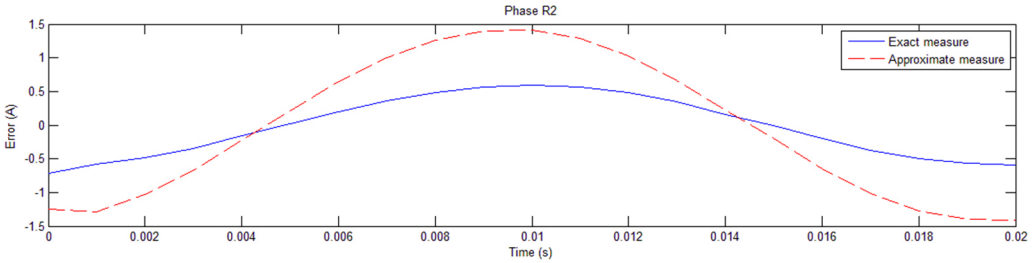
Phase R2
Exact measure
Approximate measure
Error (A)
Time (s)

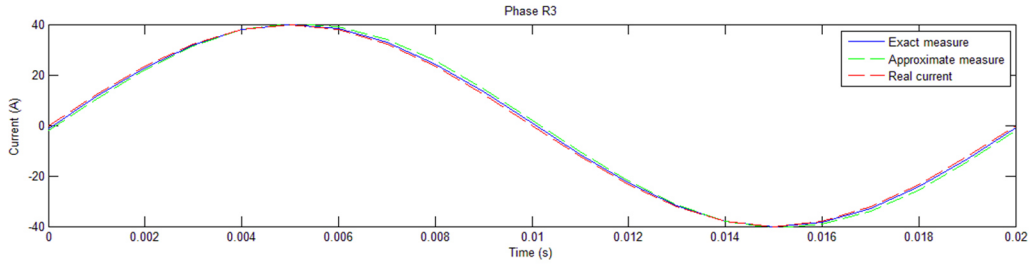
Phase R3
Exact measure
Approximate measure
Real current
Current (A)
Time (s)

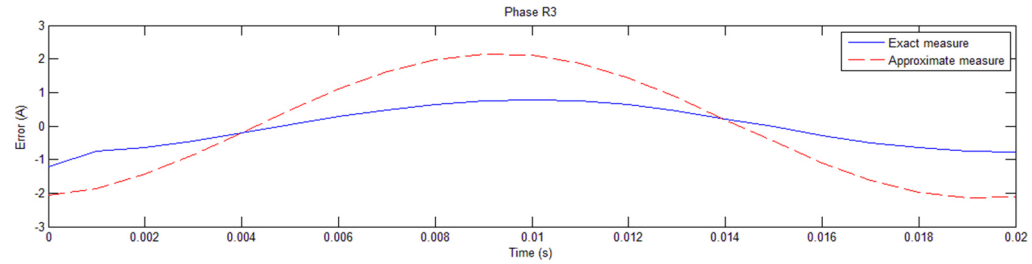
Phase R3
Exact measure
Approximate measure
Error (A)
Time (s)

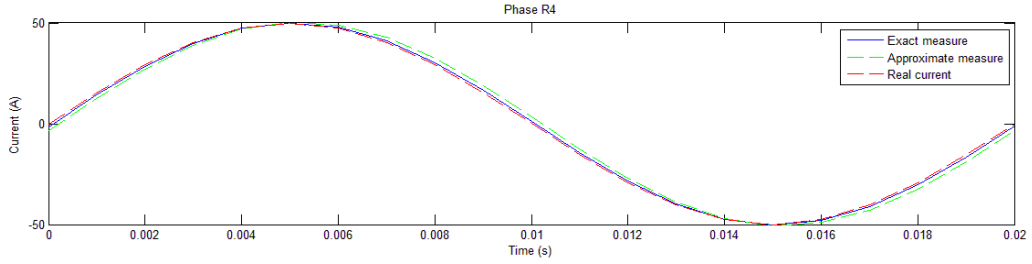
Phase R4
Exact measure
Approximate measure
Real current
Current (A)
Time (s)

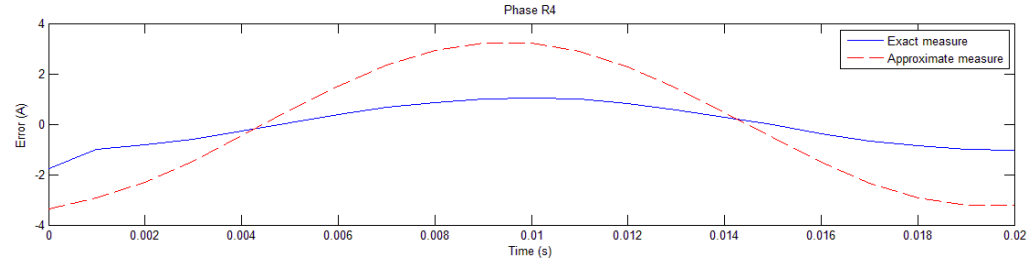
Phase R4
Exact measure
Approximate measure
Error (A)
Time (s)

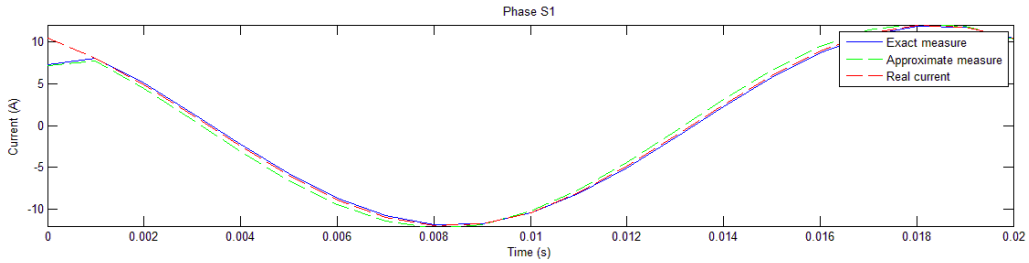
Phase S1
Exact measure
Approximate measure
Real current
Current (A)
Time (s)

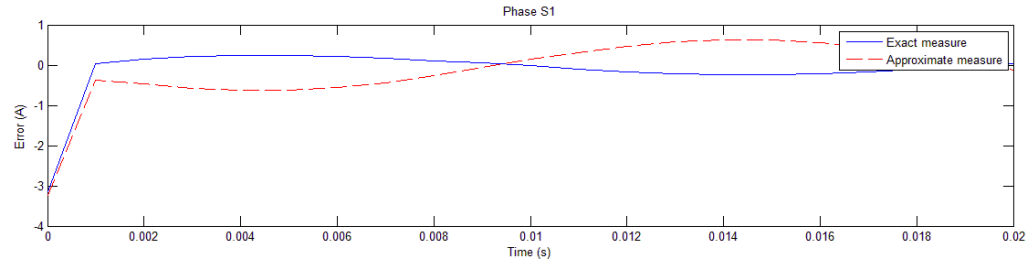
Phase S1
Exact measure
Approximate measure
Error (A)
Time (s)

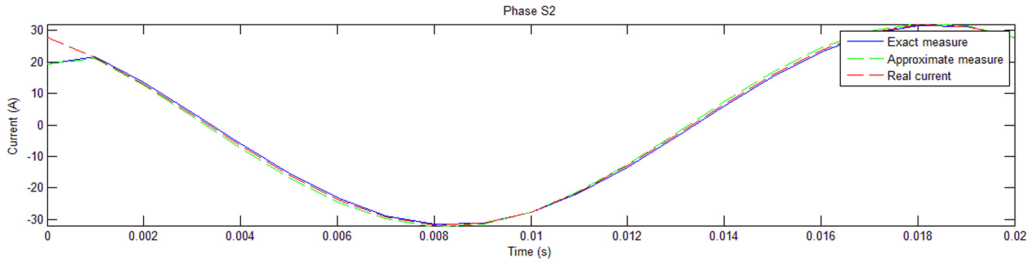
Phase S2
Exact measure
Approximate measure
Real current
Current (A)
Time (s)

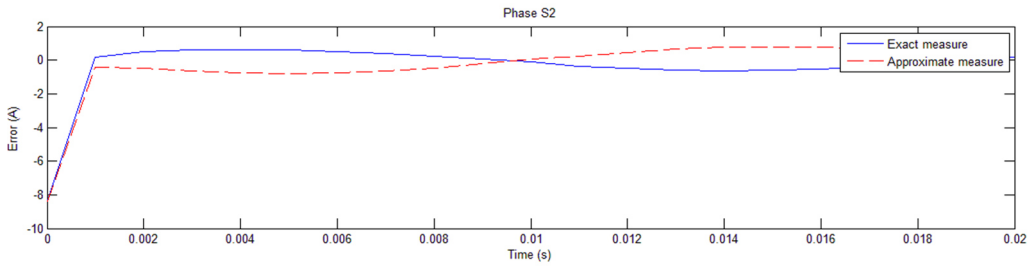
Phase S2
Exact measure
Approximate measure
Error (A)
Time (s)

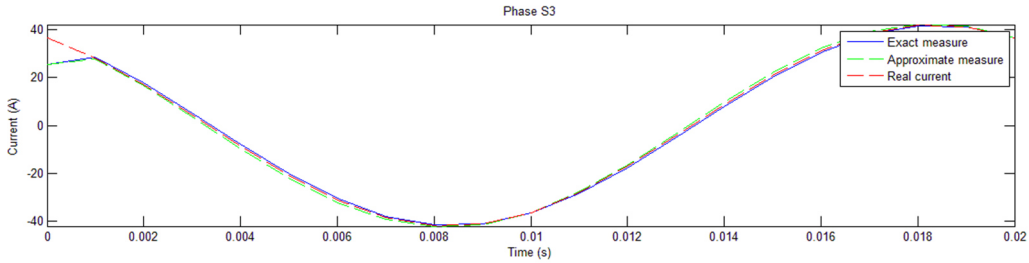
Phase S3
Exact measure
Approximate measure
Real current
Current (A)
Time (s)

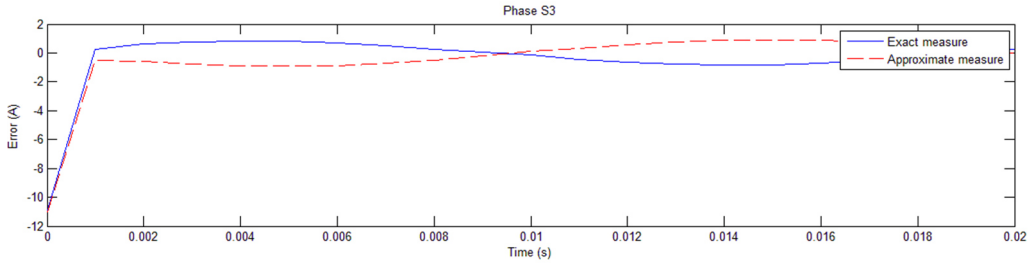
Phase S3
Exact measure
Approximate measure
Error (A)
Time (s)

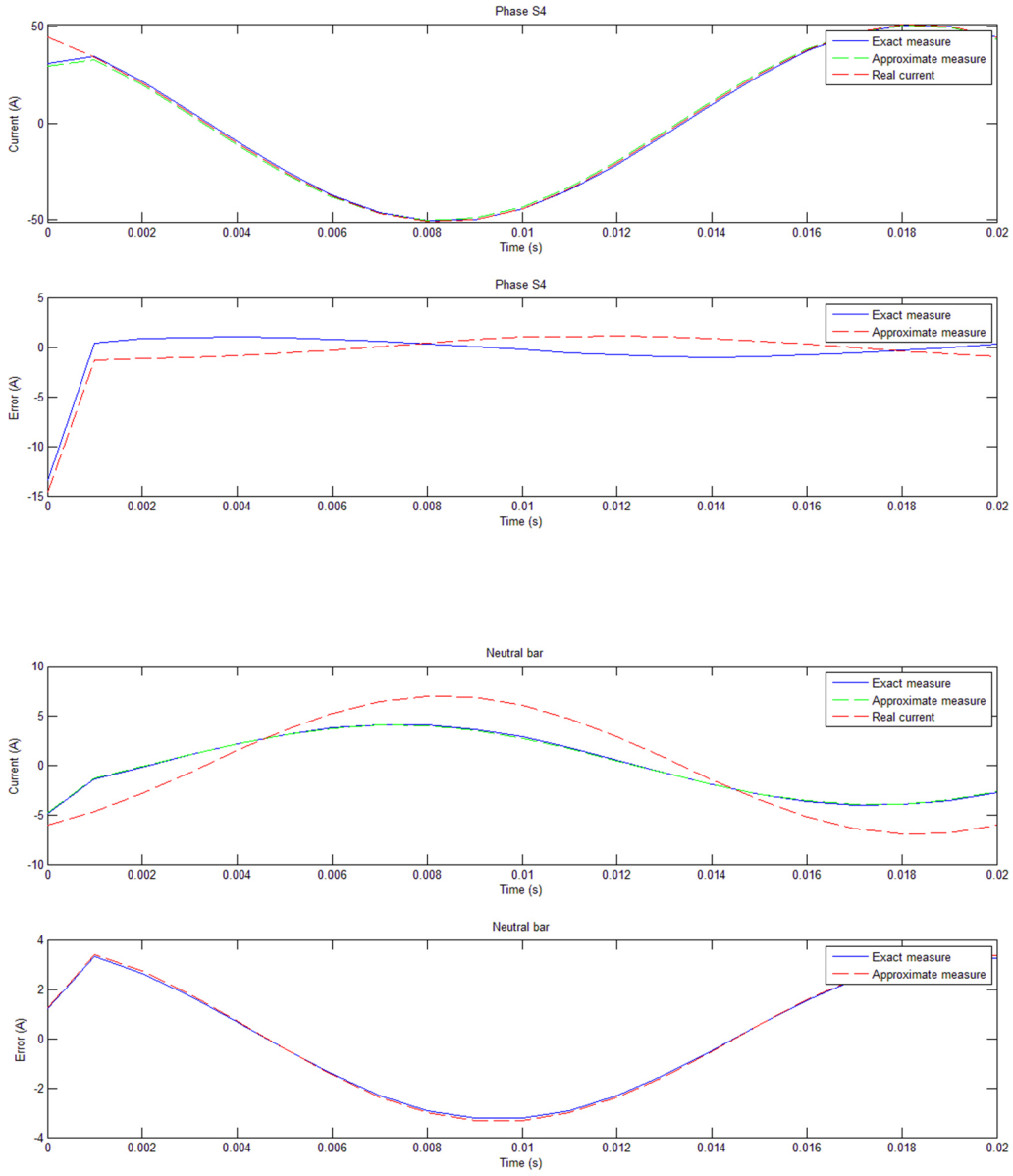

Considerations:

In these graphs it's possible to individuate a large diffusion of measure errors, so it will be necessary the integration of a corrective coefficient in order to obtain an exact measure of the current, as it was explained in the paragraph [*10.2*].

10.3.2 Results with the implementation of a corrective coefficient

As in the previous case (paragraph 10.2.2) with the implementation of the corrective coefficient is possible to make a correction in the measure system in order to obtain a perfect measurement of the current parameter.

In the next graphs are reported some example of current and error trends considering the implementation of the correctives coefficients matrix.

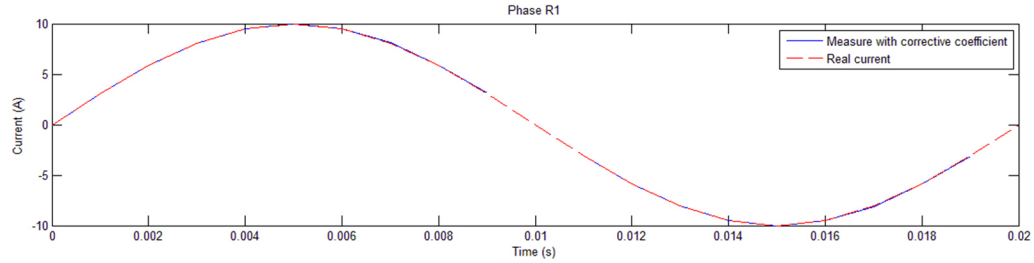

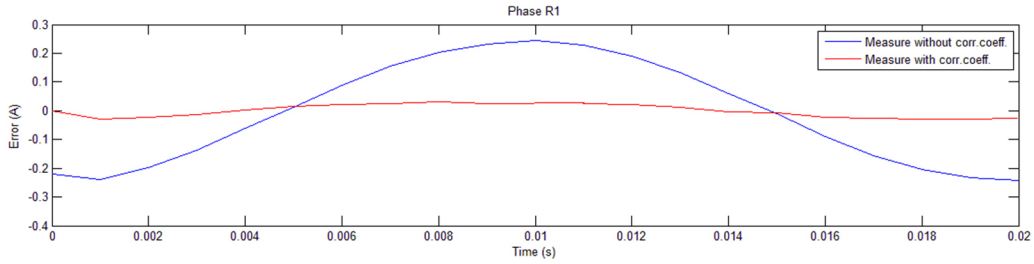

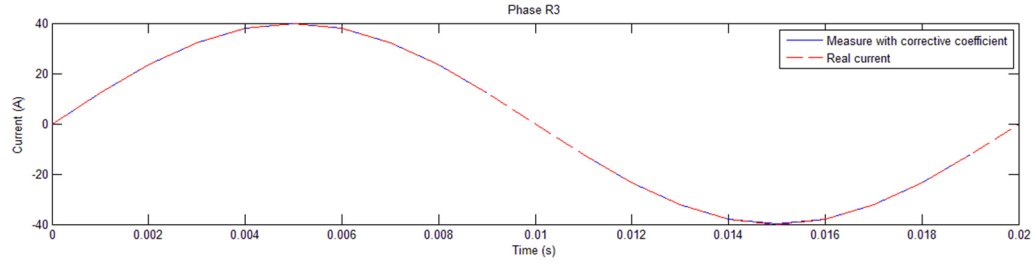

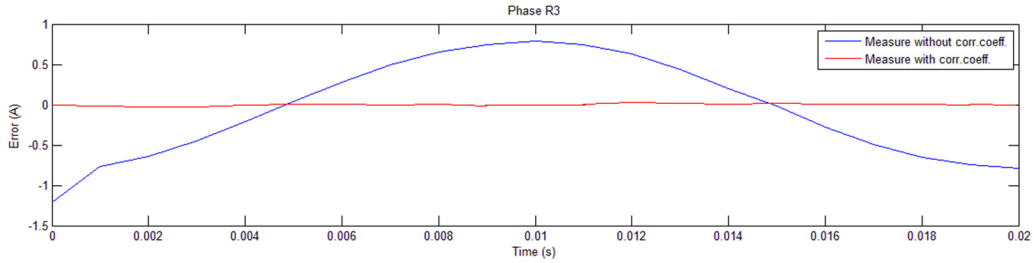

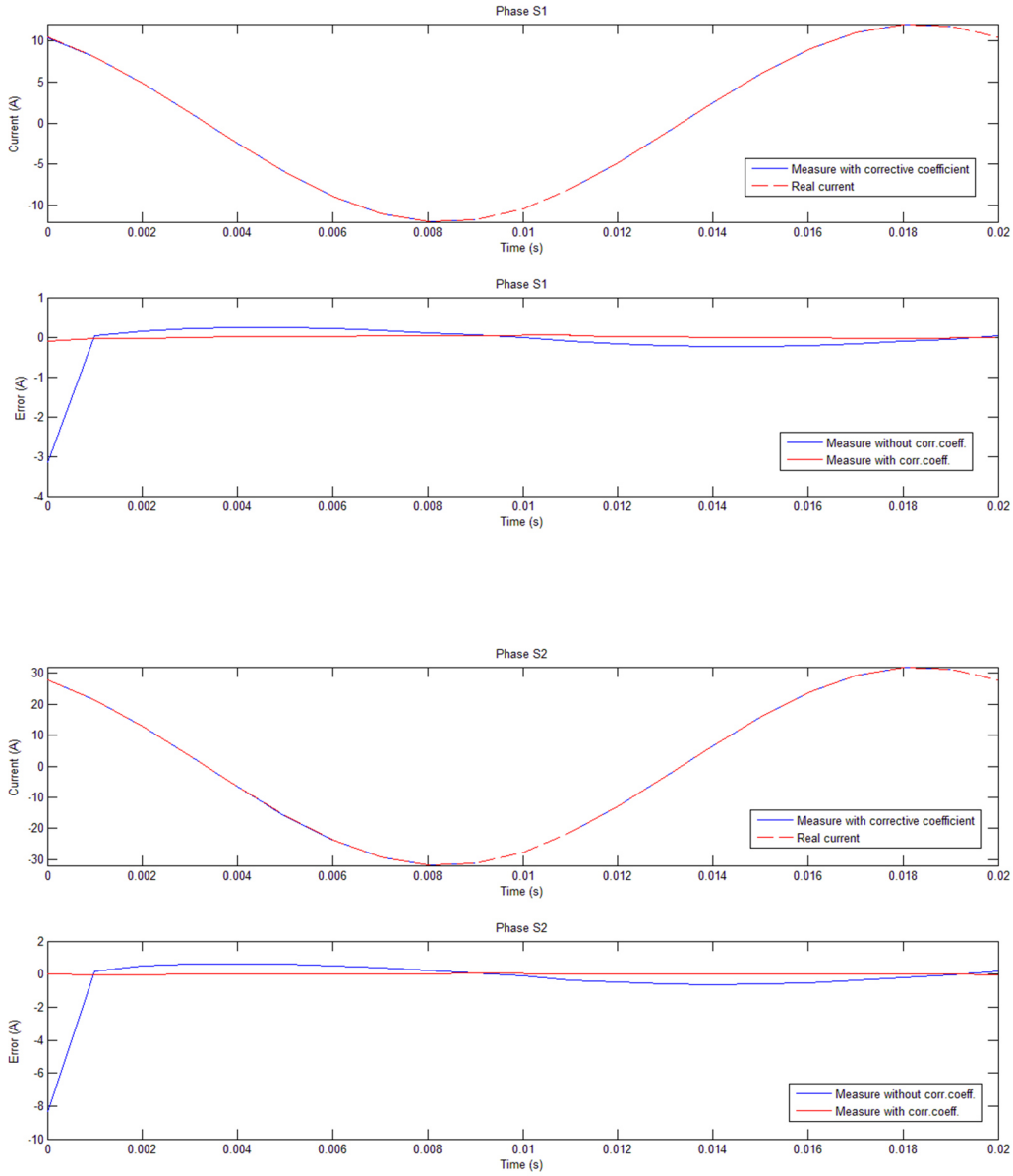

Considerations:

In the previous graphs it's possible to ascertain that with the implementation of the corrective coefficients matrix the error in the measure it will be zero for every bar considerate.

Therefore, it has been reached, with the implementation of the corrective coefficients matrix, a perfect monitoring of the currents making minimum the measurement error.

10.4 Second disposition of measure sensors

An observation to do for this plane of measure it's that it will not possible to study an eventually unbalanced system because in this cut plane it's not present the neutral bar, fortunately it will be possible in the next section where it will be take into study the 3D model.

To not overfill the document with graphs and matrices it will be take into account only the main important cases of the study, not reporting for example all the graphs obtained with the study but only a final comment about them.

It will be important, for example, focalize the document to the cases that consider the mutual inductance effect because represent more likely the real subject of study.

For this reason, it will be not shown the cases in which it's neglected the mutual inductance effect, about which, the main conclusions drawn have been:

- By comparing the two K matrix it was found that, like in the paragraph [*10.1.1*], the two matrices are equal for the fact that in the steady-state there are not present the effects of the mutual inductance;
- Regarding to the graphic solutions the error is very next to zero and it's not necessary the implementation of a corrective coefficient.

10.4.1 K matrix

1. Case considering the mutual inductance effect

With this disposition of the sensors there will be take into consideration also the sensors for the T-bars and so the K matrix derived it will be a 12×12 size matrix.

All the values of the matrix elements are expressed in [μT].

$|K|=$

SENSOR \ ACTIVE PHASE	R1	S1	T1	R2	S2	T2	R3	S3	T3	R4	S4	T4
R1	-32.43	0.065472	0.01614	-0.18569	0.022153	0.012214	-0.046374	-0.0055487	0.0052294	-0.020911	-0.0087629	0.00049702
S1	0.065455	-32.454	0.065675	0.02217	-0.18523	0.022393	-0.0055493	-0.046053	-0.0053212	-0.0087627	-0.020623	-0.0085606
T1	0.016144	0.065666	-32.466	0.012218	0.022395	-0.18506	0.0052298	-0.0053211	-0.045898	0.00049838	-0.0085609	-0.020486
R2	-0.18571	0.022147	0.012217	-32.443	0.065411	0.016119	-0.18564	0.022147	0.012205	-0.046391	-0.0055453	0.0052306
S2	0.022165	-0.18517	0.022415	0.065423	-32.456	0.065653	0.022149	-0.18527	0.022383	-0.0055409	-0.046055	-0.0053219
T2	0.012218	0.022385	-0.18519	0.016121	0.065684	-32.453	0.012206	0.02239	-0.18508	0.0052323	-0.0053233	-0.045909
R3	-0.046385	-0.0055564	0.0052318	-0.18565	0.022165	0.012207	-32.439	0.06543	0.01612	-0.18576	0.022159	0.012218
S3	-0.0055481	-0.046042	-0.0053152	0.022149	-0.18539	0.022406	0.065428	-32.462	0.065666	0.022179	-0.18529	0.022405
T3	0.0052308	-0.0053184	-0.045913	0.012206	0.022401	-0.18524	0.016122	0.065667	-32.463	0.012218	0.022403	-0.18517
R4	-0.020909	-0.0087669	0.00049828	-0.046377	-0.0055418	0.0052321	-0.18572	0.022169	0.012218	-32.443	0.065437	0.016143
S4	-0.0087652	-0.020619	-0.008558	-0.005547	-0.046067	-0.0053147	0.022169	-0.18532	0.022414	0.065429	-32.449	0.065701
T4	0.00049696	-0.0085567	-0.020487	0.00523	-0.0053219	-0.045917	0.012218	0.022407	-0.18519	0.01614	0.0657	-32.447

10.4.2 Matrix $\left[\vec{B}(t)\right]$

In this case the matrices $\left[\vec{B}(t)\right]$ are derived with the input currents set to:

$$\begin{aligned}
&\vec{I}_{R1} = I_1 \sin(2\pi\ 50\ t) \\
&\vec{I}_{R2} = I_2 \sin(2\pi\ 50\ t) \\
&\vec{I}_{R3} = I_3 \sin(2\pi\ 50\ t) \\
&\vec{I}_{R4} = I_4 \sin(2\pi\ 50\ t) \\
&\vec{I}_{S1} = I_1 \sin(2\pi\ 50\ t + 2\pi / 3) \\
&\vec{I}_{S2} = I_2 \sin(2\pi\ 50\ t + 2\pi / 3) \\
&\vec{I}_{S3} = I_3 \sin(2\pi\ 50\ t + 2\pi / 3) \\
&\vec{I}_{S4} = I_4 \sin(2\pi\ 50\ t + 2\pi / 3) \\
&\vec{I}_{T1} = I_1 \sin(2\pi\ 50\ t + 2\pi / 3) \\
&\vec{I}_{T2} = I_2 \sin(2\pi\ 50\ t + 2\pi / 3) \\
&\vec{I}_{T3} = I_3 \sin(2\pi\ 50\ t + 2\pi / 3) \\
&\vec{I}_{T4} = I_4 \sin(2\pi\ 50\ t + 2\pi / 3)
\end{aligned} \qquad I_1 = I_2 = I_3 = I_4 = 1,\ 50,\ 100\ [A]$$

Where I_1, I_2, I_3, I_4 are the peak values of the alternative current considered and the electrical system considered it's symmetrical and balanced.

To not overfill the document, it's presented below only the resulting matrix referred to the peak component of current set to 1[A]. All the values are in μT.

$|B(t)|=$

Time [s]	R1	S1	T1	R2	S2	T2	R3	S3	T3	R4	S4	T4
0	0.0050249	-18.419	17.539	0.0045087	-18.415	17.568	0.0041491	-18.425	17.536	0.0057623	-18.47	17.561
0.001	-9.5148	-21.58	30.541	-9.5976	-21.596	30.512	-9.5821	-21.589	30.547	-9.5109	-21.589	30.521
0.002	-18.706	-13.65	31.785	-18.824	-13.661	31.759	-18.809	-13.656	31.802	-18.691	-13.66	31.762
0.003	-26.074	-4.0492	29.61	-26.214	-4.0433	29.595	-26.202	-4.0424	29.638	-26.05	-4.064	29.59
0.004	-30.914	6.0007	24.529	-31.062	6.0294	24.529	-31.054	6.0269	24.567	-30.884	5.9819	24.513
0.005	-32.701	15.493	17	-32.844	15.546	17.014	-32.84	15.541	17.044	-32.668	15.472	16.99
0.006	-31.294	23.482	7.8106	-31.416	23.558	7.8378	-31.418	23.55	7.8571	-31.261	23.461	7.8059
0.007	-26.827	29.185	-2.1464	-26.918	29.278	-2.1086	-26.923	29.268	-2.1022	-26.798	29.166	-2.1452
0.008	-19.735	32.041	-11.897	-19.784	32.144	-11.852	-19.794	32.133	-11.86	-19.712	32.026	-11.891
0.009	-10.691	31.717	-20.463	-10.695	31.821	-20.416	-10.708	31.81	-20.436	-10.677	31.709	-20.452
0.01	-0.6231	28.331	-27.044	-0.58209	28.426	-26.998	-0.5961	28.416	-27.03	-0.62007	28.331	-27.029
0.011	9.5087	22.196	-31.001	9.5915	22.272	-30.962	9.5772	22.265	-31.001	9.5007	22.203	-30.985
0.012	18.722	13.854	-31.902	18.838	13.906	-31.874	18.825	13.901	-31.917	18.704	13.869	-31.886
0.013	26.069	4.1539	-29.643	26.207	4.1751	-29.627	26.196	4.1739	-29.671	26.042	4.1745	-29.629
0.014	30.9	-5.9396	-24.527	31.047	-5.9507	-24.525	31.04	-5.9482	-24.565	30.866	-5.9146	-24.516
0.015	32.636	-15.427	-16.971	32.777	-15.469	-16.983	32.774	-15.463	-17.014	32.6	-15.399	-16.964
0.016	31.306	-23.471	-7.8173	31.426	-23.541	-7.8419	31.428	-23.532	-7.8623	31.27	-23.444	-7.8159
0.017	26.829	-29.177	2.1474	26.918	-29.267	2.1126	26.924	-29.256	2.1052	26.797	-29.153	2.1431
0.018	19.739	-32.044	11.903	19.788	-32.146	11.862	19.797	-32.134	11.868	19.714	-32.024	11.893
0.019	10.693	-31.721	20.47	10.697	-31.825	20.427	10.709	-31.812	20.446	10.677	-31.708	20.456
0.02	0.62594	-28.351	27.064	0.58409	-28.446	27.024	0.59785	-28.435	27.054	0.62099	-28.345	27.047

10.4.3 Graphical results

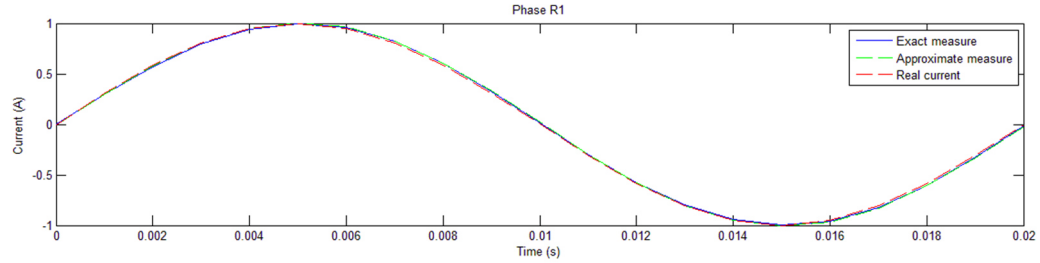

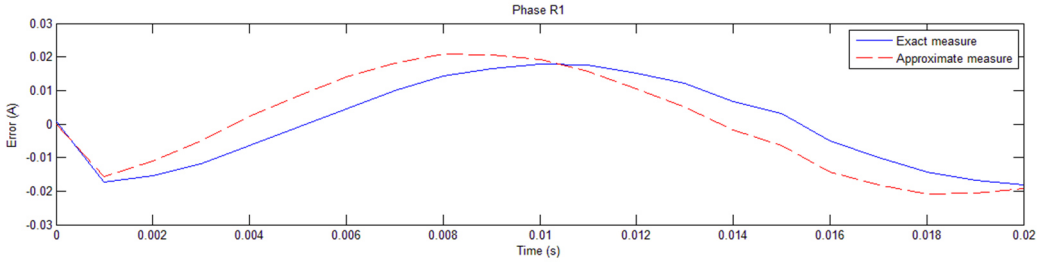

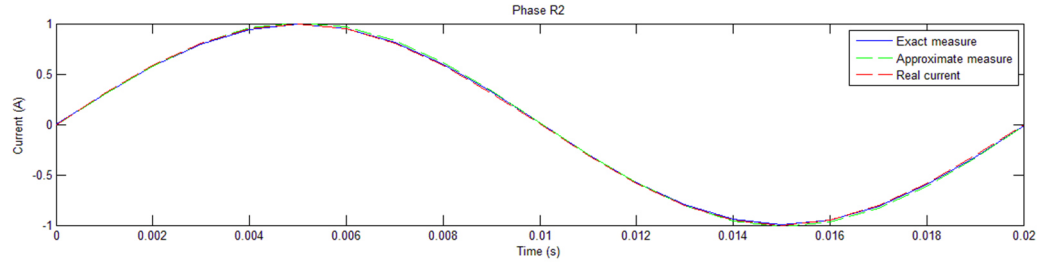

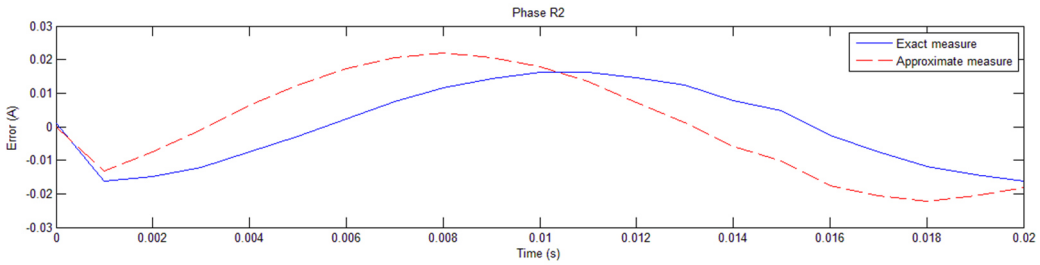

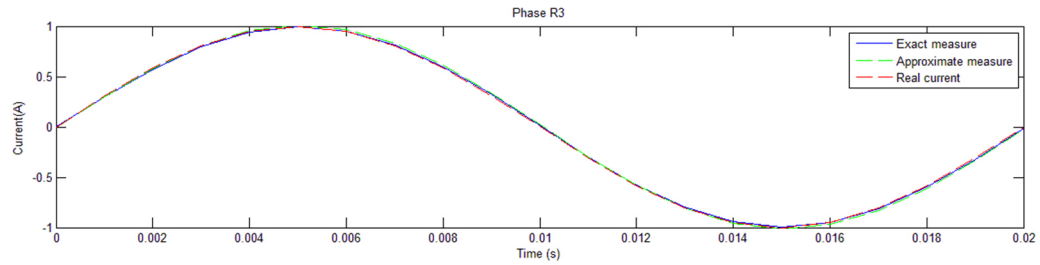

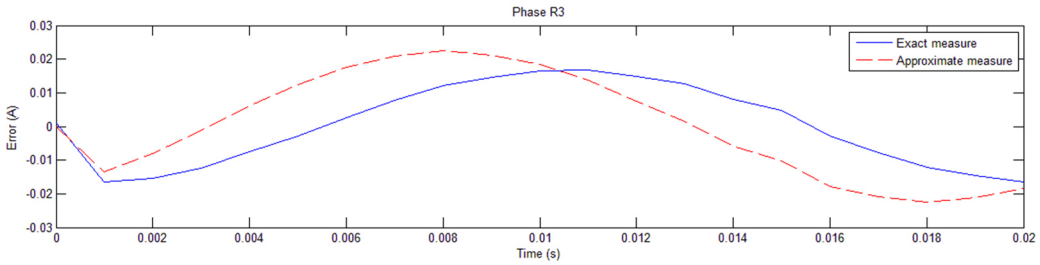

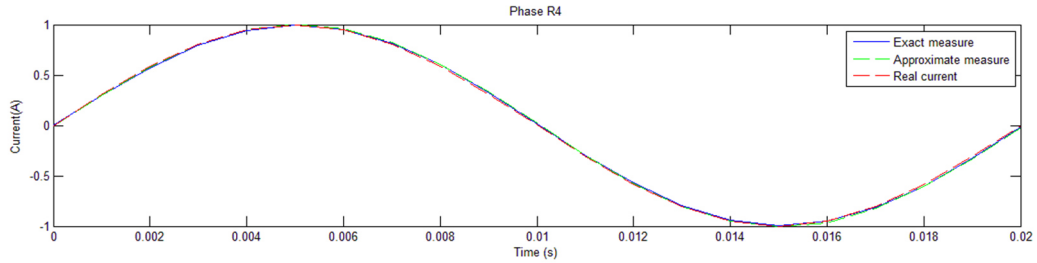
Phase R4
Current(A)
Time (s)
Exact measure
Approximate measure
Real current

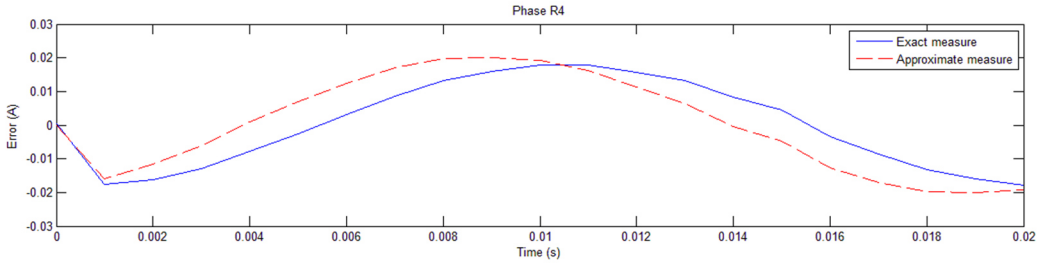
Phase R4
Error (A)
Time (s)
Exact measure
Approximate measure

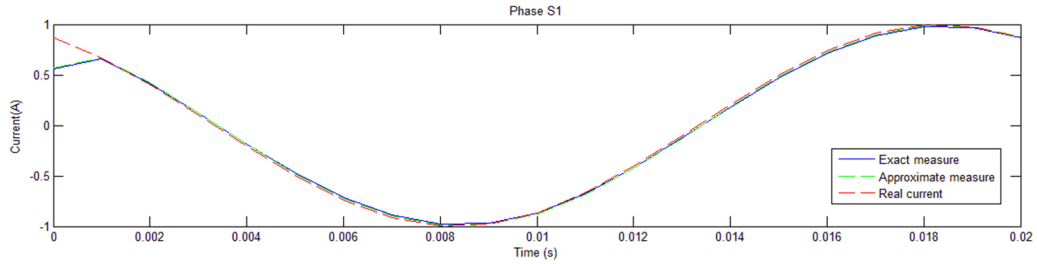
Phase S1
Current(A)
Time (s)
Exact measure
Approximate measure
Real current

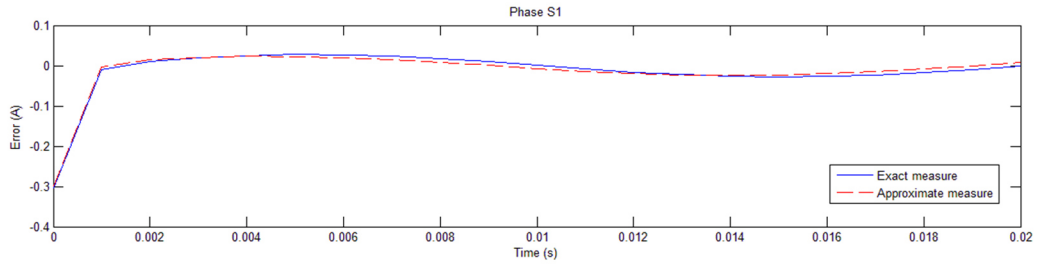
Phase S1
Error (A)
Time (s)
Exact measure
Approximate measure

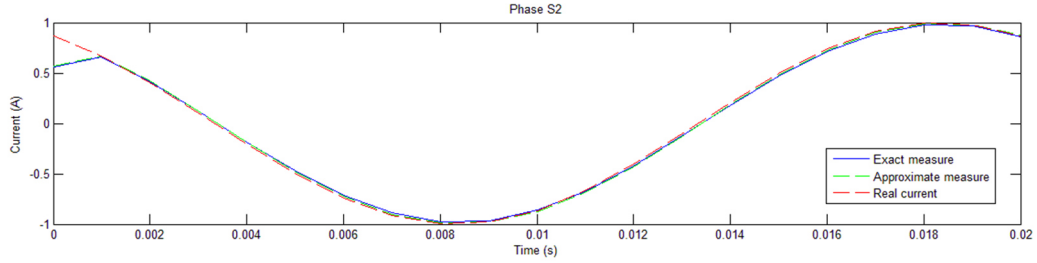
Phase S2
Current (A)
Time (s)
Exact measure
Approximate measure
Real current

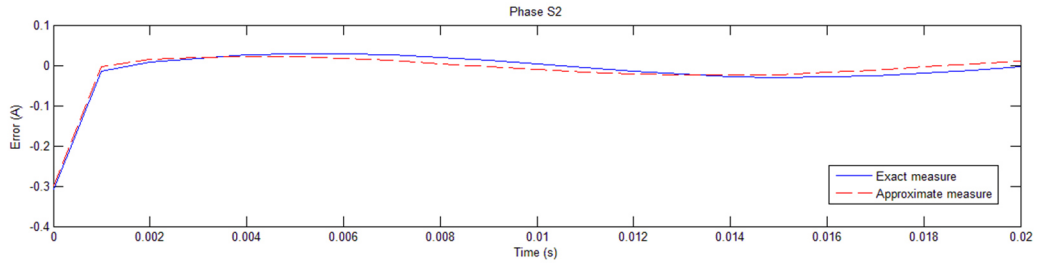
Phase S2
Error (A)
Time (s)
Exact measure
Approximate measure

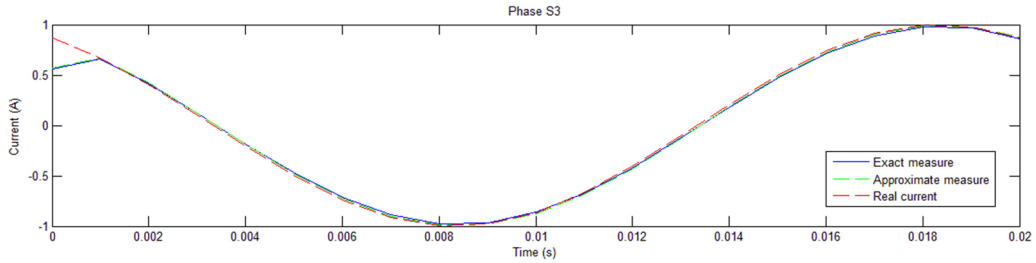
Phase S3
Current (A)
Time (s)
Exact measure
Approximate measure
Real current

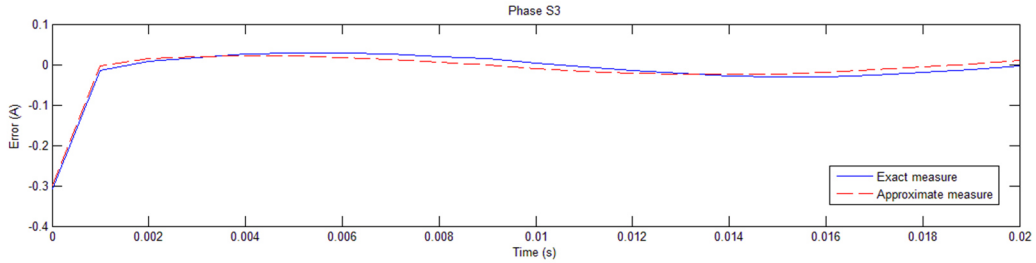
Phase S3
Error (A)
Time (s)
Exact measure
Approximate measure

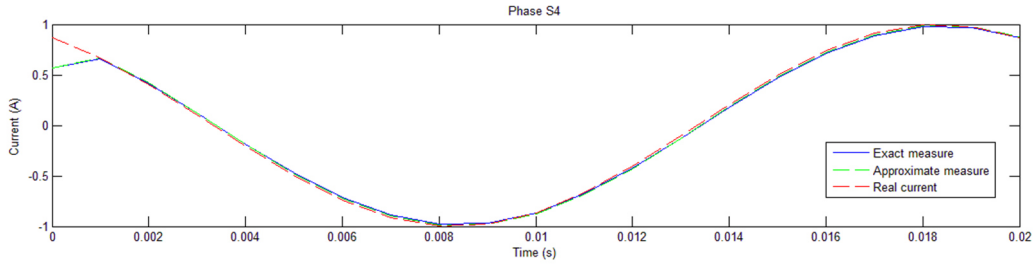
Phase S4
Current (A)
Time (s)
Exact measure
Approximate measure
Real current

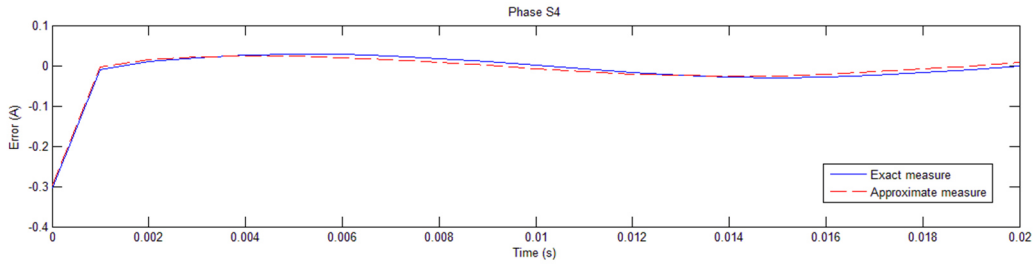
Phase S4
Error (A)
Time (s)
Exact measure
Approximate measure

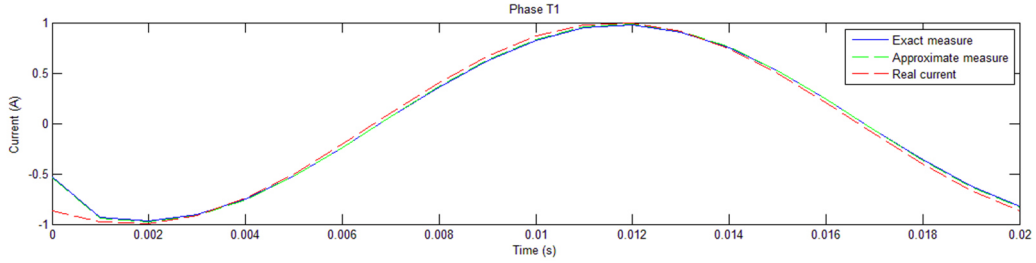
Phase T1
Current (A)
Time (s)
Exact measure
Approximate measure
Real current

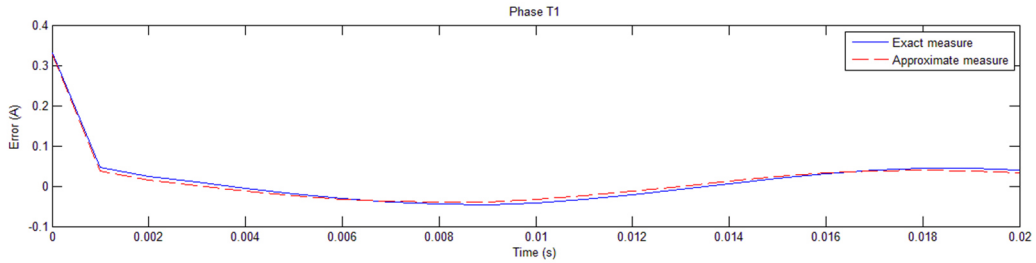
Phase T1
Error (A)
Time (s)
Exact measure
Approximate measure

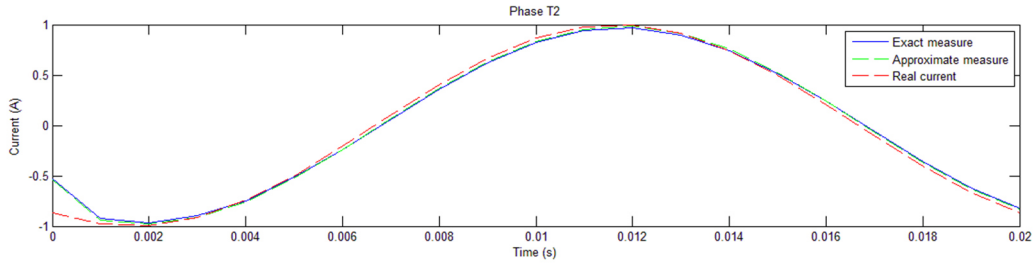
Phase T2
Exact measure
Approximate measure
Real current
Current (A)
Time (s)

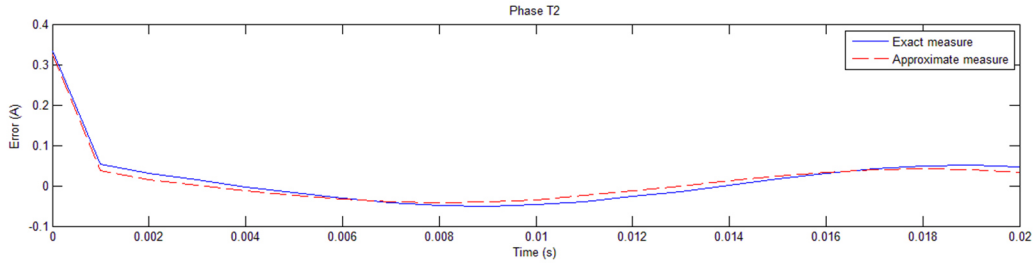
Phase T2
Exact measure
Approximate measure
Error (A)
Time (s)

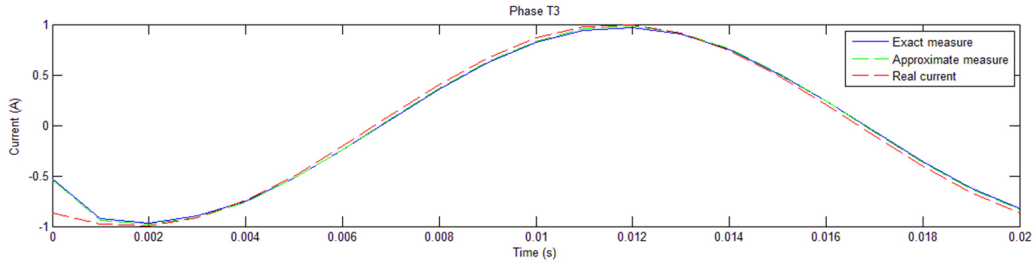
Phase T3
Exact measure
Approximate measure
Real current
Current (A)
Time (s)

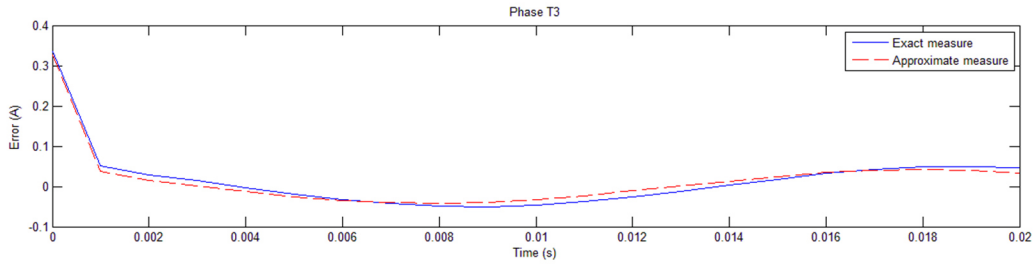
Phase T3
Exact measure
Approximate measure
Error (A)
Time (s)

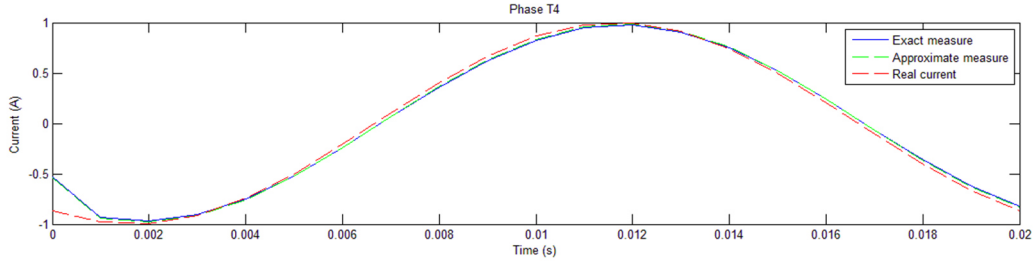
Phase T4
Exact measure
Approximate measure
Real current
Current (A)
Time (s)

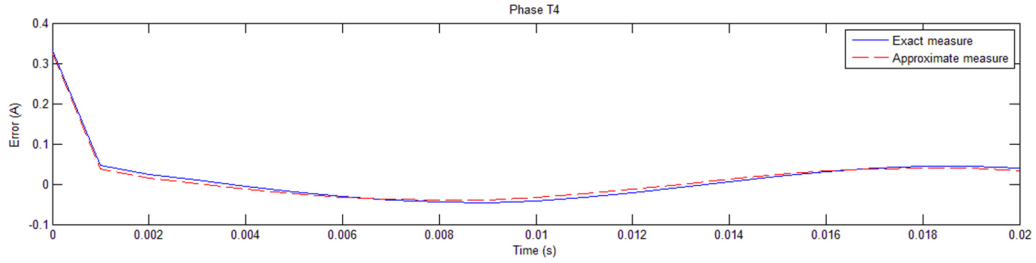
Phase T4
Exact measure
Approximate measure
Error (A)
Time (s)

Considerations:

In these graphs it's possible to individuate a large diffusion of measure errors, especially for the firsts instant of time. Thus it will be necessary the integration of a corrective coefficient in order to obtain an exact measure of the current.

10.4.4 Implementation of a corrective coefficient

The corrective coefficients matrix used in this case it's the following:

$$|K|_{corr} = \begin{vmatrix}
Inf & 0.6489 & 0.6176 & Inf & 0.6449 & 0.6151 & Inf & 0.6451 & 0.6137 & Inf & 0.6508 & 0.6187 \\
0.9437 & 0.9839 & 0.9525 & 0.9477 & 0.9787 & 0.9464 & 0.9463 & 0.9782 & 0.9472 & 0.9429 & 0.9845 & 0.9525 \\
0.9736 & 1.0239 & 0.9753 & 0.9745 & 1.0186 & 0.9694 & 0.9739 & 1.018 & 0.9704 & 0.9724 & 1.0248 & 0.9752 \\
0.9853 & 1.182 & 0.9895 & 0.985 & 1.1733 & 0.9839 & 0.9846 & 1.1727 & 0.9851 & 0.984 & 1.1865 & 0.9894 \\
0.9933 & 0.8805 & 1.0081 & 0.9922 & 0.8793 & 1.0032 & 0.9921 & 0.8788 & 1.0044 & 0.9919 & 0.8778 & 1.008 \\
0.999 & 0.9453 & 1.0393 & 0.9973 & 0.9428 & 1.0355 & 0.9973 & 0.9423 & 1.037 & 0.9975 & 0.9442 & 1.0393 \\
1.0048 & 0.964 & 1.1512 & 1.0025 & 0.9613 & 1.1515 & 1.0027 & 0.9608 & 1.154 & 1.0034 & 0.9633 & 1.1512 \\
1.0122 & 0.9747 & 0.6166 & 1.0091 & 0.9719 & 0.5973 & 1.0095 & 0.9714 & 0.5952 & 1.0107 & 0.9742 & 0.6166 \\
1.0242 & 0.9829 & 0.8902 & 1.0198 & 0.9801 & 0.8808 & 1.0205 & 0.9796 & 0.8812 & 1.0226 & 0.9826 & 0.8902 \\
1.0537 & 0.9893 & 0.932 & 1.0461 & 0.9865 & 0.9243 & 1.0475 & 0.986 & 0.9249 & 1.0519 & 0.9892 & 0.932 \\
Inf & 1 & 0.9502 & Inf & 1 & 0.9501 & Inf & 1 & 0.9503 & Inf & 1 & 0.9501 \\
0.9432 & 1.012 & 0.9669 & 0.9473 & 1.0094 & 0.9603 & 0.946 & 1.0089 & 0.9613 & 0.942 & 1.0125 & 0.9669 \\
0.9745 & 1.0392 & 0.9789 & 0.9753 & 1.0369 & 0.9729 & 0.9747 & 1.0363 & 0.9739 & 0.9731 & 1.0405 & 0.979 \\
0.9851 & 1.2125 & 0.9906 & 0.9847 & 1.2116 & 0.985 & 0.9844 & 1.211 & 0.9861 & 0.9837 & 1.2188 & 0.9907 \\
0.9929 & 0.8715 & 1.008 & 0.9917 & 0.8678 & 1.003 & 0.9916 & 0.8672 & 1.0044 & 0.9914 & 0.8679 & 1.0082 \\
0.997 & 0.9413 & 1.0375 & 0.9952 & 0.9381 & 1.0336 & 0.9953 & 0.9376 & 1.0352 & 0.9955 & 0.9397 & 1.0377 \\
1.0052 & 0.9636 & 1.1522 & 1.0028 & 0.9606 & 1.1521 & 1.003 & 0.96 & 1.1548 & 1.0037 & 0.9626 & 1.1527 \\
1.0123 & 0.9744 & 0.6169 & 1.0091 & 0.9715 & 0.5985 & 1.0095 & 0.971 & 0.5961 & 1.0107 & 0.9737 & 0.616 \\
1.0244 & 0.983 & 0.8906 & 1.02 & 0.9802 & 0.8816 & 1.0207 & 0.9796 & 0.8818 & 1.0227 & 0.9825 & 0.8904 \\
1.0539 & 0.9894 & 0.9323 & 1.0463 & 0.9867 & 0.9248 & 1.0476 & 0.9861 & 0.9254 & 1.0519 & 0.9891 & 0.9322 \\
Inf & 1 & 0.9502 & Inf & 1 & 0.9501 & Inf & 1 & 0.9503 & Inf & 1 & 0.9501
\end{vmatrix}$$

And it has been tested its independence from the variation of the input current with the method used in the paragraph [*10.2.1*].

The charts obtained with the implementation of the corrective coefficient matrix are following showed:

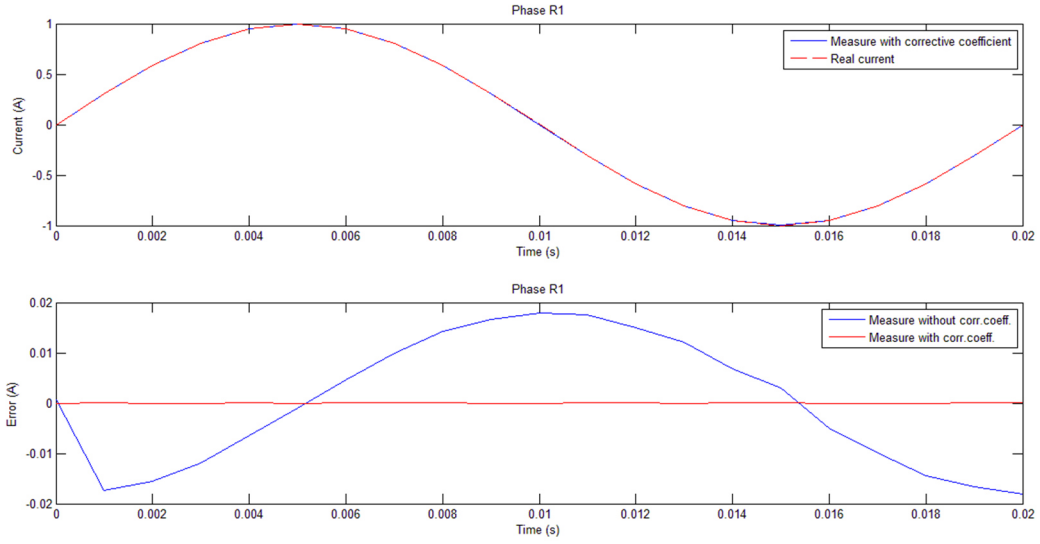

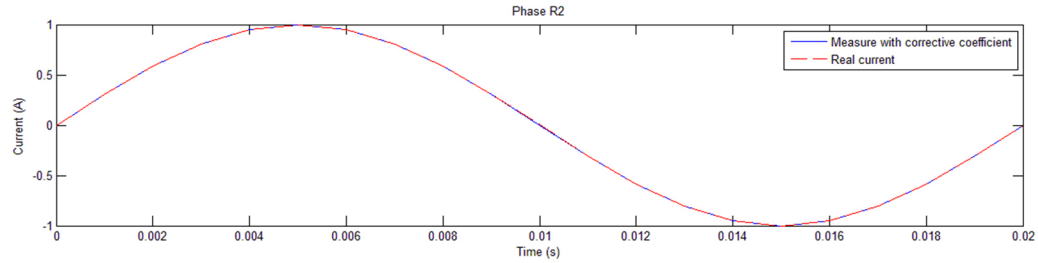
Phase R2
Measure with corrective coefficient
Real current
Current (A)
Time (s)

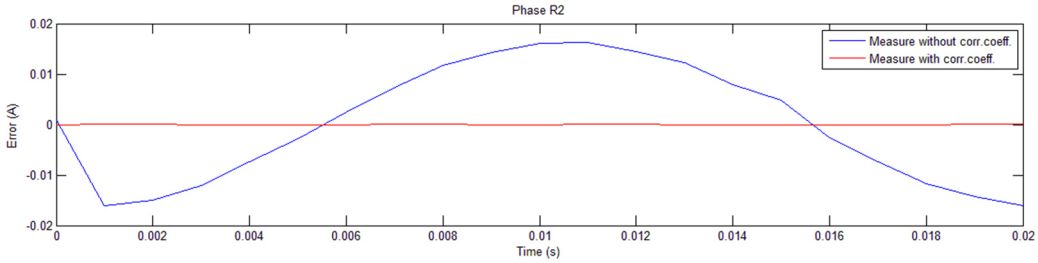
Phase R2
Measure without corr.coeff.
Measure with corr.coeff.
Error (A)
Time (s)

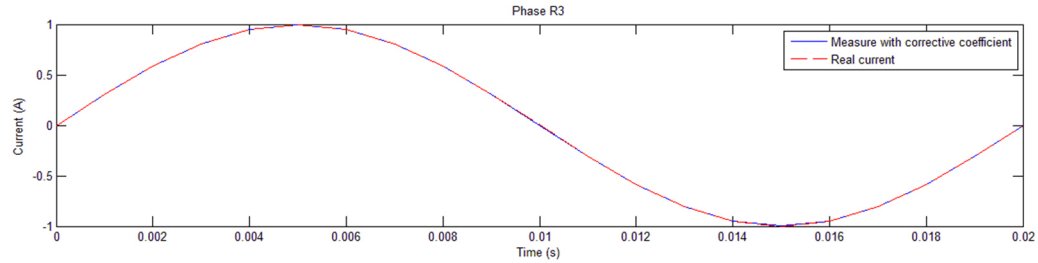
Phase R3
Measure with corrective coefficient
Real current
Current (A)
Time (s)

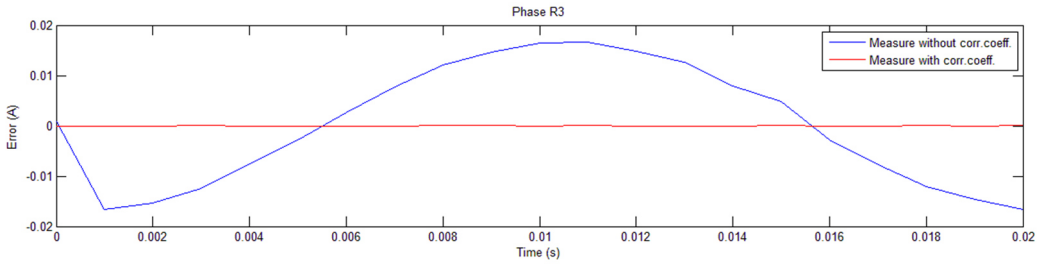
Phase R3
Measure without corr.coeff.
Measure with corr.coeff.
Error (A)
Time (s)

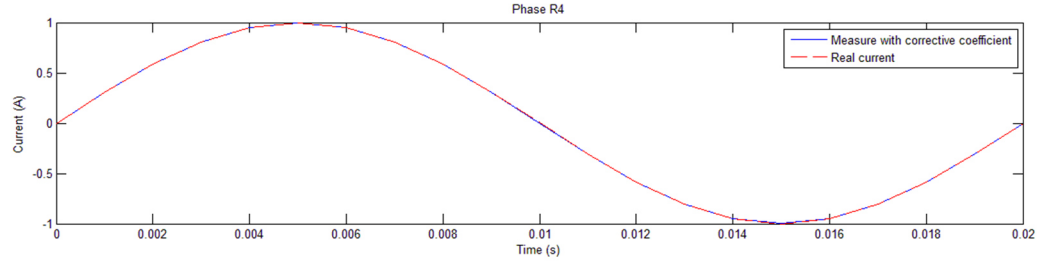
Phase R4
Measure with corrective coefficient
Real current
Current (A)
Time (s)

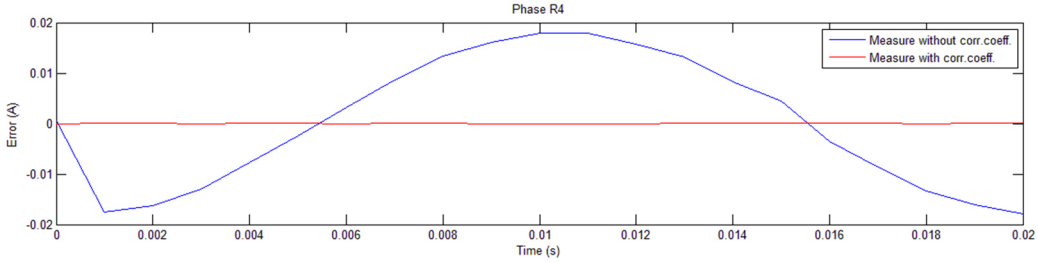
Phase R4
Measure without corr.coeff.
Measure with corr.coeff.
Error (A)
Time (s)

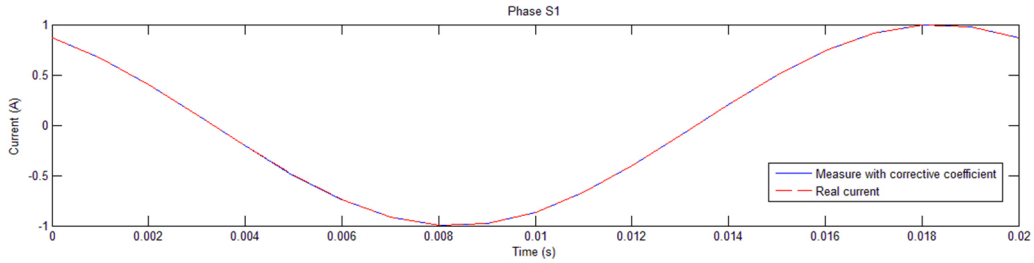
Phase S1
Current (A)
Time (s)
Measure with corrective coefficient
Real current

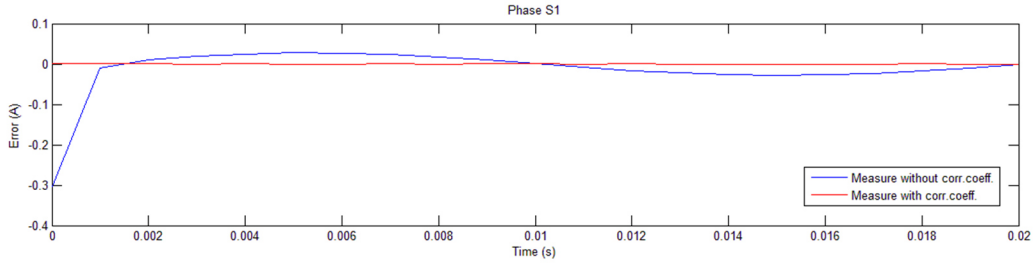
Phase S1
Error (A)
Time (s)
Measure without corr.coeff.
Measure with corr.coeff.

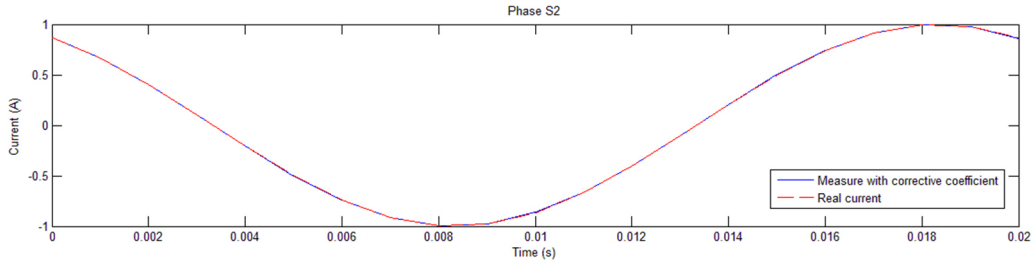
Phase S2
Current (A)
Time (s)
Measure with corrective coefficient
Real current

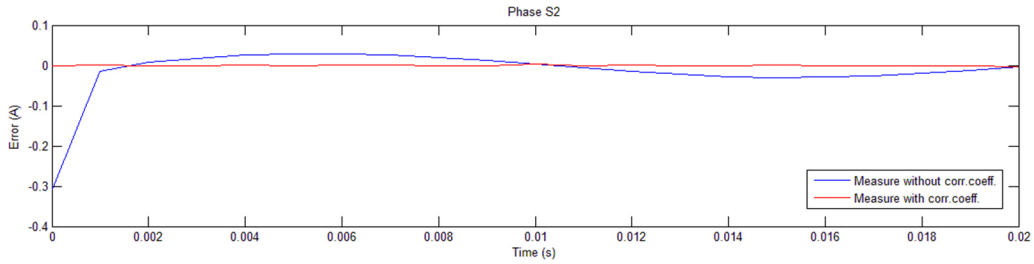
Phase S2
Error (A)
Time (s)
Measure without corr.coeff.
Measure with corr.coeff.

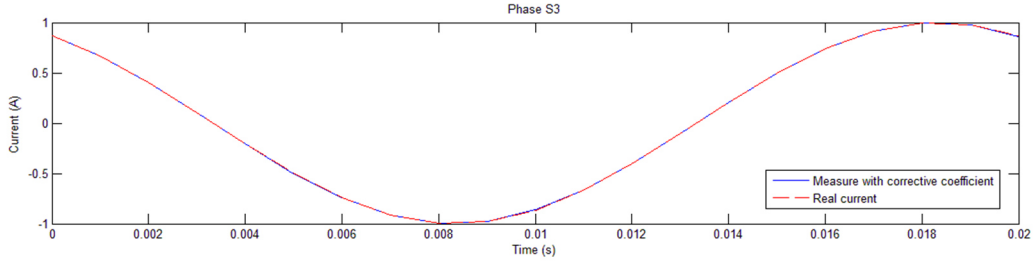
Phase S3
Current (A)
Time (s)
Measure with corrective coefficient
Real current

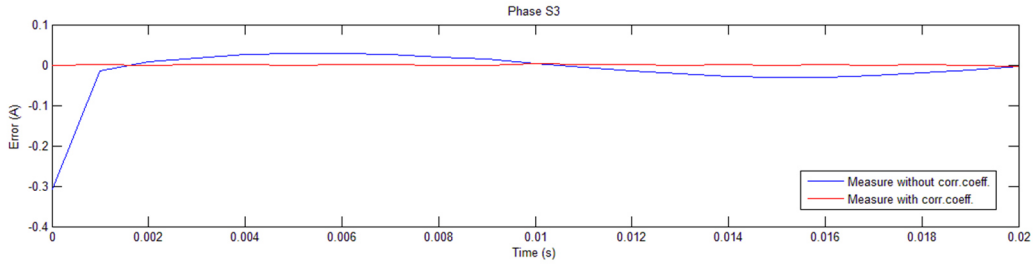
Phase S3
Error (A)
Time (s)
Measure without corr.coeff.
Measure with corr.coeff.

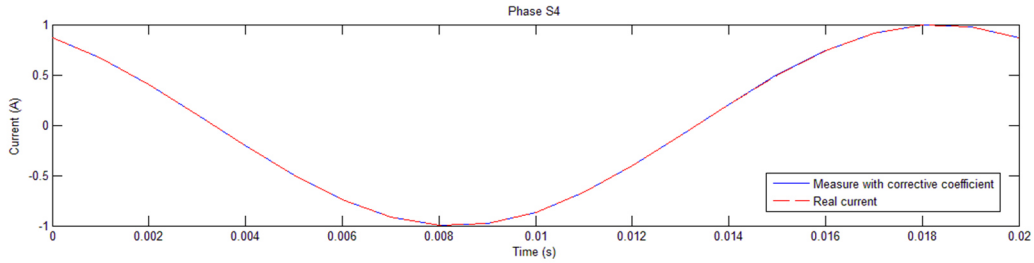
Phase S4
Current (A)
Time (s)
Measure with corrective coefficient
Real current

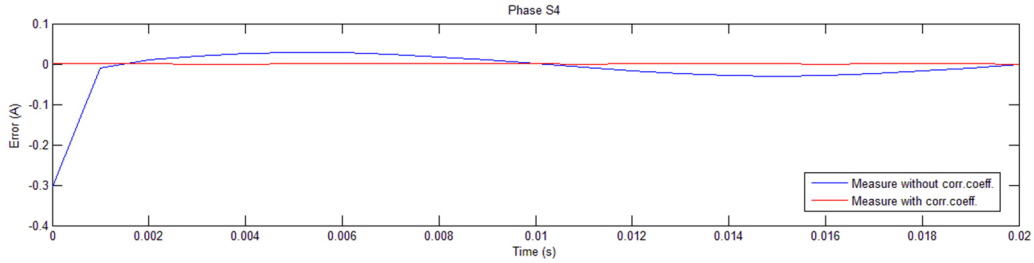
Phase S4
Error (A)
Time (s)
Measure without corr.coeff.
Measure with corr.coeff.

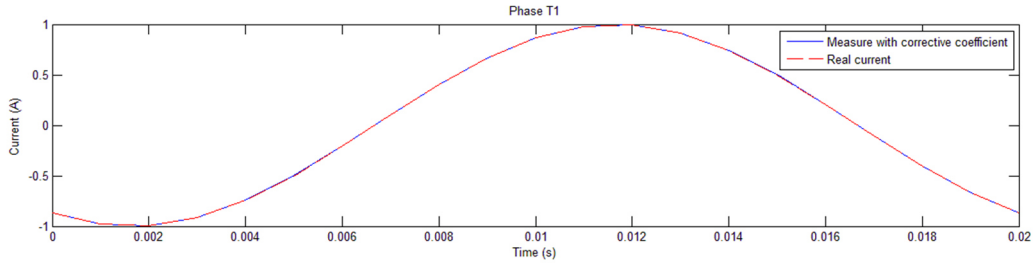
Phase T1
Current (A)
Time (s)
Measure with corrective coefficient
Real current

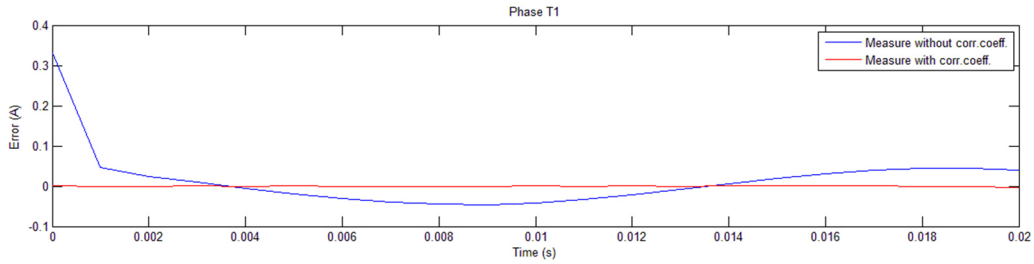
Phase T1
Error (A)
Time (s)
Measure without corr.coeff.
Measure with corr.coeff.

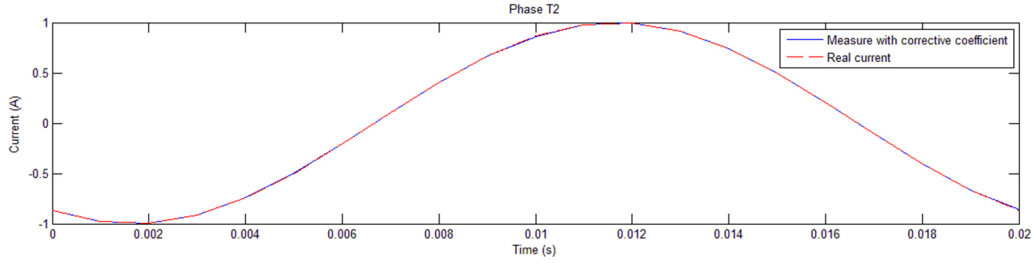
Phase T2
Current (A)
Time (s)
Measure with corrective coefficient
Real current

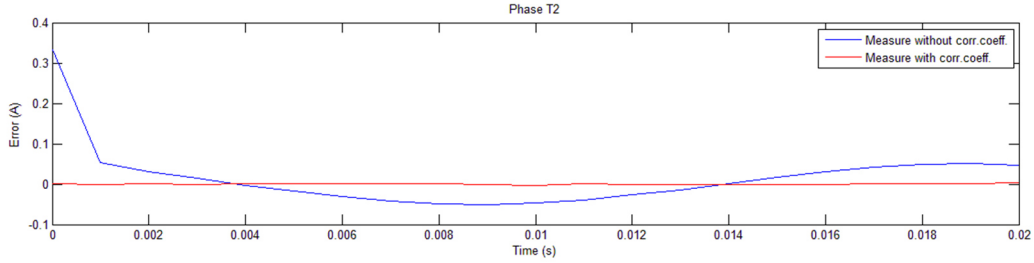
Phase T2
Error (A)
Time (s)
Measure without corr.coeff.
Measure with corr.coeff.

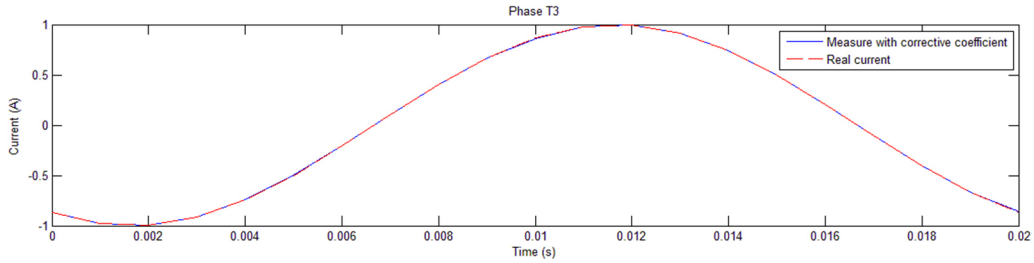

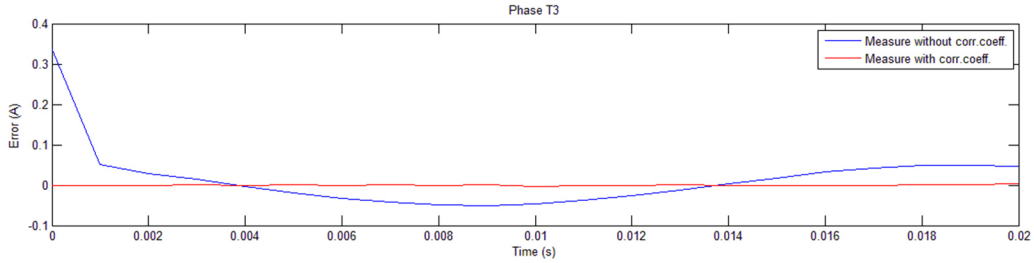

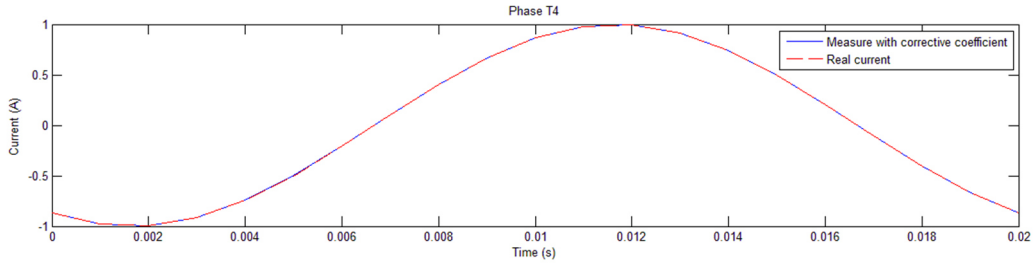

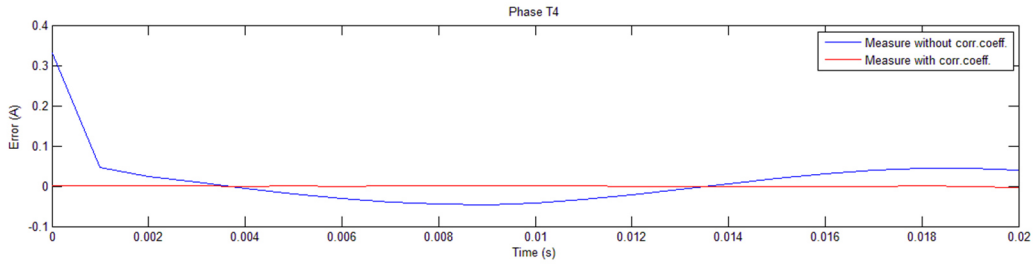

Considerations:

In the previous graphs it's possible to ascertain that with the implementation of the corrective coefficients matrix the error in the measure it will be zero for every bar considerate.

Therefore, it has been reached, with the implementation of the corrective coefficients matrix, a perfect monitoring of the currents making minimum the measurement error.

11 STUDY OF THE ERROR - 3D CASE

In this section there will be report the matrices $[K]$ necessary for the study of the measurement system in the 3D model.

With the 3D case have arisen some technical problems using the Comsol software for the simulations. In fact, it was encountered an actual limit of the software that don't allow to simulate the model in the time domain with the tool "single turn coil". This fact did not to allow to simulate the model in the time domain but only in the stationary domain, for which there have been found only the matrices $[K]$.

A possibility to remedy the problem was to consider, instead of the "single turn coil" tool, the "multi turn coil" tool. In this case the program allowed to do the simulations in the time domain but it was found that this tool wasn't right for the present model, because it's aimed to the simulation of wounded coil and the results weren't reliable.

Finally, given the present impossibility to resolve the problem, it was chosen to contact the Comsol technical support and they took charge of the problem.

Anyway, when the problem it will resolved, the main things to do will be find out the matrices $[\vec{B}(t)]$ and using the matrices $[K]$, reported in this paragraph, thin order to make the same probes made with the 2D case.

For the probes there will be used the same points of measure found in the 2D case, in the two different configurations, in order to figure out the graphs of current and error trends and eventually to consider the implementation of a corrective coefficient.

The eventually matrices and coefficients resulted from this study there will be implemented in the Arduino programming code.

11.1 First disposition of measure sensors

11.1.1 K matrix

$|K|=$

ACTIVE PHASE	R1	S1	T1	R2	S2	T2	R3	S3	T3	R4	S4	T4	N
SENSOR R1	-32.831	0.64935	0.064916	0.18281	0.06524	0.02508	0.047487	0.030478	0.019069	0.023636	0.021008	0.015083	-0.25363
S1	0.63765	-32.242	0.074873	0.74573	0.14848	0.017161	0.084	0.047224	0.024651	0.032649	0.029718	0.019841	-0.017548
T1	-0.016379	0.020836	-41.843	-0.00076916	0.0013288	0.0059477	-0.000099054	0.0012607	-0.0045018	-0.000011399	-0.00035084	-0.0043903	-0.006204
R2	0.18092	0.62021	0.037156	-32.901	0.70329	0.10003	0.18258	0.079605	0.031798	0.047832	0.042738	0.026765	0.044387
S2	0.08024	0.15893	0.039628	0.63347	-32.234	0.071027	0.75593	0.17375	0.036873	0.084181	0.06646	0.037603	0.038975
T2	0.00071056	0.0029088	0.0044554	0.0052482	0.0071025	-41.487	0.0023752	0.0016328	0.0035037	0.00029369	0.00071127	-0.0079722	0.004481
R3	0.046782	0.10108	0.053244	0.17361	0.56795	0.0606	-32.401	0.71724	0.11734	0.18495	0.099857	0.049942	0.028835
S3	0.030835	0.072691	0.031282	0.079954	0.16647	0.036241	0.65216	-32.086	0.089938	0.71884	0.17978	0.040458	0.022486
T3	0.00055222	0.0012622	-0.020766	0.0021416	0.0081692	-0.0079593	-0.0084621	0.038211	-40.771	0.0047122	0.0015656	-0.011191	0.0088087
R4	0.022088	0.054103	-0.15496	0.046227	0.088622	-0.14997	0.18056	0.64904	-0.14671	-33.231	0.72189	-0.13497	0.01764
S4	0.016361	0.035189	-0.42328	0.029421	0.051382	-0.41943	0.078297	0.14633	-0.41483	0.64543	-31.876	-0.37138	0.013975
T4	0.00016618	-0.00068652	-0.048138	0.00038718	0.0010814	-0.048015	0.00072758	0.0022699	-0.035405	0.0024133	0.0067524	-41.816	0.0077246
N	0.11937	0.0060035	-0.031879	-0.057347	-0.026702	-0.014737	-0.03161	-0.022529	-0.015328	-0.020274	-0.01851	-0.013876	-11.24

11.2 Second disposition of measure sensors

11.2.1 K matrix

$$|K| =$$

ACTIVE PHASE	R1	S1	T1	R2	S2	T2	R3	S3	T3	R4	S4	T4	N
SENSOR R1	33.578	-0.0010866	0.0040244	0.21132	0.013566	0.0047912	0.10094	0.017959	0.0059098	0.090435	0.016529	0.0064048	-0.051197
S1	0.059496	33.508	-0.019856	-0.014134	0.12151	-0.0029567	-0.000075164	0.019666	0.0038455	0.0053538	0.012076	0.0034113	0.0013297
T1	-0.031699	0.10237	33.178	0.0037069	-0.026505	0.12132	-0.00036798	-0.0032312	0.017822	-0.00029669	0.0019316	0.0071699	0.0029815
R2	0.28495	-0.002466	-0.0016212	33.222	-0.018261	-0.0024319	0.31962	-0.0027458	-0.0016343	0.20431	0.0030403	-0.00036753	-0.00037135
S2	-0.025385	0.135	-0.00064085	-0.23951	33.901	-0.018269	-0.00837	0.15516	-0.0015241	-0.00004477	0.055951	0.0053444	0.000548
T2	0.000037404	-0.013045	0.1396	0.057285	-0.013654	33.456	-0.0040611	-0.025759	0.12291	-0.0010839	-0.00076403	0.021897	-0.00085155
R3	0.034221	-0.0073832	0.00026906	0.12446	-0.012447	-0.0010285	34.104	-0.029595	-0.0018831	0.17376	-0.013987	-0.0010933	-0.000054654
S3	-0.001958	0.23899	0.0033524	-0.025502	0.35556	-0.0033847	0.046039	33.407	-0.020249	-0.015365	0.34777	-0.0033635	-0.00037954
T3	-0.001093	0.00069895	0.050448	-0.0012501	-0.016121	0.15709	0.0021415	0.12141	33.457	0.0039958	-0.022455	0.14358	-0.0015593
R4	0.0065104	0.0033247	0.0013407	0.016125	0.0043594	0.0006666	0.1137	-0.0011556	-0.00060904	33.127	-0.017535	-0.0014472	-0.000067175
S4	0.0012794	0.039497	0.00052835	-0.0037214	0.047588	0.0010037	-0.027005	0.15504	-0.0056375	0.096221	33.148	-0.02276	-0.00025002
T4	-0.00026899	0.0042918	0.22029	-0.00070784	-0.00086493	0.23127	0.00079253	-0.0097933	0.3402	0.12483	0.035878	33.593	-0.0013959
N	-0.072972	-0.031906	-0.014629	-0.081502	-0.028286	-0.014203	-0.082411	-0.026277	-0.01368	-0.079888	-0.025117	-0.013212	-11.927

12 MONITORING OF MAGNETORESISTIVE SENSORS WITH THE IMPLEMENTATION OF AN ARDUINO® BOARD

Arduino is an open-source prototyping platform based on easy-to-use hardware and software. [12]

The Arduino boards provide sets of digital and analog I/O pins that can interface to various expansion boards and other circuits. The boards feature serial communication interfaces, including Universal Serial Bus (USB) for loading programs from personal computers. For programming the microcontrollers, the Arduino project provides an integrated development environment (IDE) based on a programming language named Processing, which also supports the languages C and C++.

Arduino boards are available commercially in preassembled form, or as do-it-yourself kits. The hardware design specifications are openly available, allowing the Arduino boards to be produced by anyone.

These microcontrollers permit to create devices that interact with their environment using sensors and actuators, for this reason they are particularly useful in the present project in study. In fact, it's also possible to connect to their board a number of magnetoresistive sensors, this in order to obtain the correspondent values of measure and process them through the programming code.

Arduino boards are available commercially in preassembled form, or as do-it-yourself kits. The hardware design specifications are openly available, allowing the Arduino boards to be produced by anyone.

12.1 Arduino advantages

The mains advantages in the use of an Arduino system are:

- Arduino boards are relatively inexpensive compared to other microcontroller platforms.
- The Arduino Software (IDE) runs on Windows, Macintosh OSX, and Linux operating systems. Most microcontroller systems are limited to Windows.
- The Arduino Software (IDE) is easy-to-use for beginners, yet flexible enough for advanced users to take advantage of as well.
- The Arduino software is published as open source tools, available for extension by experienced programmers. The language can be also expanded through C++ libraries.

In the case of study in this investigation the main reason that lead to the use of an Arduino systems principally the cost-effectiveness advantage, in fact as it will be explain in the paragraph [12.7], the final total cost of the hardware tools implemented in the project will be very low.

12.2 Arduino model: MEGA 2560

The Arduino Mega 2560 is a microcontroller board with 54 digital input/output pins, 16 analogue inputs, 4 UARTs (hardware serial ports), a 16 MHz crystal oscillator, a USB connection, a power jack, an ICSP header, and a reset button. It's possible to connect it to a computer with a USB cable or power it with a AC-to-DC adapter or battery to get started.

This microcontroller it will be used in the project for the purpose to monitor all the sensor in the panel in order to derive the values of current and voltage and process them to figure out, for every circuit, some parameters of the electric system, as active power P, reactive power Q, apparent power S, cosφ.

It has been chosen this particular model of microcontroller because it's the model that provides the higher number of acquisition channels (16 analogue inputs) among all the Arduino boards. In fact, in this project there will be necessary, as it will be explained in the paragraph [12.3], the presence of all the 16 channels of the Arduino board.

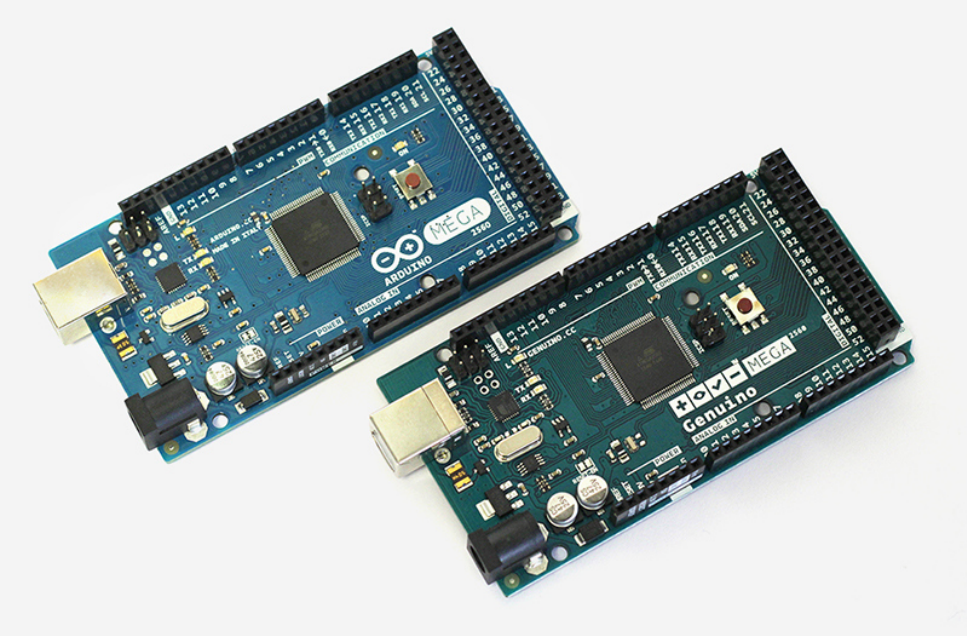

Fig. 12.1 Arduino Mega (version for USA) and Genuino Mega (version not for USA)

12.2.1 Technical specs

Microcontroller	ATmega2560
Operating Voltage	5 V
Input Voltage (recommended)	7-12 V
Input Voltage (limit)	6-20 V
Digital I/O Pins	54 (of which 15 provide PWM output)
Analog Input Pins	16
DC Current per I/O Pin	20 mA
DC Current for 3.3V Pin	50 mA
Flash Memory	256 KB
SRAM	8 KB
EEPROM	4 KB
Clock Speed	16 MHz
Length	101.52 mm
Width	53.3 mm
Weight	37 g

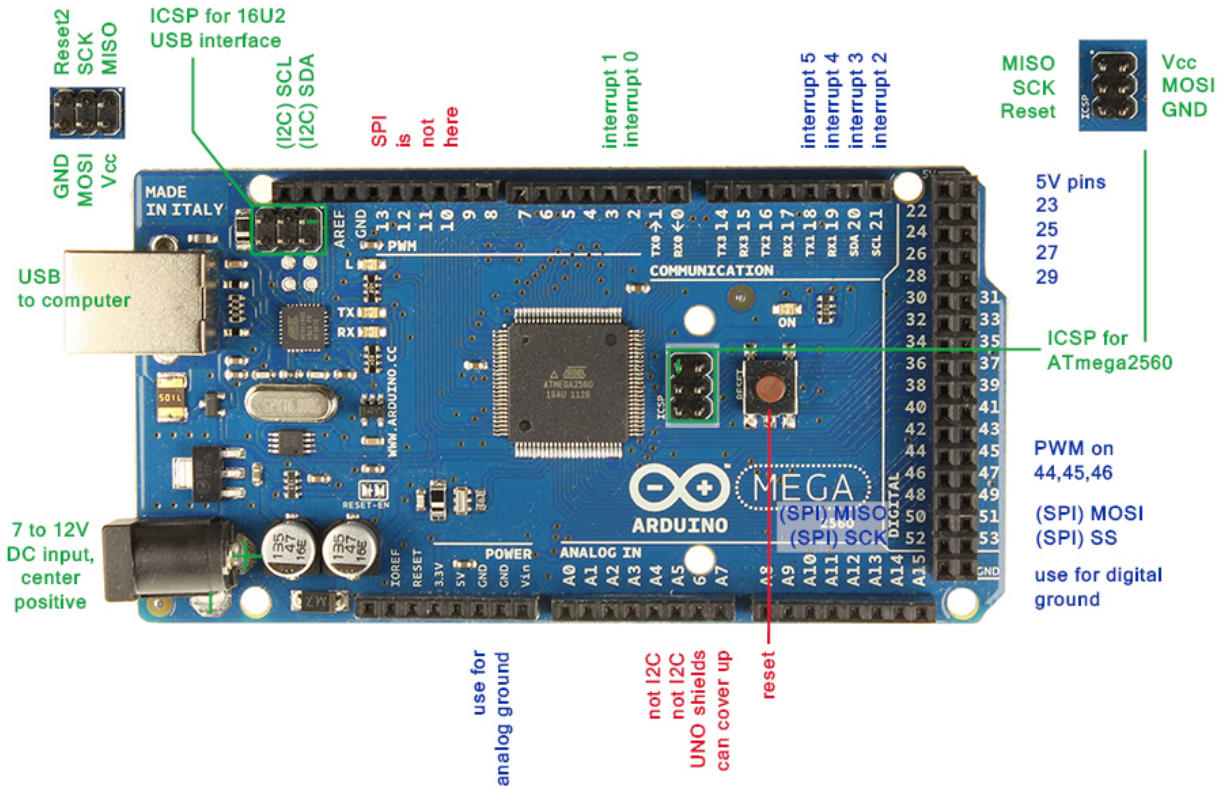

Fig. 12.2 MCU MEGA 2560

12.3 Connection system between the sensors and the MCU MEGA 2560

About the installation of the measurement system in the electric panel it has to be made some considerations.

On the one hand it's present the analogic system, formed by the sensors, and on the other hand there is the digital system, formed by the Arduino board. To connect the two systems there will be, for sure, some electronic wire and also it will be necessary an Analog to Digital Converter, already installed in the board.

For the connection of the sensors to the board it will not be connected every sensor installed in the panel with every channel but it will be used another methodology for the connection. This methodology it'll consist in add up every couple of sensors of every bar with an Operational Amplifier (OA). Then every OA it will be connected to the input channels of the board, bringing the output value of the OA (sum of the values of the two sensors) to the inputs channels of the board.

Another important thing in the system construction it will be the realization of an adapting circuit that will have to do the following things:

- Provide the power supply to the sensors (2.16 ÷ 3.6 V) and to the OA (±10 or ÷15 A);
- Adapt the output level of voltage of the OA (who depend to the output voltage signals of the sensors) to the admitted range of the Arduino board (0 ÷ 5 V).

As regards the last point, more precisely it will be necessary to adapt the output level of the OA introducing an offset of 2.5V. This because the sensors will work with sinusoidal values, that are positive and negative, so in order to maintain every value in the range it will be better maintain the signals between the values -2.5V and +2.5V.

Regarding the input channels in the board, as anticipated before, there will be used all the 16 inputs channels because there will be installed 12 OA for all the 12 bars (3 phases × 4 circuits) more 1 OA for the neutral bar and the other channels will be necessary for the 3 voltages of the 3 phases. These voltages will be measured probably with a voltage transformer.

12.4 Limitations encountered with the implementation of the MCU

A limitation encountered with the implementation of the Arduino board for the reading of the data from the sensors was that it's not possible to measure all the channels at once. This because there is only one converter with a multiplexer, which acts as the channel selector to be read. So the multiplexer every time selects a channel and then does the reading. In our case we have to read 16 channels and the time to change the selection from a channel to another is more or less fixed, but not instantaneous. Therefore, there will always be a slight delay in the switching from one channel to another.

This fact limits the initial idea to measure simultaneously all the channels, namely all the currents flowing in all the phases of the circuits. This simultaneous measure it would have been useful to measure, through the current and voltage derived for every phase, the eventually gap between the phases and thus the correspondent active power P and reactive power Q.

12.5 Exceedance of technical limitations

An idea to exceedance the limitation previously encountered it's explained in this paragraph.

Moving on the MCU programming part (elaborate with the Arduino software IDE), to read a channel exists a proper function named "analogRead", easy and fast to implement. The problem is that this function simplifies the program code, but not optimizes the process speed.

First of all, it's necessary to point out that there will be considered the channels in pairs, confronting two channels at a time.

Then, the main idea in order to resolve the problem it's, instead of using the "analogRead" function, acting

directly on the ADC and its records. This can speed up the operation of switching from a channel to another. More precisely, it will be used a timer that it will impose the time in which a reading is performed in the ADC.

In this case the timer it will programmed at a speed of 12.8 kHz.

At this frequency is generated a read command of the ADC, which causes what is called an "interruption". An interruption stop automatically what has been programmed into the principal loop and proceeds to execute what has been programmed into the function associated to the interruption function, in this case the reading of two ADC channels. When it has done the reading of two ADC channels, the running loop continues from where it had left.

Thus, the procedure is that every 78,125 μs (12.8 kHz) it's realized the consecutive measure of two channels (voltage and current of a given phase), and it's stored in two vectors with 512 samples. Then in the loop there will be performed the operations in order to obtain the values of interest (mean value, rms, power and so on) and send them, through the serial port, to the monitor of the Arduino GUI.

To obtain a high speed of the ADC it's necessary to use it through its registers. The idea is that the ADC has a multiplication factor (named "prescaler") that controls the rate of conversion. This factor can speed up the operations but at the expense of the accuracy of the reading.

In our case, with the settings explained before, there is only a delay of 10 μs between the reading of two channels. This it means that there is only a temporal gap of 0.25° between the phases and it has not a great influence in the measuring of P and Q.

12.6 Development of the programming code

The main parts composing the programming code and the main functions utilized in its development are presented in this paragraph.

The complete programming code it will be reported in the Appendix B.

The code was drawn up with the IDE Arduino software and the objective of the program code it's to control the board in order to obtain from the sensors the respective value of Voltage and Current and process them with the purpose of figure out the electric parameters in interest, like the values of P, Q, S, cosφ and the respective RMS values.

In general terms, concerning on what explained before, the board is programmed to do the same steps:

- It sample two channels filling the 512 samples for each one;
- When the samples are filled, it disables the "interruption" command to proceeding with the calculation of the parameters (P, Q, S etc.);
- The data are sent through the serial port and it will be re-enable the function ''interruption'';
- In some point it has been changed the channel identifier in order to proceed to measure other two channels, and so on till to read all the 16 channels.

Regarding the Arduino codes, they are written in a modified C language and usually are composed by the following three main parts:

- Definition of constants and their type (integer, long, etc.), with the possibility to include other defined libraries that can bring other useful functions;
- The development of the function "setup" where the device it's initialized and the configuration of some of its functionality it's performed, as the speed of sending data;
- The development of the function "loop", where there are included all the instructions that the program will going to do continuously in a closed loop.

The programming code used to control the MCU MEGA 2560 (reported in the Appendix B) is composed by the followings parts:

- Definition of constants, parameters, and types of parameters;
- Initialization of the serial port for the data sending;
- Configuration of the ADC;
- Configuration of the Timer;
- Function to be executed during interruptions;
- Main loop functions;
- Several functions in order to calculate the average value, RMS, power and other signals captured;
- Function to send data via serial port.

12.7 Total approximate cost for the hardware used in the project

The prices expressed in this paragraph will be indicative and are reported only to make an idea of the cost-effectiveness of the monitoring system developed.

The estimation includes the Arduino board that has a price of 35 €, the sensors that have a price of about 8€ buying more than 10 sensors and the OA that generally have a price that don't overcome 1 €.

The totally sum it will be, considering that there will be necessary 26 sensors and 13 OA, of about 250 €.

These prices are indicative because they depend on the quantities bought of every element.

It's important to consider that in this estimation are not included the cables for the wiring and the resistances, that fortunately are not expensive, and other eventually components necessary for the installation.

13 FINAL CONSIDERATIONS AND FUTURE WORKS

The main goals obtained with the present investigation were the obtaining of two different configurations for the positioning of the sensors in the panel and the obtaining, for every configuration, of a number of theoretical relationships necessary for the right measurement of the currents.
In particular, the choice between the two different configurations will depend to the geometry limitations that will be encountered in the sensors installation stage. In this case it will be chosen the configuration that permits the faster and easier way for the installation.
Regarding the theoretical relationships encountered in the study, as for example the various matrices and correctives coefficients, they will be implemented in a future moment in the Arduino programming code, in order to obtain a perfect measurement of the current through the values of MF measured by the sensors.
Another goal achieved it has been the develop of a part of the total implementation of the programming code for the Arduino board, the discovery of a limitation in its use and the overcoming of this limitation.
Regarding the objective of the work, to project a cheap monitoring system, it can be said that the system it will have a good cost-effectiveness, as it can be seen in the paragraph [*12.7*].

In order to actuate the real functioning of the measurement system the future works to do will be for first find out in the 3D model the main theoretical relationships for the monitoring of the currents, as it was done in the 2D model.
Then it will be necessary also to develop the wiring of the circuits with also the implementation of the OA and the installations of the sensors. After that it will be necessary a further developing of the Arduino programming code, with the implementation of the theoretical relationships discussed before and finally the realization of some tests in order to verify the correct operating of the system.

Appendix A : Matlab algorithms

Appendix A.1

```
clear all

K= [-32.43      0.0654     0.0161   -0.1857     0.0221     0.0122   -0.0463    -0.0055     0.0052   -0.0209   -0.0087     0.0004
     0.0654    -32.454     0.0656    0.0221    -0.1851     0.0223   -0.0055    -0.0460    -0.0053   -0.0087   -0.0206    -0.0085
     0.0161     0.0656   -32.4661    0.0122     0.0224    -0.1851    0.0052    -0.0053    -0.0459    0.0004   -0.0085    -0.0204
    -0.1856     0.0221     0.0122   -32.443     0.0654     0.0161   -0.1856     0.0221     0.0122   -0.0463   -0.0055     0.0052
     0.0221    -0.1852     0.0223    0.0654    -32.456     0.0656    0.0221    -0.1853     0.0224   -0.0055   -0.0460    -0.0053
     0.0122     0.0223    -0.1850    0.0161     0.0656    -32.453    0.0122     0.0224    -0.1852    0.0052   -0.0053    -0.0459
    -0.0463    -0.0055     0.0052   -0.1856     0.0221     0.0122   -32.439     0.0654     0.0161   -0.1857    0.0221     0.0122
    -0.0055    -0.0460    -0.0053    0.0221    -0.1852     0.0223    0.0654    -32.462     0.0656    0.0221   -0.1853     0.0224
     0.0052    -0.0053    -0.0458    0.0122     0.0223    -0.1850    0.0161     0.0656    -32.463    0.0122    0.0224    -0.1851
    -0.0209    -0.0087     0.0004   -0.0463    -0.0055     0.0052   -0.1857     0.0221     0.0122   -32.443    0.0654     0.0161
    -0.0087    -0.0206    -0.0085   -0.0055    -0.0460    -0.0053    0.0221    -0.1852     0.0224    0.0654   -32.449     0.0657
     0.0004    -0.0085    -0.0204    0.0052    -0.0053    -0.0459    0.0122     0.0224    -0.1851    0.0161    0.0657   -32.447 ]

      % K matrix obtained with all the input currents set to 1A

   B= [-32.575    %Array of measured values of B with all the circuit powered with a
current of 1A
     -32.558
     -32.609
     -32.711
     -32.663
     -32.718
     -32.707
     -32.669
     -32.728
     -32.589
     -32.553
     -32.591];

 Kinv = inv(K);

 I = mtimes(Kinv,B);  %Array of currents calculate with the use of the matrix K.
```

Appendix A.2

```
set(0,'DefaultFigureWindowStyle','docked')

K = [ 32.448    -0.63872  -0.17978   -0.07918   -0.046106  -0.029409   -0.020951   -0.015426   -0.014192    0.26106
     -0.63766    32.441   -0.73116   -0.17971   -0.083036  -0.0461     -0.03025    -0.020949   -0.018561    0.016993
     -0.17971   -0.73139   32.447    -0.63771   -0.17963   -0.07915    -0.04609    -0.029401   -0.024522   -0.045264
     -0.079154  -0.17966  -0.63783    32.444    -0.73108   -0.17969    -0.083028   -0.046095   -0.03387    -0.039465
     -0.046097  -0.08303  -0.17971   -0.7313     32.453    -0.63794    -0.17966    -0.079151   -0.044139   -0.02936
     -0.0294    -0.04608  -0.079147  -0.17961   -0.63741    32.43      -0.73094    -0.17969    -0.033091   -0.021429
     -0.020949  -0.03025  -0.046103  -0.083045  -0.17975   -0.73166     32.46      -0.63797     0.11414    -0.016435
     -0.015421  -0.020943 -0.029397  -0.04608   -0.079129  -0.17957    -0.63729     32.446      0.29887    -0.012736
      0.014605   0.01875   0.02434    0.033251   0.045202   0.058239    0.026484   -0.3162      12.451      0.014702
     -0.10356    0.054683  0.0536     0.039178   0.028929   0.02147     0.016761    0.013215    0.014712    12.451 ];



% K matrix

B = [ -0.94151  19.699  -1.8639    19.568   -1.8395    19.598   -2.579     18.303  -41.631
       8.7127   21.372   8.4175    21.355    8.456     21.352    7.8569    20.418  -50.742
       17.964   12.798   17.834    12.808    17.89     12.824    17.334    12.028  -49.74
       25.459   2.8306   25.498    2.8657    25.567    2.8975    25.1      2.3156  -44.67
       30.462  -7.4153   30.665   -7.3578    30.74    -7.3141    30.405   -7.621   -35.646
       32.488  -16.936   32.834   -16.862    32.907   -16.81     32.738   -16.81   -23.317
       31.329  -24.798   31.783   -24.714    31.848   -24.66     31.859   -24.352  -8.7766
       27.096  -30.217   27.611   -30.132    27.662   -30.081    27.853   -29.495   6.607
       20.227  -32.691   20.752   -32.614    20.784   -32.57     21.136   -31.764   21.336
       11.391  -31.991   11.871   -31.929    11.881   -31.897    12.359   -30.949   33.983
       1.4268  -28.136   1.8161   -28.096    1.8021   -28.079    2.3603   -27.082   43.282
      -8.6819  -21.525  -8.4234   -21.51    -8.4592   -21.51    -7.8761   -20.562   48.349
      -17.939  -12.801  -17.837   -12.814   -17.891   -12.83    -17.34    -12.022   48.68
      -25.437  -2.8306  -25.504   -2.8694   -25.571   -2.9004   -25.105   -2.3128   44.265
      -30.438   7.4154  -30.667    7.354    -30.74     7.3114   -30.406    7.6213   35.5
      -32.452   16.931  -32.823    16.853   -32.895    16.803   -32.725    16.805   23.272
      -31.298   24.79   -31.774    24.702   -31.838    24.65    -31.849    24.343   8.7668
      -27.085   30.225  -27.621    30.136   -27.671    30.087   -27.861    29.502  -6.6066
      -20.218   32.701  -20.762    32.62    -20.792    32.578   -21.144    31.772  -21.336
      -11.36    31.954  -11.86     31.889   -11.868    31.858   -12.347    30.91   -33.972
      -1.4041   28.118  -1.8116    28.074   -1.7966    28.059   -2.3548    27.061  -43.315 ];

% Matrix of values of MF for all the temporal instants from t=0[s] to t=0,02[s] with
intervals of 0,01[s]



t =[0     %temporal intervals
   0.001
   0.002
   0.003
   0.004
   0.005
   0.006
   0.007
   0.008
   0.009
   0.01
   0.011
   0.012
   0.013
   0.014
   0.015
   0.016
   0.017
   0.018
   0.019
   0.02 ];

invK=inv(K(1:9,1:9));
IR=sin(2*pi*50*t);          %input currents set in the Comsol model
IS=sin(2*pi*50*t+2*pi/3);
IT=sin(2*pi*50*t+4*pi/3);
ITt=4*sin(2*pi*50*t+4*pi/3);
```

```
Iinput =[IR IS IR IS IR IS IR IS ITt];    % Array of input currents
```

```
%% Exact calculation
Im=zeros(21,9);
for i=1:21
Im(i,:)=(invK*B(i,:)')' % calculation of currents
End
```

```
%% Approximate calculation
 Iap=zeros(21,9);
for i=1:9
Iap(:,i)=B(:,i)/K(i,i); % calculation of currents
End
```

```
error_exacto=(Im-Iinput); %error in the exact case
error_aprox=(Iap-Iinput); %error in the approximate case
```

```
%% Graphs for phase R

k=1;
for i=1:2:8
figure()
subplot(2,1,1)
plot(t,Im(:,i))
hold on
plot(t,Iap(:,i),'--g')
plot(t,IR,'--r')
str=sprintf('Fase R%1d',k);
ylabel('Corriente (A)')
xlabel('Tiempo (s)')
title(str)
legend('Medida exacta','Medida aproximada','Real')
axis([0 0.02 -1 1])

subplot(2,1,2)
plot(t,error_exacto(:,i))
hold on
plot(t,error_aprox(:,i),'--r')
legend('Medida exacta','Medida aprox.')
ylabel('Error (A)')
xlabel('Tiempo (s)')
title(str)
k=k+1;
end
```

```
%%  Graphs for phase S

k=1;
for i=2:2:8
figure()
subplot(2,1,1)
plot(t,Im(:,i))
hold on
plot(t,Iap(:,i),'--g')
plot(t,IS,'--r')
str=sprintf('Fase S%1d',k);
ylabel('Corriente (A)')
xlabel('Tiempo (s)')
title(str)
legend('Medida exacta','Medida aproximada','Real')
axis([0 0.02 -1 1])

subplot(2,1,2)
```

```
plot(t,error_exacto(:,i))
hold on
plot(t,error_aprox(:,i),'--r')
legend('Medida exacta','Medida aprox.')
ylabel('Error (A)')
xlabel('Tiempo (s)')
title(str)
k=k+1;
end
```

```
%%  Graphs for the phase T

k=1;
i=9;
figure()
subplot(2,1,1)
plot(t,Im(:,i))
hold on
plot(t,Iap(:,i),'--g')
plot(t,ITt,'--r')
str=sprintf('Fase barra T');
ylabel('Corriente (A)')
xlabel('Tiempo (s)')
legend('Medida exacta','Medida aproximada','Real')
axis([0 0.02 -4 4])

subplot(2,1,2)
plot(t,error_exacto(:,i))
hold on
plot(t,error_aprox(:,i),'--r')
legend('Medida exacta','Medida aprox.')
ylabel('Error (A)')
xlabel('Tiempo (s)')
title(str)
k=k+1;

set(0,'DefaultFigureWindowStyle','normal')
```

Appendix B: Arduino algorithms

```
  #define samples 512  // Numero de muestras a tomar

  volatile int Count = 0; // Necesario emplear variables volatiles para el paso de datos
entre la interrupcion y la funcion principal
  volatile int sensor1[samples]; // Vector para almacenar el numero de muestras definidas
en "samples"
  volatile int sensor2[samples]; // Vector para almacenar el numero de muestras definidas
en "samples"

  double S1medio = 0;
  double S2medio = 0;
  double S1rms = 0;
  double S2rms = 0;
  double pot=0;
  double S=0;
  double Q=0;
  double fdp=0;


  // Define various ADC prescaler
  const unsigned char PS_16 = (1 << ADPS2);
  //const unsigned char PS_32 = (1 << ADPS2) | (1 << ADPS0);
  //const unsigned char PS_64 = (1 << ADPS2) | (1 << ADPS1);
  //const unsigned char PS_128 = (1 << ADPS2) | (1 << ADPS1) | (1 << ADPS0);

  const unsigned char CHAN0 = 0; // Canal A0 / Canal A8 si MUX5=1
  //const unsigned char CHAN1 = (1<<MUX0); // Canal A1 / Canal A9 si MUX5=1
  const unsigned char CHAN2 = (1<<MUX1); // Canal A2 / Canal A10 si MUX5=1
  //const unsigned char CHAN3 = (1<<MUX1)|(1<<MUX0); // Canal A3 / Canal A11 si MUX5=1
  const unsigned char CHAN4 = (1<<MUX2); // Canal A4 / Canal A12 si MUX5=1
  //const unsigned char CHAN5 = (1<<MUX2)|(1<<MUX0); // Canal A5 / Canal A13 si MUX5=1
  const unsigned char CHAN6 = (1<<MUX2)|(1<<MUX1); // Canal A6 / Canal A14 si MUX5=1
  //const unsigned char CHAN7 = (1<<MUX2)|(1<<MUX1)|(1<<MUX0); // Canal A7 / Canal A15
si MUX5=1
  int canal=0;
  int CanalCount=0;


  void setup(void)
  {
    Serial.begin(115200);     // Velocidad de transferencia del puerto serie para
visualizar los datos recogidos en el monitor

    cli();//stop interrupts

    ConfigADC(CHAN0); // Función de configuración del ADC

    ConfigTimer();

    sei();//allow interrupts
  }


  ///// Función de configuración del ADC

  void ConfigADC(const unsigned char CHANNEL)
  {
    DIDR0 = 0x00;   //Digital input disabled on all ADC
    ADMUX = 0x00;   //clearing registers.
    ADCSRA = 0x00;
    ADCSRB = 0x00;

    ADCSRA |= PS_16;    // prescaler a 16

    if (CanalCount>6)
      {
```

```
        ADCSRB |= (1<<MUX5);
      }

    ADMUX |= (0<<REFS1)|(1<<REFS0)|CHANNEL;

    ADCSRA |= (1 << ADEN); // Se habilita el convertidor

  }

  ///// Función de configuración del temperizador

  void ConfigTimer(void)
  {

    //set timer1 interrupt at 12800Hz
    TCCR1A = 0;// set entire TCCR1A register to 0
    TCCR1B = 0;// same for TCCR1B
    TCNT1  = 0;//initialize counter value to 0
    // set compare match register for 12800hz increments
    OCR1A = 1249;// = (16*10^6) / (12800*1) - 1 (must be <65536)
    // turn on CTC mode
    TCCR1B |= (1 << WGM12);
    // Set CS10 bits for 1 prescaler
    TCCR1B |=  (1 << CS10);
    // enable timer compare interrupt
    TIMSK1 |= (1 << OCIE1A);

   }

  ///// Función de lectura ejecutada en cada interrupción

  ISR(TIMER1_COMPA_vect)
  {
       if(Count>=samples)
       return;

       ADCSRA|=(1<<ADSC);//iniciar conversion
       loop_until_bit_is_clear(ADCSRA, ADSC);  // ADSC es limpiado cuando la conversion
termina
       sensor1[Count] = ADC ;// Lectura del registro directamente y se almacena (0-
1024).

       ADMUX +=1;  // Cambio al siguiente canal (contiguo al inicialmente indicado en
la función setup)

       ADCSRA|=(1<<ADSC);//iniciar conversion
       loop_until_bit_is_clear(ADCSRA, ADSC);  // ADSC es limpiado cuando la conversion
termina
       sensor2[Count] = ADC ;// Lectura del registro directamente y se almacena (0-
1024).

       ADMUX -=1;    // Vuelvo al canal anterior.

       Count = Count + 1;  // Incremento del puntero para el almacenamiento en los
vectores de datos correspondiente
  }


  ///// Función principal

  void loop(void)
  {

    if(Count==samples)     // Presenta todas las muestras por el monitor serie
    {
      cli(); // Deshabilito interrupciones pra enviar los datos
      Count=0; // Reinicio del puntero para las muestras

      int t0=micros();

      Media();
```

```
    RMS();
    Potencia();

    //Resultados();
    Datos();

    S1medio=0;
    S2medio=0;
    S1rms=0;
    S2rms=0;
    pot=0;
    S=0;
    Q=0;
    fdp=0;

    canal=canal+2;
    CanalCount=CanalCount+2;

    if (CanalCount>15 | canal>6)
    {
      canal=0;
    }

    if (CanalCount>15)
    {
      CanalCount=0;
      //Serial.println("******************");
    }

    ConfigADC(canal);
    int tf=micros()-t0;
    //Serial.println(tf);

    sei(); // Habilito interrupciones
   }

}


//// Función cálculo de valor medio

void Media(void)
{
    for (int i=0; i < samples; i++) // Envío de los datos por puerto serie
    {
      S1medio+=(double)sensor1[i];
      S2medio+=(double)sensor2[i];
    }

    S1medio=S1medio/(double)samples;
    S2medio=S2medio/(double)samples;

}


//// Función cálculo RMS

void RMS(void)
{
    for (int i=0; i < samples; i++) // Envío de los datos por puerto serie
    {

      S1rms+=sq((double)sensor1[i]);
      S2rms+=sq((double)sensor2[i]);
//      S1rms+=sq((double)sensor1[i]-S1medio);
//      S2rms+=sq((double)sensor2[i]-S2medio);
    }

    S1rms=sqrt(S1rms/(double)samples);
    S2rms=sqrt(S2rms/(double)samples);
```

```
  }


  //// Función cálculo potencia

  void Potencia(void)
  {
      for (int i=0; i < samples; i++) // Envío de los datos por puerto serie
      {
        pot+=((double)sensor1[i])*((double)sensor2[i]);
        //pot+=((double)sensor1[i]-S1medio)*((double)sensor2[i]-S2medio);
      }

      pot=pot/(double)samples;
      S=S1rms*S2rms;
      Q=sqrt(sq(S)-sq(pot));
      fdp=pot/S;

  }

  //// Función envío de datos

  void Datos(void)
  {
      Serial.write('A');   // send a capital A
      Serial.println();
      delay(1);

      for (int i=0; i < samples; i++) // Envío de los datos por puerto serie
      {
       Serial.print(sensor1[i]);
       Serial.print(",");
       Serial.println(sensor2[i]);

      }

    Serial.flush();  // Se supone que fuerza al código a esperar que se envíen todos los
datos

    delay(1);
  }



  //// Función envío de resultados

  void Resultados(void)
  {   //Serial.write('A');   // send a capital A
      Serial.print("    Canal ");
      Serial.println(CanalCount);
      delay(1);

       Serial.print("Valor medio sensor 1 = ");
       Serial.println(S1medio);
       Serial.print("Valor medio sensor 2 = ");
       Serial.println(S2medio);
       Serial.print("Valor RMS sensor 1 = ");
       Serial.println(S1rms);
       Serial.print("Valor RMS sensor 2 = ");
       Serial.println(S2rms);
       Serial.print("Potencia aparente = ");
       Serial.println(S);
       Serial.print("Potencia activa = ");
       Serial.println(pot);
       Serial.print("Potencia reactiva = ");
       Serial.println(Q);
       Serial.print("Factor de potencia = ");
       Serial.println(fdp);

    Serial.flush();  // Se supone que fuerza al código a esperar que se envíen todos los
datos
```

BIBLIOGRAPHY

[1] Popović R S 2004 *Hall Effect Devices* (Bristol: Institute of Physics Publishing)

[2] Banjević M, Liakou F, Furrer B, Dimitrijević S, Blagojević M, Dimitropoulos P D and Popović R S , 2011. *Open-loop CMOS current transducer with low temperature cross sensitivity*

[3] Thomson, W. (18 June 1857), "*On the Electro-Dynamic Qualities of Metals: Effects of Magnetization on the Electric Conductivity of Nickel and of Iron*" (PDF)

[4] *The Nobel Prize in Physics 2007*, Nobel Media AB, 9 Oct 2007, retrieved 25 Jun 2014

[5] T. McGuire and R. Potter. *Anisotropic magnetoresistance in ferromagnetic 3d alloys*.

[6] Richard Fitzpatrick *(*2007*). "Ampère's Circuital Law"*.

[7] Heinz E Knoepfel (2000). *Magnetic Fields: A comprehensive theoretical treatise for practical use.*

[8] Official Comsol web site.
Link: https://www.comsol.com/blogs/modeling-coils-in-the-acdc-module/

[9] Official Comsol web site.
Link: https://www.comsol.com/blogs/exploiting-symmetry-simplify-magnetic-field-modeling/

[10] Official Comsol web site.
Link: https://www.comsol.com/blogs/how-to-choose-between-boundary-conditions-for-coil-modeling/

[11] Official Comsol web site.
Link: https://www.comsol.com/blogs/meshing-considerations-linear-static-problems/

[12] *"Arduino - Introduction"*. arduino.cc.

Trabajo Fin de Grado
Ingeniería de la Energía

Medida de Corrientes en Cuadros de Distribución BT mediante el uso de Sensores de Campo Magnético

Autor: Enrico Leorato
Tutores: Prof. Juan Carlos del Pino López
Prof. Pedro Luis Cruz Romero

Dep. de Ingeniería Eléctrica
Escuela Técnica Superior de Ingeniería
Universidad de Sevilla

Sevilla, 2016

Resumen en castellano del Trabajo Fin de Grado

I. Introducción

En los sistemas de energía, las corrientes generalmente, fluyen a través de conductores planos de cobre o de aluminio llamados barras colectoras (en inglés bus bars). Por lo tanto, actualmente, existe una demanda práctica de desarrollo de aplicaciones de medición de los parámetros eléctricos que caracterizan estas barras.

La presente investigación tiene como propósito la elaboración de un sistema de supervisión de corriente aplicable a barras colectoras con las principales características de ser económico y de realizar la medición de la corriente automáticamente sin la intervención manual, con instrumentos de medida, por parte del usuario.

Las barras consideradas en esto proyecto son empleadas en un cuadro de distribución en BT destinado al uso en el sector industrial. Esto cuadro es idealizado para la alimentación de cuatro circuitos trifásicos que proporcionan energía a distintos grupos de cargas eléctricas.

Dada su implementación en un cuadro, la futura finalidad real de este sistema de medición de corrientes podrá ser la posibilidad de obtener las principales características eléctricas de cada circuito conectado al cuadro, como por ejemplo la curva de carga.

En la aplicación desarrollada en esta investigación se supone que el campo magnético que se forma al alrededor de una barra colectora sea proporcional a la corriente aplicada en cada momento. Por lo tanto, es posible averiguar los parámetros eléctricos que caracterizan una barra midiendo y analizando el campo magnético por ella generado.

Con el fin de analizar el campo magnético, se tuvo en cuenta, principalmente por la relación coste-eficacia, la instalación en el panel de una serie de sensores magnetoresistivos apoyados por un microcontrolador Arduino® (modelo MEGA 2560), especialmente programado para el caso en estudio. El funcionamiento de estos sensores es caracterizado da el efecto AMR (anisotropic magnetoresistance) y los sensores usados son los sensores Honeywell HMC5883L, elegidos por su rentabilidad y tamaño pequeño.

El principal desarrollo del proyecto se realizó mediante un modelo 3D del panel de distribución, diseñado con el apoyo del software Solidworks® y posteriormente implementado en el software de simulación COMSOL Multiphysics® para el análisis de elementos finitos.

El uso del software de simulación FEM ha sido fundamental con el fin de detectar la posición correcta y la configuración de los sensores. El objetivo principal obtenido mediante las simulaciones FEM fue la eliminación de la influencia del campo magnético de dispersión en las medidas de los sensores. Esto ha sido posible a través de una configuración diferencial de los sensores, como será explicado en el documento.

Al final de la obra se ha alcanzado un nivel bastante avanzado del proyecto, llegando a conseguir el correcto funcionamiento, a nivel de simulación, del sistema de medición y consiguiendo también en la idealización de un algoritmo Arduino® para controlar el microprocesor que soporta los sensores.

El correcto funcionamiento del sistema de simulación ha sido verificado mediante un estudio gráfico de las tendencias de las corrientes medidas, desarrollado en un entorno Matlab.

II. Consideraciones teóricas para la medida del campo magnético

El objetivo del proyecto es obtener una correcta medida del campo magnético generado por cada barra con el propósito de adquirir un perfecto sistema de medida de la corriente que fluye por cada barra y entonces por cada circuito.

El principal problema encontrado para conseguir este objetivo fue descubrir la disposición de los sensores alrededor de las barras que habría permitido de medir solo el campo generado por la barra de interés y no el campo magnético de dispersión creado por las otras barras.

Una solución práctica a este problema fue obtenida yendo a posicionar los sensores como en la siguiente imagen donde se consideran dos conductores eléctricos atravesados por una corriente:

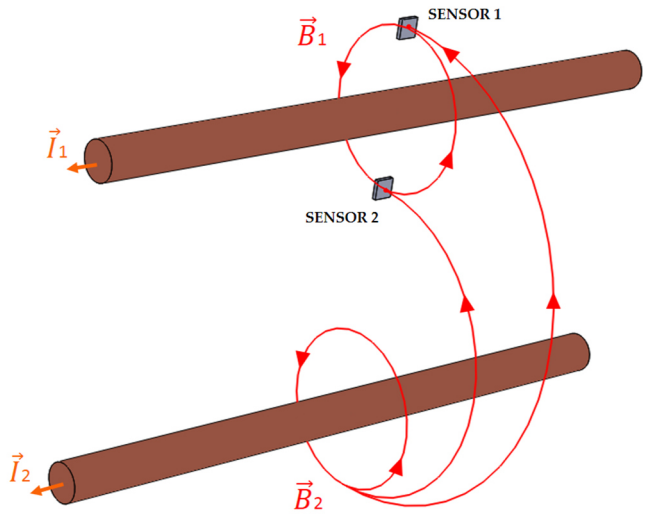

Fig. a *Detección de campo magnético por parte de los sensores. Caso con dos cables eléctricos.*

Como puede observarse en la imagen, los sensores 1 y 2, instalados por la medida del campo magnético producido por el primero conductor, son influenciados también da las líneas de campo magnético generadas por el otro conductor.

La idea clave para la eliminación de los campos de dispersión fue en la configuración de los sensores y en su posicionamiento. De hecho, usando una configuración diferencial de los sensores y colocándolos (en la medida de lo posible) cercanos à la barra en consideración, se han podido eliminar los efectos, sobre la medida, de los campos magnéticos externos.

La configuración diferencial en particular, ha permitido que calculando la suma de los valores obtenidos por los dos sensores se lograra la eliminación de los valores referidos al campo externo. Esto por el hecho de que ambas líneas de campo son entrantes en los sensores, pero los sensores teniendo una configuración diferencial van a eliminar estos valores cuando se realice la suma de las dos medidas.

En la próxima imagen está representado el mismo concepto, pero adaptado al caso en cuestión:

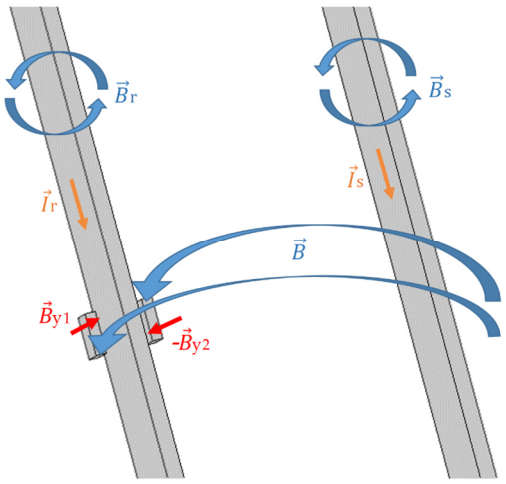

Fig.b *Detección de campo magnético por parte de los sensores. Caso con dos barras colectoras.*

En la imagen $\vec{B}_{y1}$ y $-\vec{B}_{y2}$ son los valores impostados para los sensores en configuración diferencial.

III. Desarrollo de la geometría en Solidworks®

En las siguientes imágenes está representado el cuadro en consideración en su forma real y en su forma modelizada con el 3D CAD software Solidworks.

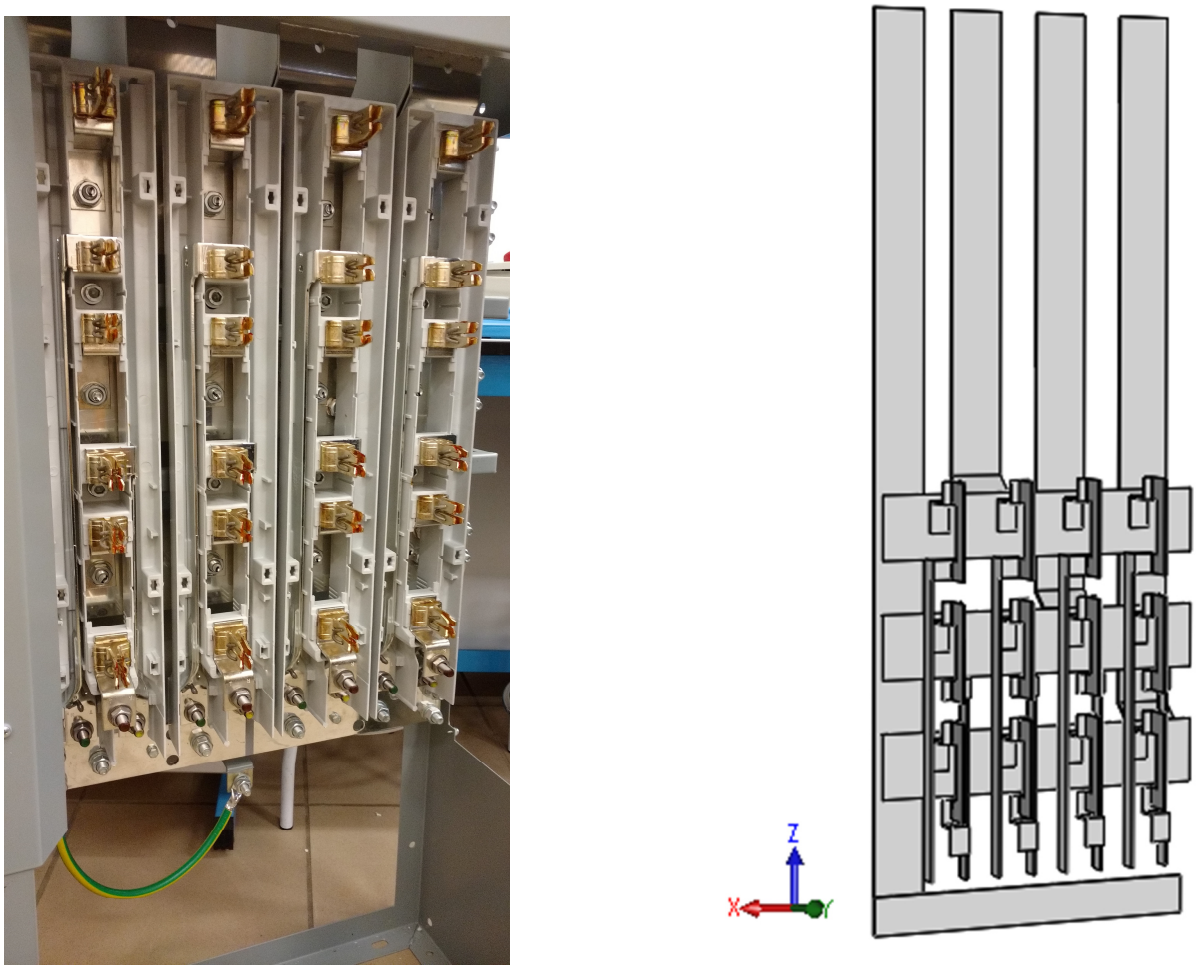

Fig.b *Cuadro en su forma real y en su forma modelizada*

Las características eléctricas son:

- In = 400 A
- Vn = 400 V

Las características geométricas son reportadas en la próxima página, donde se consideran las principales medidas del cuadro usadas en la modelización en Solidworks.

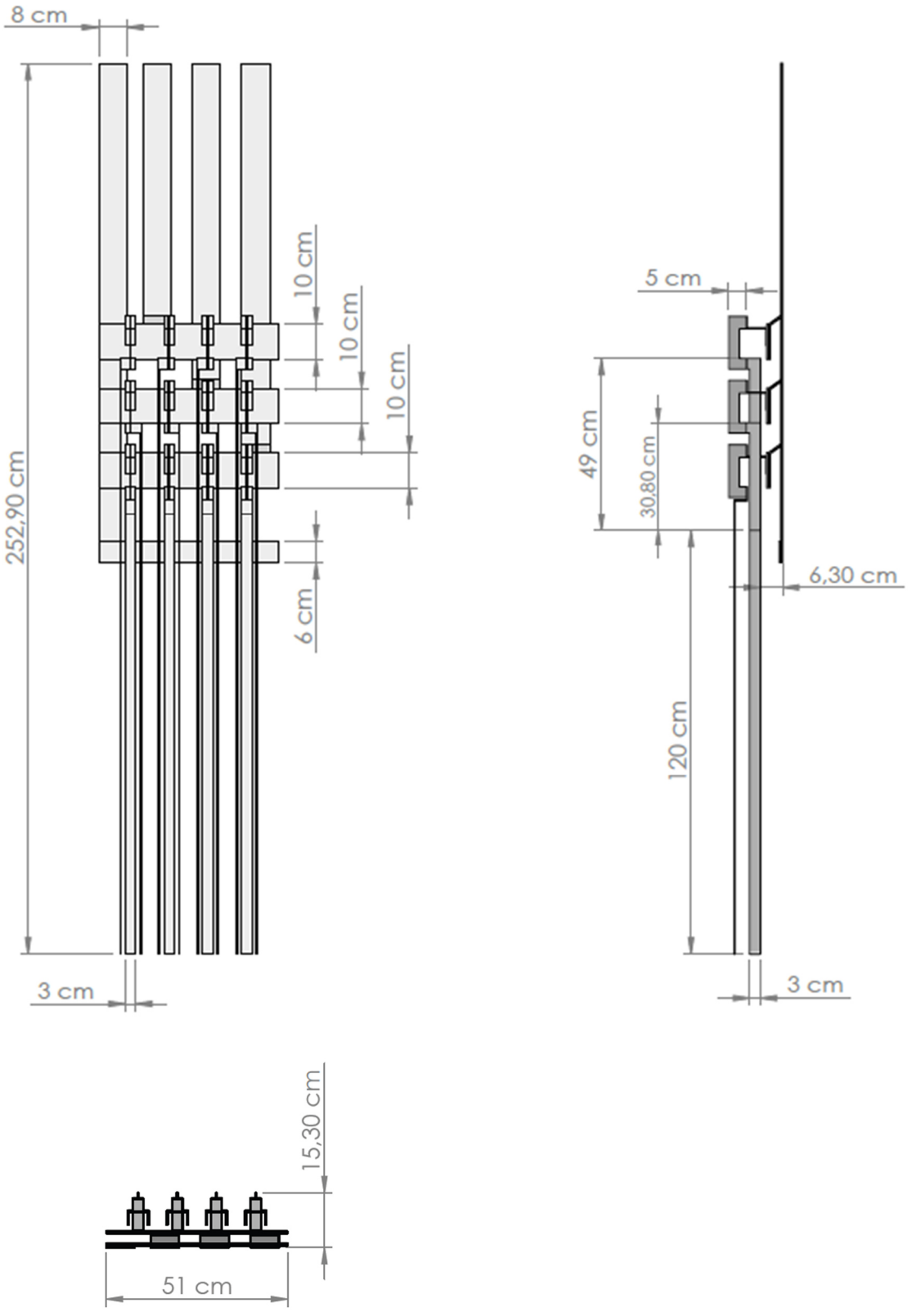

Fig.c *Principales medidas del cuadro modelizado*

IV. Implementación de la geometría en COMSOL Multiphysics®

Luego haber creado la geometría en Solidworks esa fue importada en COMSOL Multiphysics para permitir un análisis FEM.

La implementación en COMSOL del modelo fue caracterizada da los siguientes pasos:

- Construcción de dos dominios externos para la limitación de el volumen de cálculo e para obtener un circuito cerrado por la corriente;
- Planteamiento de los respectivos materiales por cada parte del modelo. En particular aluminio para las barras y aire para los dos dominios externos;
- Aplicación de las Boundary Condition al dominio exterior, in particular se utilizaron Magnetic Insulation Boundary Conditions para permitir el retorno de corriente a través del dominio exterior;
- Inserción de una oportuna Mesh para la parte de las barras de aluminio y los dos dominios de aire.

V. Desarrollo del estudio del modelo para el posicionamiento de los sensores.

La parte más sustancial del trabajo fue la parte de análisis del modelo en Comsol con el propósito de simular la instalación de los sensores y su vigilancia de las corrientes.

Para desarrollar esta parte del trabajo se decidió repartir el estudio del modelo entre diferentes planos 2D obtenidos "cortando" el modelo 3D en planos de interés. Por cada plano de corte fue considerado una posible disposición de los sensores.

Este procedimiento ha permitido simplificar el estudio, reducir el tiempo de cálculo y simplificar la geometría a examinar.

Los principales planes de corte son los siguientes:

- Un plano x-y obtenido cortando el modelo a la altura de z = 35,25 cm;
- Un plano x-z obtenido cortando el modelo a la altura de y = 11,4 cm;
- Un plano x-z obtenido cortando el modelo a la altura de y = 6,9 cm.

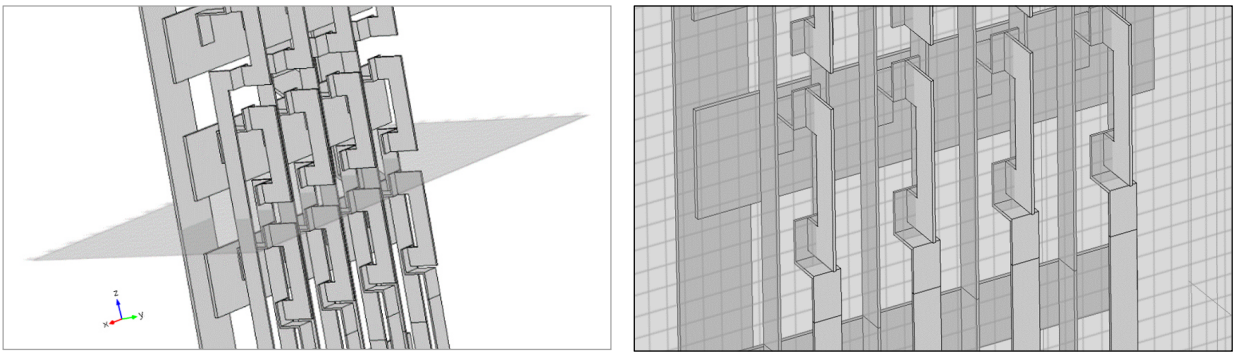

Fig.d *Planes de corte para los sensores de la primera disposición, vistas en 3D.*

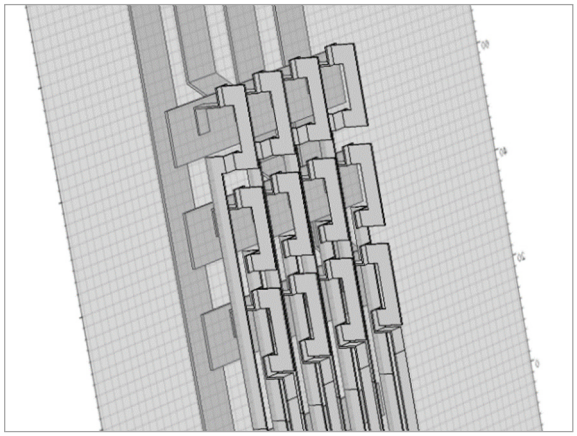

Fig. e *Plan de corte para los sensores de la segunda disposición, vistas en 3D.*

De esta manera, se dividió el estudio del modelo en las dos siguientes posibles disposiciones de sensores:

- Primera posible disposición de sensores, compuesta por los primeros dos planos de corte (Z = 35,25 cm e Y = 11,4 cm), donde en el plan de corte z fueron dispuestos los sensores de las fases R, S y en el plan y los sensores de las fases T;
- Segunda posible disposición de sensores, compuesta por el tercero plan de corte (y = 6,9 cm), donde fueron dispuestos todos los sensores de todas las fases.

La presencia de los sensores fue simulada, en el modelo de simulación, con el uso de una herramienta virtual que permite medir el campo magnético y sus componentes vectoriales en un punto dado.

Los pasos principales para la aplicación de los puntos de medición en el plan de corte 2D fueron:

Tener en cuenta la posición en la que es posible insertar los sensores en el cuadro eléctrico real, tratando de seguir una cierta simetría física;

- Encontrar el sitio con la menor distancia entre los sensores;
- Aclarar la componente vectorial del campo que permite obtener la mejor medida del campo posible;
- Hacer un breve estudio sobre la distribución del campo magnético al alrededor de las barras eléctricas. Esto con el fin de averiguar el sitio cerca de las barras que presenta la mayor magnitud de campo magnético para el componente vectorial tomado en consideración.

Estos puntos son ampliamente explicados en el documento.

Las posiciones resultantes obtenidas para los puntos de medida (o sea los sensores en el cuadro real) son reportadas en la siguiente página.

- **Primera disposición de sensores**

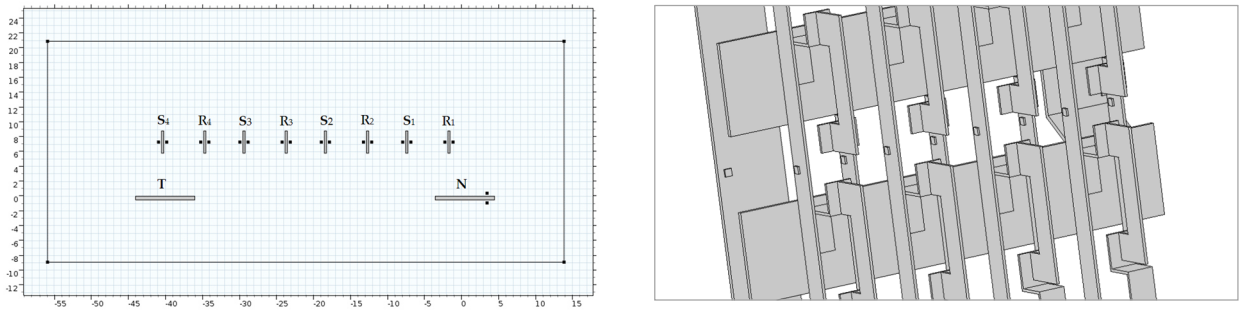

Fig.f *Posición de los puntos de medidas en el plan 2D y respectivos sensores modelizados en el modelo 3D. Caso barras R-S de la primera disposición de los sensores.*

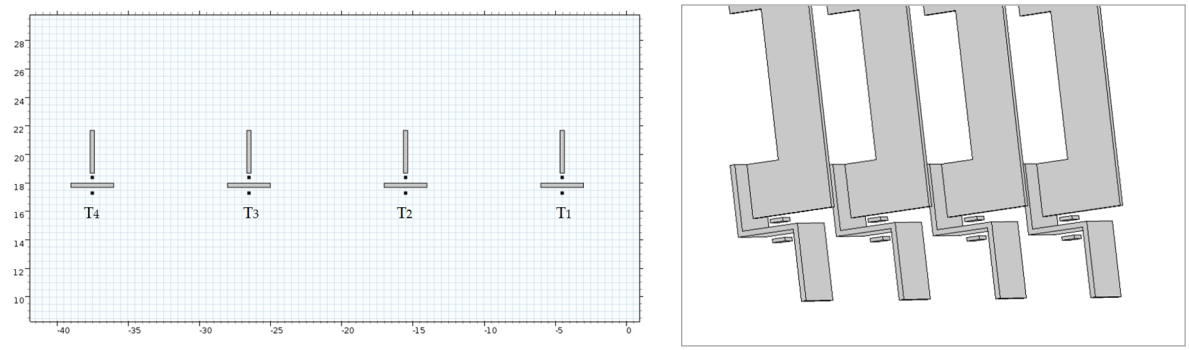

Fig.*Errore. Nel documento non esiste testo dello stile specificato.****g*** *Posición de los puntos de medidas en el plan 2D y respectivos sensores modelizados en el modelo 3D. Caso barras T de la primera disposición de los sensores.*

- **Segunda disposición de sensores**

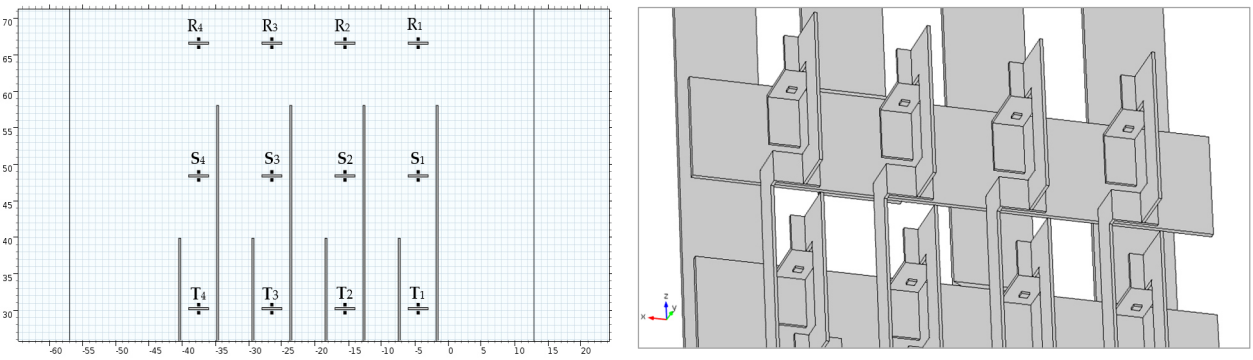

Fig.h *Posición de los puntos de medidas en el plan 2D y respectivos sensores modelizados en el modelo 3D. Caso de la segunda disposición de los sensores.*

VI. Derivación del valor de la corriente

En lo que respecta a la derivación de la corriente fue usado un método, ampliamente explicado en el documento, en cuyo se buscó una relación entre la corriente (incógnita que se debe medir) y el campo magnético (factor medido a través de los sensores).

Esta relación se expresa en una matriz llamada $[K]$, compuesta por elementos constantes, derivada a través de un estudio del estado estable del modelo en Comsol considerando el principio de superposición de los efectos. Una fase importante del estudio fue asegurarse de que la matriz se quedara constante independientemente de las corrientes inyectadas en las pletinas.

Cada elemento de esta matriz representa el valor de medida de cada sensor obtenido con las barras alimentadas una a una. Un ejemplo de matriz $[K]$ y su relación con la corriente y el campo magnético puede ser el siguiente:

$$\left[\vec{B}\right] = [K] \cdot \left[\vec{I}\right]$$

$$\begin{bmatrix} B_{R1} \\ B_{S1} \\ B_{T1} \\ B_{R2} \\ B_{S2} \\ B_{T2} \\ B_{R3} \\ B_{S3} \\ B_{T3} \\ B_{R4} \\ B_{S4} \\ B_{T4} \end{bmatrix} = \begin{bmatrix} K_{R1R1} & K_{R1S1} & K_{R1T1} & K_{R1R2} & K_{R1S2} & K_{R1T2} & K_{R1R3} & K_{R1S3} & K_{R1T3} & K_{R1R4} & K_{R1S4} & K_{R1T4} \\ K_{S1R1} & K_{S1S1} & K_{S1T1} & K_{S1R2} & K_{S1S2} & K_{S1T2} & K_{S1R3} & K_{S1S3} & K_{S1T3} & K_{S1R4} & K_{S1S4} & K_{S1T4} \\ K_{T1R1} & K_{T1S1} & K_{T1T1} & K_{T1R2} & K_{T1S2} & K_{T1T2} & K_{T1R3} & K_{T1S3} & K_{T1T3} & K_{T1R4} & K_{T1S4} & K_{T1T4} \\ K_{R2R1} & K_{R2S1} & K_{R2T1} & K_{R2R2} & K_{R2S2} & K_{R2T2} & K_{R2R3} & K_{R2S3} & K_{R2T3} & K_{R2R4} & K_{R2S4} & K_{R2T4} \\ K_{S2R1} & K_{S2S1} & K_{S2T1} & K_{S2R2} & K_{S2S2} & K_{S2T2} & K_{S2R3} & K_{S2S3} & K_{S2T3} & K_{S2R4} & K_{S2S4} & K_{S2T4} \\ K_{T2R1} & K_{T2S1} & K_{T2T1} & K_{T2R2} & K_{T2S2} & K_{T2T2} & K_{T2R3} & K_{T2S3} & K_{T2T3} & K_{T2R4} & K_{T2S4} & K_{T2T4} \\ K_{R3R1} & K_{R3S1} & K_{R3T1} & K_{R3R2} & K_{R3S2} & K_{R3T2} & K_{R3R3} & K_{R3S3} & K_{R3T3} & K_{R3R4} & K_{R3S4} & K_{R3T4} \\ K_{S3R1} & K_{S3S1} & K_{S3T1} & K_{S3R2} & K_{S3S2} & K_{S3T2} & K_{S3R3} & K_{S3S3} & K_{S3T3} & K_{S3R4} & K_{S3S4} & K_{S3T4} \\ K_{T3R1} & K_{T3S1} & K_{T3T1} & K_{T3R2} & K_{T3S2} & K_{T3T2} & K_{T3R3} & K_{T3S3} & K_{T3T3} & K_{T3R4} & K_{T3S4} & K_{T3T4} \\ K_{R4R1} & K_{R4S1} & K_{R4T1} & K_{R4R2} & K_{R4S2} & K_{R4T2} & K_{R4R3} & K_{R4S3} & K_{R4T3} & K_{R4R4} & K_{R4S4} & K_{R4T4} \\ K_{S4R1} & K_{S4S1} & K_{S4T1} & K_{S4R2} & K_{S4S2} & K_{S4T2} & K_{S4R3} & K_{S4S3} & K_{S4T3} & K_{S4R4} & K_{S4S4} & K_{S4T4} \\ K_{T4R1} & K_{T4S1} & K_{T4T1} & K_{T4R2} & K_{T4S2} & K_{T4T2} & K_{T4R3} & K_{T4S3} & K_{T4T3} & K_{T3R3} & K_{T3S3} & K_{T4T4} \end{bmatrix} \begin{bmatrix} I_{R1} \\ I_{S1} \\ I_{T1} \\ I_{R2} \\ I_{S2} \\ I_{T2} \\ I_{R3} \\ I_{S3} \\ I_{T3} \\ I_{R4} \\ I_{S4} \\ I_{T4} \end{bmatrix}$$

Hay que tener en cuenta que la matriz $[K]$ es diferente por cada plan de estudio analizado.

Para obtener el valor de la corriente se ha hecho un estudio del modelo en Comsol en el dominio del tiempo con el objetivo de sacar los valores vectoriales de campo magnético medidos por los sensores al variar del tiempo. Los valores de tiempo tenidos en consideración son los valores desde t = 0 [s] hasta t = 0,02 [s] con intervalos de 0,01 [s], es decir:

$$t = (0;\ 0{,}001;\ 0{,}002 \ldots 0{,}019;\ 0{,}02)$$

De esta forma se ha podido sacar la matriz de las corrientes sinusoidales en dependencia del tiempo usando la siguiente relación:

$$\left[\vec{I}(t)\right] = [K]^{-1} \cdot \left[\vec{B}(t)\right]$$

Todo esto fue desarrollado por las dos posibles disposiciones de sensores tomadas en cuenta, yendo a sacar por cada caso la matriz $[K]$ y la matriz $\left[\vec{B}(t)\right]$ porque en cada caso los valores cambian segundo la disposición de los sensores y el número de barras incluidas en el cálculo.

En el proyecto fue analizado también el caso donde se desprecian los efectos de inducción mutua que se producen entre las barras y el sistema desequilibrado de corrientes.

VII. Resultados

Los resultados se han obtenidos de forma gráfica con el uso del software Matlab gracias à la implementación de un programa de cálculo dedicado. En la siguiente imagen está representado un ejemplo de los resultados obtenidos considerando solo la pareja de puntos de medida de la primera barra de la fase R:

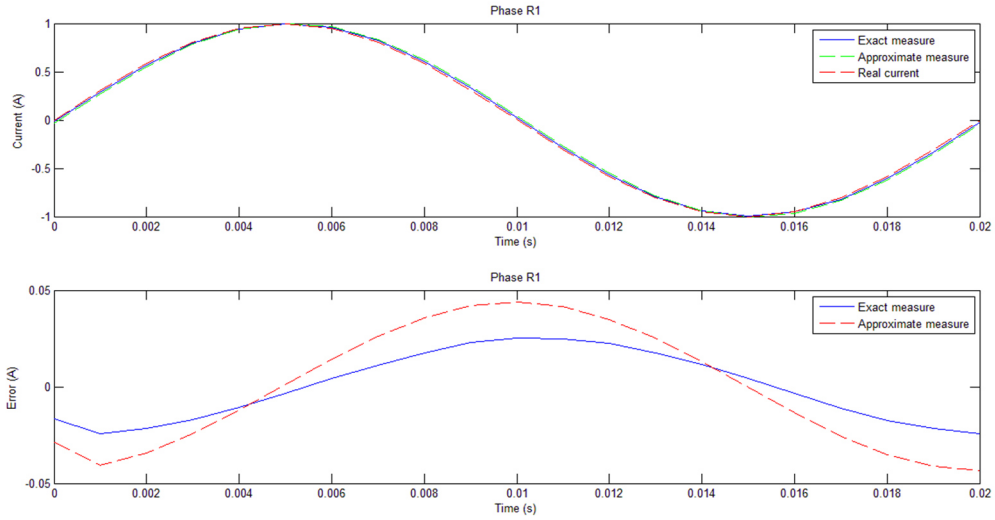

Fig. i *Evolución de la corriente y respectivo error*

Las curvas representadas se obtuvieron a través de las subsiguientes ecuaciones:

- Exact measure (gráfico corrientes) : $\left[\vec{I}(t)\right]_{exact} = \left[K\right]^{-1} \cdot \left[\vec{B}(t)\right]$
- Approximate measure (gráfico corrientes) : $\left[\vec{I}(t)\right]_{approx.} = \frac{\left[\vec{B}(t)\right]}{\left[K\right]}$
- Exact measure (gráfico error) : $e_{exact} = \left[\vec{I}(t)\right]_{exact} - \left[\vec{I}(t)\right]_{input}$
- Approximate measure (gráfico error): $e_{approx.} = \left[\vec{I}(t)\right]_{approx.} - \left[\vec{I}(t)\right]_{input}$

Donde:

$\left[\vec{I}(t)\right]_{input}$ es la matriz de las corrientes inyectadas en las barras en la simulación (Real current en el gráfico);

$\left[\vec{I}(t)\right]_{exact}$ es la corriente medida con el método de la matriz K.

Por el hecho que, como se puede ver en el gráfico, la medida de corriente está afectada por un error se ha pensado de introducir una matriz de coeficientes correctivos, presentada en el documento, que ha permitido corregir el error de medida. El resultado de esta implementación se puede ver claramente en el siguiente grafico donde se aprecia un error prácticamente nulo.

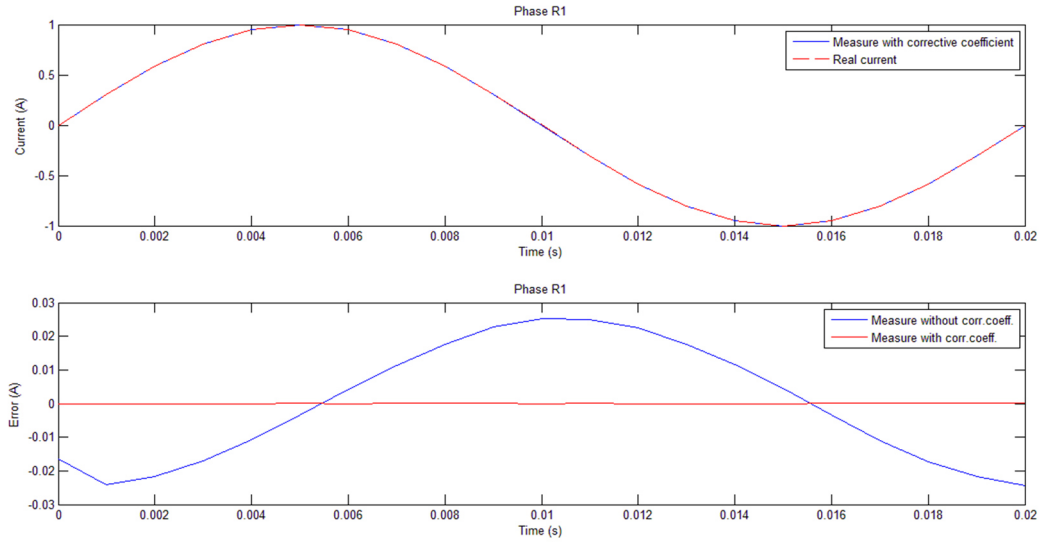

Fig.j *Evolución de la corriente y respectivo error con la implementación del factor correctivo*

VIII. Vigilancia de sensores Magnetoresistivos a través de la aplicación de un microcontrolador Arduino®

Las principales ventajas que han llevado à la elección del uso de un microcontrolador y un sistema de programación Arduino han sido el hecho que las pizarras electrónicas Arduino son relativamente baratas en comparación con otras plataformas de microcontroladores y permiten con facilidad de monitorear los sensores elegidos. Además, el software de Arduino (IDE) para la programación de las pizarras es gratuito.

El modelo de microcontrolador usado fue "MEGA 2560" elegido por el hecho que ese modelo, entre todos los modelos de microcontroladores de Arduino, era lo que tenía más canales de ingreso (en total 16).

De hecho, la configuración de conexión no será una conexión directa sensor-canal sino los valores medidos por los dos sensores puestos en cada pletina serán sumados por un amplificador operacional. El resultado de la suma será lo que se lleve a un determinado canal para su adquisición. Por eso se tendrán en total 12 canales para las fases de todos los circuitos (4 circuitos × 3 fases) más un canal para el neutro y tres para las tensiones.

Además, será necesario también realizar un circuito de adaptación para alimentar a los sensores y los operacionales, así como para adaptar los niveles de salida de éstos al rango admitido por Arduino.

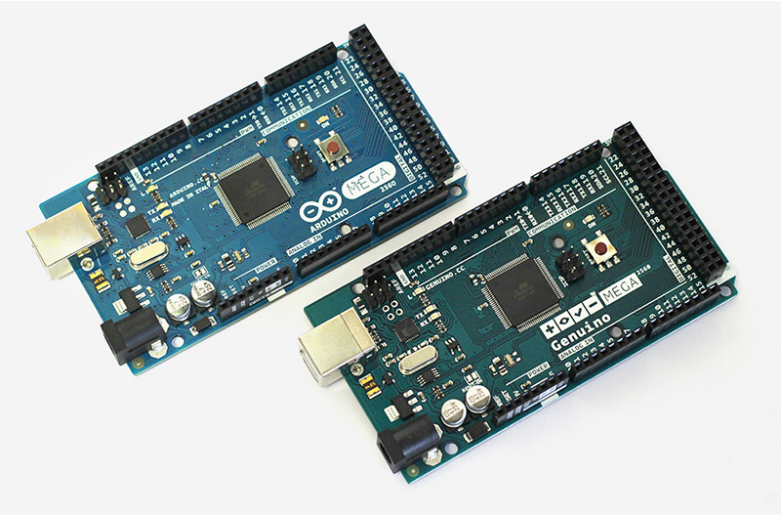

Fig.k *Arduino Mega (versión para EE.UU.) y Genuino Mega (versión no para EE.UU.)*

Una limitación encontrada en la implementación del microcontrolador Arduino es que no es posible medir todos los canales a la vez. Esto se debe a que sólo hay un convertidor con un multiplexor, que actúa como el selector de canales al ser leído. En nuestro caso tenemos que leer 16 canales y el tiempo para cambiar la selección de un canal a otro es más o menos fijo, pero no es instantáneo. Por lo tanto, eso supone que hay un ligero retraso en la conmutación de un canal a otro.

Todo esto ha llevado algunos problemas en la consecución del objetivo de medir, a través de la corriente y la tensión derivada para cada fase, la diferencia de tiempo entre las fases y por lo tanto la correspondiente potencia activa P y potencia reactiva Q.

La resolución de este problema fue conseguida considerando los canales por pares, con el fin de obtener los parámetros de V e I entre las dos fases y consiguientemente el respectivo desfase.

Por segundo yendo a implementar un temporizador programándolo para el funcionamiento à la velocidad de 12.8 kHz y cambiando la gestión del almacenamiento de los datos.

Luego fue necesario, para disminuir al mínimo el tiempo entre la lectura del primer canal y del segundo, aumentar la velocidad de lectura de los datos usando el ADC a través de sus registros, controlando la velocidad de conversión. Con este método se ha obtenido una lectura de dos canales casi instantáneamente, caracterizada por una diferencia entre un canal y el otro de 10 μs de diferencia (que sería como 0.25º de desfase temporal que apenas influye a la hora de medir P y Q).

Al final de toda la programación del microcontrolador se ha conseguido en obtener un programa que desde la lectura de los sensores va a calcular y mostrar en el monitor de Arduino todos los parámetros principales (P, Q, S, cosφ y los respectivos valores efectivos y medios) para la supervisión del sistema eléctrico conectado al cuadro.

IX. Conclusiones

Los principales objetivos obtenidos con la presente investigación han sido la obtención de dos configuraciones diferentes para el posicionamiento de los sensores en el panel y la obtención, para cada configuración, de un número de relaciones teóricas necesarias para la medición correcta de las corrientes.

Otra meta alcanzada ha sido el desarrollo de una parte de la implementación total del código de programación para la placa Arduino, el descubrimiento de una limitación en su uso y la superación de la misma.

En cuanto a los costes del sistema de medida en cuenta, se ha podido ver que la realización de este sistema tiene una buena relación coste-eficacia.

La futura continuación del desarrollo del proyecto será centrada sobre el cableado de los circuitos y la instalación de los amplificadores operacionales y de los sensores.

Además de este, habrá que desarrollar el código de programación de Arduino, incluyendo las relaciones teóricas obtenidas en el proyecto y, por último, habrá que realizar alguna prueba con el fin de comprobar el correcto funcionamiento del sistema instalado.